

# AccuTOF™ LC series

DTRT™ (Direct Analysis in Real Time)

## Applications Notebook

Edition April 2022





## Table of Contents

<b>Introduction and Fundamentals .....</b>	<b>1</b>
Direct Analysis in Real Time (DART™) Mass Spectrometry (R. B. Cody, J. A. Laramée, J. M. Nilles, H. D. Durst, JEOL News, 40, 8 – 12, 2005) .....	1
The AccuTOF™ Atmospheric Pressure Interface: an Ideal Configuration for DART™ and Ambient Ionization (MSTips No. 221) .....	7
Accurate Isotope Data is Essential for Determining Elemental Compositions.....	13
DART™ Contamination Resistance: Analysis of Compounds in Saturated Salt and Buffer Solutions (MSTips No. D016) .....	17
<b>Drugs.....</b>	<b>19</b>
Direct Analysis of Drugs in Pills and Capsules with No Sample Preparation (MSTips No. D013) .....	19
Instantaneous Screening for Counterfeit Drugs with No Sample Preparation (MSTips No. D009) .....	20
<b>Food, Flavor, and Fragrance .....</b>	<b>21</b>
Using Solid Phase Microextraction with AccuTOF™-DART™ for Fragrance Analysis.....	21
Rapid Detection of Melamine in Dry Milk Using AccuTOF™-DART™.....	22
Flavones and Flavor Components in Two Basil Leaf Chemotypes .....	23
“No-prep” Analysis of Lipids in Cooking Oils and Detection of Adulterated Olive Oil (MSTips No. D019) .....	25
Detection of Oleocanthal in Freshly Pressed Extra-Virgin Olive Oil (MSTips No. D017) .....	29
Rapid Detection of Fungicide in Orange Peel (MSTips No. D014) .....	30
Instantaneous Detection of Opiates in Single Poppy Seeds (MSTips No. D008) .....	31
Detection of Lycopene in Tomato Skin (MSTips No. D006).....	32
Detection of Unstable Compound Released by Chopped Chives (MSTips No. D004) .....	33
Distribution of Capsaicin in Chili Peppers (MSTips No. D003) .....	34

Identifying “Buried” Information in LC/MS Data (MSTips No. D002) .....	35
Direct analysis of caffeine in soft drinks and coffee and tea infusions.....	37
Rapid screening of stobilurins in crude solid materials (wheat grains) using DART™-TOFMS ...	39
Analysis of stobilurins in wheat grains using DART™-TOFMS .....	41
Analysis of deoxynivalenol in beer .....	43
<b>Forensic and Homeland Security .....</b>	<b>45</b>
AccuTOF™-DART™ Analysis of Smokeless Powders.....	45
Fiber analysis by thermal desorption/pyrolysis DART™ .....	47
X-Ray Fluorescence Helps Identify Peaks in DART™ Mass Spectrum of Electrical Tape - ElementEye JSX-1000S and AccuTOF™-DART™ .....	51
Clandestine Methamphetamine Labs: Rapid Impurity Profiling by AccuTOF™-DART™ .....	55
“Laundry Detective”: Identification of a Stain.....	57
Direct analysis of stains on cloth caused by cosmetic foundation (MSTips No. D023) .....	58
Detection of the Peroxide Explosives TATP and HMTD .....	59
Detection of Explosives in Muddy Water (MSTips No. D012) .....	60
Rapid Detection and Exact Mass Measurements of Trace Components in an Herbicide (MSTips No. D011) .....	61
Instantaneous Detection of Illicit Drugs on Currency (MSTips No. D010) .....	62
Instantaneous Detection of Explosives on Clothing (MSTips No. D005).....	63
Instantaneous Detection of the “Date-Rape” Drug – GHB (MSTips No. D001) .....	64
Chemical Analysis of Fingerprints .....	65
Analysis of Biological Fluids.....	67
<b>Materials and Chemistry.....</b>	<b>71</b>
End group structural analysis of polyphenylene sulfide by thermal desorption / pyrolysis DART™- TOFMS (MSTips No. 353).....	71
Analysis of polystyrene end group structure by thermal desorption/pyrolysis (TDP) DART™- TOFMS (MSTips No. 318).....	73
Rapid Confirmation of Synthetic Compounds Using DART™ –Direct Mass Spectrometric Analysis from NMR Sample Tubes– (MSTips No. 223).....	76



Identification of Contamination on Welding Wires Using Cross-Platform Techniques in SEM and Mass Spec .....	77
AccuTOF™-DART™ analysis of motor oils .....	81
Analysis of duct tapes by thermal desorption and pyrolysis mass spectrometry and X-ray-fluorescence spectroscopy (MSTips No. 232) .....	85
Analysis of low polar compound by DART™ ~ analysis of organic electroluminescence materials ~ (MSTips No. D032) .....	93
Analysis of highly polar compound by DART™ ~ analysis of ionic liquid ~ (MSTips No. D031) ..	94
Analysis of Organic Contaminant on Metal Surface (MSTips No. D030) .....	95
Chemical Reaction Monitoring with the AccuTOF™-DART™ Mass Spectrometer .....	96
Direct Analysis of Organometallic Compounds .....	97
Rapid Analysis of p-Phenylenediamine Antioxidants in Rubber (MSTips No. D021) .....	101
Identification of Polymers (MSTips No. D020) .....	103
Rapid Analysis of Glues, Cements, and Resins (MSTips No. D018) .....	105
Direct Analysis of Adhesives (MSTips No. D015) .....	107
<b>Biological Species Identification and Classification .....</b>	<b>111</b>
A High Throughput Ambient Mass Spectrometric Approach to Species Identification and Classification from Chemical Fingerprint Signatures (Musah, R. A. <i>et al.</i> , <i>Sci. Rep.</i> 5, 11520; doi: 10.1038/srep11520 (2015)) .....	111

- For any question or inquiry regarding this Applications Notebook, please contact your local JEOL representative, or use the Product Information Request form on our Global Web Site:  
[https://www.jeol.co.jp/en/support/support\\_system/contact\\_products.html](https://www.jeol.co.jp/en/support/support_system/contact_products.html)
  - The contact information on each applications note is that at the time of the initial publication and might not be current.
  - The contact information and affiliations of the authors on the JEOL News articles are those at the time of the initial publication and might not be current.
  - The URLs referred in each applications note or article are those at the time of initial publication and some of them might not be valid any longer.



# Direct Analysis in Real Time (DART<sup>™</sup>) Mass Spectrometry

Robert B. Cody<sup>†</sup>, James A. Laramée<sup>††</sup>,  
J. Michael Nilles<sup>†††</sup>, and H. Dupont Durst<sup>††††</sup>

<sup>†</sup>JEOL USA, Inc.

<sup>††</sup>EAI Corporation

<sup>†††</sup>Geo-Centers Inc.

<sup>††††</sup>Edgewood Chemical Biological Center

## Introduction

Mass Spectrometry (MS) is one of the fastest-growing areas in analytical instrumentation. The use of mass spectrometry in support of synthetic, organic, and pharmaceutical chemistry is well established. Mass spectrometry is also used in materials science, environmental research, and forensic chemistry. It has also evolved into one of the core methods used in biotechnology. However, currently available ion sources place extreme restrictions on the speed and convenience of sample analysis by mass spectrometry. Here we report a method for using mass spectrometry to instantaneously analyze gases, liquids, and solids in open air at ground potential under ambient conditions.

Traditional ion sources used in mass spectrometry require the introduction of samples into a high vacuum system. Traditional ion sources operated in vacuum include electron ionization (EI)[1], chemical ionization (CI)[2], fast atom bombardment (FAB)[3], and field desorption/field ionization (FD/FI)[4]. These techniques have been used successfully for decades. However, the requirement that samples be introduced into a high vacuum for analysis is a severe limitation. Gas or liquid samples must be introduced through a gas chromatograph or a specially designed inlet system. Solid samples must be introduced by using a direct insertion probe and a vacuum lock system. Direct insertion probes can result in vacuum failure and/or contamination of the

ion source if too much sample is introduced.

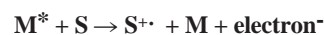
Atmospheric pressure ion sources such as atmospheric pressure chemical ionization (APCI)[5], electrospray ionization (ESI)[6-8], matrix-assisted laser desorption ionization (MALDI)[9-10] and atmospheric pressure photoionization (APPI)[11] have broadened the range of compounds that can be analyzed by mass spectrometry. However, these ion sources require that samples be exposed to elevated temperatures and electrical potentials, ultraviolet irradiation, laser radiation, or a high-velocity gas stream. Safety considerations require that the ion source be fully enclosed to protect the operator from harm.

The new ion source reported herein overcomes these limitations. The new technique, referred to as Direct Analysis in Real Time (DART<sup>™</sup>), has been coupled to the AccuTOF-LC<sup>™</sup> atmospheric pressure ionization mass spectrometer to permit high-resolution, exact mass measurements of gases, liquids, and solids[12,13]. DART successfully sampled hundreds of chemicals, including chemical agents and their signatures, pharmaceuticals, metabolites, pesticides and environmentally significant compounds, peptides and oligosaccharides, synthetic organics, organometallics, drugs of abuse, explosives, and toxic industrial chemicals. These chemicals were detected on a variety of surfaces such as concrete, human skin, currency, airline boarding passes, fruits and vegetables, body fluids, cocktail glasses, and clothing. The composition of drug capsules and tablets was directly analyzed.

sources used in hand-held detectors for chemical weapons agents (CWAs), drugs, and explosives. The discovery that DART could be used for positive-ion and negative-ion non-contact detection of materials on surfaces, as well as for detection of gases and liquids, led to the development of a commercial product.

DART is based on the atmospheric pressure interactions of long-lived electronic excited-state atoms or vibronic excited-state molecules with the sample and atmospheric gases. The DART ion source is shown in **Figure 1**. A gas (typically helium or nitrogen) flows through a chamber where an electrical discharge produces ions, electrons, and excited-state (metastable) atoms and molecules. Most of the charged particles are removed as the gas passes through perforated lenses or grids and only the neutral gas molecules, including metastable species, remain. A perforated lens or grid at the exit of the DART provides several functions: it prevents ion-ion and ion-electron recombination, it acts as a source of electrons by surface Penning ionization, and it acts as an electrode to promote ion drift toward the orifice of the mass spectrometer's atmospheric pressure interface.

Several ionization mechanisms are possible, depending on the polarity and reaction gas, the proton affinity and ionization potential of the analyte, and the presence of additives or dopants. The simplest process is Penning ionization [14] involving transfer of energy from the excited gas  $M^*$  to an analyte  $S$  having an ionization potential lower than the energy of  $M^*$ . This produces a radical molecular cation  $S^{+\bullet}$  and an electron ( $e^-$ ).



Penning ionization is a dominant reaction mechanism when nitrogen or neon is used in the DART source. Nitrogen or neon ions are effectively removed by the electrostatic lenses and are never observed in the DART back-

## Background and Principle of Operation

DART grew out of discussions at JEOL USA, Inc. between two of the authors (Laramée and Cody) about the possibility of developing an atmospheric pressure thermal electron source to replace the radioactive

<sup>†</sup>11 Dearborn Road, Peabody, Massachusetts, USA.

<sup>††</sup>1308 Continental Drive, Suite J, Abingdon, MD 21009

<sup>†††</sup>Box 68 Gunpowder Branch, APG, MD 21010

<sup>††††</sup>Aberdeen Proving Grounds, Maryland USA

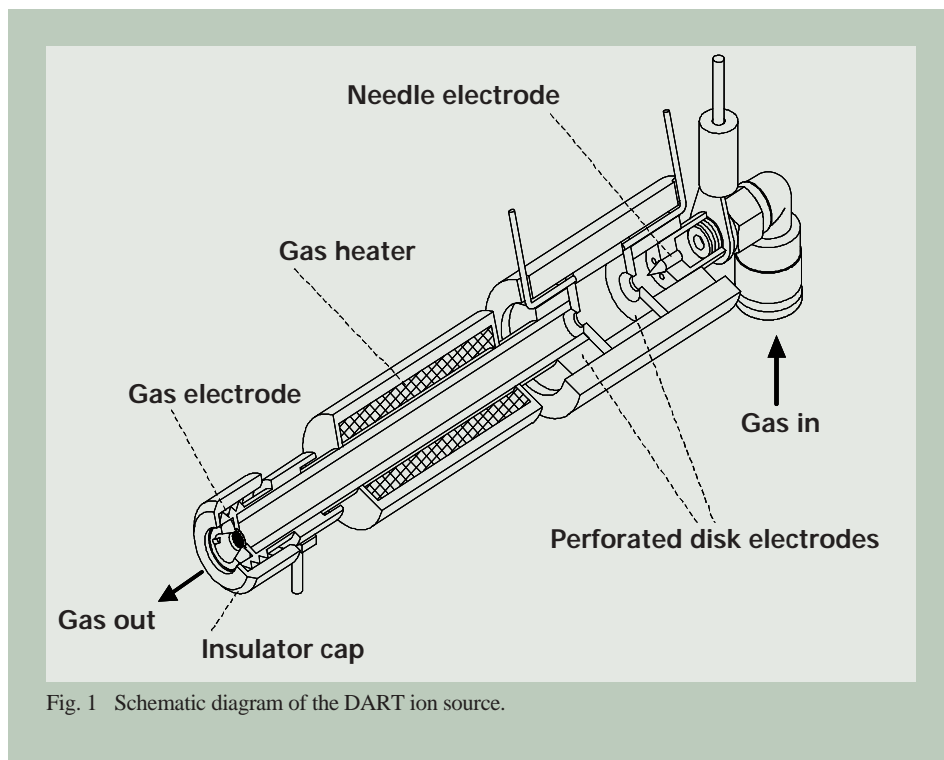
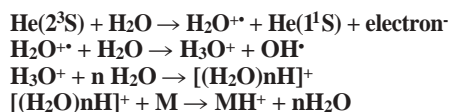


Fig. 1 Schematic diagram of the DART ion source.

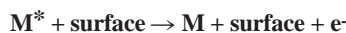
ground mass spectrum.

When helium is used, the dominant positive-ion formation mechanism involves the formation of ionized water clusters followed by proton transfer reactions:



The helium  $2^3\text{S}$  state has an energy of 19.8 eV. Its reaction with water is extremely efficient [15] with the reaction cross section estimated at  $100 \text{ \AA}^2$ . Because of this extraordinarily high cross section, DART performance is not affected by humidity.

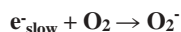
Negative-ion formation occurs by a different mechanism. Electrons ( $e^-$ ) are produced by Penning ionization or by surface Penning ionization:



These electrons are rapidly thermalized by collisions with atmospheric pressure gas



Thermal electrons undergo electron capture by atmospheric oxygen



to produce  $\text{O}_2^-$ , which reacts with the analyte to produce anions. The DART negative-ion reagent mass spectra are virtually identical for nitrogen, neon, and helium. However, negative-ion sensitivity increases for DART gases in the following order:



This is due to the increased efficiency in forming electrons by Penning ionization and

surface Penning ionization as the internal energy of the metastable species increases.

The polarity of the DART ion source is switched between positive-ion mode and negative-ion mode by changing the polarity of the disk electrode and grid. The polarity of the discharge needle is not changed, so the plasma is not interrupted. This permits rapid switching between positive and negative modes.

Other reactions are possible. The presence of traces of dopants such as ammonium (e.g. from ammonium hydroxide headspace vapor) or chloride (e.g. from methylene chloride vapor) can modify the chemistry allowing the chemist to tailor the experiment for specific analyses.

DART produces relatively simple mass spectra characterized by  $\text{M}^+$ ; and/or  $[\text{M}+\text{H}]^+$  in positive-ion mode, and  $\text{M}^-$  or  $[\text{M}-\text{H}]^-$  in negative-ion mode. Fragment ions are observed for some compounds. The degree of fragmentation can be influenced by the choice of gas, the temperature, and the AccuTOF orifice 1 potential. Alkali metal cation attachment and double-charge ions are not observed.

The mechanism involved in desorption of materials from surfaces by DART is less well characterized. Thermal desorption plays a role if the gas stream is heated. However, the analysis by DART of inorganic materials such as sodium perchlorate or organic salts having little or no vapor pressure is evidence of other processes. It is postulated that the transfer energy to the surface by metastable atoms and molecules facilitates desorption and ionization.

In contrast with other ion sources that use metastable species [16-23], the DART ion source does not operate under reduced pressure, apply a high electrical potential to the analyte, or expose the analyte directly to the discharge plasma. Argon, used in many of these ion sources, is not well suited for use with DART because argon metastables are rapidly quenched in the presence of water vapor [20] by a reaction involving homolytic

cleavage of the water bond without concomitant ion formation. None of these ion sources are designed for direct analysis of gases, liquids, and solids in open air under ambient conditions.

## Experimental

A DART<sup>tm</sup> source [24] was installed on a JEOL AccuTOF LC<sup>tm</sup> time-of-flight mass spectrometer. The DART source replaces the standard electrospray ionization (ESI) source supplied with the AccuTOF. No vacuum vent is required. The ion sources can be exchanged and made operational within minutes.

The mass spectrometer operates at a constant resolving power of approximately 6000 (FWHM definition). Typical atmospheric pressure interface conditions are: orifice 1 = 30V, and both orifice 2 and ring lens are set to 5V. The AccuTOF ion guide voltage is varied as needed depending on the lowest  $m/z$  to be measured. Orifice 1 temperature is typically kept warm (80 degrees C) to prevent contamination. Although there is some electrical potential on the exposed orifice 1, the voltage and current are so low that there is absolutely no danger to the operator, even with prolonged direct contact.

The DART source is operated with typical gas flows between 1.5 and 3 liters per minute. Gas temperature is programmable from ambient temperature up to approximately 350 degrees C (gas heater temperature from OFF to a maximum of 550 degrees C). Typical potentials are: discharge needle 2 kV to 4 kV, electrode 1: 100V, grid: 250 V. Gas, liquid, or solid samples positioned in the gap between the DART source and mass spectrometer orifice 1 are ionized.

Because the mass spectrometer orifice is continually bathed in hot inert gas, the DART source is remarkably resistant to contamination and sample carryover. Mass scale calibration is easily accomplished by placing neat poly-

ethylene glycol average molecular weight 600 (PEG 600) on a glass rod or a piece of absorbent paper in front of the DART source. In positive-ion mode, this produces a series of  $[M+H]^+$  and  $[M+H-H_2O]^+$  peaks from  $m/z$  45 up to beyond  $m/z$  1000. By including background peaks, the calibrated mass range can be extended down to  $m/z$  18 or 19. Negative-ion spectra of PEG are characterized by  $[M+O_2-H]^-$  and  $[(C_2H_4O)_n+O_2-H]^-$  ion series.

The reference spectrum can be acquired within seconds. There is no memory effect or carryover of the reference compound -- the PEG peaks do not persist after the reference standard is removed. For these reasons, a full reference mass spectrum can be quickly and easily included in each data file, and accurate mass measurements are routinely acquired for all samples.

## Applications

The DART ion source has been used to analyze an extremely wide range of analytes, including drugs (prescription, over-the-counter, veterinary, illicit, and counterfeit) in dose form or in body fluids or tissues, explosives and arson accelerants, chemical weapons agents and their signatures, synthetic organic or organometallics compounds, environmentally important compounds, inks and dyes, foods, spices and beverages. An important benefit of DART is that materials can be analyzed directly on surfaces such as glass, TLC plates, concrete, paper, or currency without requiring wipes or solvent extraction.

Drugs can be detected in pill form by placing the pill in front of the DART source for a few minutes. An example is shown below (Figure 2) for the rapid detection of illicit drugs in pills confiscated by a law-enforcement agency. The intact pills were simply placed in front of the DART source and analyte ions were observed within seconds. Exact mass and isotopic measurements confirmed the elemental compositions of the labeled components. All labeled assignments in the following examples were confirmed by exact mass measurements.

Drug counterfeiting is becoming a serious and widespread public health problem. Counterfeit drugs are not only illegal, but dangerous; they may contain little or no actual drug content, or they may contain completely different drugs with potentially toxic consequences.

DART can be used to rapidly screen for counterfeit drugs. An example is shown below in Figure 3 where DART was used to analyze a sample of a real drug containing the anti-malarial dihydroartemisinin, and a counterfeit drug containing no active ingredients.

DART has been applied to the direct detection of drugs and metabolites in raw, unprocessed body fluids, including blood, urine, perspiration, and saliva. An example is shown below in Figure 4 for the negative-ion analysis of the urine of a subject taking prescription ranitidine. No extraction or other processing was used: a glass rod was dipped in raw urine and placed in front of the DART source.

For easy viewing, only abundant components are labeled in this figure. A more complete list of assignments is given in Table 1. Assignments are made for compounds com-

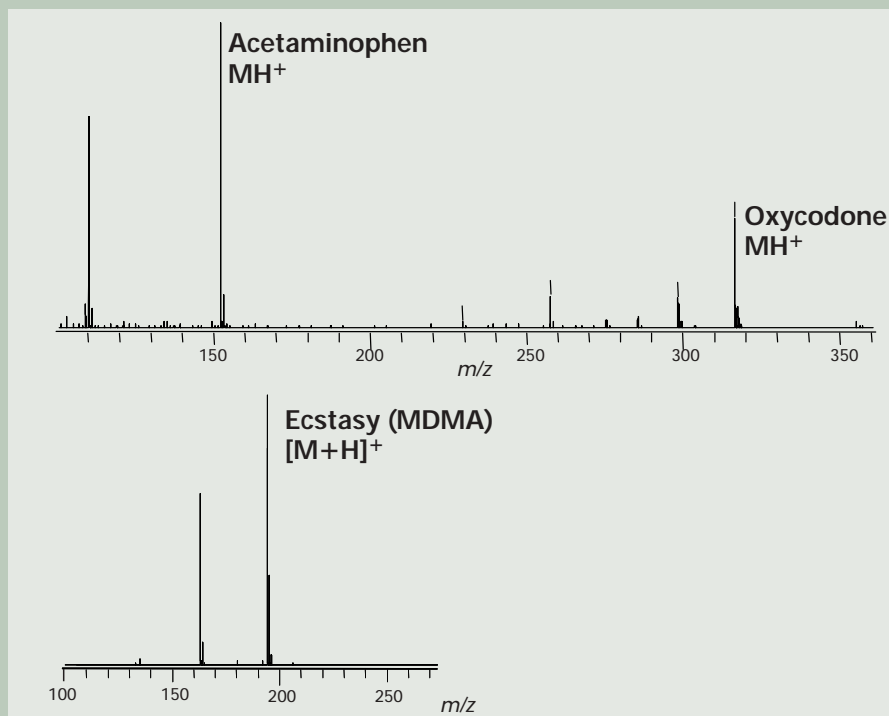


Fig. 2 DART mass spectra of two pills: An analgesic containing acetaminophen plus oxycodone (top) and methylenedioxyamphetamine ("ecstasy", bottom).

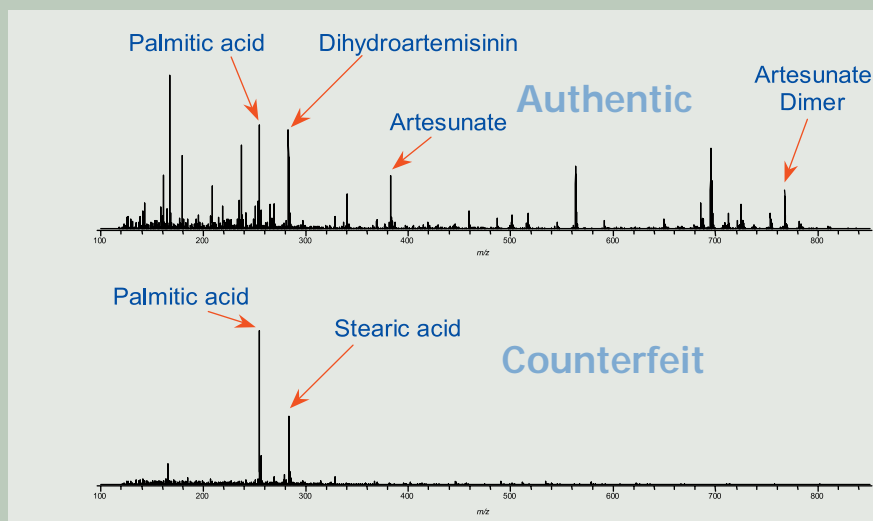


Fig. 3 Rapid detection of counterfeit drug. The top mass spectrum shows the authentic drug and the bottom mass spectrum shows the counterfeit drug.

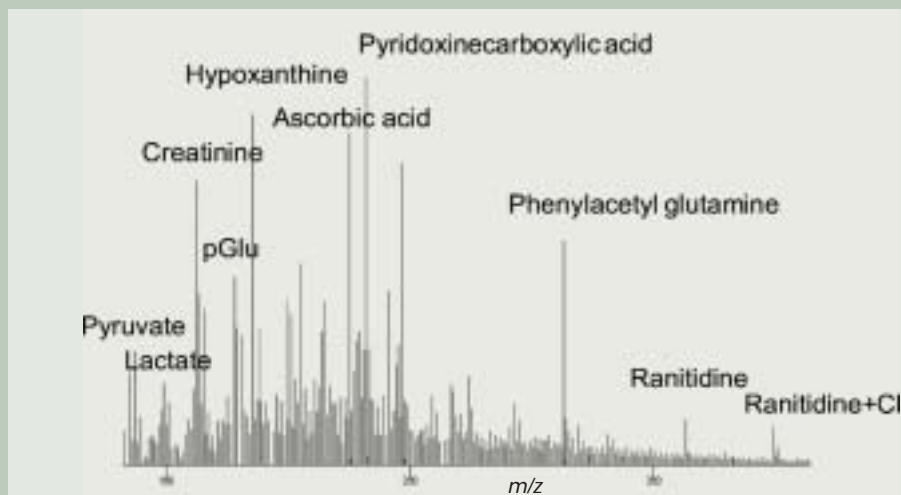


Fig. 4 Negative-ion DART analysis of the urine of a subject taking prescription ranitidine.



Table 1 Assignments for Compounds Detected in Negative-Ion DART Mass Spectrum of Raw Urine.

Name	Meas.	Calc.	Diff(u)	Abund.
GBL	85.0295	85.0290	0.0006	11.0317
Pyruvic_acid	87.0084	87.0082	0.0002	7.1700
Lactic_acid	89.0236	89.0239	-0.0002	8.3658
Cresol	107.0492	107.0497	-0.0004	.9294
Uracil	111.0153	111.0195	-0.0041	14.3328
Creatinine	112.0513	112.0511	0.0002	81.6851
Purine	119.0354	119.0358	-0.0004	31.9510
Niacin	122.0277	122.0242	0.0035	3.1489
Dihydro_methyluracil	127.0486	127.0508	-0.0021	23.3773
pGlu	128.0353	128.0348	0.0006	59.2337
Methylmaleic_acid	129.0212	129.0188	0.0024	37.1191
Me_succinate/diMe_malonate	131.0368	131.0358	0.0010	19.3593
Deoxyribose	133.0489	133.0501	-0.0012	28.3521
Hypoxanthine	135.0306	135.0307	-0.0001	100.0000
Adipic_acid	145.0469	145.0501	-0.0032	11.7389
Methyl_hypoxanthine	149.0454	149.0463	-0.0009	37.5243
Hydroxymethyl_methyl_uracil	155.0453	155.0457	-0.0003	55.5832
a-aminoadipic_acid	160.0568	160.0610	-0.0042	9.5885
Methionine_sulfoxide	164.0419	164.0381	0.0037	11.7609
Methylxanthine	165.0408	165.0412	-0.0004	32.4341
Formiminoglutamic_acid	173.0536	173.0562	-0.0027	12.3531
Ascorbic_acid	175.0285	175.0243	0.0042	23.1998
Hippuric_acid	178.0513	178.0504	0.0009	66.4487
Glucose	179.0552	179.0556	-0.0004	39.7499
Dimethylxanthine	179.0552	179.0569	-0.0017	39.7499
Pyridoxinecarboxylic_acid	182.0479	182.0453	0.0026	34.7913
Hydroxyindoleacetic_acid	190.0542	190.0504	0.0037	5.4133
Dimethyluric_acid	195.0527	195.0518	0.0009	23.7577
AAMU (caffeine metabolite)	197.0667	197.0675	-0.0007	79.6617
Cinnamalidinemalonic_acid	217.0483	217.0501	-0.0017	60.5399
AFMU (caffeine metabolite)	225.0643	225.0624	0.0019	21.9092
Cytidine	242.0801	242.0777	0.0024	3.4545
Uridine	243.0641	243.0617	0.0024	21.1156
Phenylacetyl_glutamine	263.1033	263.1032	0.0001	48.9665
Adenosine	266.0861	266.0889	-0.0028	1.4869
Ranitidine	313.1321	313.1334	-0.0013	8.7459
Ranitidine+Cl	349.1113	349.1101	0.0011	11.7296

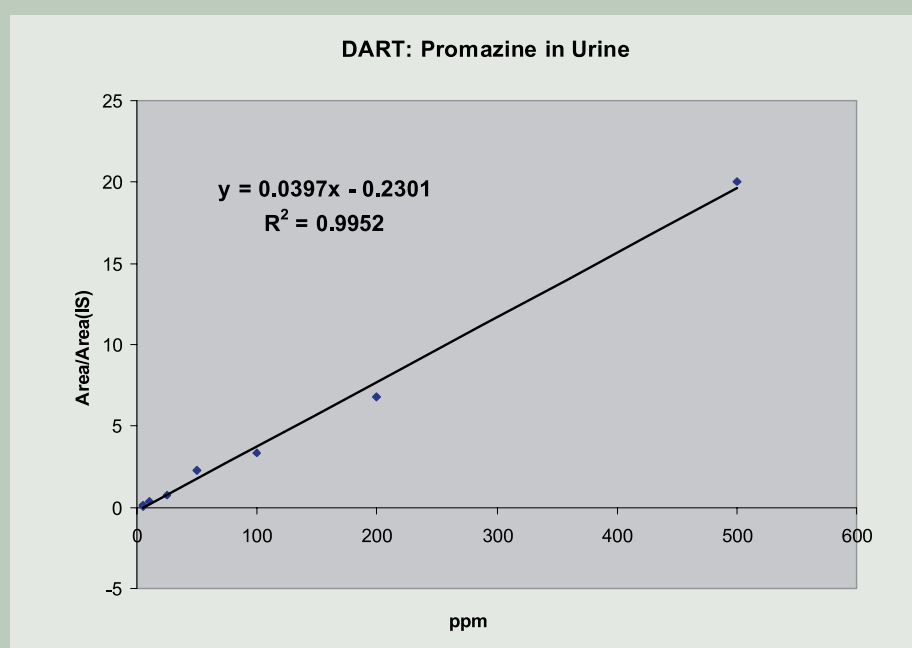


Fig. 5 Rapid quantitative analysis by DART of promazine in urine. Chlorpromazine was added as an internal standard.

monly encountered in urine that have elemental compositions that match the measured  $m/z$  values. It is interesting to note that the basic drug, ranitidine, is observed as an  $[M-H]^-$  species in the negative-ion mass spectrum as well as an abundant  $[M+H]^+$  species in the positive-ion mass spectrum. Ranitidine metabolites are also observed [11] in the positive-ion mass spectrum (not shown).

DART can be used for quantitative analysis. The absolute abundance of ions produced by DART depends on the positioning of the target in the gas stream. However, the use of an internal standard permits rapid quantitative analysis of drugs in urine, plasma, or other body fluids. Figure 5 shows a working curve obtained for urine samples spiked with promazine at the 1 to 500 ppm level. Chlorpromazine (50 ppm) was added as an internal standard. Undiluted urine samples were applied to a glass rod. Each analysis was complete within seconds of placing the rod in front of the DART source. This approach has also been used to screen for the “date rape” drug gamma hydroxy butyrate (GHB) in urine [24] and for the rapid quantitative analysis of developmental drugs in plasma.

The detection of explosives is important for forensics and security. DART has been applied to the detection of nitro explosives such as nitroglycerine, TNT, and HMX, inorganic explosives such as ammonium nitrate, perchlorate and azide, and peroxide explosives such as TATP and HMTD. Examples are shown in Figures 6 and 7.

The high dynamic range of the DART-AccuTOF combination can permit the identification of trace-level impurities for quality control and similar applications. An example is shown in Figure 8 and Table 2 for the exact-mass analysis of 1% propazine and 0.2% simazine in a sample of the herbicide atrazine.

## Conclusion

A new ion source has been developed that permits the analysis of gases, liquids, and solids in open air under ambient conditions. No solvents or high-pressure gases are used. The sample is not directly exposed to high voltages, laser beams or radiation or plasma. The combination of this source with a high-resolution time-of-flight mass spectrometer permits rapid qualitative and quantitative analysis of a wide variety of materials.

## Acknowledgment

Technical assistance and keen scientific insight were unselfishly provided by (in alphabetical order) Daniel Banquer, Ted Boileau, William Creasy, Daniel Evans, Drew McCrady, Michael McKie, Michael Nilles, Edward Owen, Gary Samuelson, Philip Smith, John Stuff, and Dean Tipple. The authors would like to thank Prof. Facundo Fernandez of Georgia Tech University for the dihydroartemisinin and counterfeit drug sample.

## Additional Information

Additional applications and digital videos showing DART analysis are available on the internet at <http://www.jeolusa.com/ms/msprod->

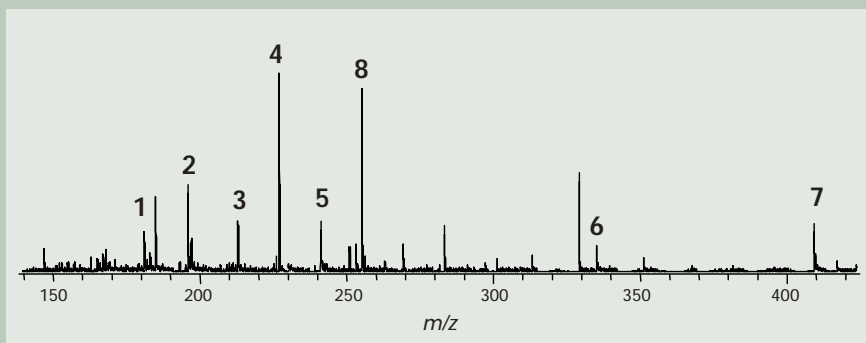


Fig. 6 3 ppm explosives spiked into muddy water. 1=DNT, 2=amino-DNT, 3=trinitrobenzene, 4=TNT, 5=RDY+TFA, 6=Tetryl, 7=HMX+TFA, 8=palmitate in the water background (used as lock mass). Headspace vapor from a 0.1% aqueous solution of trifluoroacetic acid was used to produce TFA adducts.

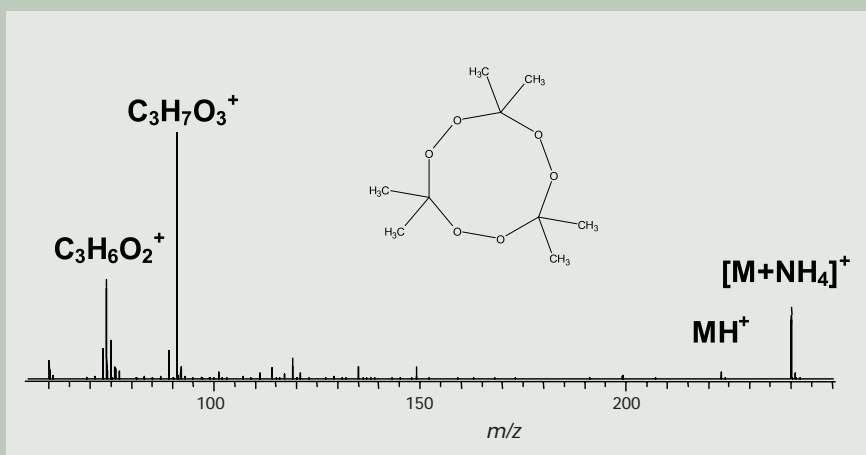


Fig. 7 Positive-ion DART mass spectrum of triacetone triperoxide (TATP). Ammonium hydroxide headspace vapor provided a source of  $\text{NH}_4^+$ .

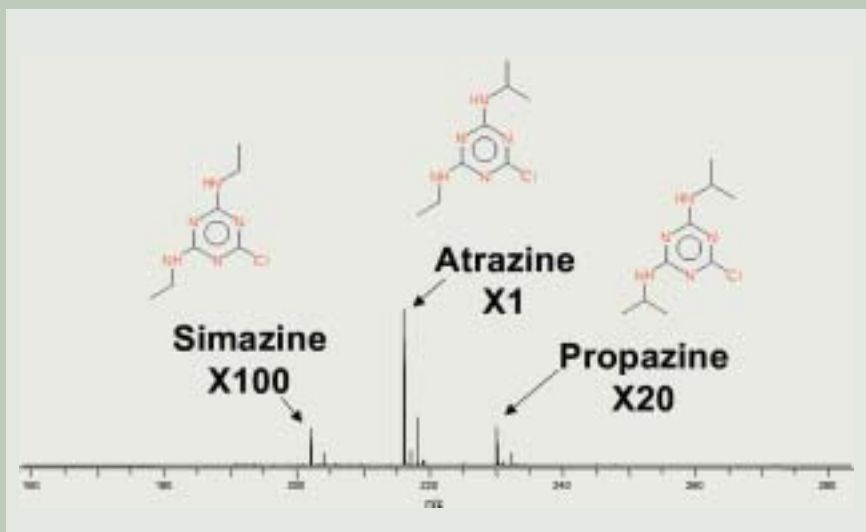


Fig. 8 Exact-mass analysis of trace simazine and propazine in a sample of the herbicide atrazine.

Table 2 DART measured masses for  $[\text{M}+\text{H}]^+$  from atrazine and trace impurities.

Compound	Composition	Measured	Calculated	Diff. (mmu)
Atrazine	$\text{C}_8\text{H}_{15}\text{N}_5\text{Cl}$	216.10159	216.10160	-0.01
Propazine	$\text{C}_9\text{H}_{17}\text{N}_5\text{C}$	230.11760	230.11725	+0.35
Simazine	$\text{C}_7\text{H}_{13}\text{N}_5\text{Cl}$	202.08440	202.08595	+1.60

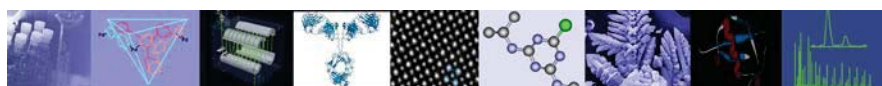
saccutof\_dart.html. Chemical agent data is available from the authors upon request.

## References

- [1] Dempster, A. J. *Phys. Rev.*, **11**, 316-324, (1918).
- [2] Munson, M. S. B.; Franklin, F. H. *J. Am. Chem. Soc.*, **88**, 2621, (1966).
- [3] Barber, M.; Bordoli, R. S.; Elliott, G. J.; Sedgwick, R. D.; Tyler, A. N. *J. Chem. Soc. Chem. Commun.*, **325**, (1981).
- [4] Beckey H. D. *Research/Development*, **20**(11), 26-29, (1969).
- [5] Horning, E. C.; Horning, M. E.; Carroll, D. I.; Dzidic, I.; Stilwell, R. N.; *Anal. Chem.*, **45**, 936-943, (1973).
- [6] Dole, M. Mack, L. L. Hines, R. L.; Mobley, R. C.; Ferguson, L. D. Alice, M. A. *J. Chem. Phys.*, **49**, 2240, (1968).
- [7] Aleksandrov, M. L.; Gall, L. N. Krasnov, N. V. Nikolaev, V. I. Pavlenko, V. A.; Shkurov, V. A. *Dokl. Akad. Nauk. SSSR*, **277**, 379-383, (1984).
- [8] Fenn, J. B.; Mann, M.; Meng, C. K.; Wong, S. F. *Science*, **246**, 64-71, (1989).
- [9] Tanaka, K.; Waki, H.; Ido, Y.; Akita, S.; Yoshida, Y. *Rapid. Commun. Mass Spectrom.*, **2**, 151-153, (1988).
- [10] Karas, M.; Hillenkamp, F. *Anal. Chem.*, **60**, 2299-2301, (1988).
- [11] Robb, D. B.; Covey, T. R.; Bruins, A. P. *Anal. Chem.*, **72**, 3653-3659, (2000).
- [12] Cody, R. B.; Laramee, J. A.; Durst, H. D. *Anal. Chem.*, **77**(8), 2297 - 2302, (2005).
- [13] Patents pending.
- [14] Penning, F. M. *Naturwissenschaften*, **15**, 818, (1927).
- [15] Mastwijk, H. C. Cold Collisions of Metastable Helium Atoms, Ph.D. Thesis, University of Utrecht, Netherlands, (1997).
- [16] Faubert, D.; Paul, G.J.C., Giroux, J.; Bertrand, M. J. *Int. J. Mass Spectrom. Ion Proc.*, **124**, 69, (1993).
- [17] Faubert, D.; L'Heureux, A.; Peraldi, O.; Mousselm, M.; Sanchez, G.; Bertrand, M. J.; "Metastable Atom Bombardment (MAB) Ionization Source: Design, Optimization and Analytical Performances" in *Adv. Mass Spectrom.: 15th International Mass Spectrometry Conference*, Wiley: Chichester, UK, 431-432, (2001).
- [18] [http://www.jeol.com/ms/docs/map\\_note.pdf](http://www.jeol.com/ms/docs/map_note.pdf).
- [19] Tsuchiya, M. Kuwabara, H.; *Anal. Chem.*, **56**, 14, (1984).
- [20] Tsuchiya, M. *Mass Spectrom. Rev.*, **17**, 51, (1998).
- [21] Tsuchiya, M. *Analytical Sciences*, **14**, 661-676, (1998).
- [22] Hiraoka, K.; Fujimaki, S.; Kambara, S.; Furuya, H.; Okazaki, S. *Rapid Commun. Mass Spectrom.*, **18**, 2323-2330, (2004).
- [23] McLuckey, S. A.; Glish, G. L.; Asano, K. G.; Grant, B. C., *Anal. Chem.*, **60**, 2220, (1988).
- [24] Guzowski, J. P., Jr.; Broekaert, J. A. C.; Ray, S. J.; Hieftje, G. M. J. *Anal. At. Spectrom.*, **14**, 1121-1127, (1999).
- [25] IonSense, Inc., 11 Dearborn Road, Peabody, MA USA 01960.
- [26] Jagerdeo, E.; Cody, R. B. unpublished results.







## The AccuTOF® Atmospheric Pressure Interface: an Ideal Configuration for DART® and Ambient Ionization

### Introduction

The DART ion source was developed on the JEOL AccuTOF time-of-flight mass spectrometer which allows the exit of the DART source to be positioned within millimeters of the sampling orifice (orifice 1) of the mass spectrometer atmospheric pressure interface (API). The AccuTOF vacuum system is robust, highly resistant to contamination, and capable of pumping helium DART gas without assistance.

### The AccuTOF API

Figure 1 shows a schematic diagram of the AccuTOF atmospheric pressure interface. The API consists of two off-axis skimmers (designated "orifice 1" and "orifice 2") with an intermediate ring lens, followed by a bent RF ion guide. The off-axis skimmer design traps contamination -- ions are electrostatically guided upward toward orifice 2 whereas neutral molecules are pumped downward. Any contamination that enters the API is either pumped away into the rough pump (RP) or trapped on the lower part of orifice 2. The bent RF ion guide provides an additional level of protection. This makes the AccuTOF an ideal mass spectrometer for DART analysis of dirty "real-world" samples such as mud, biological fluids, melted chocolate, polymers, and even crude oil. In addition, orifice 1 is easily accessible and is operated at low voltage and current, making it a convenient platform for ambient ionization sources.

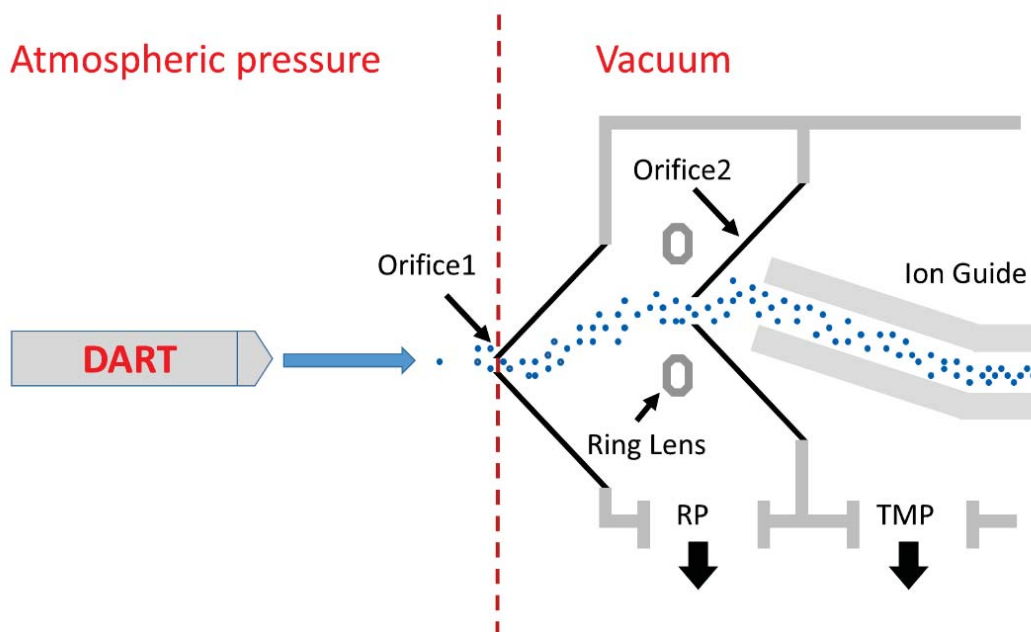


Figure 1. Schematic diagram of the AccuTOF atmospheric pressure interface (API)

AccuTOF® is a registered trademark of JEOL Ltd. (Akishima Japan)

DART® is a registered trademark of JEOL USA, Inc. (Peabody, MA USA)



Figure 2 shows the DART source mounted on the AccuTOF with the exit of the ceramic insulator positioned approximately 1 cm from the apex of orifice 1. This is the optimal positioning of the DART source for normal operation.

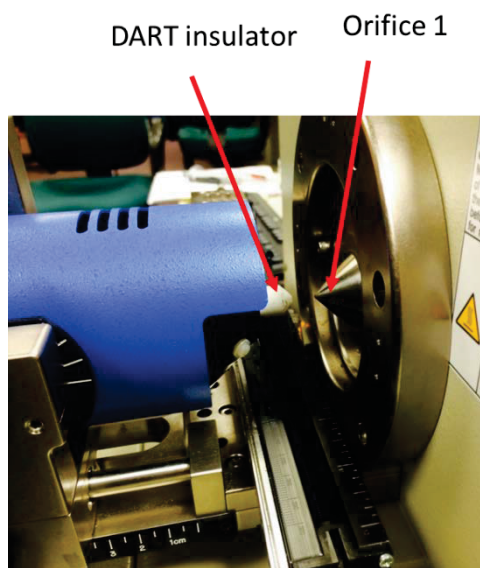


Figure 2. The white DART ceramic insulator cap is positioned approximately 1 cm from the apex of orifice 1 (the silver cone on the right).

## The Vapur® Interface

### Description

The vacuum systems of other mass spectrometer systems are not capable of handling the additional pumping burden and may shut down if the DART is operated with helium. The Vapur® interface allows the DART source to be used with non-JEOL mass spectrometers. It consists of a ceramic tube mounted on a custom flange and an auxiliary pumping stage (Figure 3 and Figure 4) that is used as an interface for mounting the DART on ALL non-JEOL mass spectrometers and for mounting certain DART accessories that require additional clearance.

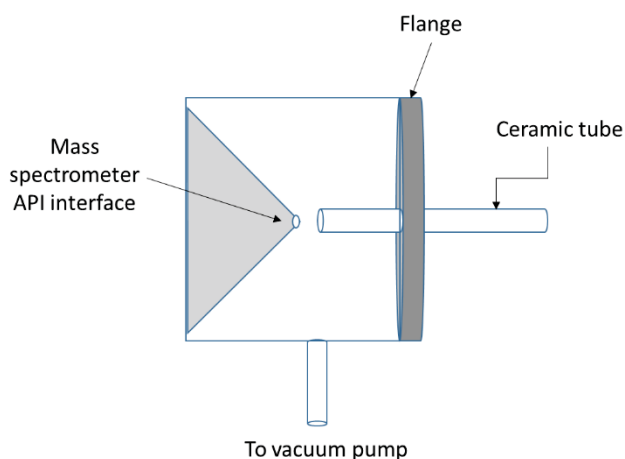


Figure 3. Schematic diagram of Vapur interface. On the AccuTOF, the gap between orifice 1 and the exit of the Vapur ceramic tube should be 2 mm for optimal performance.

Vapur® is a registered trademark of IonSense LLC (Saugus, MA USA)

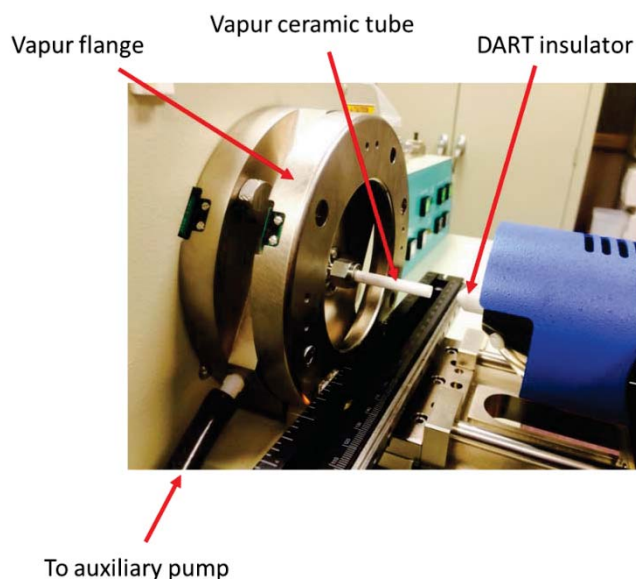
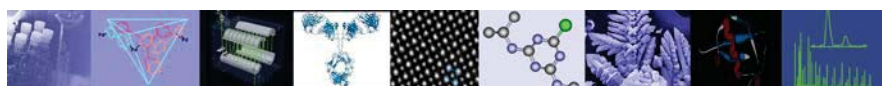


Figure 4. The Vapur interface mounted on the AccuTOF DART.

#### Loss of signal

The large diameter of the Vapur interface's ceramic tube improves reproducibility for some analyses by reducing gas turbulence and it provides space for mounting some accessories such as the IonSense 3+D Scanner. However, increasing the gas flow path increases the likelihood of ion-molecule reactions occurring, which can cause a loss of signal for samples that do not have a high proton affinity. Figure 5a shows the normal DART positive-ion low-mass background without the Vapur installed. The dominant reagent ions are protonated water and proton-bound water dimer. Figure 5b shows the background measured with the Vapur installed. Protonated water is barely visible, even at a magnification of 25X. The other peaks are trace impurities in the gas lines and in the background that have a higher proton affinity than water.

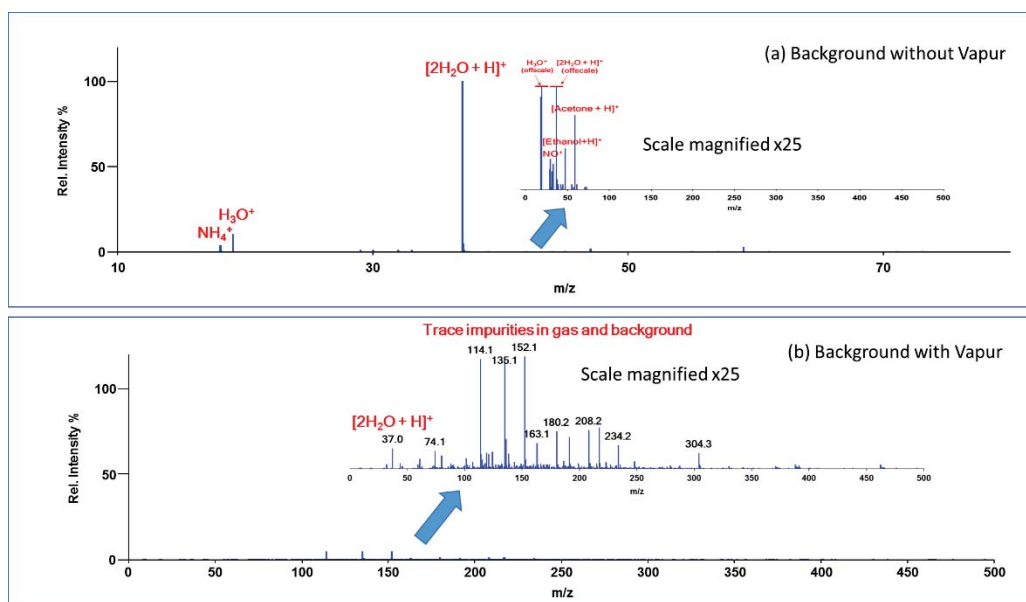


Figure 5. (a) positive-ion low-mass DART background without the Vapur installed, showing the dominant reagent ions with trace laboratory solvent peaks and (b) the low-mass background observed with the Vapur installed.



Nonpolar compounds are particularly susceptible to signal loss due to ion-molecule reactions at atmospheric pressure. Figure 6 illustrates the signal loss for a roughly equimolar mixture of epitestosterone and quinine with trace levels of methyl stearate as the Vapur is installed. The methyl stearate signal is completely lost, epitestosterone's signal reduced by a factor of 6, and even the relatively polar quinine is attenuated by a factor of 2.

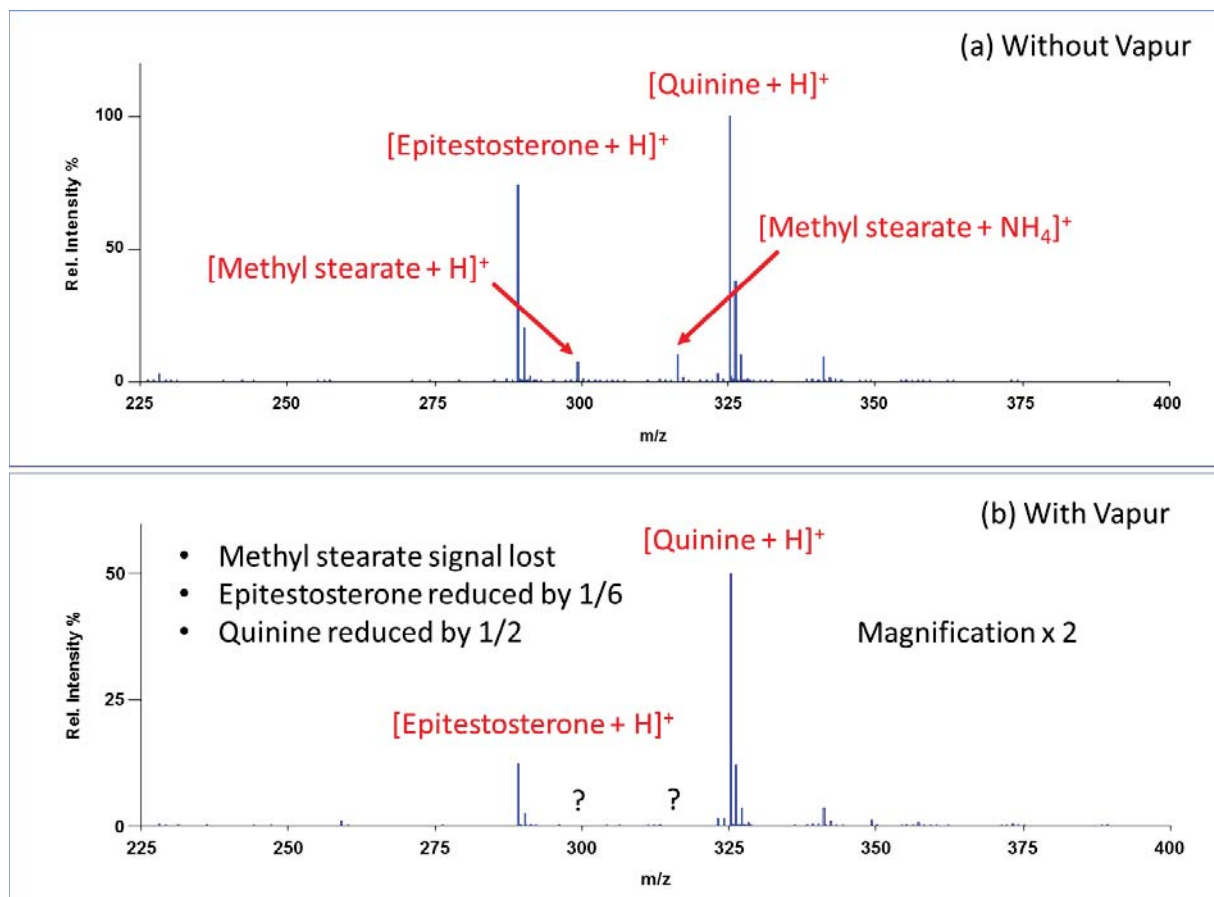


Figure 6. Comparison of signal for quinine, epitestosterone, and methyl stearate (a) without the Vapur interface and (b) with the Vapur interface.

### Differences in ionization chemistry

Samples such as ethers and carbonyls measured with the Vapur interface installed tend to form ammonium adducts preferentially. This results from ion-molecule reactions occurring during sample transport through the Vapur, which favor ammonium over hydronium due to the high proton affinity of trace atmospheric ammonia. Samples without a strongly basic site that normally produce proton adducts by DART without the Vapur may be observed as ammonium adducts if the Vapur is installed. Figure 7 shows the comparison of the DART mass spectra measured for a polyethylene glycol (PEG) sample measured without the Vapur (Figure 7a) and with the Vapur (Figure 7b). Proton and ammonium adducts are observed in both spectra, but the proton adducts dominate in Figure 7a, whereas ammonium adducts dominate in Figure 7b.

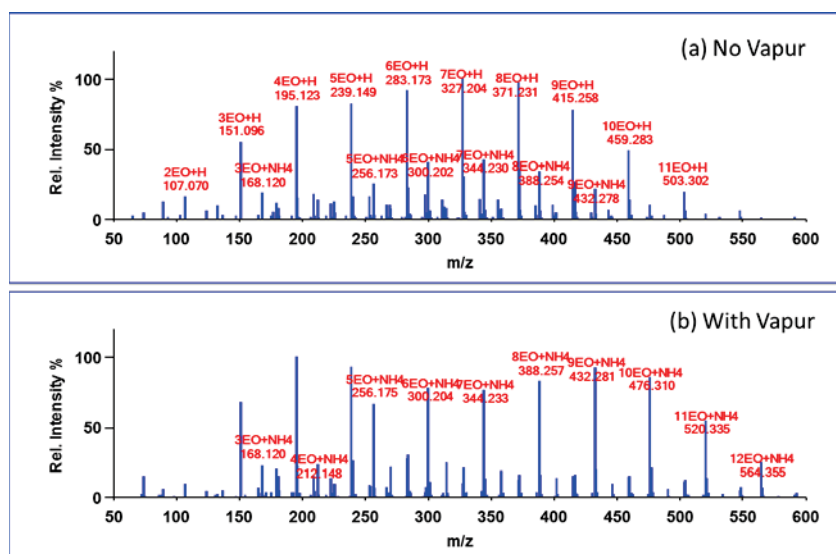


Figure 7. Positive-ion DART mass spectra of a PEG sample measured (a) with no Vapur and (b) with the Vapur installed.

### Sample Carryover

Sample carryover in the Vapur is a problem for some samples. Therefore it is important to limit sample quantity when using the Vapur and to check for cross-contamination between samples. Figure 8 shows an example for the analysis of a sample containing 1% diisobutyl phthalate in isopropanol. Samples were introduced by depositing them onto the sealed end of a melting point tube and positioning the tube in the DART gas stream for several seconds. Three replicate measurements were made for the sample, followed by a mass reference standard (Jeffamine® M-600, Huntsman Corporation). Figure 8a shows the results of the sample measurement without the Vapur installed, and Figure 8b shows the results of the same measurements with the Vapur installed. The red arrows indicate the time at which each sample was introduced into the DART gas stream. Note that the total ion current and reconstructed ion current chronogram (RIC) for diisobutyl phthalate show increasing contamination in Figure 8b as the DIBP is adsorbed onto the ceramic tube. The results obtained without the Vapur do not show any sample carryover and it is easy to determine when each sample was measured.

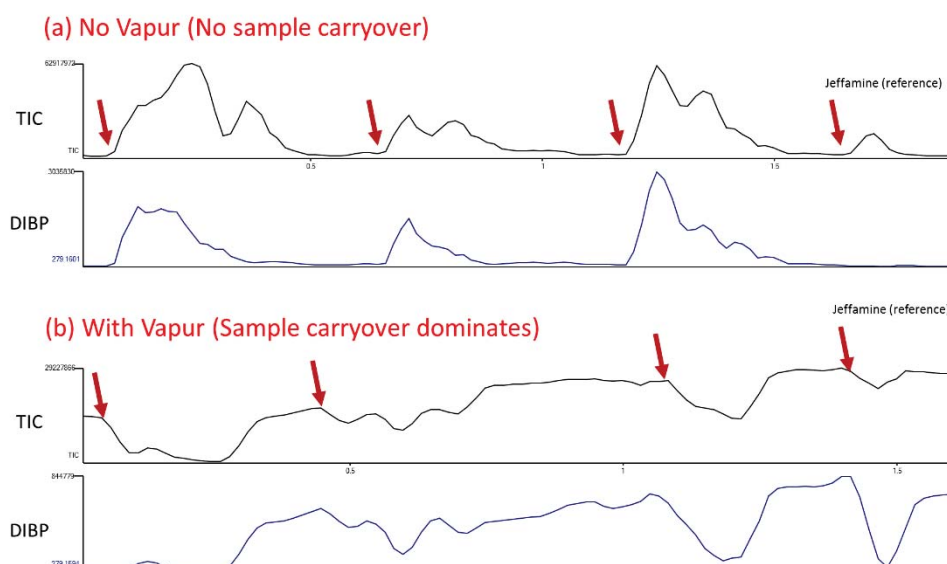


Figure 8. Chronograms for three replicate measurements of a sample containing diisobutyl phthalate (DIBP) (a) with no Vapur and (b) with the Vapur installed.



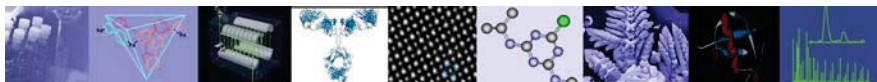
### Vapur Summary

- |   |  |
|---|--|
| <ul style="list-style-type: none"> <li>• Features</li> <li>• Assists weaker vacuum systems to pump helium.</li> <li>• Improves reproducibility by reducing effects of turbulence</li> <li>• Provides a universal DART interface.</li> </ul> | <ul style="list-style-type: none"> <li>• Problems</li> <li>• Required for DART on ALL mass spectrometers <u>EXCEPT THE JEOL AccuTOF.</u></li> <li>• Ion-molecule reactions occur as ions are transported over a longer distance</li> <li>• Loss of non-polar and reactive compounds including the air peaks</li> <li>• Ammonium adducts dominate over <math>MH^+</math></li> <li>• Increased oxidation</li> <li>• Problems with sample carryover if compounds stick to the Vapur ceramic tube.</li> <li>• Requires an extra vacuum pump</li> </ul> |
|---|--|

### Conclusion

The AccuTOF mass spectrometer atmospheric pressure interface is an ideal platform for use with the DART and ambient ionization sources. It permits the use of the DART without additional pumps, interfaces, or hardware that can cause sample carryover, loss of signal, or changes in the DART ionization chemistry.





# Accurate Isotope Data is Essential for Determining Elemental Compositions

## Introduction

Elemental compositions are commonly determined from high-resolution mass spectra and accurate mass measurements. Given a measured mass ( $m/z$ ) and a range of elements that can be present, software calculates the exact mass for each combination of elements and reports all elemental combinations that match the measured mass within a specified error tolerance. Improving the mass accuracy reduces the number of elemental compositions, but mass accuracy alone may not be sufficient to determine the correct elemental composition for an unknown sample.

JEOL AccuTOF™ mass spectrometers (the AccuTOF™-DART®, the AccuTOF™-GCX and the AccuTOF™-GCX Plus) are capable of accurate isotope measurements that can be used to determine elemental compositions from high-resolution mass spectra. Matching the measured abundances and exact masses for isotope peaks can be more effective than mass accuracy alone.

## Experimental

A JEOL AccuTOF™-DART® mass spectrometer was used to acquire positive-ion mass spectra at a resolving power of  $>10,000$  (FWHM). The DART was operated in positive-ion mode with helium gas and a gas heater temperature of  $350^{\circ}\text{C}$ . Chlorpromazine was analyzed by dipping a melting point tube into a dilute solution of chlorpromazine in dichloromethane and dangling the tip of the tube in the DART gas stream. Jeffamine® M-600 (Huntsman) copolymer was measured in the same data file as an external calibrant for exact mass measurements. Mass Mountaineer™ software was used for elemental composition determinations from accurate mass measurements and isotope matching.

## Example

The pesticide chlorpyrifos has the elemental composition  $\text{C}_9\text{H}_{11}\text{Cl}_3\text{NO}_3\text{PS}$ . The major peaks in the positive-ion DART mass spectrum in Figure 1 correspond to the protonated molecule of chlorpyrifos.

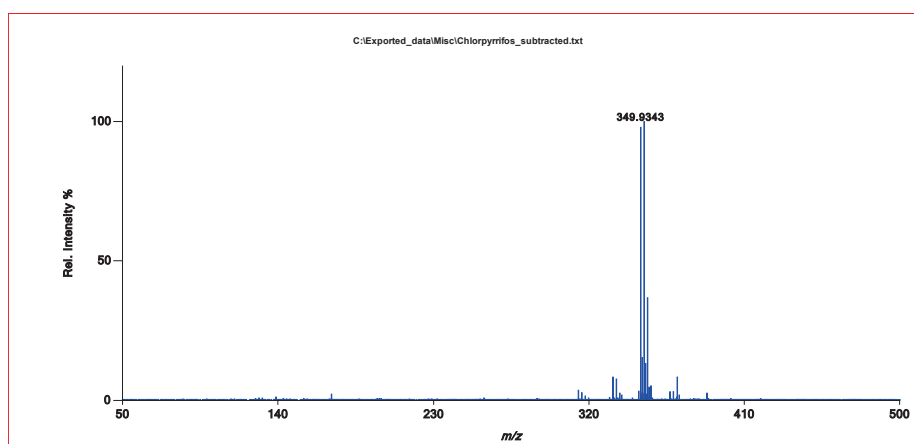
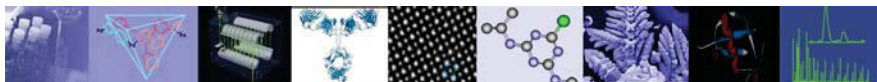
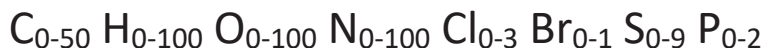


Figure 1. Positive-ion AccuTOF-DART mass spectrum of the pesticide chlorpyrifos



The measured monoisotopic mass is 349.93427, which differs from the calculated exact mass by 0.00016 u, that is, 0.16 millimass units (mmu) or 0.5 parts per million (ppm). The range of elements used for elemental compositions was:



with the maximum limits for the X+2 elements Cl, Br, and S determined automatically by the Mass Mountaineer program. Using the measured monoisotopic mass and an error tolerance of 2 mmu (5.7 ppm), there are 99 possible elemental compositions for even-electron ions (protonated molecules). If we let the software calculate the exact masses and theoretical isotope abundances for each of the 99 possible compositions and match these against the measured isotope masses and abundances, the correct composition is readily determined as the best match (Figure 2 and Table 1). The correct compound (chlorpyrifos) is the only entry found in the 2017 NIST Mass Spectral Database for this composition.

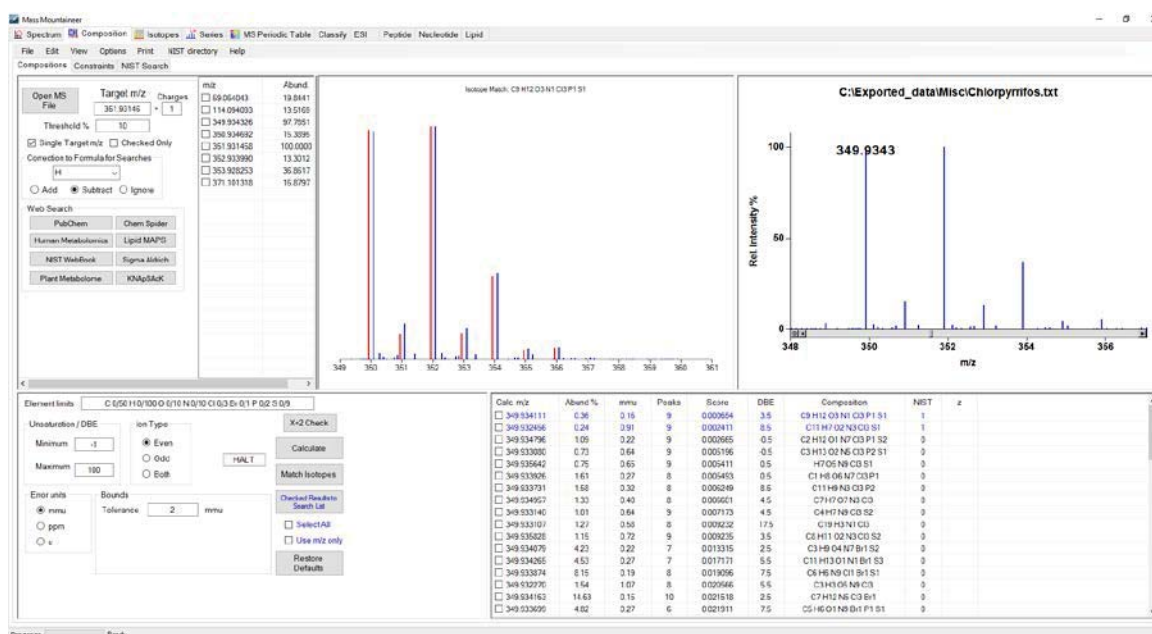


Figure 2. Mass Mountaineer elemental composition determination with isotope matching shows the correct elemental composition for chlorpyrifos.



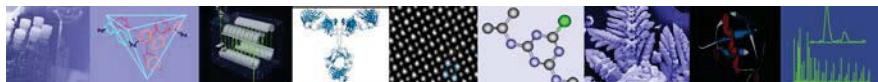


Table 1. The top 10 isotope match results for measured monoisotopic  $m/z$  349.93427 using the data from the mass spectrum shown in Figure 1. The correct composition (in red) has the lowest isotope match score, indicating the best match. One entry (chlorpromazine) is found in the NIST database for this composition minus a proton.

Calc. $m/z$	Abund % <sup>a</sup>	mmu <sup>b</sup>	Peaks <sup>c</sup>	Score <sup>d</sup>	DBE <sup>e</sup>	Composition	NIST
<b>349.93411</b>	<b>0.36</b>	<b>0.16</b>	<b>9</b>	<b>0.000654</b>	<b>3.5</b>	<b>C9 H12 O3 N1 Cl3 P1 S1</b>	<b>1</b>
349.93246	0.24	0.91	9	0.002411	8.5	C11 H7 O2 N3 Cl3 S1	1
349.9348	1.16	0.23	8	0.003367	-0.5	C2 H12 O1 N7 Cl3 P1 S2	0
349.93373	1.58	0.32	8	0.006249	8.5	C11 H9 N3 Cl3 P2	0
349.93496	1.33	0.4	8	0.006601	4.5	C7 H7 O7 N3 Cl3	0
349.93564	0.79	0.69	8	0.006847	0.5	H7 O5 N9 Cl3 S1	0
349.93393	1.72	0.29	7	0.007164	0.5	C1 H8 O6 N7 Cl3 P1	0
349.93308	0.83	0.72	7	0.008588	-0.5	C3 H13 O2 N5 Cl3 P2 S1	0
349.93311	1.27	0.58	8	0.009232	17.5	C19 H3 N1 Cl3	0

- a. RMS abundance error for 9 isotope peaks found in the measured mass spectrum  
b. RMS mass error for 9 isotope peaks found in the measured mass spectrum  
c. Number of isotope peaks found in the measured spectrum that match the calculated isotopes  
d. Isotope match score. A lower score indicates a better match,  
e. Double-bond equivalents ("unsaturation" or "rings + double bonds")

What would be the result of having better mass accuracy, but without isotope matching? Even if we were to measure the mass exactly (no error!) and limit the mass tolerance to 0.15 mmu (0.4 ppm), there are eight possible elemental compositions. Two possible compositions fall within an error tolerance of 0.1 ppm.

Calc. $m/z$	mmu	ppm	DBE*	Composition
349.934079	-0.03	-0.09	2.5	C3 H9 O4 N7 Br1 S2
349.934028	-0.08	-0.24	3.5	C5 H9 O7 N3 P1 S3
349.934202	0.09	0.26	3.5	C6 H9 O6 N3 Cl1 S3
349.933989	-0.12	-0.35	2.5	C6 H12 O1 N5 Cl2 Br1 P1
349.934163	0.05	0.15	2.5	C7 H12 N5 Cl3 Br1
349.933997	-0.11	-0.33	8.5	C9 H6 O2 N5 Cl2 S2
<b>349.934111</b>	<b>0</b>	<b>0</b>	<b>3.5</b>	<b>C9 H12 O3 N1 Cl3 P1 S1</b>
349.933983	-0.13	-0.37	13.5	C13 H1 O9 N1 Cl1

\* Double-bond equivalents

## Conclusion

Mass accuracy alone is often not enough to determine the elemental composition of an unknown. JEOL AccuTOF™ mass spectrometers provide accurate masses and accurate isotope data with software that provides powerful capabilities for elemental composition determinations.



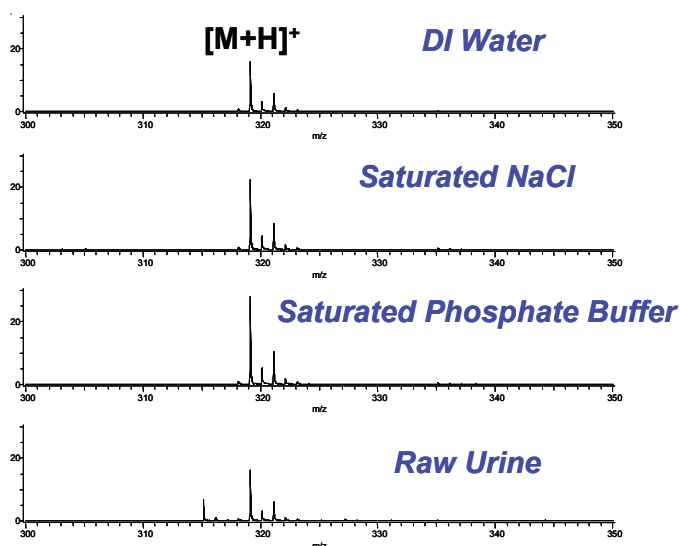
## DART Contamination Resistance: Analysis of Compounds in Saturated Salt and Buffer Solutions

DART provides very simple mass spectra that are free of multiple charging and alkali metal cation adducts such as  $[M+Na]^+$  and  $[M+K]^+$ . This facilitates identification of target compounds in mixtures and simplifies assignment of elemental compositions for unknowns.

50 ppm solutions of chlorpromazine were prepared in ultrapure deionized (DI) water, aqueous solutions of saturated sodium chloride and saturated potassium

phosphate buffer, and raw urine. Two microliters of each solution were applied to glass melting point tubes and analyzed by DART.

The mass spectra are shown below. All spectra are characterized by  $[M+H]^+$  and there is no evidence of  $[M+Na]^+$  or  $[M+K]^+$ . Sample suppression is not observed at this concentration.



*DART analysis of chlorpromazine in various solutions.*

*Note: Ranitidine ( $m/z$  315) is also present in the urine background.*

### Conclusion

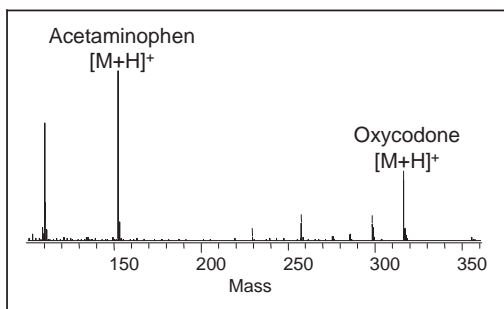
DART provides simple mass spectra, free of alkali metal cation adducts, even when analytes are present in concentrated salt or buffer solutions.



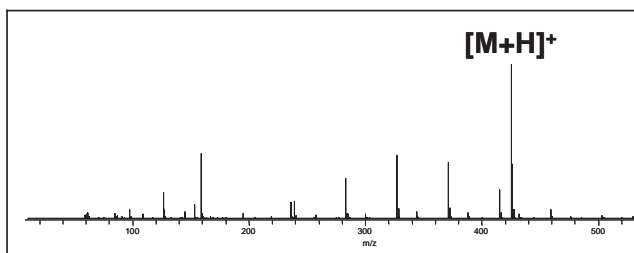
## Direct Analysis of Drugs in Pills and Capsules with No Sample Preparation

The AccuTOF™ equipped with Direct Analysis in Real Time (DART™) is capable of analyzing drugs in pills and capsules with no sample preparation. In most cases, the pill can simply be placed in front of the DART and the active ingredients can be detected within seconds. This application note shows a wide variety of pills that have been analyzed by using DART. The examples include

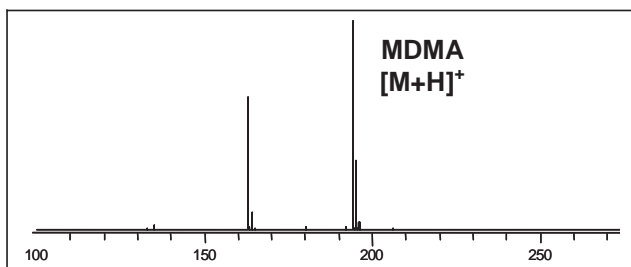
prescription drugs, over-the-counter medicines, and illicit drugs that were confiscated by a law-enforcement agency.



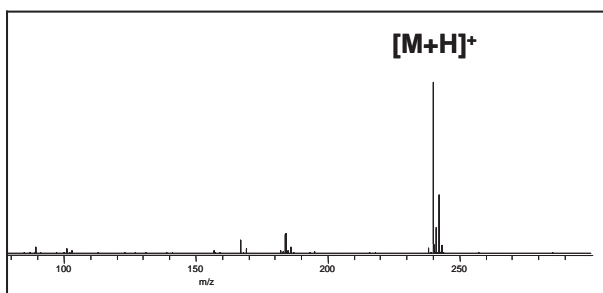
Endocet tablet (oxycodone: narcotic)



Lotensin Tablet (Benazepril: Antihypertensive)



"Ecstasy" (MDMA: illegal drug)



Generic Wellbutrin (Bupropion antidepressant)

### Examples of Pills and Medicines that Have Been Analyzed Directly by DART

#### OTC Medicines

- Ibuprofen (anti-inflammatory)
- Naproxen sodium (anti-inflammatory)
- Aspirin (anti-inflammatory)
- Acetaminophen ("Tylenol" painkiller)
- Sudafed® (pseudoephedrine decongestant)
- Melatonin (sleep aid)
- Chlortrimeton (antihistamine)
- Cough syrup (guaiafenesin and dextromethorphan)
- Codeine with Tylenol® (painkiller)

#### Prescription Drugs

- Generic Wellbutrin® (Bupropion antidepressant)
- Zantac® (ranitidine: histamine H<sub>2</sub>-receptor antagonist) Sealed capsule.
- Lipitor® (atorvastatin: treatment of hypercholesterolemia)
- Endocet® (oxycodone plus acetaminophen)
- Levsin® sublingual tablet (Hyoscyamine anticholinergic)

#### Dietary Supplements and Herbal Medicines

- Coenzyme Q10 with Vitamin E and Di- and Triglycerides
- Magnolia Bark (Chinese herbal medicine)
- Conjugated Linoleic Acid ("CLA" weight-loss formulation)

#### Confiscated Illicit Drugs

- Dimethoxyamphetamine plus methamphetamine
- Methylenedioxymethamphetamine ("Ecstasy" or MDMA)
- OxyContin®

All brand names are registered trademarks of their respective manufacturers.

## Instantaneous Screening for Counterfeit Drugs with No Sample Preparation

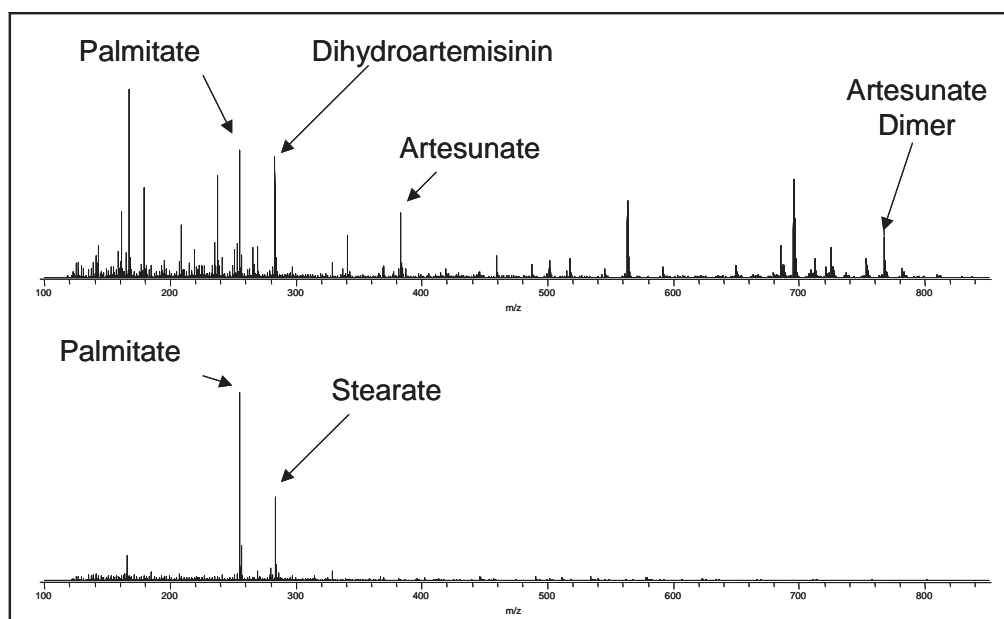
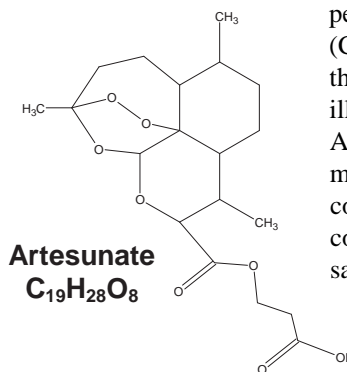
Drug counterfeiting is becoming a serious and widespread public health problem. The number of FDA open investigations into drug counterfeiting rose sharply from 2000 to 2001 and has remained high in recent years<sup>1</sup>. Counterfeit drugs are not only illegal, but dangerous; they may contain little or no actual drug content, or they may contain completely different drugs with potentially toxic consequences. The problem is worldwide; it has been reported that nearly 50% of all anti-malarial drugs in Africa are thought to be counterfeit<sup>1</sup>.

Direct Analysis in Real Time (DART™) offers a simple solution to screening for counterfeit drugs. DART can detect the presence or absence of drugs in medicines within seconds by simply placing the pill or medicine in front of the mass spectrometer. In combination with the AccuTOF, DART provides exact masses and accurate isotopic patterns that provide elemental compositions for known and unknown substances.

The top spectrum (below left) shows a sample of a genuine drug containing the anti-malarial compound "Guilin B" containing artesunate (structure below right), and the bottom spectrum shows a counterfeit drug containing only binders (stearate and palmitate) and no

active ingredient<sup>2</sup>. The samples were placed in front of the DART with no sample preparation and the mass spectra were obtained within seconds.

It is noteworthy that the peak at  $m/z$  283.15476 in the genuine drug is assigned the composition  $C_{15}H_{23}O_5^-$  (dihydroartemisinin or a fragment from artesunate). The measured  $m/z$  differs from the calculated  $m/z$  by only 0.2 millimass units and is easily distinguished by its exact mass measurement from the peak at  $m/z$  283.26405 ( $C_{18}H_{35}O_2^-$  or stearate) in the phony drug. This illustrates the value of AccuTOF's exact mass measurements in making correct assignments for compounds having the same integer mass.



<sup>1</sup> [http://www.fda.gov/oc/initiatives/counterfeit/report02\\_04.html#scope](http://www.fda.gov/oc/initiatives/counterfeit/report02_04.html#scope)

<sup>2</sup> Samples were provided courtesy of Prof. Facundo Fernandez, Georgia Institute of Technology

# AccuTOF™-DART™

## Using Solid Phase Microextraction with AccuTOF-DART™ for Fragrance Analysis

### Introduction

Solid phase microextraction (SPME) is a well established sampling technique that is often used to isolate volatile organic components in gaseous mixtures. Once the compounds have been collected, the SPME fibers are typically placed into a heated GC inlet which thermally desorbs these components into a GC-MS system for analysis. Normally, this analysis can take between 10 and 30 minutes to complete depending on the complexity of the samples. In this work, the Direct Analysis in Real Time (DART™) heated gas stream is used to desorb and directly introduce a SPME sample into a high-resolution mass spectrometer. This methodology produces comparable information to the traditional GC-MS technique but streamlines the results into only a few seconds of analysis time.

### Experimental

A Supelco DVB/Carboxen/PDMS StableFlex SPME fiber was placed in an enclosed plastic bag with a banana for 10 minutes during each analysis. For direct analysis of the SPME fiber, the JEOL AccuTOF-DART™ system was set to the following parameters: needle voltage 3500V, discharge electrode 150V, grid electrode 250V, helium temperature 200 degrees C, and helium flowrate 2.3 L/

min. A JEOL GC-Mate II high resolution sector bench top system equipped with a DB5-HT (0.25mm × 30m) was used for the GC-MS portion of the analysis. The GC-Mate II was set to the following parameters: inlet temperature 250 degrees C, split ratio 30, and helium flowrate 1.2 mL/min. The GC oven was set for the following temperature profile: 40 degrees C held for 2 min, ramp from 40 to 260 degrees C at 20 degrees C/min, 260 degrees C held for 2 min.

### Results and Conditions

Figure 1 shows a typical AccuTOF-DART™ mass spectrum obtained for a banana headspace sample. At first glance, this spectrum might appear complex, but using the JEOL-provided ChemSW *Search from List Software*, all of the [M+H]<sup>+</sup>, [M+NH<sub>4</sub>]<sup>+</sup>, and [2M+H]<sup>+</sup> for each alcohol, acetate, and butyrate were identified, summed together, and normalized in a matter of seconds. Additionally, these results were directly comparable to the data obtained for the traditional GC-MS analysis done using the GC-Mate II. Figure 2 shows a side-by-side comparison of these data sets. This work clearly demonstrates that the AccuTOF-DART™ can be used with SPME to quickly produce results that are comparable to traditional analysis techniques.

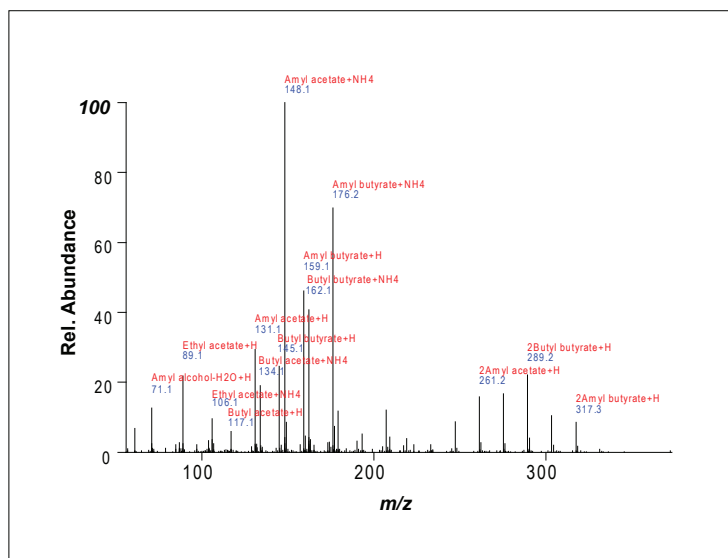


Figure 1. AccuTOF-DART mass spectrum for banana fragrance from SPME fiber.

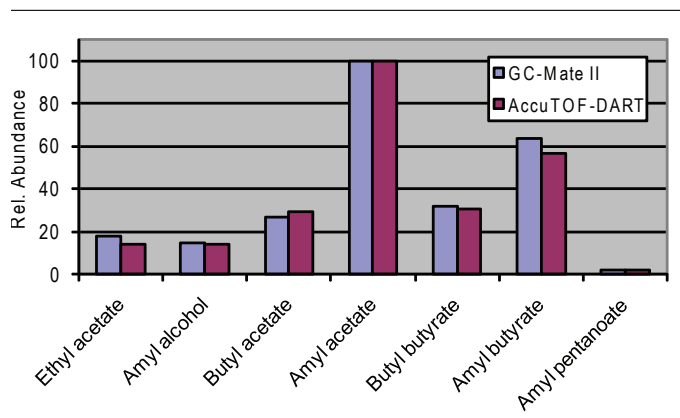


Figure 2. Comparison of relative abundances observed for compound using GC-MS and DART-MS analysis.

## Rapid Detection of Melamine in Dry Milk Using AccuTOF-DART

### Introduction

Recent events have led to the recall of both pet food and dairy food products from international consumer markets. In both cases, melamine was added to these products to show a higher chemical signature for proteins, which in turn would increase the reported quality of the food. Unfortunately, the effect of this melamine addition caused the death of both pets and babies that consumed these tainted products. As a result, there is growing government and consumer concern towards the presence of melamine in food products.<sup>1, 2</sup> Because of this concern, there is a need for a rapid and accurate test to quickly determine the presence of melamine in these food products. Previously, the JEOL AccuTOF-DART was shown to be an effective technique for determining the presence of melamine in pet food.<sup>3</sup> In this work, we extend the application of AccuTOF-DART to show that melamine can be rapidly detected when it is present in dry nonfat milk.

### Experimental

Solid melamine granules were artificially spiked into commercially available dry nonfat milk at levels between 1000ppm and 500 ppb. These samples were then pulverized with a mortar and pestle to homogenize the mixtures. For analysis, the AccuTOF-DART system was set to the following parameters: needle voltage 3500V, discharge

electrode 150V, grid electrode 40V, Helium temperature 150 degrees C, and He flowrate 2.3 L/min. A melting point tube was dipped and swirled through the melamine/milk mixture and then placed in the Helium stream between the DART and the AccuTOF atmospheric pressure interface. The data was collected in a matter of seconds from the moment the samples were introduced into the DART stream. A representative mass spectrum is shown in Figure 1 that shows the high resolution and isotopic data for the melamine  $[M+H]^+$ . Additionally, a semi-quantitative calibration curve was constructed to show the ability of the AccuTOF-DART to measure melamine in dry milk over a dynamic range of concentrations (Figure 2). Furthermore, using this methodology, the AccuTOF-DART was able to detect 1 ppm of melamine in dry milk, which is below the United States Food and Drug Administration's maximum allowable concentration of 2.5 ppm.<sup>1</sup>

### Conclusion

Unlike other analytical techniques, the AccuTOF-DART methodology described above does not require time consuming extractions or chromatographic methods to detect melamine in dry milk. Additionally, within seconds of sampling the tainted milk, the AccuTOF-DART provides high resolution and isotopic data to identify melamine.

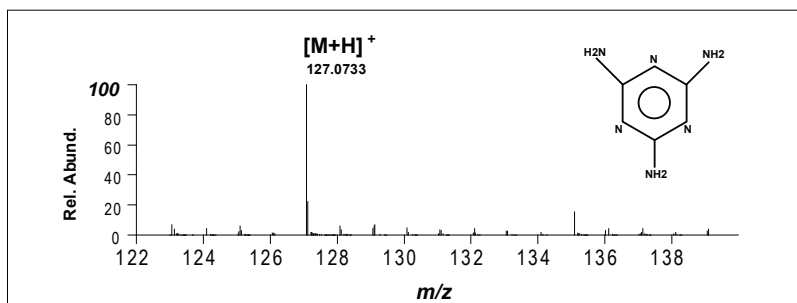


Figure 1. Mass spectrum of melamine in dry nonfat milk.

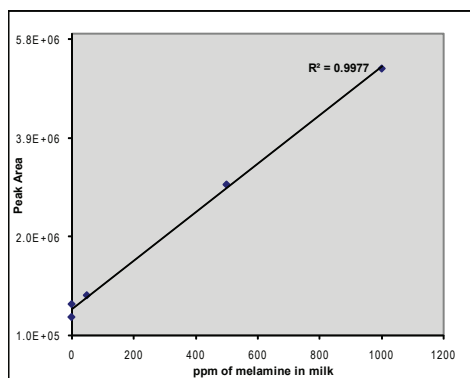


Figure 2. Semi quantitative calibration curve for melamine in dry nonfat milk.

### References

- 1 Kwisnek, S. FDA Issues Interim Safety and Risk Assessment of Melamine and Melamine-related Compounds in Food. *FDA News* **2008**, [cited 2008 October 21]; Available from: <http://www.fda.gov/bbs/topics/NEWS/2008/NEW01895.html>.
- 2 Statement of EFSA on risks for public health due to the presences of melamine in infant milk and other milk products in China. *The EFSA Journal* **2008**, 807: p. 1-10.
- 3 Vail, T., P.R. Jones, and O.D. Sparkman. Rapid and unambiguous identification of melamine in contaminated pet food based on mass spectrometry with four degrees of confirmation. *J Anal Toxicol.* **2007**, 31(6): p. 304-12.



## Flavones and Flavor Components in Two Basil Leaf Chemotypes

The chemical composition of herbs and spices can vary dramatically between different species and different growing conditions. Herbs grown under different conditions that have different essential oil compositions are referred to as chemotypes.

Basil is an herb that has widely varying chemotypes<sup>1,2</sup>. The difference between basil leaves from two different sources was easily observed by using DART. A leaf from a basil plant purchased at a grocery store was compared with a leaf from a Vietnamese restaurant. A small particle from each leaf was analyzed placed in front of the DART source. Mass spectra were obtained within seconds. Elemental compositions were confirmed by exact masses and accurate isotopic abundance measurements.

The resulting mass spectra (Figure 1) show dramatic differences between the two leaves. The basil leaf from the Vietnamese restaurant has a pleasing licorice-like flavor and a fragrant licorice-and-lemon aroma whereas the grocery store basil has a very mild clove flavor and a weak aroma. Both leaves contain terpenes and sesquiterpenes. The mass spectrum of the restaurant basil leaf (top figure) shows an abundant estragole (methyl chavicol, or *p*-allyl anisole) peak and a smaller citral peak. The grocery-store basil shows a weak eugenol peak. Furthermore, the restaurant basil leaf shows an abundance of hydroxymethoxyflavones. Flavones and related compounds are of interest because of possible antioxidant activity or other health benefits<sup>3,4</sup>. The grocery store basil shows only weak peaks for these compounds.

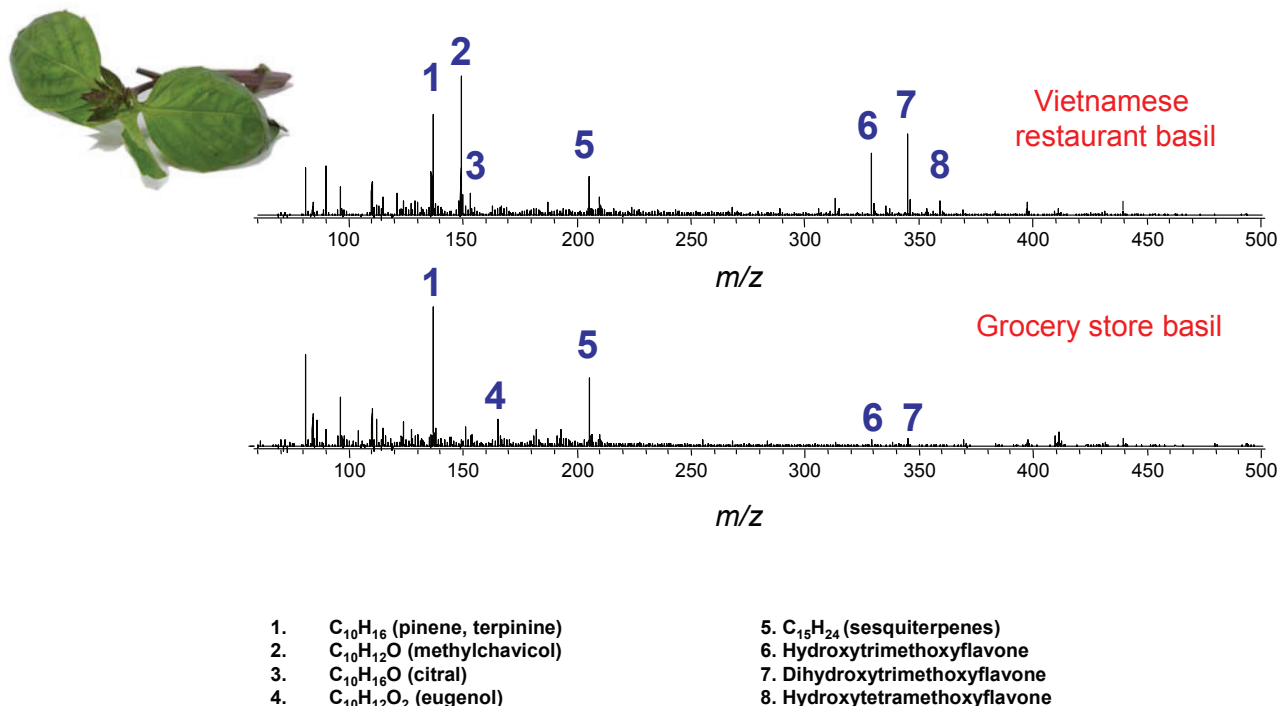


Figure 1. DART analysis of two different basil leaves.

### Conclusion

DART can rapidly detect flavor components and antioxidants in herbs and spices and can be used to discriminate between different chemotypes.

### References

- <sup>1</sup> <http://www.plantphysiol.org/cgi/content/full/136/3/3724>
- <sup>2</sup> <http://www.hort.purdue.edu/newcrop/CropFactSheets/basil.html>
- <sup>3</sup> <http://www.hort.purdue.edu/newcrop/ncnu02/pdf/juliani.pdf>
- <sup>4</sup> <http://lpi.oregonstate.edu/infocenter/phytochemicals/flavonoids/index.html>



## “No-prep” Analysis of Lipids in Cooking Oils and Detection of Adulterated Olive Oil

### Introduction

Dietary fats are categorized according to the level of unsaturation. Oils are a mixture of triglycerides and free fatty acids. Olive oil contains a high concentration of monounsaturated fatty acids, while other oils such as Canola and safflower oil contain larger amounts of polyunsaturated fatty acids. Characterizing the type of lipids present is important for quality control and for detecting adulteration of more expensive oils (e.g. olive oil) with cheaper products. Analysis by HPLC is time-consuming and requires solvents and consumables. DART provides a convenient alternative: no solvents are required and the analysis can be completed in seconds.

### Experimental

Analysis was carried out by using a JEOL AccuTOF-DART™ mass spectrometer operated in positive-ion mode at a resolving power of >6000 (FWHM). The

DART source was operated with helium and the gas heater was set to 375°C. Melting point tubes were dipped in oil samples and placed in front of the DART ion source for a few seconds. A cotton swab dipped in dilute ammonium hydroxide was placed nearby to enhance formation of  $[M+NH_4]^+$  from triglycerides. A spectrum of PEG 600 was measured between samples to permit exact mass measurements.

### Results

Figure 1 shows the DART mass spectrum of a grocery-store olive oil and Figure 2 shows a comparison of mass spectra for different cooking oils. Free fatty acids (Figure 3), squalene and di- and triglycerides (Figure 4) are detected as  $[M+NH_4]^+$ . The relatively high abundance of free fatty acids in Figure 1 (bottom) is a result of thermal decomposition and is only observed at higher gas temperatures for large amounts of (neat) oil. However, the abundant peaks for the free

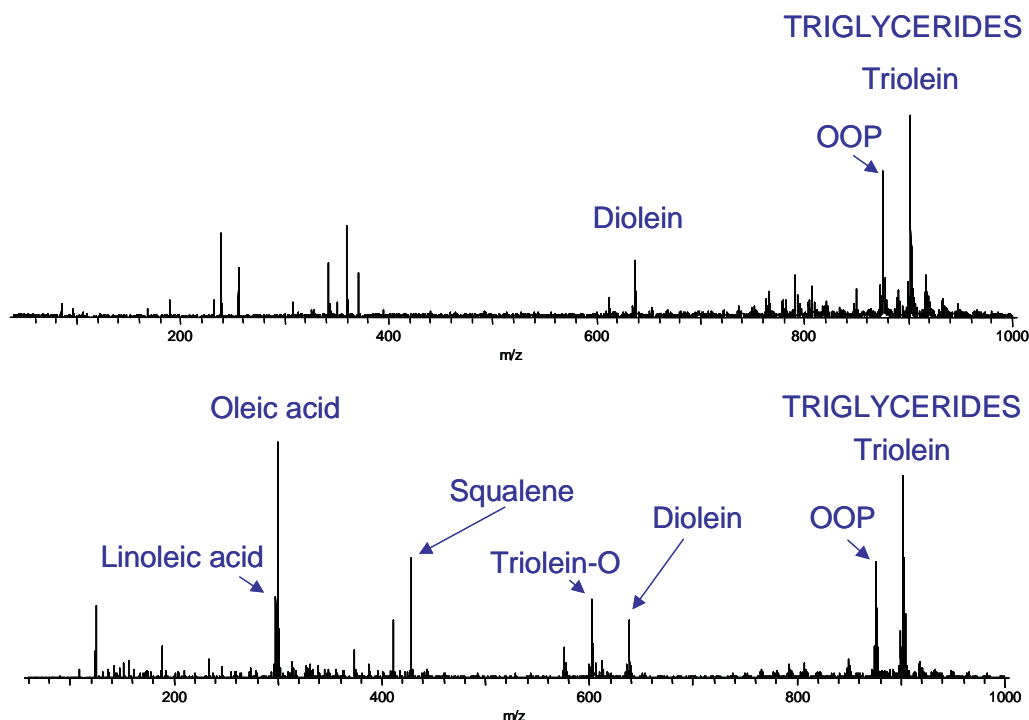


Figure 1. Medium-quality grocery store olive oil. Top: dilute solution of olive oil in hexane, bottom: neat oil (DART at 375°C).

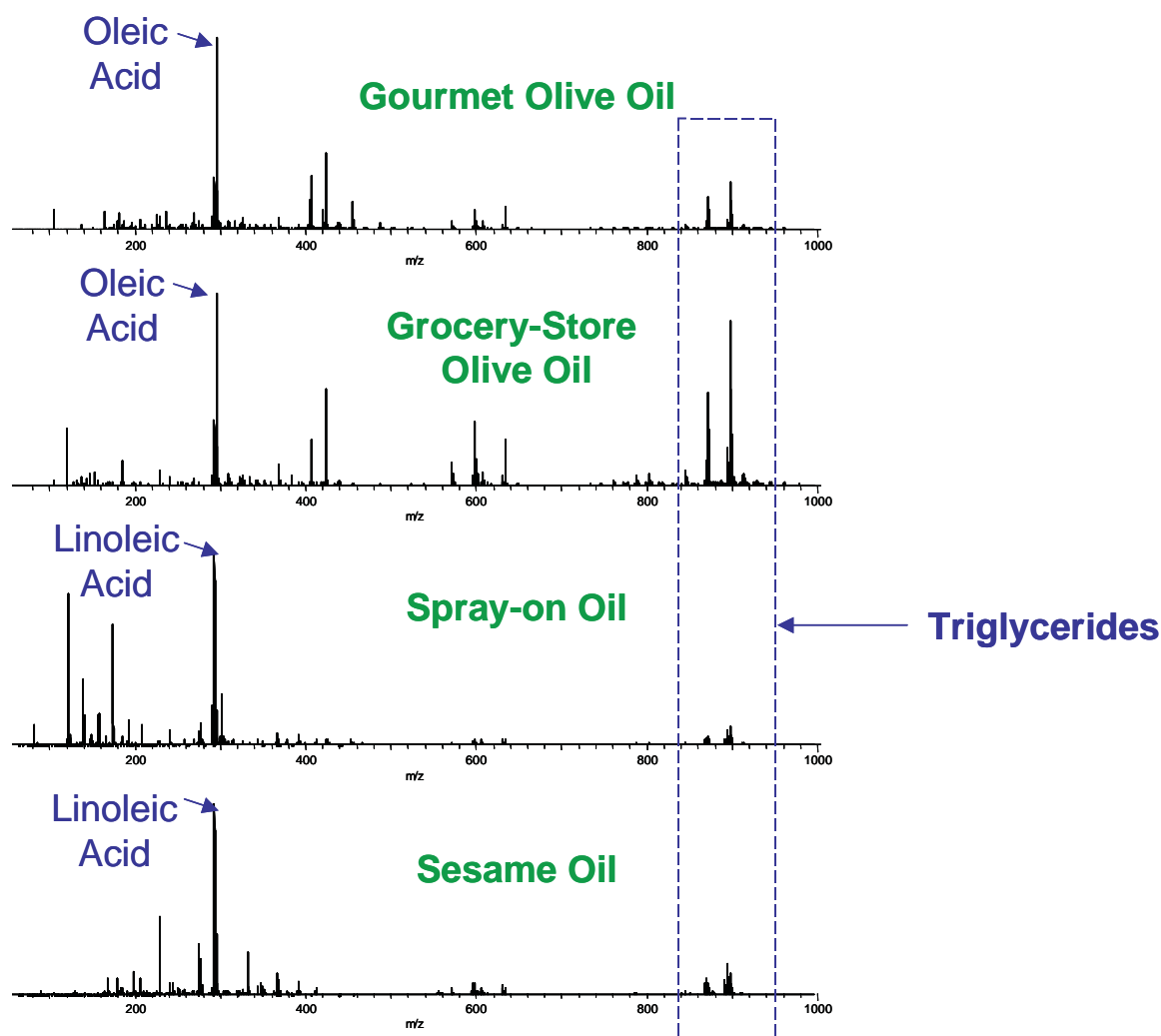


Figure 2. Comparison of cooking oils

fatty acids under these conditions make it easy to see differences in the overall fatty acid content of the oil.

Of the  $C_{18}$  fatty acids, oleic acid (O) comprises 55-85% of olive oil<sup>1</sup>, while the Omega-6 fatty acid linoleic acid (L) is present at about 9% and the Omega-3 fatty acid linolenic acid (Ln) is present at less than 1.5%. Other fatty acids including the  $C_{16}$  palmitic acid (P) are also detected.

The triglycerides are readily detected (Figure 4) and their elemental compositions confirmed by exact mass measurements (Table 1) and isotope pattern matching. Triolein (OOO) is the major component in olive oil,

while increasing unsaturation is observed for the Canola/safflower oil blend and the sesame oil.

Elemental compositions were confirmed for the triglyceride  $[M+NH_4]^+$  peaks by exact mass measurements and isotope pattern matching. Examples for triolein (OOO) and OOP are shown in Table 1. Figure 5 shows the DART mass spectrum of an olive oil sample to which 50% of the Canola/safflower oil blend has been added. In comparison with the unadulterated olive oil (Figures 3 and 4), the adulterated oil is easily recognized by the higher degree of unsaturation and the relatively higher abundance of linoleic and linolenic acids.

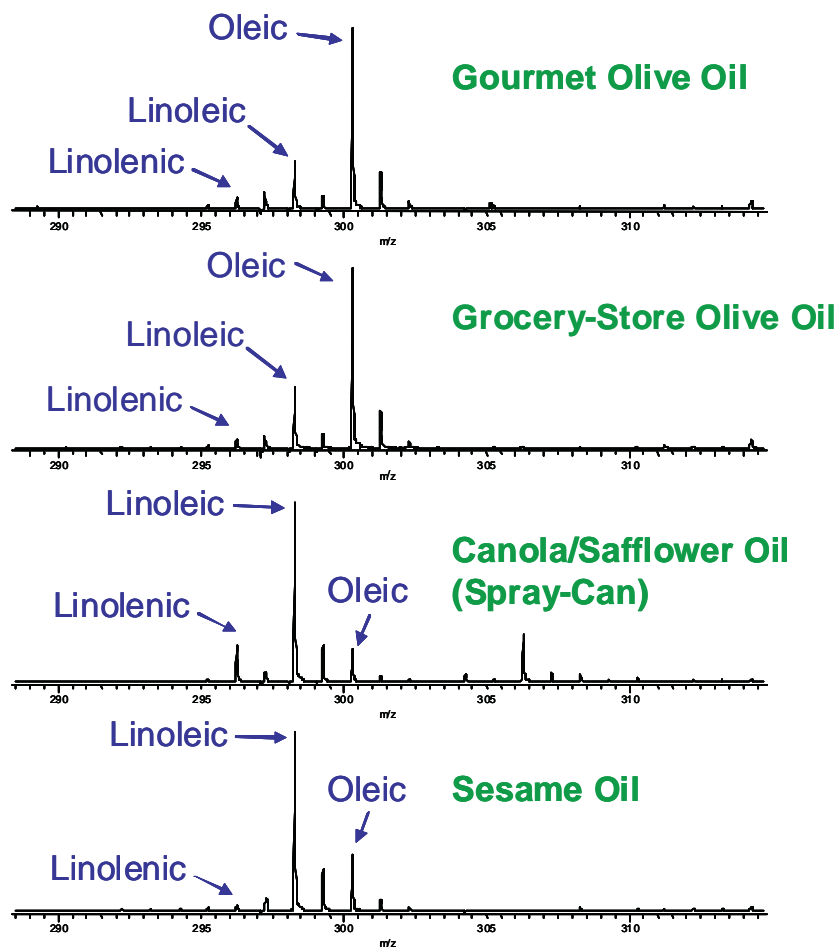


Figure 3. Enlarged view of free fatty acid region

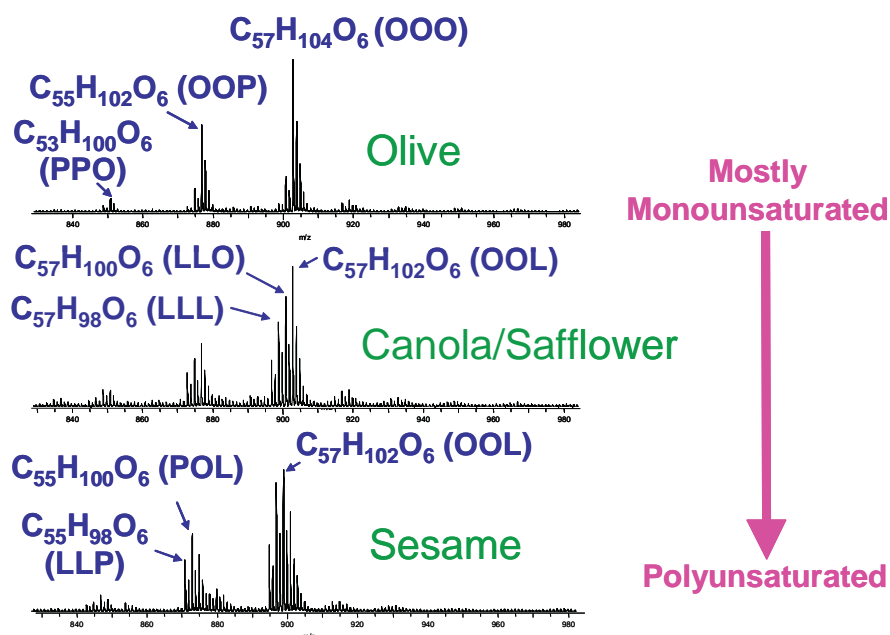


Figure 4. Enlarged view of triglycerides in cooking oils

Meas. mass (um)	Abund. (%)	Difference (mmu)	Unsaturation	Compositions
876.801270	25.14	-0.75	3.5	C55 H106 O6 N1 (OOP)
902.816040	35.62	-1.61	4.5	C57 H108 O6 N1 (OOO)

Table 1. Elemental compositions from exact mass measurements

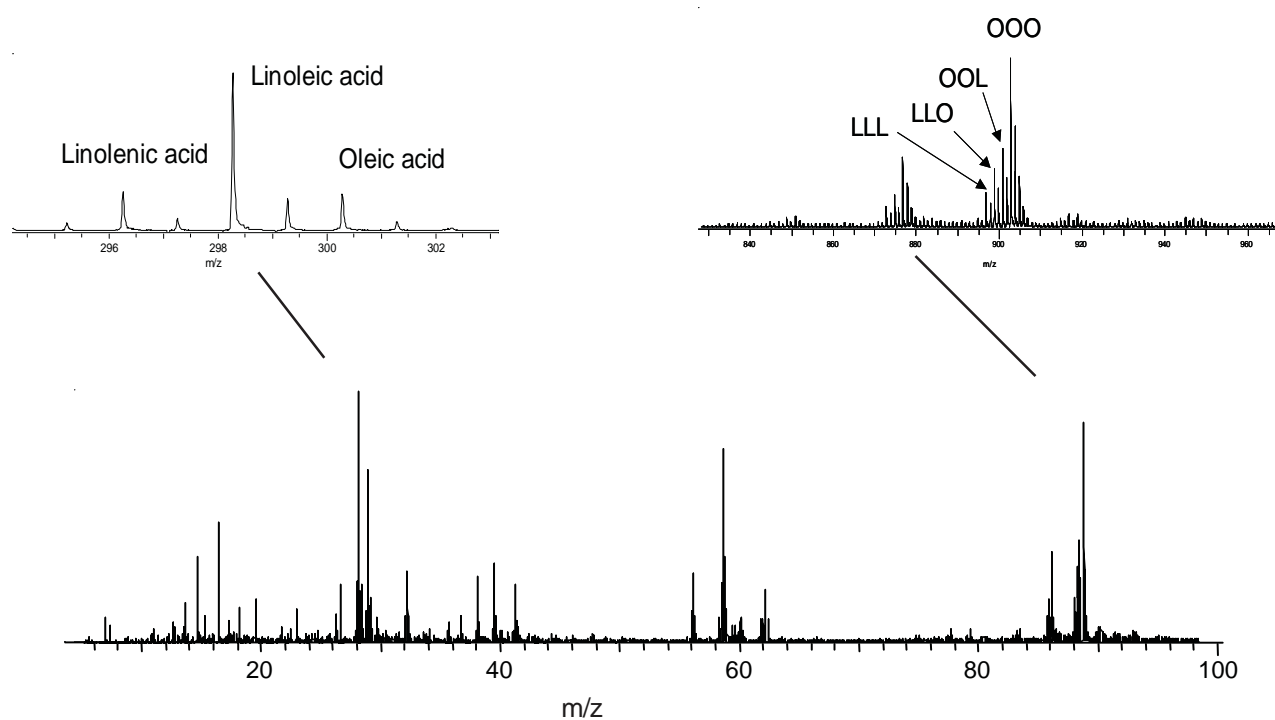


Figure 5. DART mass spectrum of adulterated olive oil

## Conclusion

DART can characterize lipids such as fatty acids and mono-, di-, and triglycerides in cooking oils and detect adulterated olive oil within seconds and with no sample preparation.

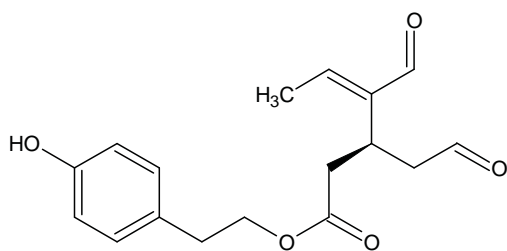
## Reference

1. <http://www.oliveoilsource.com/olivechemistry.htm>

## Detection of Oleocanthal in Freshly Pressed Extra-Virgin Olive Oil

According to a recent report in *Nature*<sup>1</sup>, freshly pressed extra-virgin olive oil contains a compound, oleocanthal, that has properties similar to the common anti-inflammatory drug, ibuprofen.

We used DART to rapidly examine cooking oils for the presence of this compound. Fresh-pressed extra-virgin olive oil from a specialty food store was compared with a medium-quality grocery-store brand. Sesame oil and a low-quality spray-on cooking oil were also examined. No sample preparation was required. Glass melting point tubes were dipped into the oil samples and then placed in front of the DART source for analysis. The DART source was operated with helium in positive-ion mode at a gas heater temperature of 350°C. A cotton swab dipped in dilute aqueous ammonium hydroxide was placed nearby to permit the formation of  $[M+NH_4]^+$  for triglycerides and other oil components. A mass spectrum of neat PEG 600 on a glass rod was acquired and stored in the same data file to provide an external calibrant for exact mass measurements.



Oleocanthal

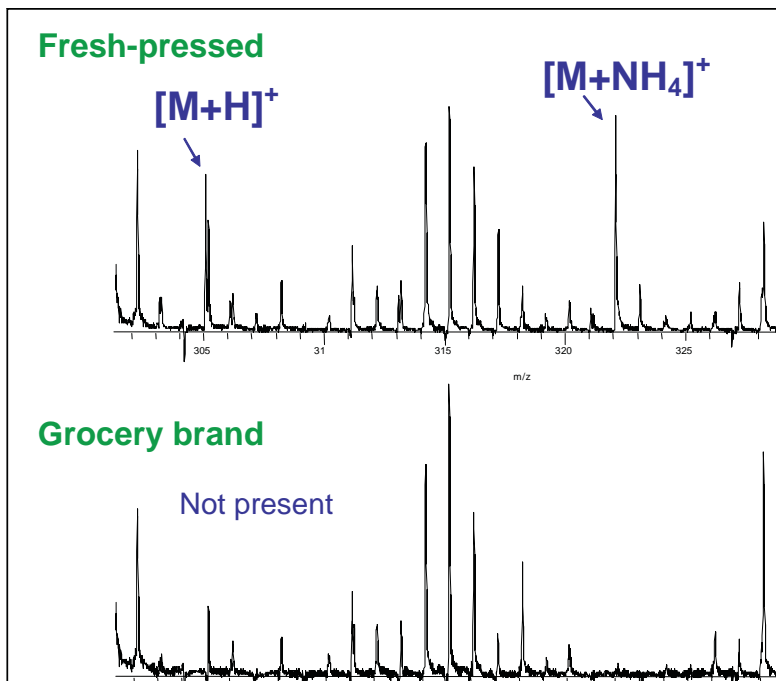


Figure 1. Positive-ion DART mass spectra of two olive oils. Enlarged view of the region where oleocanthal peaks are observed.

The oleocanthal was readily observed in the fresh-pressed oil as  $[M+H]^+$  and  $[M+NH_4]^+$ . The measured masses confirmed the expected composition with excellent mass accuracy.

### Conclusion

DART can detect the presence of natural products in cooking oils. Analysis is rapid (within seconds) and no sample preparation is required.

### Reference

<sup>1</sup>Beauchamp, G.K.; Keast, R. S. J.; Morel, D.; Lin, J.; Pika, J.; Han, Q.; Lee, C.-H.; Smith, A. B.; Breslin, P. A. S. *Nature*, **437**, 45-46 (Sept. 2005). "Phytochemistry: Ibuprofen-like activity in extra-virgin olive oil."

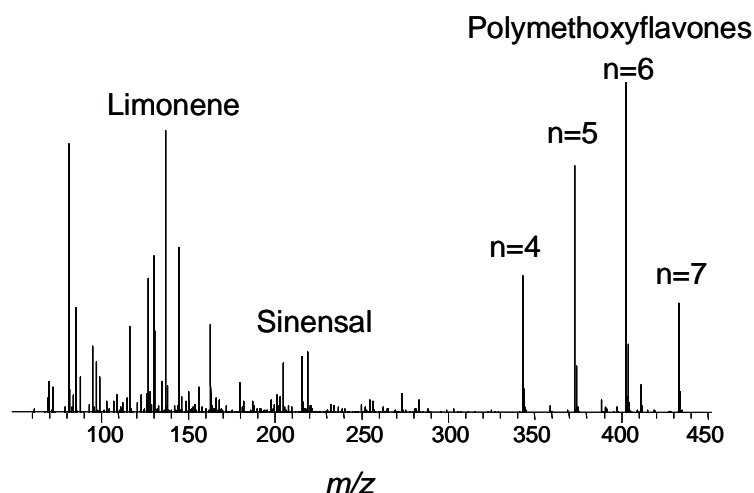
Meas. mass (um)	Diff. (mmu)	Composition	Assignment
305.138977	0.09	C <sub>17</sub> H <sub>21</sub> O <sub>5</sub>	$[M+H]^+$
322.165955	0.50	C <sub>17</sub> H <sub>24</sub> O <sub>5</sub> N <sub>1</sub>	$[M+NH_4]^+$

## Rapid Detection of Fungicide in Orange Peel

Thiabendazole is an anthelmintic and a highly persistent systematic benzimidazole fungicide that is widely used for controlling spoilage in citrus fruit. It is considered a General Use Pesticide (GUP) in EPA Toxicity Class III – Slight Toxicity.

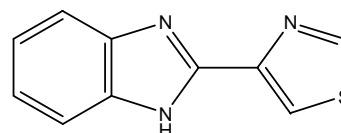
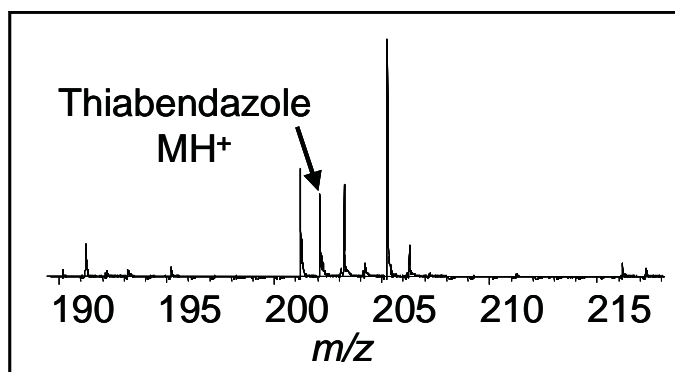
A small piece of orange peel (a few square millimeters in size) from a Florida orange was placed in

the DART sampling region. Compounds present in the peel were detected within seconds. Among these were the familiar orange-oil flavor components such as limonene and sinensal as well as polymethoxylated flavones that are attributed with antioxidant and cholesterol-reducing properties.



An enlarged view of the region near  $m/z$  202 is shown below. The large peak at  $m/z$  205.1949 has the elemental composition  $C_{15}H_{24}$ , assigned as the  $[M+H]^+$

for farnesene. Residual thiabendazole was detected as  $[M+H]^+$  at  $m/z$  202.0444, which differs by only 0.0005 from the theoretical  $m/z$  of 202.0439.



**Thiabendazole**

$C_{10}H_7N_3S$

Measured: 202.0444 Da

Calculated: 202.0439 Da

Difference: 0.0005 Da

**Conclusion:** DART was used for the rapid detection of trace pesticides on fruit.



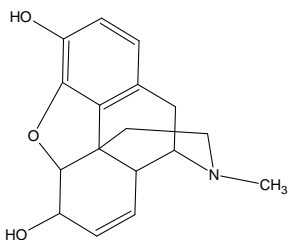
## Instantaneous Detection of Opiates in Single Poppy Seeds

Poppy seed is a common flavoring ingredient that is known to contain small amounts of opiates. Maximum morphine and codeine concentrations are estimated to be about 33 and 14 micrograms respectively per gram of seed<sup>1</sup>. Consumption of typical amounts of baked goods containing poppy seeds has not been shown to cause any ill effects. However, ingestion of poppy seeds may result in false positives from drug tests.

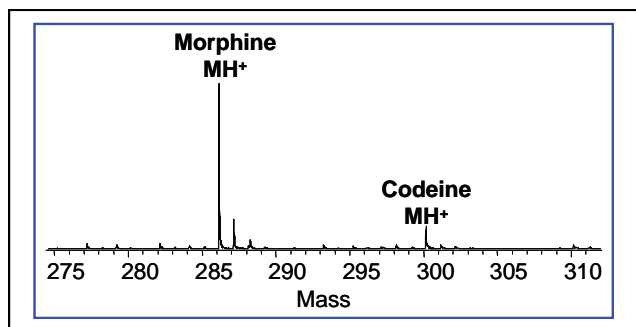
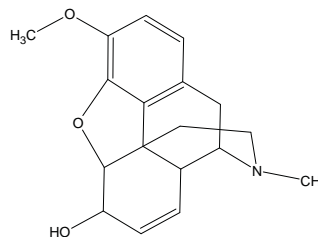
Single poppy seeds from different sources were analyzed independently in two different laboratories by using the DART™/AccuTOF™ combination. The resulting mass spectra were nearly identical.



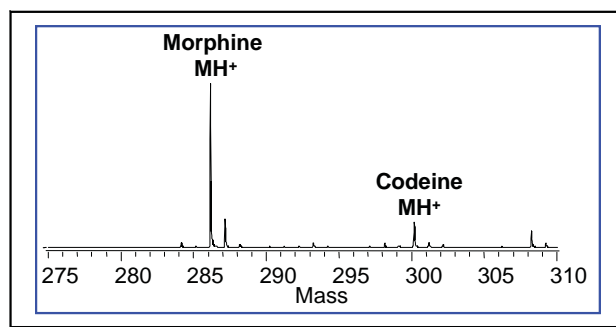
**Morphine C<sub>17</sub>H<sub>19</sub>NO<sub>3</sub>**



**Codeine C<sub>18</sub>H<sub>21</sub>NO<sub>3</sub>**



**Poppy seed # 1 (DART in Maryland)**



**Poppy seed # 2 (DART in Massachusetts)**

**Measured Mass**

286.1443 Da

300.1611 Da

**Mass Error (mmu)**

<0.001

0.001

**Elemental Composition**

C<sub>17</sub>H<sub>20</sub>N<sub>1</sub>O<sub>3</sub> (Morphine)

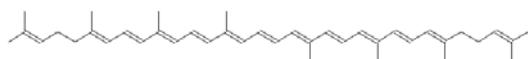
C<sub>18</sub>H<sub>22</sub>N<sub>1</sub>O<sub>3</sub> (Codeine)

<sup>1</sup>Opiate concentrations following the ingestion of poppy seed products – evidence for the poppy seed defense. Medway, C.; George, S.; Braithwaite, R. *Forensic Sci. Int.* vol. 96 (1998), pp. 29-38.

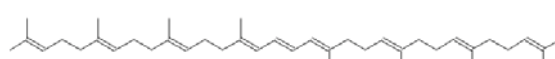
## Detection of Lycopene in Tomato Skin

Tomatoes are rich in lycopene, a hydrocarbon antioxidant that is the source of the red coloring in ripe tomatoes. The potential benefits of nutritional antioxidants such as lycopene have received a great deal of attention in the popular media.

A piece of tomato skin was placed in front of the DART and the positive-ion mass spectrum was recorded. Peaks were quickly observed at the expected exact masses for lycopene and  $[M+H]^+$  ( $C_{40}H_{57}^+$ ,  $m/z$  537.4460) and phytoene  $[M+H]^+$  ( $C_{40}H_{65}^+$ ,  $m/z$  545.5086).



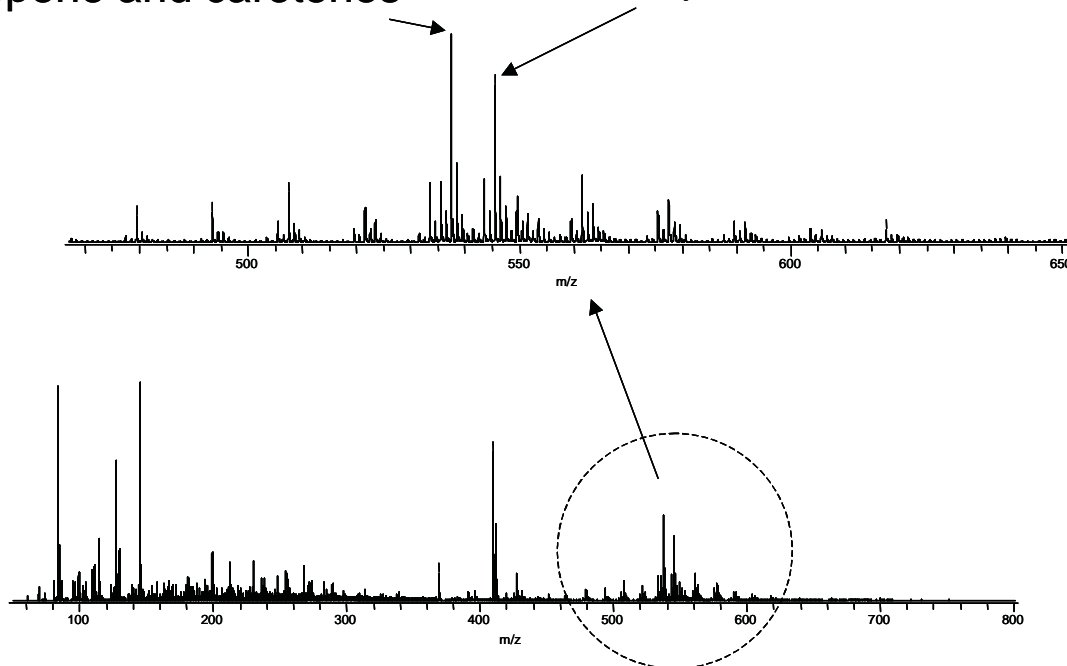
**Lycopene**



**Phytoene**

**Lycopene and carotenes**

**Phytoene**

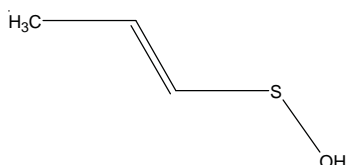


## Detection of Unstable Compound Released by Chopped Chives

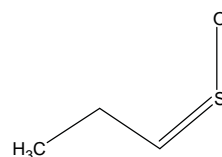
Every cook knows that chopping onions releases chemicals that cause eye irritation. The lachrymator released by chopped onions and related plants is formed by the action of a pair of enzymes on a cysteine derivative to ultimately form propanethial S-oxide ( $C_3H_6SO$ ), the compound that causes eye irritation.

This compound is reactive and unstable and is therefore difficult to analyze by conventional mass spectrometry techniques.

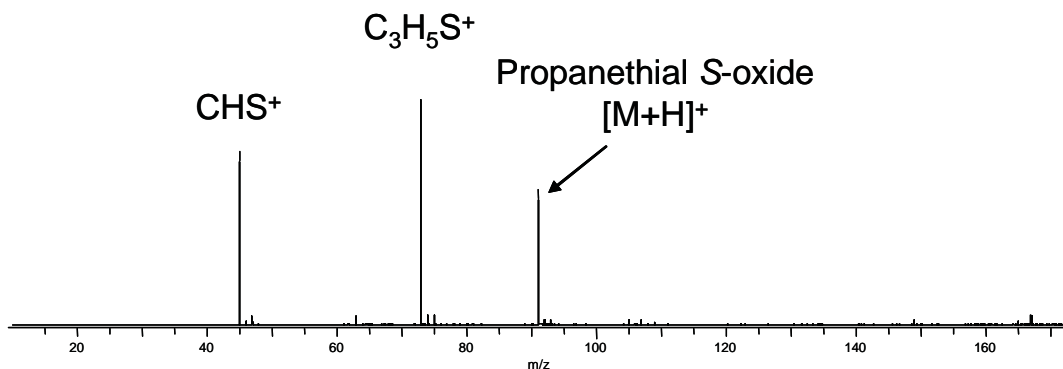
However, DART was easily able to detect propanethial S-oxide when a freshly cut chive bulb was placed in front of the mass spectrometer. The sample was analyzed at atmospheric pressure under ambient conditions and no sample preparation was required, other than cutting into the chive bulb. The compound was detected as  $[M+H]^+$  ( $C_3H_7SO^+$ ,  $m/z$  91.0139).



*Sulfenic acid released by enzymatic reactions when an onion is cut*



*Propanethial S-oxide lachrymator in onion*



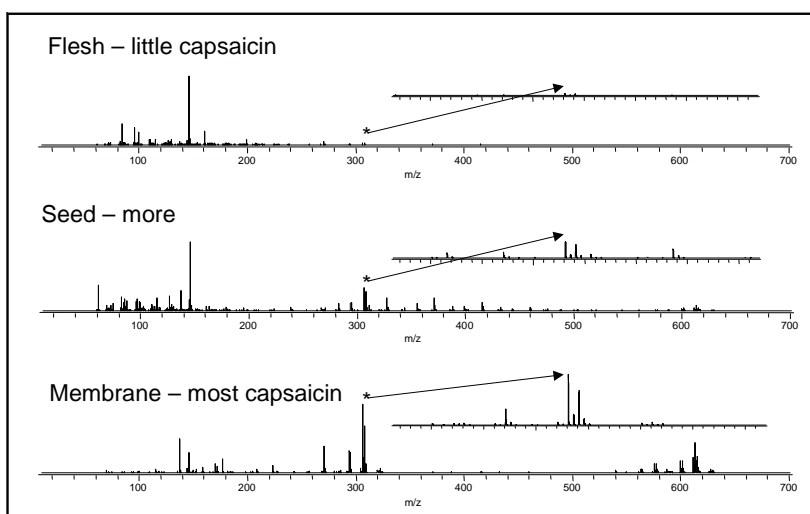
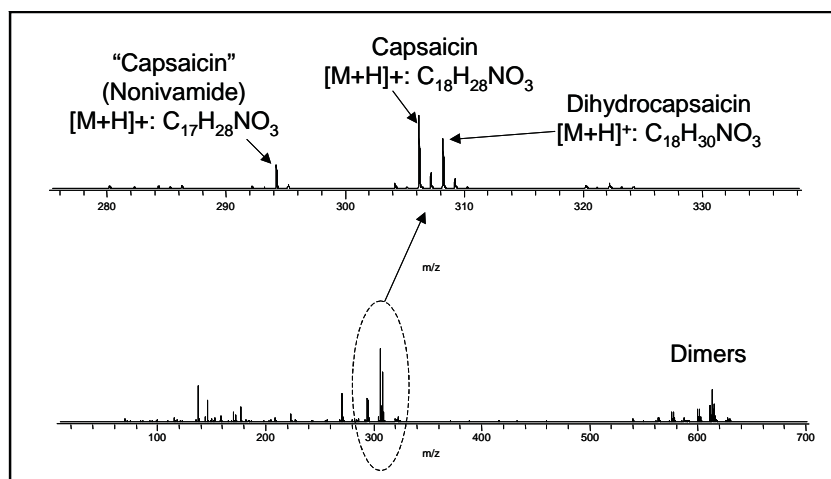
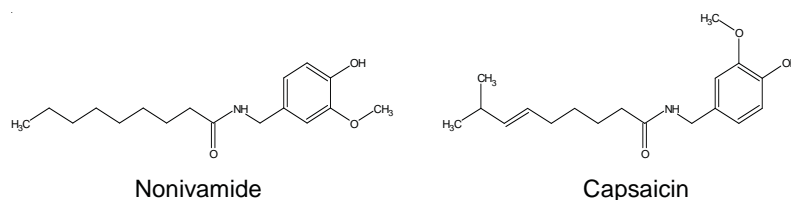
*Lachrymator detected from freshly chopped chive bulbs placed in front of the mass spectrometer.*

## Distribution of Capsaicin in Chili Peppers

Capsaicin ( $C_{18}H_{27}NO_3$ ) is the molecule that causes the hot, burning sensation when you eat chili peppers. Capsaicin, dihydrocapsaicin ( $C_{18}H_{29}NO_3$ ), and a related compound, nonivamide ( $C_{17}H_{27}NO_3$ ) are found in different concentrations in different parts of the pepper pod.

We examined different parts of a hot pepper to determine which part of the pepper contains the highest

concentration of capsaicin. Different sections of the pepper were placed between the DART and the AccuTOF orifice. Little capsaicin was found in the fleshy part of the pepper; higher concentrations were found in the pepper seeds. The highest concentration of capsaicin was found in the membrane inside the pepper pod onto which the seeds are attached.



## Identifying “Buried” Information in LC/MS Data

It is not always easy to identify minor unknown components in complex LC/MS datasets. The new DART™ ion source screened for components that were not immediately recognized in LC/MS analysis of tea samples.

LC/TOFMS datasets can contain high-resolution, exact-mass data for all ionized components of a complex mixture. Even with concurrent UV detection and chromatographic enhancement software, it is not always easy to identify all of the components that are present in the dataset. Furthermore, suppression effects may mask important information. Here, a new technique known as Direct Analysis in Real Time (DART™) was used to screen tea samples and provide elemental compositions for minor components that were “buried” in LC/MS data collected for tea analysis. DART is a powerful new ionization method that permits direct analysis of solid, liquid, or gas samples at atmospheric pressure and ground potential. DART has been applied to rapid in-situ analysis of a very wide range of materials ranging from drugs to explosives, foods, and beverages.

### Experimental Conditions

Drinking-quality green tea was analyzed directly by dipping a glass rod into the liquid and placing the rod between the DART source and the mass spectrometer orifice. Analysis was complete within 30 seconds. Following the tea analysis, a piece of filter paper dipped in PEG 600 was placed in front of the DART to provide reference masses for exact mass measurements. LC/MS conditions were described in a previous application note. (<http://www.lcgc.com/lcgc/article/articleDetail.jsp?id=87195>).

### Results and Conclusions

Elemental compositions for several components are given in Table 1 for several compounds identified by DART. Compositions were identified by combined exact-mass measurements and isotope pattern matching for the observed  $[M+H]^+$  species. Candidate compositions were proposed by searching the mass spectral database for suitable compounds having the correct elemental composition. Following DART analysis, reconstructed ion mass chromatograms were generated from the LC/MS data for the exact mass of each component.

DART is ideal for screening because the analysis is rapid, suppression is minimal, solvent adducts are not observed, and exact mass measurements are simple and accurate. The presence of several isomers having these candidate compositions was confirmed by the RIC's. The LC/MS data shows well-separated isomers and provides quantitative information about each component.

- |                        |   |
|------------------------|---|
| 1. $C_6H_4O_2^+$       | Benzoquinone                                    |
| 2. $C_4H_4O_2^+$       | Furanone  |
| 3. $C_5H_4O_2^+$       | Furfural, pyranone                              |
| 4. $C_6H_6O_3^+$       | Maltol  |
| 5. $C_7H_6O_3^+$       | Sesamol, dihydroxybenzaldehydes, salicylic acid |
| 6. $C_{15}H_{10}O_6^+$ | Kaempferol                                      |
| 7. $C_{15}H_{10}O_7^+$ | Quercetin                                       |
| 8. $C_{15}H_{10}O_8^+$ | Myricetin                                       |

Table 1. Elemental compositions and some candidate compounds identified by DART in green tea.

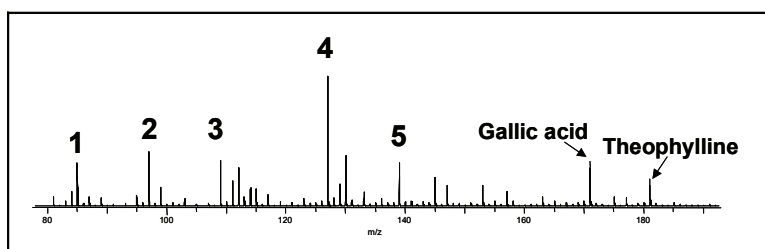


Figure 1. Portion of positive-ion DART mass spectrum for green tea sampled with a glass rod. Larger components such as #6-8, caffeine and catechin were detected but are not shown here.

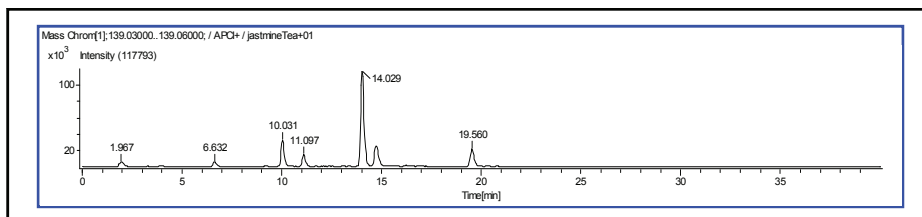


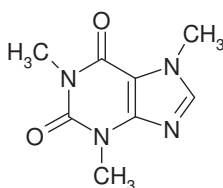
Figure 2. Reconstructed mass chromatogram for  $m/z$  139.0395 ( $C_7H_7O_3^+$ ).



## ***Direct analysis of caffeine in soft drinks and coffee and tea infusions***

Caffeine (Figure 1), a xanthine alkaloid acting as psychoactive stimulant and mild diuretic in human, is an integral part of diet of many people. It is often found in natural products such as tea, coffee and cocoa beans, cola nuts and many others. Analysis of caffeine in various foods and beverages is an important task for analytical laboratories, as its content is considered in assessment of product quality (coffee, cocoa beans and tea). Due to its physiological effect, the amount of caffeine is regulated in selected foods in EU. Maximum limits are set for some soft drinks to which caffeine is added. HPLC methods employing UV detection are commonly used for its control. While for soft drinks and coffee/tea infusions, the sample preparation is not too much time demanding, LC separation of sample components becomes a limiting step in laboratory throughput. Employing AccuTOF-DART system offers straightforward examination of caffeine content in tens of samples per hour, thanks to omitting separation step. Isotope dilution is used for target analyte quantification.

**Figure 1** Structure of caffeine (1,3,7-trimethylxanthine, CAS Number: 58-08-2).



### ***Experimental***

#### **Samples**

The samples were prepared for analysis in following way:

- (i) Soft drinks (ice tea, cola drink, energy drink) were decarbonized by sonication.
- (ii) Soluble coffee 2 g were diluted in 100 mL of boiling water.
- (iii) Ground coffee beans and tea leaves (5 g) were extracted with 100 mL of boiling water under shaking (1 min).

All liquid samples were diluted 50 times and 5 µl of aqueous solution containing 5 µg of isotope labeled internal standard (<sup>13</sup>C<sub>3</sub>-caffeine) were added to 1 mL of each diluted sample.



DART-TOFMS measurements

The DART ion source was operated in positive ion mode with helium as the ionizing medium at a flow rate of 2.7 L/min. The gas beam was heated to 300 °C, discharge needle voltage set to 3000 V, perforated and grid electrode voltages were +150 V and +250 V, respectively. Accurate mass spectra were acquired in a range of *m/z* 50–500 employing 0.2 s recording interval; the peaks voltage value was set to 1000 V. A solution containing a mixture of poly(ethylene glycol) PEG 600 and 200 was introduced at the end of each sample analysis to compensate any mass drift.

The examined samples were introduced automatically with the use of an AutoDart sampler and Dip-it™ tips. Following steps were involved: (i) sampling tip immersed into the sample; (ii) placing of tip in front of the DART gun exit close to the ion source – mass spectrometer axis; (iii) sampling tip disposed. Five replicate measurements were carried out on examined samples.

Results

As shown in Figure 3, both caffeine and isotope labeled internal standard were detected as [M+H]<sup>+</sup> ions. The differences between exact and measured masses were as low as -0.7 mmu and -0.6 mmu, respectively.

In Figure 4 calibration plot of caffeine is shown. Each data point is an average of five repeated analyses measured over a period of five days, good linearity was obtained (*R*<sup>2</sup> = 0.9989). Table 1 summarizes the results of analyses obtained by analyses of the above samples. The repeatability of measurements was less than 8% (RSD) within an experimental series for all examined matrices. Good agreement with data obtained by reference HPLC/UV method was obtained.

Conclusions

DART-TOFMS technique was demonstrated to be suitable for accurate determination of caffeine in various beverages including coffee and tea infusions. The requirements on sample preparation are minimal: only dilution, sonication and internal standard addition are needed. The results of preliminary experiments have shown the potential of DART-TOFMS to detect also other regulated compounds in soft drinks (artificial sweeteners, acidulants, preservation agents, etc.).

Figure 3 Positive DART spectrum: diluted coffee infusion.

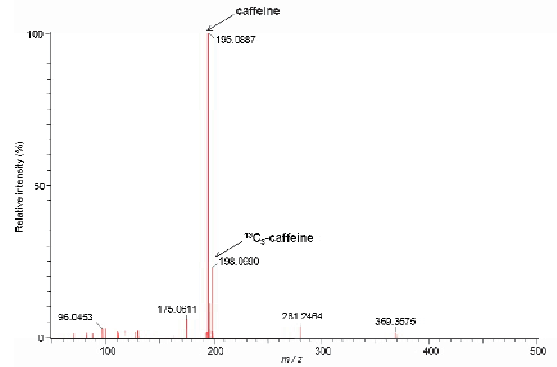


Figure 4 Calibration curve.

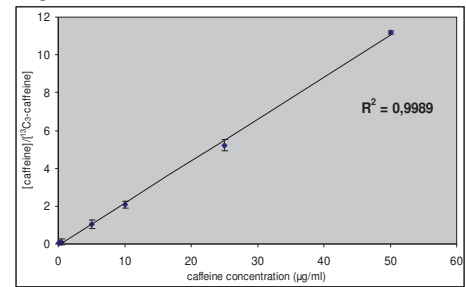


Table 1 Caffeine concentrations in examined samples.

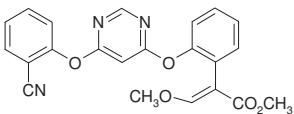
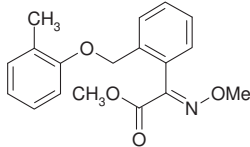
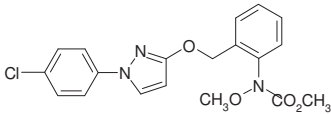
Sample	Caffeine concentration (µg/ml) <sup>a</sup>	RSD (%) <sup>b</sup>
Coffee infusion	825	7.9
Black tea infusion	103	4.2
Green tea infusion	71	3.1
Ice tea	44	5.6
Cola drink	95	4.5
Energy drink	230	3.5

<sup>a</sup> calculated to undiluted beverage, <sup>b</sup> n = 5

## ***Rapid screening of strobilurins in crude solid materials (wheat grains) using DART-TOFMS***

Direct control of solid materials for pesticide residues is a challenging task enabling fast contamination screening. In our study, we investigated direct analysis of strobilurin fungicides in milled wheat grains. Strobilurins, systemic pesticides originated from natural fungicidal derivatives, play an important role in control of various plant pathogens.<sup>1,2,3</sup> Because of their unique protective properties, significant yield enhancements and longer retention of green leaf tissue, strobilurins have been widely used in agriculture since their introduction on the market in 1992.<sup>3</sup> As other pesticides, these compounds are involved in control and monitoring surveys undertaken by regulation authorities.<sup>4</sup> Some characteristics of strobilurins are shown in Table 1.

**Table 1** Strobilurins: physico-chemical characteristics.

Compound	Structure	log Kow	water solubility (mg l <sup>-1</sup> )	molecular weight
<b>Azoxystrobin</b>		2.5	6.0	403.4
<b>Kresoxim methyl</b>		3.4	2.0	313.4
<b>Pyraclostrobin</b>		4.0	4.6	387.8

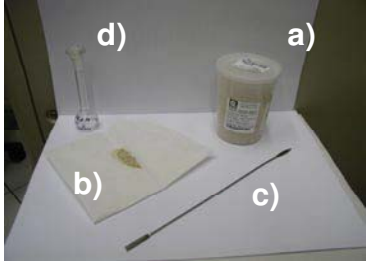
AccuTOF-DART system was used for examination of milled wheat grains containing incurred residues of azoxystrobin, kresoxim methyl and pyraclostrobin.

The DART ion source was operated in positive ion mode with helium as the ionizing medium at flow a rate of 2.7 L/min. The gas beam was heated to 130 °C and the distance between the exit of the DART gun and inlet of the mass spectrometer was 12 mm. The discharge needle voltage of the DART source was set to positive

potential of 2400 V, perforated and grid electrode voltages were +150 V and +250 V, respectively. Accurate mass spectra were acquired in a range of  $m/z$  100–500, spectra recording interval was 0.2 s; the peaks voltage value was set to 850 V. A mixture solution of poly(ethylene glycol) PEG 600 and 200 was used for calibration. The same calibrant was also introduced at the end of each sample analysis to perform mass drift compensation. The mass resolution of the mass spectrometer was typically  $6000 \pm 500$  (FWHM).

Samples were introduced manually with the use of in-hand made filtering paper envelopes containing approximately 1 g of homogenous sample. The sample was spread across the edge of the envelope (see Figure 1) and placed into the DART gas stream to ionize target analytes and detect the respective peaks.

**Figure 1** The only items needed for fast analysis of strobilurins in milled wheat grain are: a) incurred wheat grain sample, b) filtering paper, c) spatula, d) PEG solution.



In Figures 2, 3 and 4 a positive-ion DART mass spectrum of directly analyzed wheat grains samples showing the tested strobilurins as  $[M+H]^+$ . The ion identity was confirmed by elemental composition calculations as documented in Table 2 and also shown in respective Figures.

**Figure 2** a) Mass spectrum of wheat grains containing incurred residues of azoxystrobin. b) Estimation of an element composition from exact mass measurement. The highlighted column stands for target analyte.

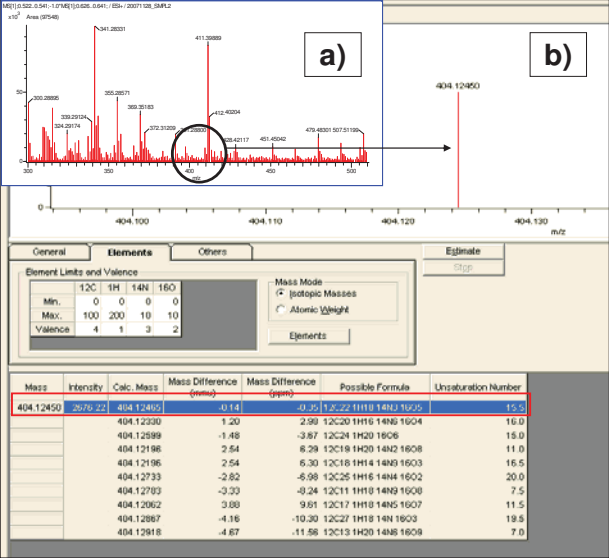


**Figure 3** a) Mass spectrum of wheat grains containing incurred residues of pyraclostrobin. b) Estimated element composition from exact mass measurement. The highlighted column stands for target analyte.

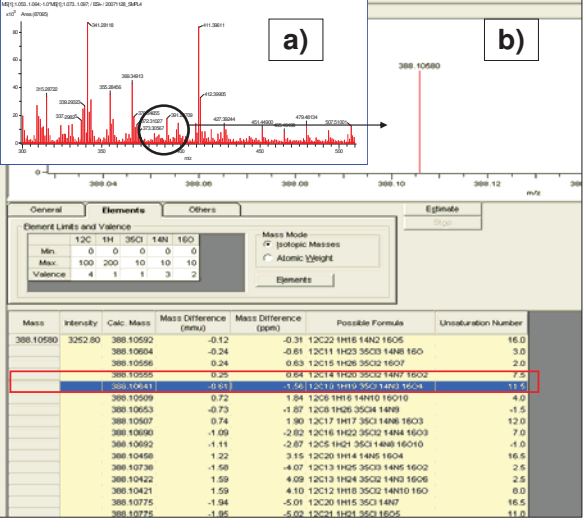


**Figure 4** a) Mass spectrum of wheat grains containing incurred residues of kresoxim-methyl. b) Estimated element composition from exact mass measurement. The highlighted column stands for target analyte.

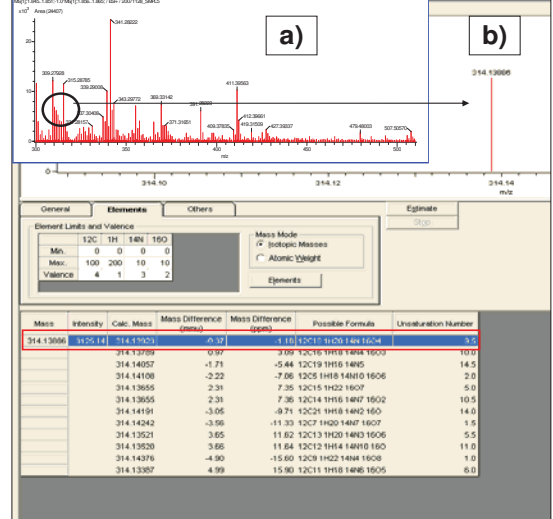


**Table 2** Strobilurins identified by exact mass after direct analysis of wheat grains containing incurred residues at different concentration levels.

Compound	Exact mass (mu)	Measured mass (mu)	Difference (mmu)	Elemental composition	Concentration (ppb)
Azoxystrobin	404.12465	404.12450	-0.14	C <sub>22</sub> H <sub>18</sub> N <sub>3</sub> O <sub>4</sub>	445
Kresoxim methyl	314.13923	314.13886	-0.37	C <sub>14</sub> H <sub>10</sub> N <sub>2</sub> O <sub>4</sub>	45
Pyraclostrobin	388.19641	388.10580	-0.61	C <sub>14</sub> H <sub>10</sub> N <sub>2</sub> O <sub>4</sub>	202

The quantification was performed using DART-TOF MS analysis of ethyl acetate extracts of wheat grains (prochloraz was used as internal standard).<sup>5</sup>

In this study, DART-TOFMS system has been demonstrated as a suitable tool for rapid screening of strobilurin fungicides, time and money consuming sample preparation and purification steps can be omitted. The exact mass measurements provide high degree of confirmation, enabled by elemental composition calculation of target analytes.

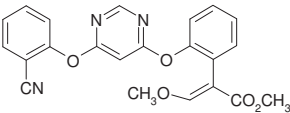
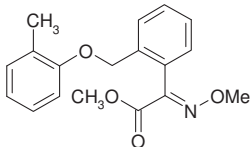
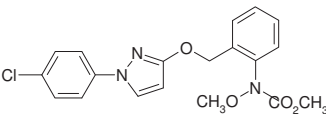
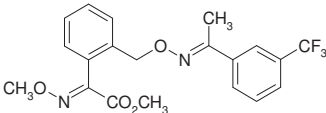
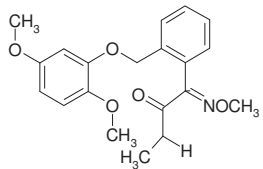
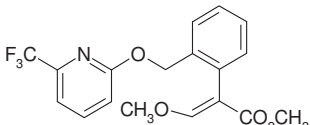
**References**

- Oerke, E.C., Dehne, H.W., Schonbeck, F., Weber, A., 1994. Crop Protection and Crop Production. Elsevier, Amsterdam, 808p
- Bartlett, D.W., Clough, J.M., Godwin, J.R., Hall, A.A., Hamer, M., Parr-Dobrzanski, B., 2002. Review: the strobilurin fungicides. *Pest Manage. Sci.* 58, 649–662.
- Sauter, H., Steglich, W., Anke, T., 1999. Strobilurins: evolution of a newclass of active substances. *Angew. Chem., Int. Ed.* 111, 1416–1438.
- [http://ec.europa.eu/food/plant/protection/resources/mrl\\_pesticide.pdf](http://ec.europa.eu/food/plant/protection/resources/mrl_pesticide.pdf)
- JEOL application report: Analysis of strobilurins in wheat grains using DART-TOFMS, 2008.

## ***Analysis of strobilurins in wheat grains using DART-TOFMS***

Strobilurins, systemic pesticides originated from natural fungicidal derivatives, play an important role in control of various plant pathogens.<sup>1,2,3</sup> Because of their unique protective properties, significant yield enhancements and longer retention of green leaf tissue, strobilurins have been widely used in agriculture since their introduction on the market in 1992.<sup>3</sup> As other pesticides, these compounds are involved in control and monitoring surveys undertaken by regulation authorities.<sup>4</sup> Some characteristics of strobilurins are shown in Table 1.

**Table 1** Strobilurins: structure and MRLs in wheat.

Compound	CAS number	Structure	MRL (mg/kg) in wheat		
			UK	Codex	EU
Azoxystrobin	131860-33-8		0.3	none	0.3
Kresoxim methyl	143390-89-0		0.05	0.05	0.05
Pyraclostrobin	175013-18-0		0.2	none	none
Trifloxystrobin	141517-21-7		0.02 <sup>a</sup>	none	none
Dimoxystrobin	149961-52-4		0.05 <sup>b</sup>	none	none
Picoxystrobin	117428-22-5		0.05 <sup>b</sup>	none	0.05 <sup>a</sup>

<sup>a</sup> proposed MRL, <sup>b</sup> temporary MRL

The AccuTOF-DART system equipped with an AutoDart HTC PAL autosampler was used for the analysis of strobilurin residues (listed in Table 1) in wheat grain extracts. Crude extracts were prepared by shaking 12.5 g of sample with 50 mL of ethyl acetate and 5 mL of Na<sub>2</sub>SO<sub>4</sub>, the suspension was then filtered and the volume was made up to 25 mL by rota vapour. Within the validation, extracts spiked with strobilurins in the range from 12 to 1200 ng/g were analyzed. For quantitative analysis, prochloraz was used as an internal standard (samples were spiked with this internal standard at a level of 250 ng/g).

The DART ion source was operated in positive ion mode with helium as the ionizing medium at a flow rate of 2.7 L/min. The gas beam was heated to 300 °C, and the optimal distance between the exit of the DART gun and inlet of the mass spectrometer was 12 mm. The discharge needle voltage set to positive potential of 3000 V, perforated and grid electrode voltages were +150 V and +250 V, respectively. Accurate mass spectra were acquired in a range of *m/z* 100–500 employing 0.2 s recording interval; the peaks voltage value was set to 1000 V. A solution containing a mixture of poly(ethylene glycol) PEG 600 and 200 was used for mass calibration. The same calibrant was introduced at the end of each sample analysis to compensate any mass drift. The mass resolution of the mass spectrometer was typically 6000 ± 500 (FWHM).

The examined samples were introduced automatically with the use of an AutoDart sampler and Dip-it™ tips. A sampling tip was immersed into the sample and then placed in front of the DART gun exit close to the source – mass spectrometer axis. Each sample was examined in six repeated runs. The TIC chromatogram of spiked wheat sample is shown in Figure 1. Due to the variability of absolute responses, the use of internal standard is obviously essential for quantitative measurements.

Figure 1 TIC chromatogram: “on-line” 6 repeated injections of spiked wheat extract followed by PEG mixture.

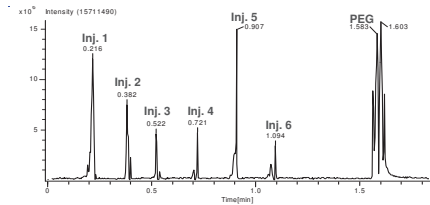


Figure 2 shows a positive-ion DART mass spectrum of crude ethyl acetate wheat extract spiked with strobilurins. Under these experimental conditions, both strobilurins and internal standard were detected as [M+H]<sup>+</sup>. In Table 2, measured and exact masses are compared, the differences ranged from -1.95 to 2.51 mmu.

Figure 2 Strobilurins (240 ng/g) and prochloraz (250 ng/g) in wheat extract.

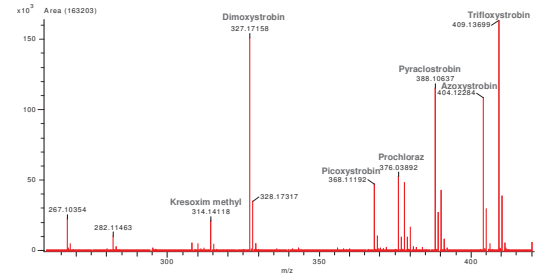


Table 2 Strobilurins identified in wheat extract by exact mass

Compound	Exact mass (mu)	Measured mass (mu)	Difference	Elemental composition
	[M+H] <sup>+</sup>	[M+H] <sup>+</sup>	(mmu)	[M+H] <sup>+</sup>
Azoxystrobin	404.12465	404.12284	1.81	C <sub>22</sub> H <sub>18</sub> N <sub>2</sub> O <sub>5</sub>
Kresoxim methyl	314.13923	314.14118	-1.95	C <sub>18</sub> H <sub>20</sub> NO <sub>4</sub>
Pyraclastrobin	388.19641	388.10637	0.04	C <sub>19</sub> H <sub>19</sub> ClN <sub>2</sub> O <sub>4</sub>
Trifloxystrobin	409.13752	409.13699	2.51	C <sub>20</sub> H <sub>18</sub> F <sub>3</sub> N <sub>2</sub> O <sub>4</sub>
Dimoxystrobin	327.17087	327.17158	-0.71	C <sub>18</sub> H <sub>16</sub> N <sub>2</sub> O <sub>5</sub>
Picoxystrobin	368.11097	368.11192	-0.95	C <sub>18</sub> H <sub>17</sub> F <sub>2</sub> NO <sub>4</sub>
Prochloraz	376.03864	376.03892	-0.28	C <sub>15</sub> H <sub>16</sub> Cl <sub>2</sub> N <sub>2</sub> O <sub>2</sub>

As Figure 3 shows, acceptable linearity was obtained for the analytes in the range from 12 to 1200 ppb.

The repeatability of measurements at a spiking level of 60 ng/g was in the range 8–15% (*n* = 6), limits of quantification (LOQs) ranged from 12 to 30 ng/g depending on the particular analyte. To prove the trueness of generated data, wheat grains with incurred strobilurin residues (reference material) were employed. Table 3 documents good agreement between the data obtained by DART-TOFMS and accredited LC-MS/MS method.

Figure 3 Calibration plots of strobilurins (analyte to internal std. intensity ratio plotted versus analyte concentration).

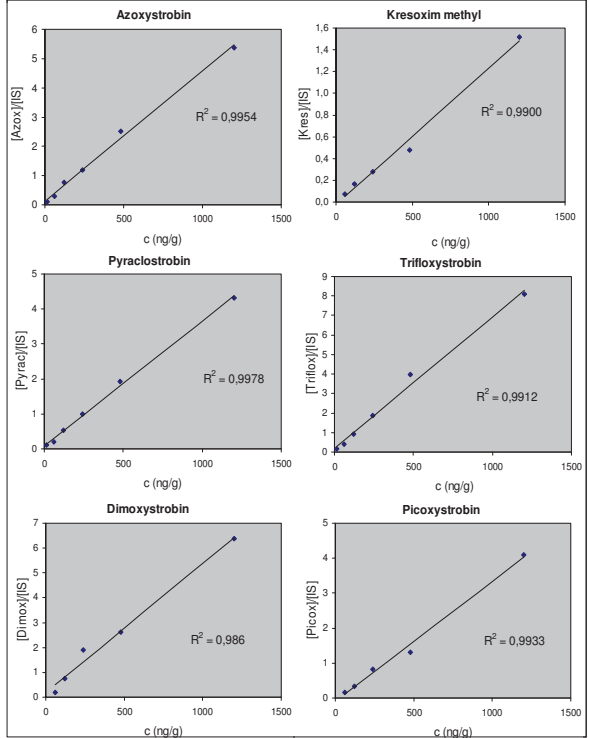


Table 3 Comparison of DART-TOFMS and LC-MS/MS method: analysis of wheat grain reference material.

Analyte	Concentration (ppb)	
	DART-TOFMS	LC-MS/MS
Azoxystrobin	445	429
Kresoxim methyl	45	52
Pyraclastrobin	202	170

Compared to conventional LC-MS/MS method, DART-TOFMS allowed significant decrease of analysis time, thus, enabled increase of sample throughput.

Although the detection limits are somewhat higher employing this new strategy as compared to the LC-MS/MS method, the DART-TOFMS enables convenient control of MRLs set for strobilurin residues in wheat grains which are in the range from 0.05 to 0.3 mg/kg.

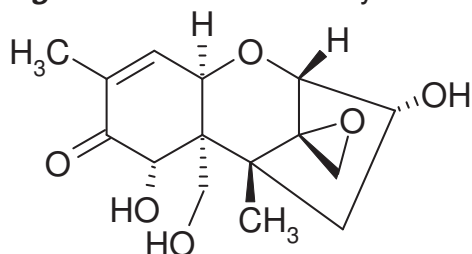
References

1. Oerke, E.C., Dehne, H.W., Schonbeck, F., Weber, A., 1994. Crop Protection and Crop Production. Elsevier, Amsterdam, 808p  
2. Bartlett, D.W., Clough, J.M., Godwin, J.R., Hall, A.A., Hamer, M., Parr-Dobrzanski, B., 2002. Review: the strobilurin fungicides. *Pest Manage. Sci.* 58, 649–662.  
3. Sauter, H., Steglich, W., Anke, T., 1999. Strobilurins: evolution of a newclass of active substances. *Angew. Chem., Int. Ed.* 111, 1416–1438.  
4. [http://ec.europa.eu/food/plant/protection/resources/mrl\\_pesticide.pdf](http://ec.europa.eu/food/plant/protection/resources/mrl_pesticide.pdf)

## ***Analysis of deoxynivalenol in beer***

Mycotoxins, toxic secondary metabolites of several fungal species, represent food safety issue of high concern. Deoxynivalenol (Figure 1), the most abundant trichothecene mycotoxin, can be found world-wide as a contaminant of wheat, barley, maize and other cereals.<sup>1,2</sup> The transmission of deoxynivalenol from barley into beer has been reported in several studies.<sup>3,4</sup> Therefore, its levels should be controlled.

**Figure 1** Structure of deoxynivalenol, trichothecene B *Fusarium* toxin.



The AccuTOF-LC time-of-flight mass spectrometer equipped with a DART ion source and AutoDart HTC PAL autosampler, was used for examination of beer in this study. Donprep<sup>®</sup> immunoaffinity columns (R-Biopharm) was employed for selective isolation of target analyte from the sample. Briefly, 10 mL of beer with added internal standard (<sup>13</sup>C<sub>15</sub>-deoxynivalenol, 500 ng/ml) were passed through the cartridge, which was then washed with 5 mL of water. Deoxynivalenol was subsequently eluted with 4.5 mL of methanol. Calibration standards containing deoxynivalenol in the range from 100 to 1500 ng/mL and fixed amount of internal standard (500 ng/mL) were prepared for quantification.

Introduction of the sample ( $n = 5$ ) into the gas beam was carried out automatically with the use of autosampler. Beer extract was placed in the sampling hole, Dip-it<sup>™</sup> sampler stick was immersed into the sample and introduced in front of the DART ion source (Figure 2). After each sample analysis, PEG mixture solution was injected for mass drift compensation. TIC chromatogram of beer sample analysis is shown in Figure 3.

Figure 2 Sample introduction.

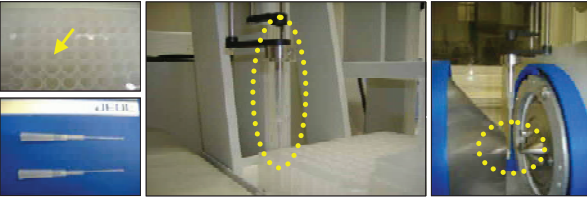
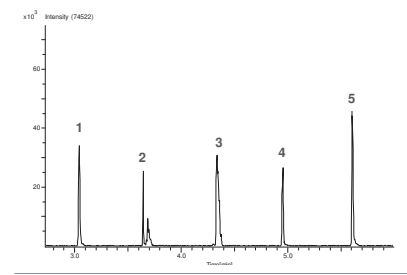


Figure 3 Repeated injections of beer sample.



To enhance negative ionization of target analytes, vial containing methylene chloride was placed beneath DART gun exit – MS orifice axis. After sample introduction, both deoxynivalenol and <sup>13</sup>C<sub>15</sub>-deoxynivalenol were immediately detected as [M+Cl]<sup>-</sup> (see Figure 4) under parameters setting shown in Table 1. Good mass accuracy was obtained (see Table 2).

**Table 1** Optimized DART ion source parameters

Parameter	Setting
Polarity	negative
Helium flow rate	2.7 L/min
Discharge needle voltage	3000 V
Perforated electrode voltage	-150 V
Grid electrode voltage	-250 V
Gas beam temperature	300 °C

Figure 4 Positive DART spectrum: deoxynivalenol and internal standard in beer extract.

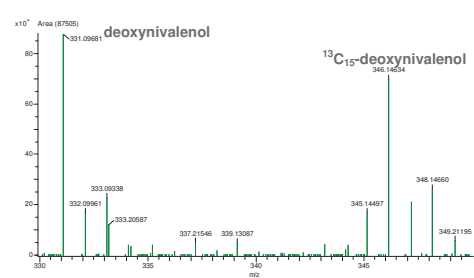
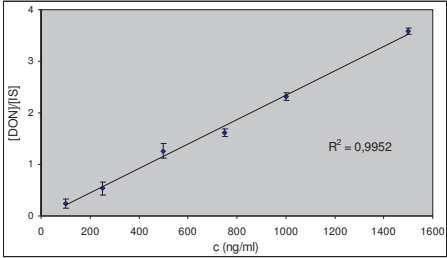


Table 2 Comparison of exact and measured masses.

Compound	Exact mass (mu)	Measured mass (mu)	Difference (mmu)	Elemental composition [M+Cl] <sup>-</sup>
Deoxynivalenol	331.09484	331.09681	-1.97	C <sub>15</sub> H <sub>20</sub> O <sub>6</sub> Cl
<sup>13</sup> C <sub>15</sub> -Deoxynivalenol	346.14516	346.14634	-1.18	<sup>13</sup> C <sub>15</sub> H <sub>20</sub> O <sub>6</sub> Cl

In Figure 5, calibration plot of deoxynivalenol is shown; analyte to internal standard ratio was linear in selected concentration range. Deoxynivalenol concentration determined with the use of DART-TOFMS in particular beer sample was 166 µg/L and repeatability of the method, estimated from five repetitive analyses, was 3%. In addition, accredited LC-MS/MS method was used for sample examination to confirm the trueness of results obtained by DART-TOFMS. The difference between deoxynivalenol obtained by respective methods was as low as 14 µg/mL.

Figure 5 Calibration curve.

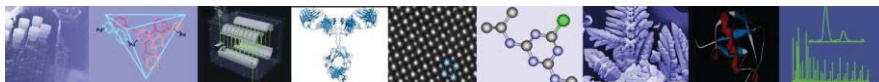


In conclusion, AccuTOF-DART has been demonstrated as a suitable to screen for deoxynivalenol in beer samples purified by simple procedure employing immunoaffinity columns.

References

- Hussein, H. S.; Brasel, J. M.: Toxicity, metabolism, and impact of mycotoxins on humans and animals, *Toxicology*, 167, 2001, 101-134.
- Wiedenbörner, M.: Encyklopedia of food mycotoxins, Springer, Berlin.
- Scott, P. M.: Mycotoxins transmitted into beer from contaminated grains during brewing, *Food Chemical Contaminants*, 79, 1996, 875-882.
- Papadoulou-Bouraoui, A.; Vrabcheva, T.; Valzacchi, S.; Stroka, J.; Anklam, E.: Screening survey of deoxynivalenol in beer from the European market by an enzyme-linked immunosorbent assay, *Food Additives and Contaminants*, 21, 2004, 607-617.





## AccuTOF-DART<sup>®</sup> Analysis of Smokeless Powders

### Introduction

Smokeless powders (Figure 1) are often used in improvised explosive devices. The formulations for smokeless powders vary between manufacturers and between brands from a given manufacturer; ingredients include energetics, stabilizers, plasticizers and deterrents. Chemical analysis of smokeless powders can provide valuable forensic evidence. Here we show that the AccuTOF-DART mass spectrometer can rapidly identify the organic components in smokeless powders and provide a chemical fingerprint that can be used to identify individual powder particles.



Figure 1. Several smokeless powders viewed under an optical microscope.

### Experimental

The AccuTOF<sup>™</sup> mass spectrometer was operated in positive-ion mode. Polyethylene glycol (PEG-600) was measured as a reference standard within each data file, but separate from the smokeless powder particle measurements. Individual particles sampled with vacuum tweezers were positioned in the DART gas stream for analysis (Figure 2). Disposable vacuum tweezers were constructed by passing a glass capillary through an Eppendorf pipette tip and inserting the pipette tip into a rubber hose connected to a low-vacuum pump. Data were acquired by using JEOL Mass Center software and mass spectra were processed by TSSPro3 software (Shrader Software Solutions, Detroit, MI).

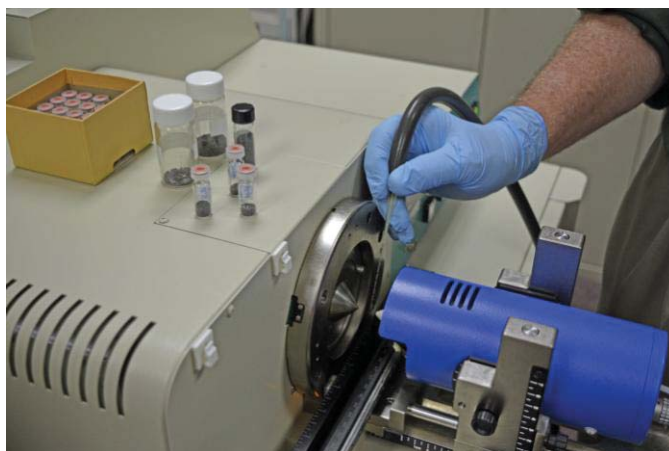
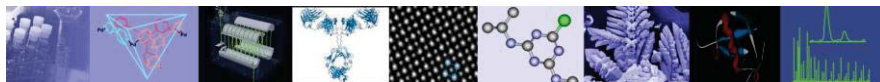


Figure 2. AccuTOF-DART analysis of a smokeless powder particle.



The DART ion source was operated with a gas heater temperature setting of  $\leq 200^{\circ}\text{C}$  to avoid damaging or detonating the smokeless powder particles. Individual samples could be analyzed within seconds. As long as the gas heater temperature did not exceed  $200^{\circ}\text{C}$ , the samples were not consumed and could be examined or reanalyzed at a later time.

A list of target compounds commonly used in smokeless powders was created in a Microsoft Excel spreadsheet. The spreadsheet contained the names and elemental compositions of the target compounds. The target compound spread sheet was used by Mass Mountaineer software ([www.mass-spec-software.com](http://www.mass-spec-software.com)) to identify compounds in the smokeless powder mass spectra based upon exact masses and isotopic data. The Mass Mountaineer program also allowed us to create and search mass spectral databases created from the mass spectra of smokeless powder standards.

## Results

The AccuTOF-DART mass spectra for several smokeless powders are shown in Figure 3a and 3b. The DART mass spectra show unique patterns of organic components typically detected as protonated molecules  $[M + H]^+$ . Because some samples from the same manufacturer showed the same organic components, but had different morphology, it appears that both morphology and DART analysis will be required for a unique identification of a specific powder.

Because labeled compounds were tentatively identified by solely by exact mass and isotopic data, the presence of isomers cannot be ruled out. Regardless, the mass spectra are reproducible and distinctive, making it possible to identify unknown particles by comparison against database spectra.

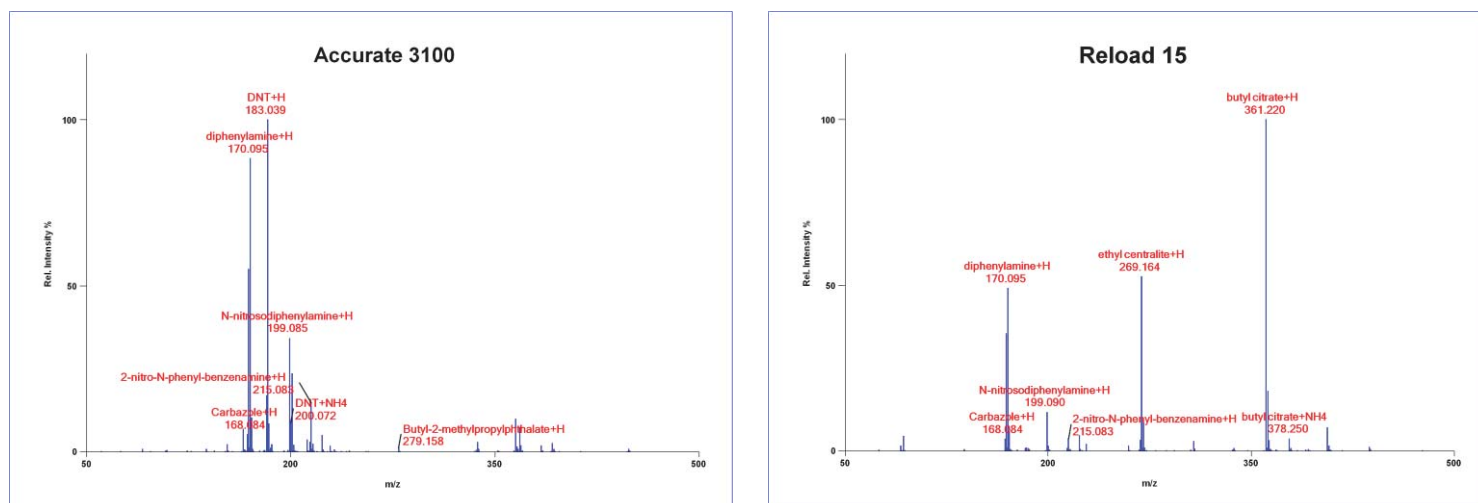


Figure 3. (a) AccuTOF-DART mass spectrum of an Accurate 3100 smokeless powder particle; (b) AccuTOF-DART mass spectrum of a Reload 15 particle.

## Conclusions

The AccuTOF-DART mass spectrometer is capable of rapid fingerprinting of organic compounds in smokeless powders. Although further work needs to be done to expand the database and validate the method, the AccuTOF-DART mass spectra (in combination with particle morphology) offer a rapid and potentially nondestructive approach for the identification of individual smokeless powder particles.

## Acknowledgement

We are grateful to John A. Meyers who suggested this work and provided background information and the initial set of smokeless powder samples that we analyzed at the 2008 Pittsburgh Conference on Analytical Chemistry and Applied Spectroscopy (PittCon).



## Fiber analysis by thermal desorption/pyrolysis DART®

### Introduction

Analyzing fiber samples has always been difficult by DART®. The problem has been that there is no easy way to hold the fiber in the gas stream without losing it into the vacuum system. A fiber can be secured in the DART gas stream with forceps or other means, but if the DART gas is too hot, the fiber can break off and be lost into the mass spectrometer vacuum system through the atmospheric pressure interface.

A thermal desorption/pyrolysis stage (The Biochromato, Inc. "ionRocket™") designed for use with DART produces highly reproducible thermal desorption profiles that show outgassing, additives, and high-quality pyrolysis DART mass spectra for materials. Because fiber samples placed in the disposable copper sample "pots" are not positioned directly in the DART gas stream, a single fiber can be analyzed without risk of loss into the vacuum system.

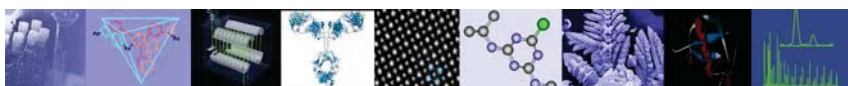
### Experimental

Mass spectra were acquired by using a JEOL AccuTOF™-DART® 4G mass spectrometer (Figure 1) equipped with a Biochromato, Inc. *ionRocket* thermal desorption and pyrolysis system (<http://biochromato.com/ionrocket/>).

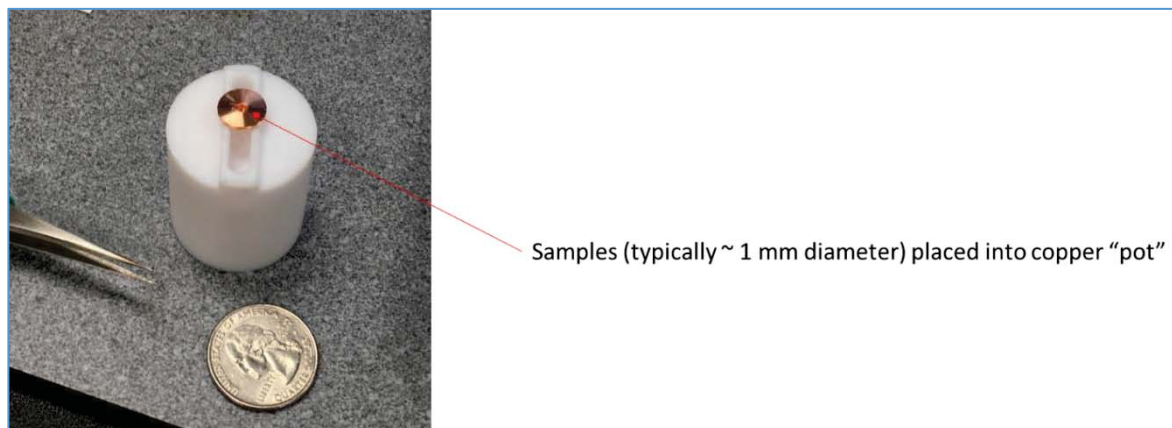


Figure 1. The ionRocket thermal desorption/pyrolysis system mounted on the AccuTOF-DART 4G mass spectrometer





A single fiber or a small clump of fibers was placed into a disposable copper sample stage (or “pot”) for the *ionRocket* (Figure 2).



*Figure 2. A copper pot used as a sample holder for the ionRocket*

The copper sample stage was placed onto the *ionRocket* heater (Figure 3) and moved into position between the exit of the DART ion source and the sampling orifice of the *AccuTOF-DART 4G* mass spectrometer. A glass tee positioned above the sample (Figure 4) guides the thermal desorption and pyrolysis products into the DART gas stream.

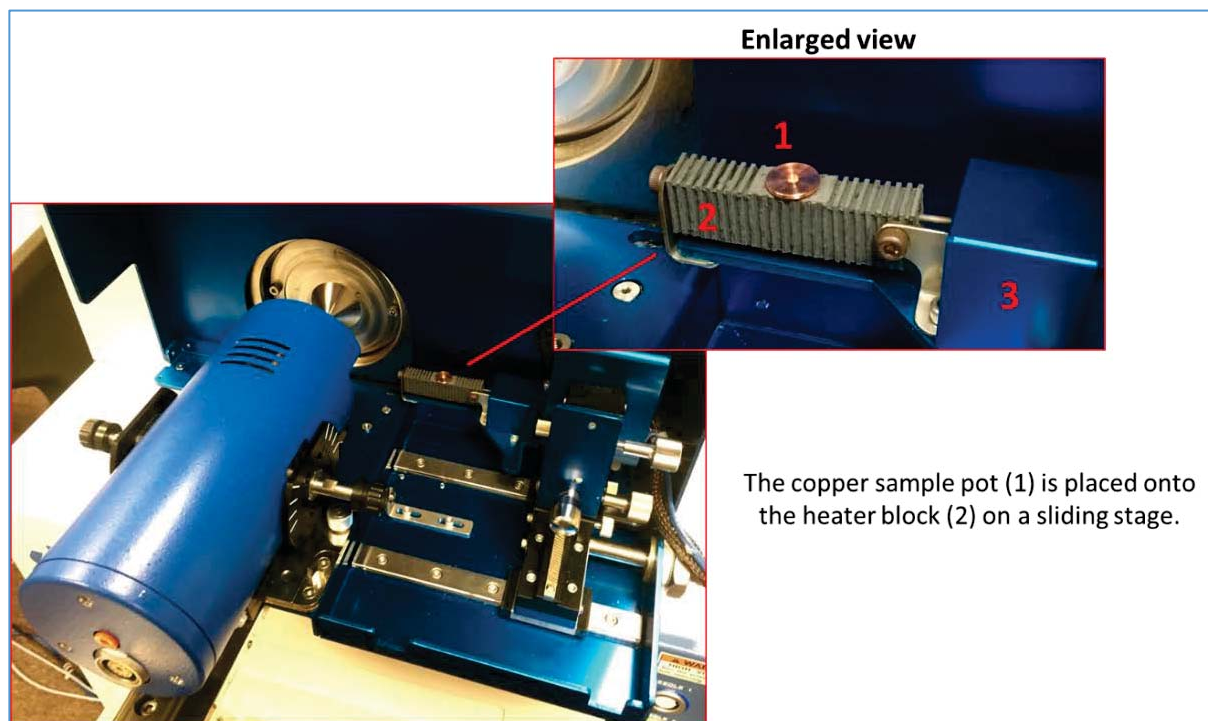
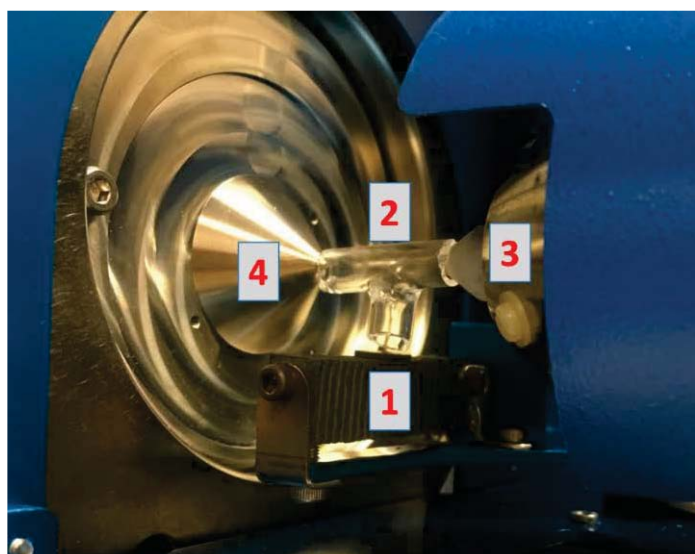


*Figure 3. A sample mounted onto the ionRocket heater block.*



The sample pot and heater block (1) slide into position below a glass tee (2) mounted between the DART exit (3) and the mass spectrometer sampling orifice (4).

Figure 4. A sample mounted on the heater block, positioned below a glass tee.

The temperature ramp was programmed from ambient temperature to 600°C at a rate of 100°C min<sup>-1</sup>. Mass spectra were acquired at a resolving power of 10,000 in positive-ion mode at a spectral acquisition rate of 1 spectrum per second for the  $m/z$  range 50-1000.

## Results

### Carpet fiber

A small tuft of fibers from the carpet in the JEOL booth at PittCon 2016 was placed onto a copper sample holder for the *ionRocket* and analyzed by the *AccuTOF-DART*. The thermal desorption profiles of selected components are shown in Figure 5. Oleamide, a common stabilizer shows a maximum abundance at temperatures below 200°C. The stabilizer 2,5-di-*t*-butylhydroquinone maximizes at temperatures just above 200°C, and high- $m/z$  pyrolysis products from the polyolefin fiber maximize at temperatures above 400°C.

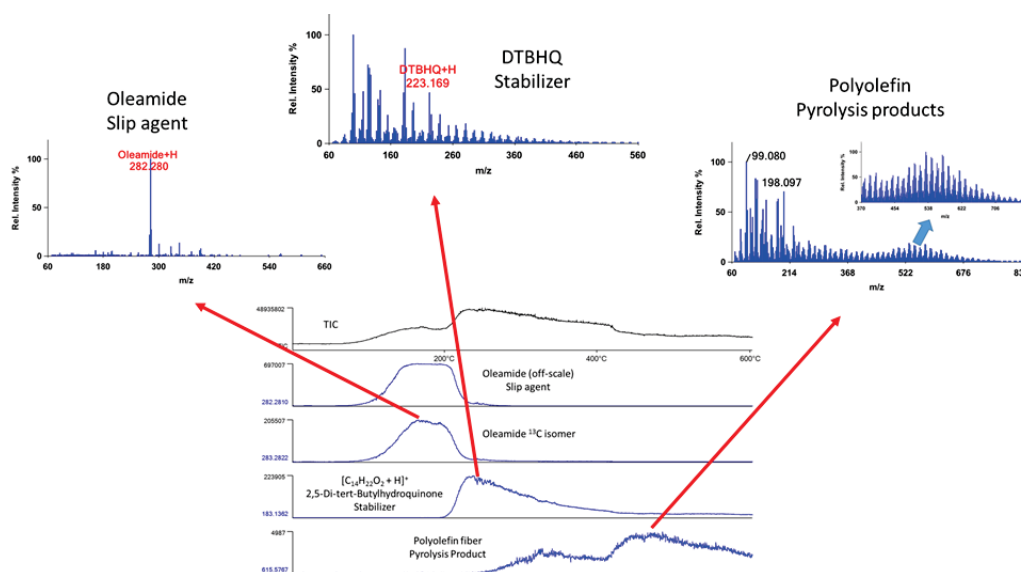
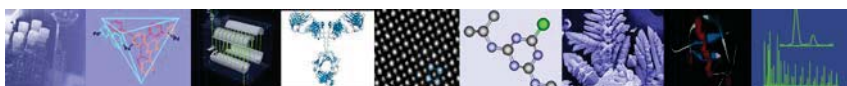


Figure 5. Thermal desorption profiles and mass spectra for components in carpet fiber.



### Fiber from a badge holder lanyard

A single fiber from the badge holder lanyard from PittCon 2016 was placed onto a copper sample holder for the *ionRocket* and analyzed by the *AccuTOF-DART* (Figure 6). At temperatures below 300°C, we detect additives such as dibutyl phthalate plasticizer. At higher temperatures, we detect pyrolysis fragments from the polyethylene terephthalate (PETE) polymer.

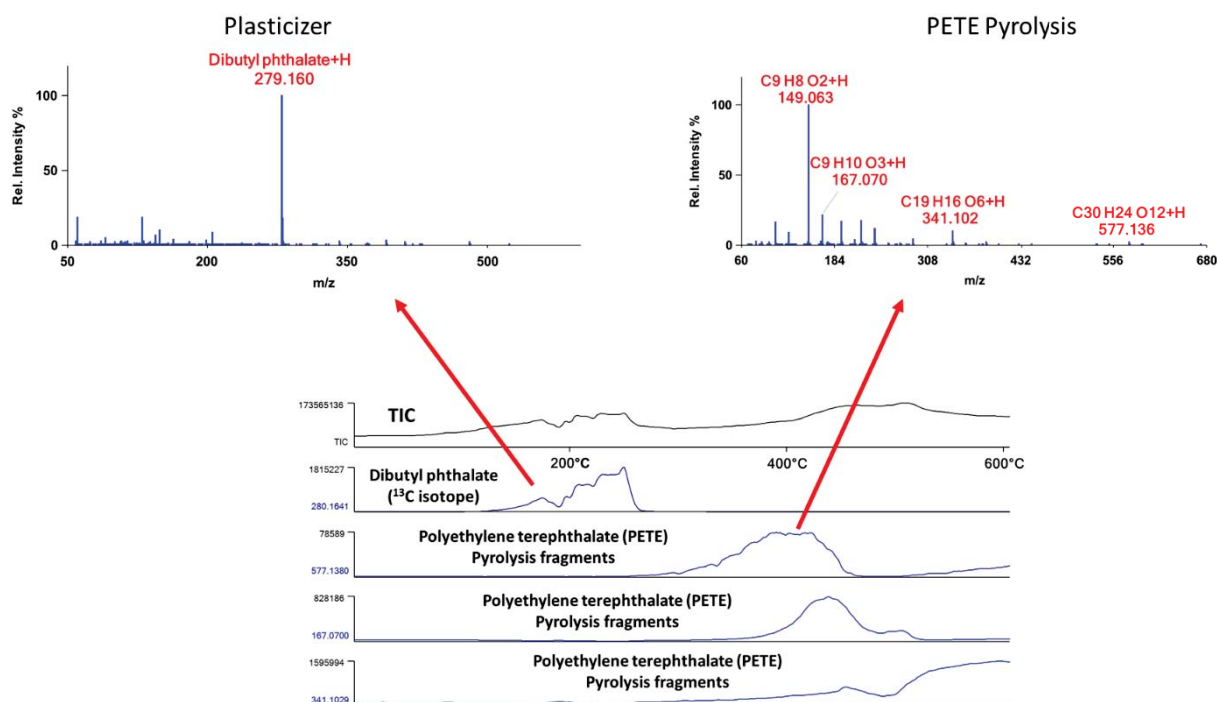


Figure 6. Thermal desorption profiles and mass spectra for components in a badge holder lanyard.

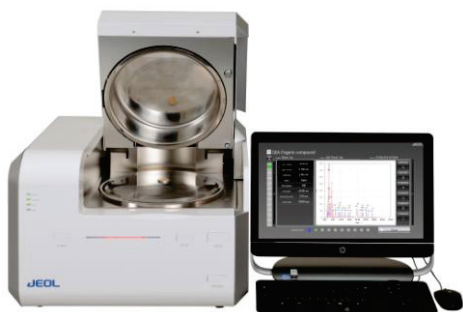
### Conclusion

Thermal desorption/pyrolysis with the *ionRocket* offers a convenient solution for the analysis of single fibers with the *AccuTOF-DART*. Accurate-mass and isotopic data measured by the *AccuTOF-DART* system allows us to detect additives and identify the base polymer. Because the fiber is not held directly in the DART gas stream, there is no risk of losing the fiber into the mass spectrometer vacuum system if the fiber decomposes upon heating.

# X-Ray Fluorescence Helps Identify Peaks in DART Mass Spectrum of Electrical Tape - ElementEye JSX-1000S and AccuTOF-DART



LC and Ambient Ionization HRTOF Mass Spectrometer JMS T100LP AccuTOF-DART™



X-ray Fluorescence Spectrometer JSX-1000S ElementEye

## Introduction

The identification of electrical tapes is important for forensic investigation of improvised explosive devices [1]. Pyrolysis mass spectrometry [2] and X-Ray Fluorescence (XRF) [3] are among the methods that are used for the forensic analysis of electrical tapes.

Direct Analysis in Real Time (DART) can be operated with a high gas temperature as an alternative to conventional pyrolysis GC/MS methods [4,5]. A sample of electrical tape analyzed with the AccuTOF-DART™ showed distinctive peaks in the negative-ion DART mass spectrum. No reasonable elemental compositions could be determined by assuming the presence of only the common organic elements: C, H, N, O, P, S, Cl, Si, and Br. X-ray fluorescence (XRF) data obtained with the ElementEye™ indicated the presence of Zn and Sb, allowing us to correctly assign the elemental compositions for the peaks observed in the DART mass spectrum.

## Experimental

A piece of electrical tape was placed in the DART gas stream with the DART gas heater set to 500°C (pyrolytic DART conditions). A sample of poly(perfluoropropyl ether) was measured in the same data file as a mass reference standard for exact mass measurements. Elemental compositions with isotope matching were determined by using Mass Mountaineer™ software. The XRF spectrum of the sample was measured with the ElementEye by using the Quick and Easy Organic Analysis method and the ElementEye reporting program. The collimator was set to 2 mm and the total analysis time was 60 seconds.

## Results and Discussion

The negative-ion DART mass spectrum in Figure 1 shows distinctive peaks with isotope patterns that suggest the presence of multiple halogens (chlorine and/or bromine). This is not unexpected considering that electrical tape can be made of polyvinyl chloride (PVC). However, no reasonable elemental composition assignments could be made by assuming only elements present in common organic polymers. To assign the elemental compositions, we needed additional information about which other elements might be present.

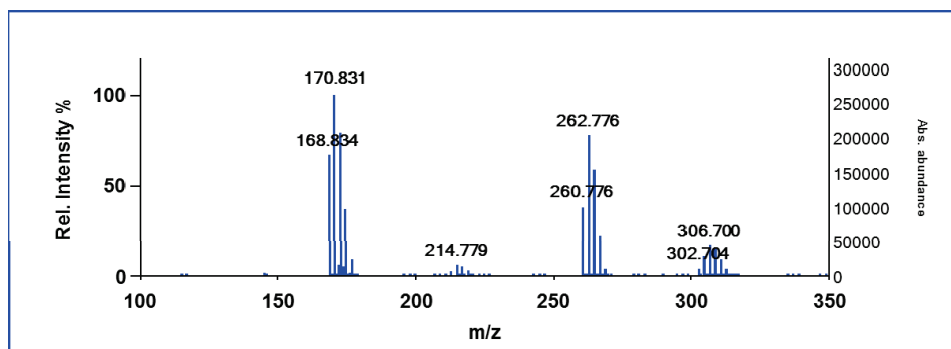
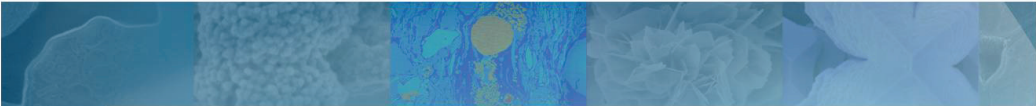


Fig. 1 Negative-ion AccuTOF-DART mass spectrum of a piece of electrical tape.





Among the elements detected in the XRF spectrum (Figure 2, Table 1) are antimony, zinc, chlorine and bromine. Adding these elements to the constraints for the elemental composition calculation for the AccuTOF-DART data allows us to correctly assign the elemental compositions for these peaks (Figure 3). The measured isotope peaks show excellent agreement with the calculated isotope patterns (Figure 4).

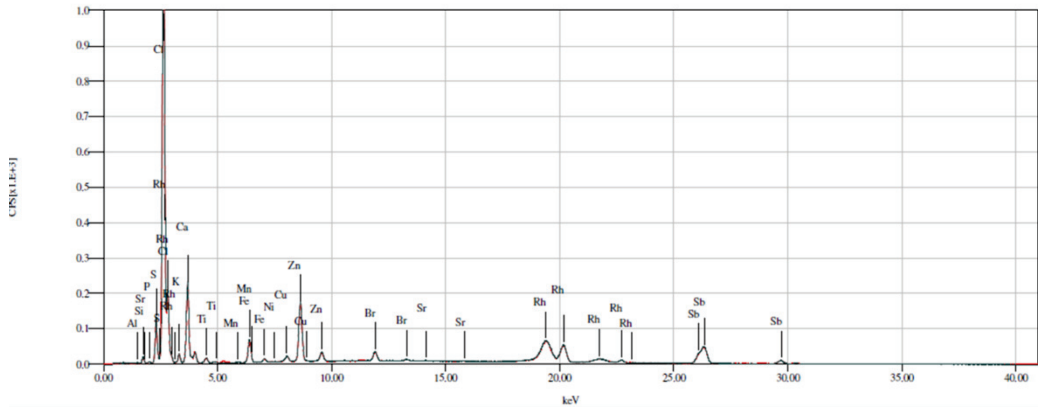


Fig. 2. XRF Spectrum of the electrical tape obtained with ElementEye

Analysis Target	Result	Unit	3sigma
Aluminium(Aluminu	1.01	%	0.30
Iron	0.18	%	0.00
Manganese	0.00	%	0.00
Nickel	0.00	%	0.00
Potassium(Kalium)	0.43	%	0.01
Silicon	1.38	%	0.05
Strontium	0.00	%	0.00
Titanium	0.10	%	0.00
Antimony(Stibium)	1.87	%	0.02
Copper	0.03	%	0.00
Zinc	0.27	%	0.00
Calcium	2.58	%	0.02
Sulfur	1.13	%	0.01
Phosphorus	0.09	%	0.01
Bromine	0.03	%	0.00
Chlorine	19.21	%	0.06

Table 1. Elements detected by the ElementEye

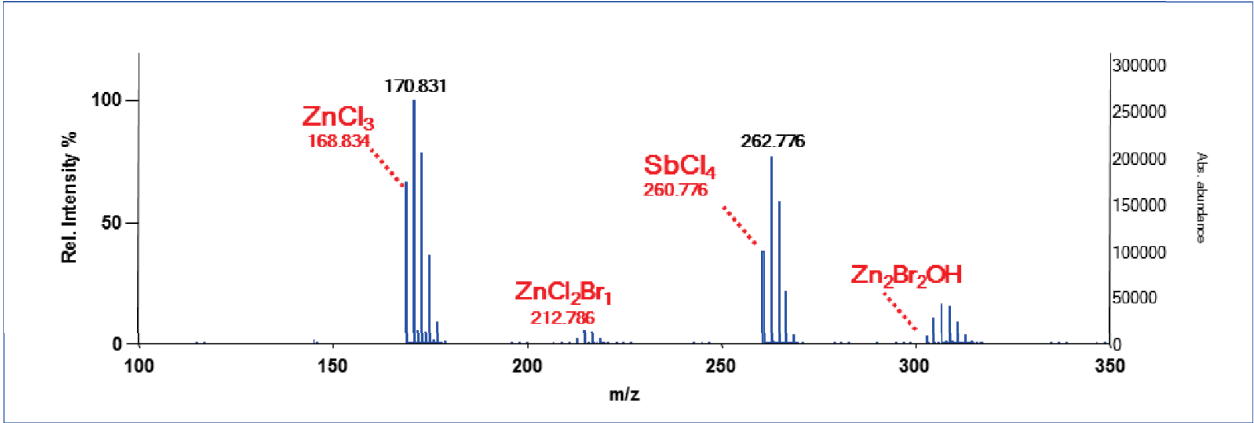


Fig. 3. Elemental composition assignments for the peaks in the mass spectrum from Figure 1 calculated after determining the presence of Zn, Sb, Cl, and Br from the XRF data.

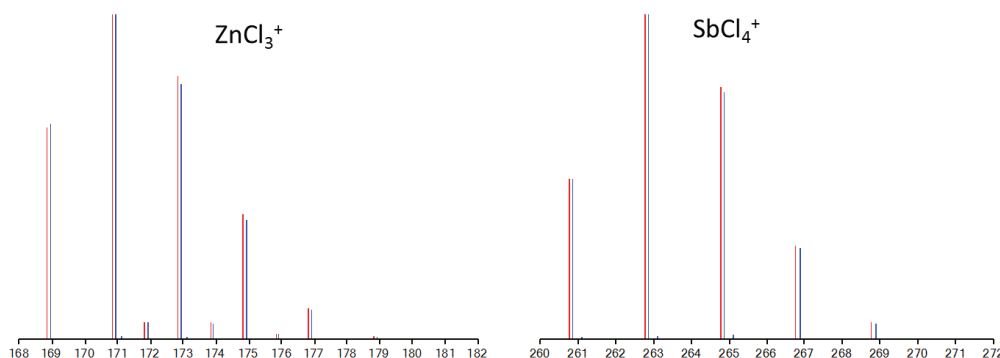


Figure 4. Comparison of calculated (red) and measured (blue) isotope peaks for  $\text{ZnCl}_3^+$  and  $\text{SbCl}_4^+$

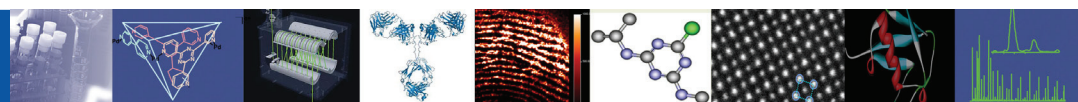
## Conclusion

Elemental composition assignments based on accurate mass and isotope measurements by mass spectrometry require the operator to provide a list of elements that may be present and their limits. If an element is omitted from the list, the correct assignment will not be reported. If too many elements are added to the list, the number of possible compositions becomes uninterpretable. The ElementEye is a rapid and convenient tool that provides complementary elemental information allowing us to assign the unknown peaks in the AccuTOF-DART data for the electrical tape sample.

## References

1. Scientific Working Group for Materials Analysis (SWGMA) Daubert Admissibility Package for Tape Evidence. <http://www.swgmat.org/Tape%20Admissibility%20Package.pdf>
2. (SWGMA), S. W. G. f. M. A. Standard Guide for Using Pyrolysis-Gas Chromatography and Pyrolysis-Gas Chromatography/Mass Spectrometry in Forensic Tape Examinations <http://www.swgmat.org/SWG%20tape%20PGC%20guideline.pdf>
3. Keto, R. O., Forensic Examination of Black Polyvinyl Chloride Electrical Tape. <http://swgmat.org/Keto-Characterization%20of%20PVC%20Tapes.pdf>.
4. Loftin, K. B., Development of Novel DART™ TOFMS Analytical Techniques for the Identification of Organic Contamination on Spaceflight-Related Substrates and Aqueous Media. Ph.D. Thesis, University of Central Florida, 2009
5. Lancaster, C.; Espinoza, E., Analysis of select Dalbergia and trade timber using direct analysis in real time and time-of-flight mass spectrometry for CITES enforcement. *Rapid Communications in Mass Spectrometry* **2012**, *26* (9), 1147-1156.





# AccuTOF-DART™

## Clandestine Methamphetamine Labs: Rapid Impurity Profiling by AccuTOF-DART™

### Introduction

Methamphetamine is a Schedule II Controlled Substance that is illegally manufactured in clandestine labs. There are several common synthetic pathways in use. For this study, methamphetamine was synthesized from phenyl-2-propanone by the (1) Leuckart synthesis or (2) Reductive Amination, or from ephedrine or pseudoephedrine by the (3) Nagai, (4) Birch, and (5) Edme syntheses. Each of these reaction sequences resulted in unique impurity profiles<sup>1-3</sup> that can be used by law enforcement to track the activities of clan labs, distribution networks, and trafficking patterns. The AccuTOF-DART was used to examine the starting materials, reaction mixtures, and final products from each reaction scheme.

### Experimental

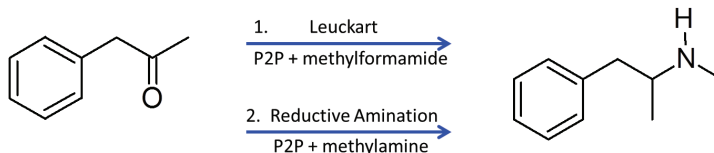
A JEOL AccuTOF-DART mass spectrometer was used for all measurements. Samples were deposited on the sealed end of melting point tubes and measured in positive-ion mode with helium DART gas and a gas heater setting of 350°C. Polyethylene glycol (average MW 600) was used as a reference standard for exact mass measurements.

### Results

Examples are given of the DART mass spectra measured for methamphetamine synthesized by the Birch (Figure 2) and Nagai (Figure 3) synthetic methods.

### Meth Synthetic Pathways

#### • Phenyl-2-propanone (P2P)



#### • Ephedrine/Pseudoephedrine

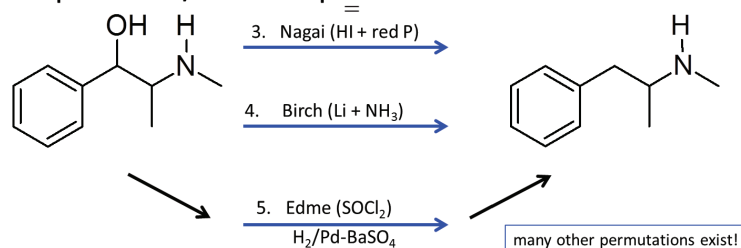


Figure 1. Common synthetic pathways for the illicit manufacture of methamphetamine.

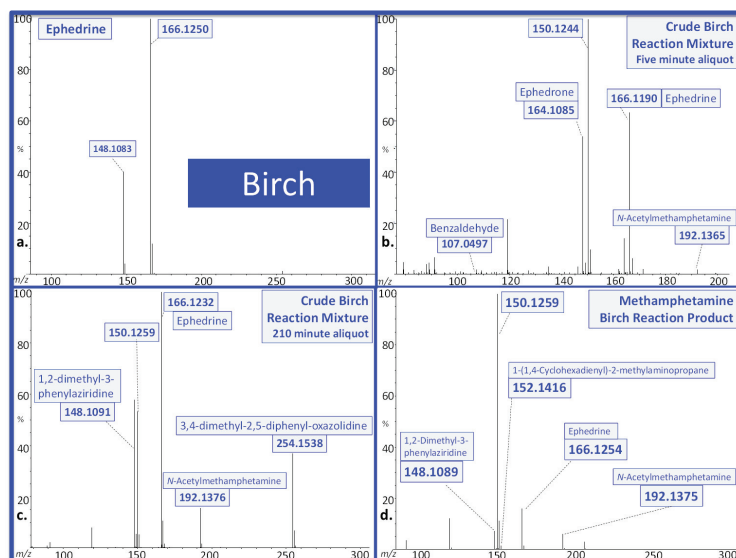


Figure 2. AccuTOF-DART mass spectra for ephedrine, crude reaction mixture at two different reaction times, and the final reaction product of a Birch synthesis.

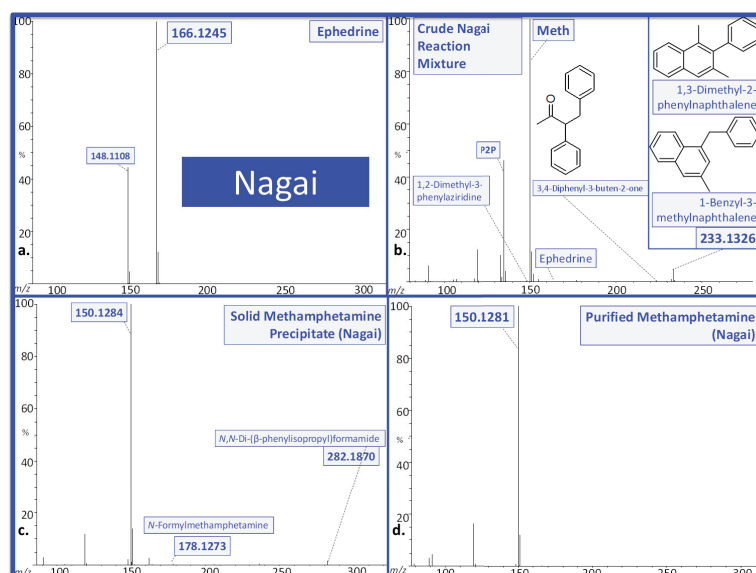


Figure 3. AccuTOF-DART mass spectra for the ephedrine starting material, reaction mixture, methamphetamine precipitate, and purified methamphetamine from a Nagai synthesis.

## Conclusion

The AccuTOF-DART can provide rapid impurity profiling that can be used by law enforcement to characterize the starting products, reaction mixtures, and semi-purified final products for methamphetamine manufactured in clandestine laboratories. The results support and complement the alternative GC/MS methods.

## Acknowledgement

These data were provided by Prof. Jason Shepard. A more complete discussion of these results for all five reaction methods will be found in a forthcoming publication (reference 4).

## References

1. Andersson, K.; Lock, E.; Jalava, K.; Huizer, H.; Jonsson, S.; Kaa, E.; Lopes, A.; Poortman-van der Meer, A.; Sippola, E.; Dujourdy, L.; Dahlén, J., Development of a harmonised method for the profiling of amphetamines VI. *Forensic Science International* 2005 169 (1), 86-99.
2. Dujourdy, L.; Dufey, V.; Besacier, F.; Miano, N.; Marquis, R.; Lock, E.; Aalberg, L.; Dieckmann, S.; Zrcek, F.; Bozenko, J. S., Jr., Drug intelligence based on organic impurities in illicit MA samples. *Forensic Science International* 2008 177 (2), 153-161.
3. Kunalan, V.; Nic Daéid, N.; Kerr, W. J.; Buchanan, H. A. S.; McPherson, A. R., Characterization of Route Specific Impurities Found in Methamphetamine Synthesized by the Leuckart and Reductive Amination Methods. *Analytical Chemistry* 2009, 81 (17), 7342-7348.
4. Shepard, J., manuscript in preparation. 2014.

## “Laundry Detective”: Identification of a Stain

The AccuTOF-DART™ was recently applied to an unusual analytical problem: finding the cause of oily stains on freshly laundered shirts (Figure 1). No cutting or extraction was required. Stained and unstained regions of the shirt were placed in the DART gas stream and the mass spectra were acquired.

The DART parameters were: helium gas, flow 3-4 LPM, gas heater set to 175 degrees C, positive-ion mode, PEG 600 exact mass reference standard. These conditions did not damage the shirt.

The mass spectrum of the stained region (Figure 2, top) showed a distinctive pattern of saturated fatty acids and their proton-bound dimers, monoglycerides, and triethanolamine. The same components were found in the dryer sheet (Figure 2, bottom). Elemental composition assignments were confirmed by exact mass measurements and computer-aided isotope pattern matching. The assignment of the fatty acids was confirmed by the presence of  $[M-H]^-$  peaks in the negative-ion DART spectrum (not shown). Fatty acid esters will not produce  $[M-H]^-$  peaks in negative-ion mode. After considering several possible sources of contamination, a matching pattern was found for the bargain-price fabric softener sheet that was placed in the clothes dryer with the shirts. The components causing the stains were released when the dryer sheet was exposed to high temperatures.

### Conclusion

AccuTOF-DART was able to determine the nature and cause of oily stains on a shirt without causing any damage to the fabric. Solutions to the problem include lowering the dryer temperature, changing to a different brand of fabric softener, and re-washing the shirts.

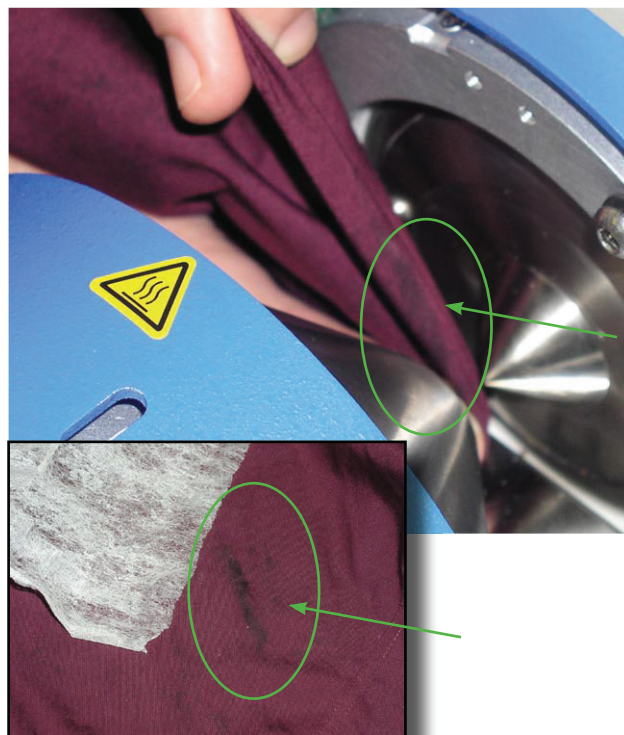


Figure 1. Oily stain on a freshly laundered shirt placed in between DART ion source and AccuTOF mass spectrometer inlet. Inset: stain on shirt circled next to used dryer sheet.

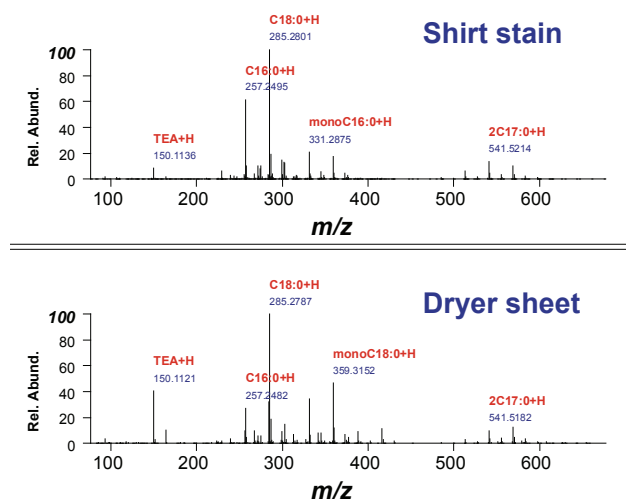


Figure 2. (Top) AccuTOF-DART mass spectrum of stain on shirt. (Bottom) AccuTOF-DART mass spectrum of fabric softener sheet placed in the dryer with the shirts.



## Direct analysis of stains on cloth caused by cosmetic

Product used : Mass Spectrometer (MS)

Foundation is one of the essential cosmetics for women. At the mean time, it often makes a stain on clothing. We directly analyzed foundation stains on cloth (Fig. 1) without sample preparation by using DART (Direct Analysis in Real Time) ion source installed on AccuTOF™ LC series. Foundation from 3 manufacturers were measured and compared.

Helium was used as the DART gas. The DART gas heater was set to 200 °C. A small piece of cloth on which foundation was deposited was presented to the DART ion source.

Ions at  $m/z$  371 were observed from the foundation of all 3 manufacturers. Based on the measured accurate masses, the elemental formula of the ions was elucidated to be  $C_{10}H_{31}O_5Si_5$  and inferred to be the  $[M+H]^+$  ions of decamethylcyclopentasiloxane. Ions at  $m/z$  223 were found only from Bland A and their elemental composition was elucidated to be  $C_{10}H_{15}O_2Si_2$  from the measured accurate  $m/z$ .

By using DART ion source, the nature and cause of stains on cloth can be determined without sample preparation.

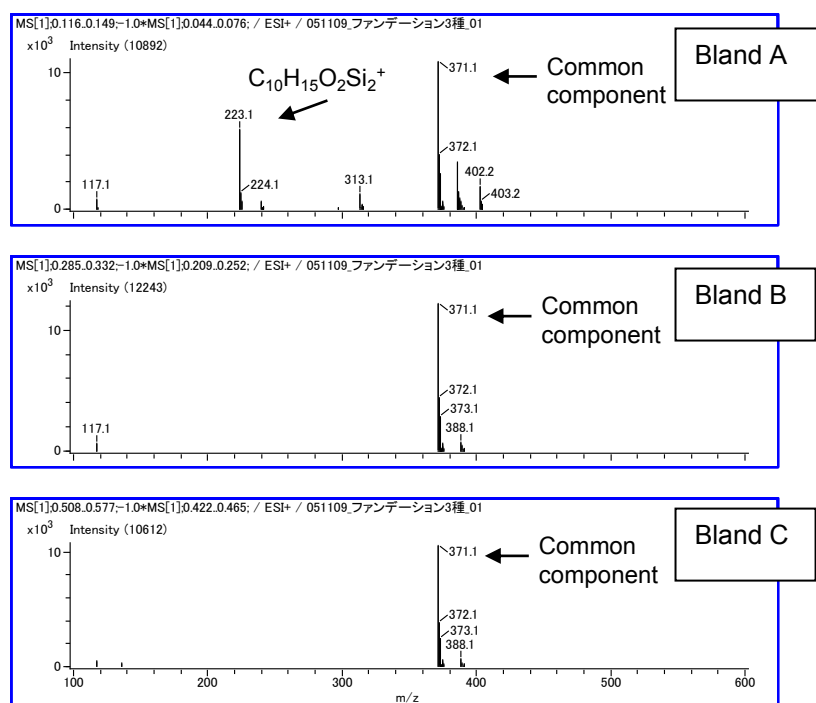


Fig. 1 A foundation stain on a piece of cloth.

Fig. 2 Mass spectra of foundation stains (Top: Bland A, Middle: Bland B, Bottom: Bland C)

Measured $m/z$	Calculated $m/z$	Error ( $\times 10^{-3}$ )	Elemental composition	Unsaturation
223.06194	223.06106	0.88	$C_{10}H_{15}O_2Si_2$	5.5
371.10100	371.10178	-0.78	$C_{10}H_{31}O_5Si_5$	0.5

Table 1 Elucidated elemental compositions of the ions found in the mass spectrum of Bland A.

Copyright © 2016 JEOL Ltd.

Certain products in this brochure are controlled under the "Foreign Exchange and Foreign Trade Law" of Japan in compliance with international security export control. JEOL Ltd. must provide the Japanese Government with "End-user's Statement of Assurance" and "End-use Certificate" in order to obtain the export license needed for export from Japan. If the product to be exported is in this category, the end user will be asked to fill in these certificate forms.

## Detection of the Peroxide Explosives TATP and HMTD

### Introduction

The explosive peroxide compounds triacetone triperoxide (TATP) and hexamethylenetriperoxide diamine (HMTD) are difficult to detect by conventional mass spectrometry methods. These compounds can be easily detected by the Direct Analysis in Real Time (DART™) ion source.

### Experimental

Measurements were made with the AccuTOF-DART mass spectrometer operated in positive-ion mode under standard conditions. Little or no heat was required to observe these compounds. Dilute solutions of standard samples of TATP and HMTD were analyzed by dipping melting point tubes into the liquid and dangling the melting point tubes in the DART ion source. Dilute aqueous ammonium hydroxide on a cotton swab was held in the DART gas stream to enhance detection of TATP as the ammoniated molecule.

### Results

TATP is readily detected as  $[M+NH_4]^+$  at  $m/z$  240.1447 (Figure 1). A trace fragment at  $m/z$  91.0399 is assigned as the  $C_3H_7O_3^+$  fragment. Exact mass measurements allow the assignment of the peak at  $m/z$  223.0968 as  $C_{12}H_{15}O_4^+$ , which is assigned as monobutyl phthalate  $[M+H]^+$ . Exact mass measurements avoid a mistaken assignment of this peak as protonated TATP ( $m/z$  223.1182), which is not observed.

HMTD is observed as the protonated molecule at  $m/z$  209.0776. This is major species observed. A few small characteristic fragment ions may also be observed in the HMTD mass spectrum.

### Conclusion

Peroxide explosives TATP and HMTD were easily detected by the AccuTOF-DART with no sample preparation. Both compounds were detected at trace levels on a variety of surfaces including fingertips, boarding passes, and cloth. Exact mass measurements confirmed the compositions and avoided mistaken assignment of a contaminant as a target analyte peak.

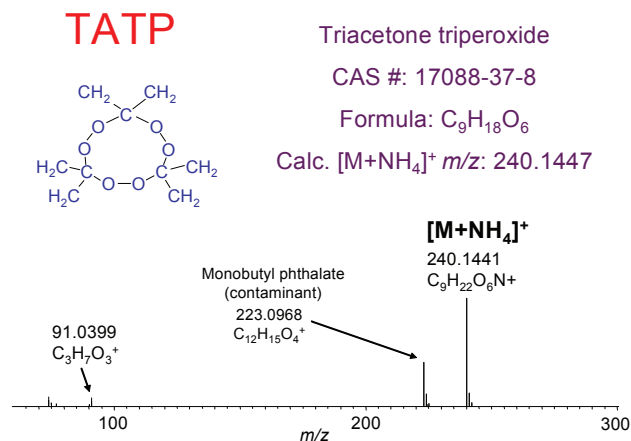


Figure 1. AccuTOF-DART mass spectrum of TATP

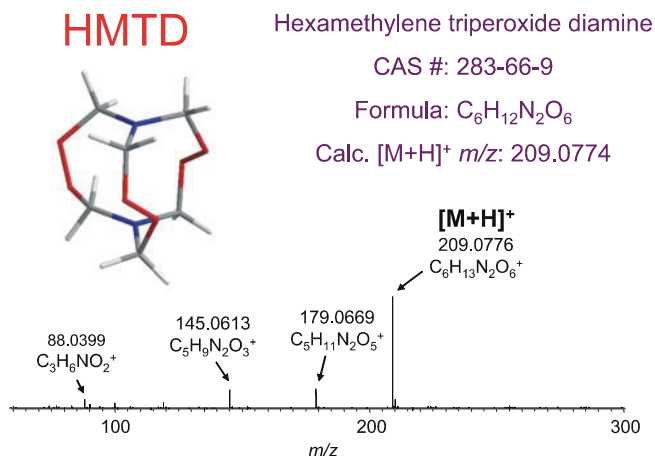


Figure 2. AccuTOF-DART mass spectrum of HMTD

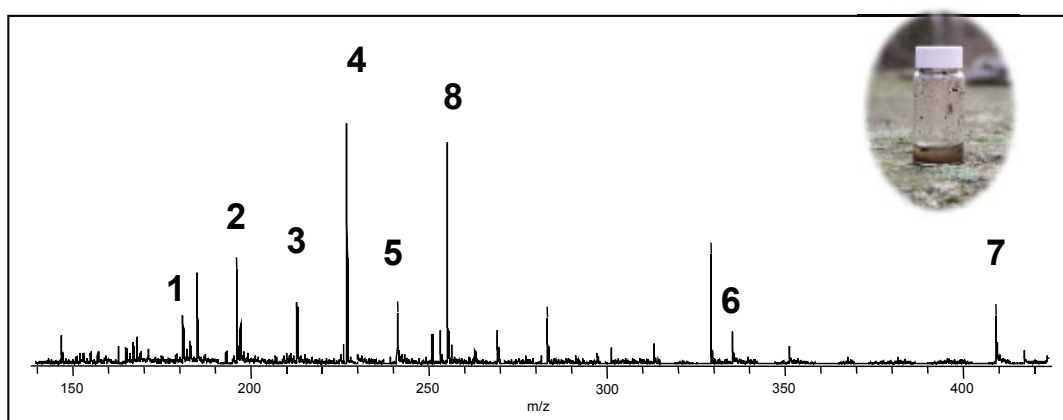


# AccuTOF™ with DART™

## Detection of Explosives in Muddy Water

The AccuTOF time-of-flight mass spectrometer equipped with Direct Analysis in Real Time (DART™) has been used to detect a wide variety of explosives in or on a variety of materials ranging from solutions to samples deposited on surfaces ranging from ABS plastic to metal, clothing and cardboard. Detection is rapid, specific, and sensitive. To demonstrate DART's ability to detect explosives in a "messy" sample, we took a sample of muddy water from a frog pond in the woods near our laboratory. The water was spiked with 3 ppm

of an explosives mixture, mixed and allowed to stand. A glass rod was dipped into the spiked water solution and then placed between the DART and the first orifice of the AccuTOF atmospheric pressure interface. An aqueous solution of 0.1% trifluoroacetic acid was placed under the glass rod to permit the formation of trifluoroacetate adducts for HMS and RDX. The results are shown in the figure below. The total time for analysis was 20 to 30 seconds.



*Explosives detected in muddy water.*

*1:dinitrotoluene (DNT) 2:amino-DNT, 3:trinitrobenzene, 4:trinitrotoluene (TNT)  
5: tetryl 6: RDX (TFA adduct) 7: HMS (TFA adduct) 8: Palmitate (in pond water).*

### Some Explosives Analyzed by DART

- Sodium perchlorate
- Nitroglycerin (NG)
- Ethylene glycol dinitrate (EGDN)
- Dinitrotoluene (DNT)
- Amino-dinitrotoluene (DNT)
- Trinitrobenzene
- Hexamethylenetriperoxidediamine (HTMD)
- Triacetone triperoxide (TATP)
- Trimethylenetrinitramine (RDX)
- Tetramethylenetetra nitramine (HMX)
- Picrylmethylnitramine (Tetryl)
- Pentaerythritol tetranitrate (PETN)

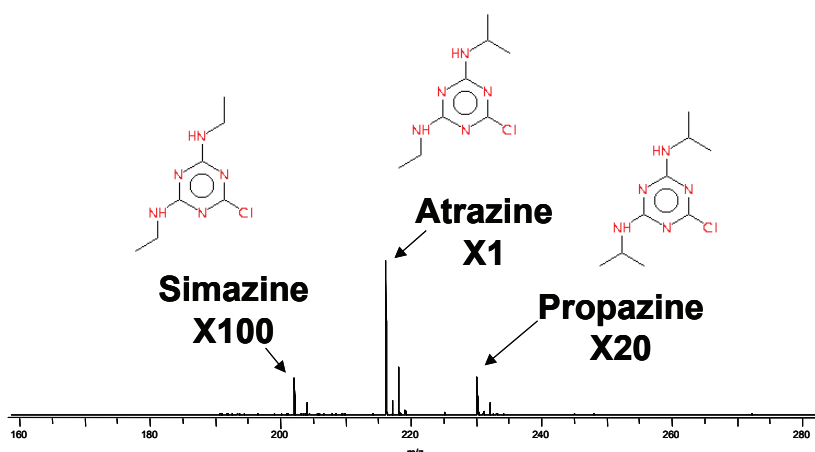
## Rapid Detection and Exact Mass Measurements of Trace Components in an Herbicide

Analytical chemists are often asked to identify trace components in manufactured compounds such as drugs, consumer products, and agricultural chemicals. A common approach to the identification of minor components is to use gas or liquid chromatography coupled with high-resolution mass spectrometry. Although this approach is effective, it may be time-consuming and difficult to set up.

The AccuTOF with Direct Analysis in Real Time (DART™) provides a rapid solution. The high dynamic range of both source and detector permit the determination of minor components in the presence of a

major component. The AccuTOF always provides high-resolution data with exact mass measurements and accurate isotope ratios that can provide elemental composition assignments for unknown compounds.

In this example, a few dust particles from a sample of atrazine herbicide containing 1% propazine and 0.2% simazine were deposited on a glass rod and placed in front of the DART. The mass spectrum shown below was measured in seconds. All three components were detected with good signal-to-noise and excellent mass accuracy and isotopic abundances.



### Exact Mass Measurements

Compound	$[M+H]^+$	Measured	Calculated	Diff. (mmu)
Atrazine	$C_8H_{15}N_5Cl$	216.10159	216.10160	-0.01
Propazine	$C_9H_{17}N_5Cl$	230.11760	230.11725	+0.35
Simazine	$C_7H_{13}N_5Cl$	202.08440	202.08595	+1.60

## Instantaneous Detection of Illicit Drugs on Currency

The widespread presence of illicit drugs on currency is an indication of the extent of the worldwide substance abuse problem. Remarkably, cocaine can be found on virtually all one-dollar bills in the United States — the upper limit for the general background level of cocaine is estimated to be 13 ng per bill<sup>1</sup>.

The Direct Analysis in Real Time (DART™) ion source, combined with the AccuTOF™ mass spectrometer can be used to sample drugs on currency within seconds. No sample preparation (extraction, wipes, etc.) or chromatography is required. The bill is placed in front of the DART and the presence of drugs can be detected immediately. Only a small portion of the bill is sampled at any given time. This allows the analyst to view the distribution of drugs on the surface of a bill, and allows the bill to be retained for reexamination at a later time.

Over the past few years, we have used DART to examine paper currency from the United States and other countries. Cocaine was found at various levels on almost all US one-dollar bills. Cocaine was detected in significant amounts on a Venezuelan 50 Bolivares bill and in large amounts on a Spanish 2000 peseta bill. New currency and larger-denomination US bills were much less likely to show the presence of cocaine and other drugs.

Figure 1 shows the presence of cocaine on a US one-dollar bill.

Cocaine is detected as  $C_{17}H_{22}NO_4^+$  ( $[M+H]^+$ ) at  $m/z$  304.15488. The assignment of this peak as cocaine was confirmed by raising the orifice potential to induce fragmentation (not shown). The cocaine fragment ion  $C_{10}H_{16}NO_2^+$  is observed at  $m/z$  182.1182. Mass measurements for both  $C_{17}H_{22}NO_4^+$  and  $C_{10}H_{16}NO_2^+$  were within one millimass unit.

Other drugs detected on dollar bills include methylphenidate (Ritalin, figure 2) and procaine. Procaine is a local anesthetic used by drug dealers as a cocaine adulterant.

Substances commonly detected on US bills include nicotine, diethyltoluamide (DEET bug repellent), sunscreen, dioctylphthalate (plasticizer), triethanolamine (from cosmetics) and glycerol and other polyols. Triethanolamine ( $[M+H]^+$ ,  $m/z$  150.1130) is easily distinguished from the illicit drug methamphetamine ( $[M+H]^+$ ,  $m/z$  150.1283) by its exact mass.

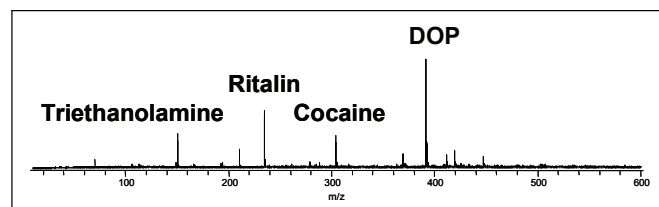
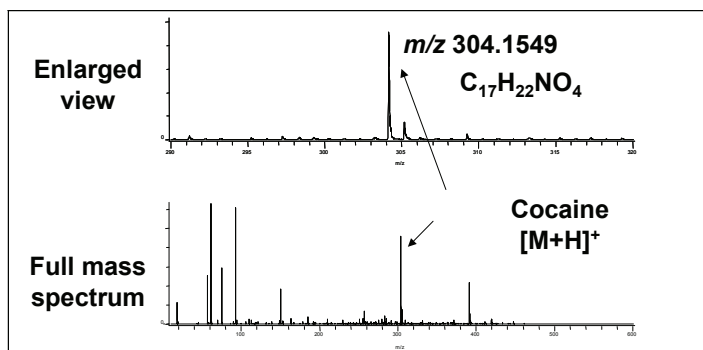


Figure 2. Ritalin and cocaine on a US \$1 bill. All compounds shown were detected as the  $[M+H]^+$  and composition assignments were verified by exact mass measurements.

Figure 1. Cocaine on a US \$1 bill.

<sup>1</sup> Paradis, D. RCMP Gas. 1997, 59, 20-22

## Instantaneous Detection of Explosives on Clothing

The detection of explosives is of vital importance in forensic applications and in preventing criminal or terrorist activity. The analytical detection of explosives on surfaces is normally done by using solvent extractions or wipes and chromatography or chromatography combined with mass spectrometry. This is inefficient because solvent extractions and wipes only result in a partial transfer of material from the surface into the sampling material. Furthermore, the chromatographic analysis can be time-consuming and requires the use of disposable solvents (an environmental concern).

The JEOL AccuTOF™ with Direct Analysis in Real Time (DART™) has demonstrated the capability to detect both volatile and involatile explosives on surfaces such

as plastic, cloth, concrete, glass, cardboard, metal, and more. No wipes or solvent extractions are required. The method is instantaneous, environmentally friendly, and does not require solvents. An example is shown in this application note.

A construction company has been recently conducting blasting to remove boulders near our offices. One of our employees happened to walk through the edge of the plume from the blasting when he arrived for work in the morning. At the end of the day, more than eight hours later, we tested him for exposure to explosives. By placing the employee's necktie in front of the DART we could easily detect nitroglycerin, as shown in Figure 1 (below). It was not necessary to take the tie off to perform the analysis.

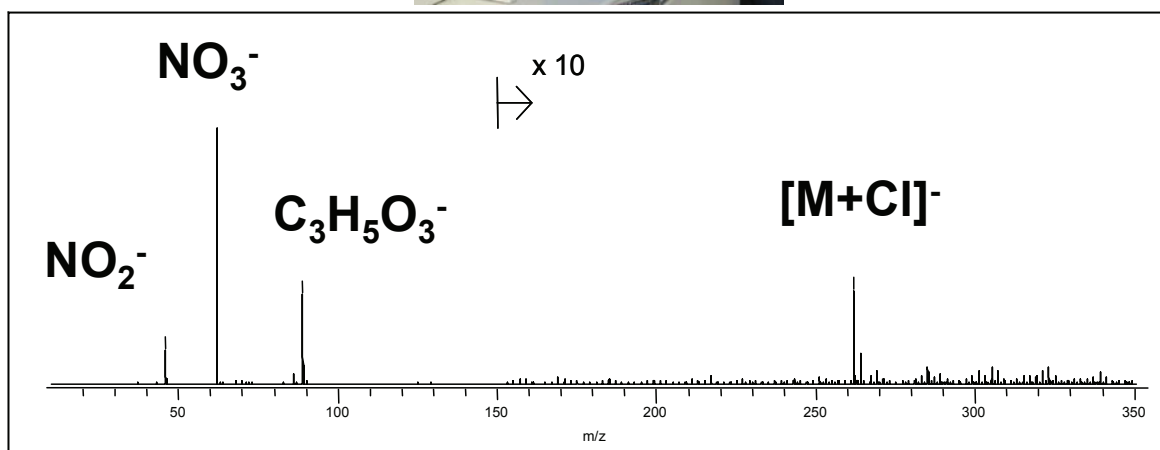


Figure 1. Nitroglycerin detected on an employee's tie after exposure to a plume from blasting. Methylene chloride vapor was placed beneath the DART to enhance the formation of  $[\text{M}+\text{Cl}]^-$ . All elemental compositions were easily confirmed by exact mass measurements.

## Instantaneous Detection of the “Date-Rape” Drug -- GHB

Gamma hydroxybutyrate (GHB) is a fast-acting central nervous system depressant<sup>1</sup>. Prior to its ban by the FDA in 1990, GHB was sold in bodybuilding formulas. It has been abused as a euphoriant. Because it is colorless and odorless, it can be added to alcoholic drinks of unsuspecting victims. An overdose can result in serious consequences, including respiratory depression and coma. GHB was classified as a Schedule I Controlled Substance in March, 2000.

Detection of GHB is problematic. GC/MS and LC/MS methods are time consuming. A rapid colorimetric assay for GHB has been developed<sup>2</sup>, but this assay suffers from some limitations. For example, ethanol produces the same colorimetric response as GHB.

The AccuTOF™ mass spectrometer equipped with Direct Analysis in Real Time (DART™) can rapidly detect GHB anion ( $C_4H_7O_3^-$ ,  $m/z$  103.0395) on surfaces, in urine, and in ethanol. No solvent extraction, wipes, or chromatography are required. Examples are shown in the figures below.

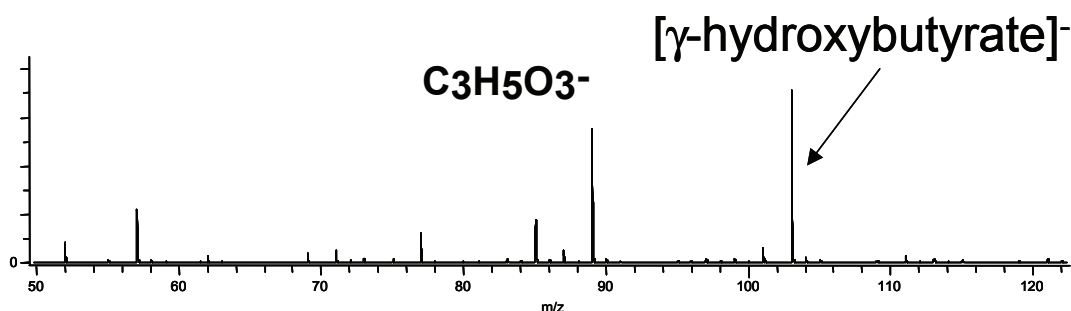


Figure 1. 10 ppm GHB (sodium salt) added to “Bombay Blue Sapphire” Gin.

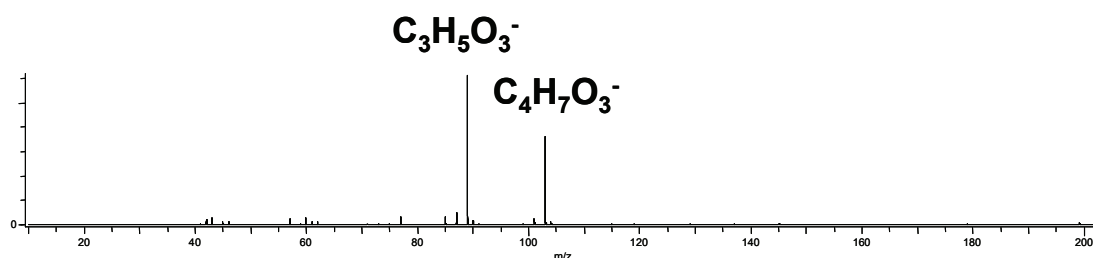


Figure 2. 100 ng of GHB (sodium salt) deposited on the rim of a glass.

<sup>1</sup><http://www.whitehousedrugpolicy.gov/publications/factsht/gamma/>

<sup>2</sup> Alston WC 2nd, Ng K. Forensic Sci Int. 2002 Apr 18;126(2):114-7. Rapid colorimetric screening test for gamma-hydroxybutyric acid (liquid X) in human urine.

## Chemical Analysis of Fingerprints

Fingerprints contain a great deal of chemical information that is not often exploited for forensic analysis. DART can detect and identify the chemical components of fingerprints, often providing information about what substances a subject has been handling.

An example is shown here for DART analysis of a single fingerprint made on a glass vial after touching an aspirin/oxycodone tablet. The aspirin and oxycodone are readily detected, along with minoxidil (hair-loss

treatment), fatty acids, urea, lactic acid, squalene, cholestadiene, and the common plasticizer BEHP bis(ethylhexylphthalate). The amino acids A, F, G, I/L, S, P, T, and V are also detected with relative abundances between 0.5% and 18%. Other lipids can be detected at higher masses (not shown). Oxycodone is readily separated at the AccuTOF's high resolving power from an unassigned interference at  $m/z$  316.

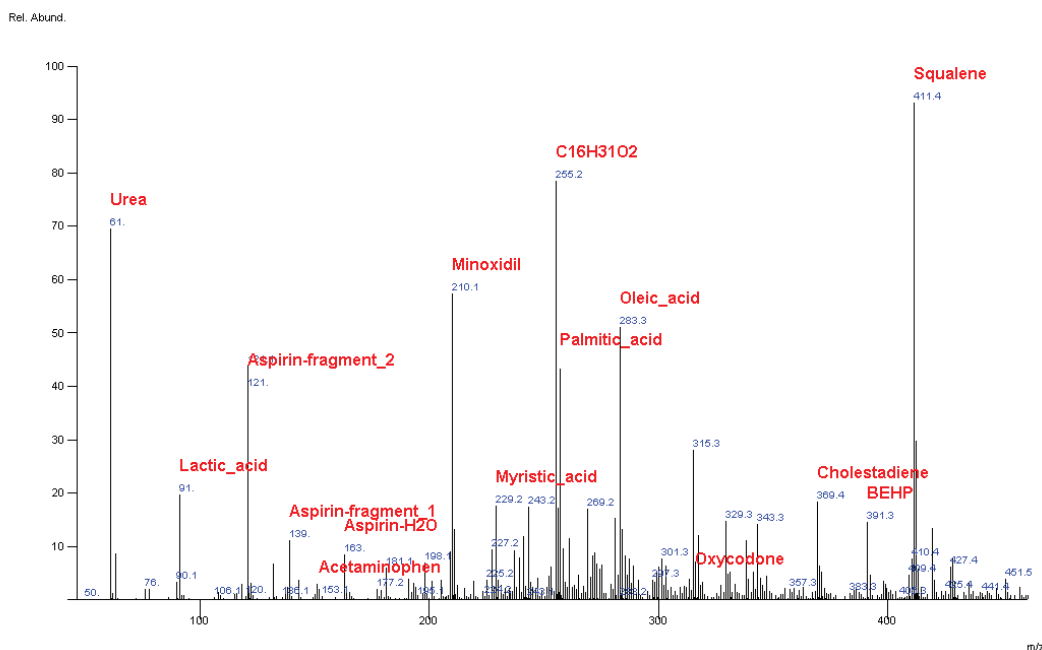


Figure 1. Fingerprint on a glass vial after touching Oxycodone tablet.

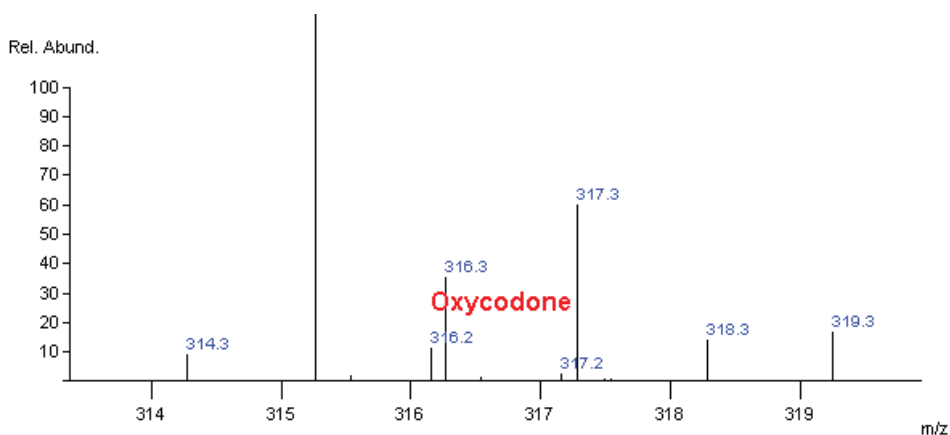


Figure 2. Enlarged view of region near  $m/z$  316, showing that oxycodone is resolved from interference at the same integer  $m/z$ .

Name	Meas.	Calc.	Diff(u)	Abund.
Oxycodone	316.1554	316.1549	0.0005	2.3573
Aspirin-H <sub>2</sub> O	163.0398	163.0395	0.0003	8.9676
Aspirin-fragment_1	139.0401	139.0395	0.0006	11.9823
Aspirin-fragment_2	121.0286	121.0290	-0.0004	42.4559
Minoxidil	210.1355	210.1355	0.0000	61.6484
Urea	61.0413	61.0402	0.0011	74.7234
Palmitic_acid	257.2477	257.2480	-0.0003	46.4336
C <sub>16</sub> H <sub>31</sub> O <sub>2</sub>	255.2324	255.2324	0.0000	84.2178
Squalene	411.3996	411.3991	0.0005	100.0000
Cholestadiene	369.3525	369.3521	0.0004	19.7204
Lactic_acid	91.0400	91.0395	0.0005	21.1630
BEHP	391.2854	391.2849	0.0005	15.6784
Oleic_acid	283.2637	283.2637	0.0000	54.9441
Myristic_acid	229.2162	229.2168	-0.0006	18.8792

Table 1. Compounds detected within 0.002 u of compounds in a list of common drugs and components in human sweat.

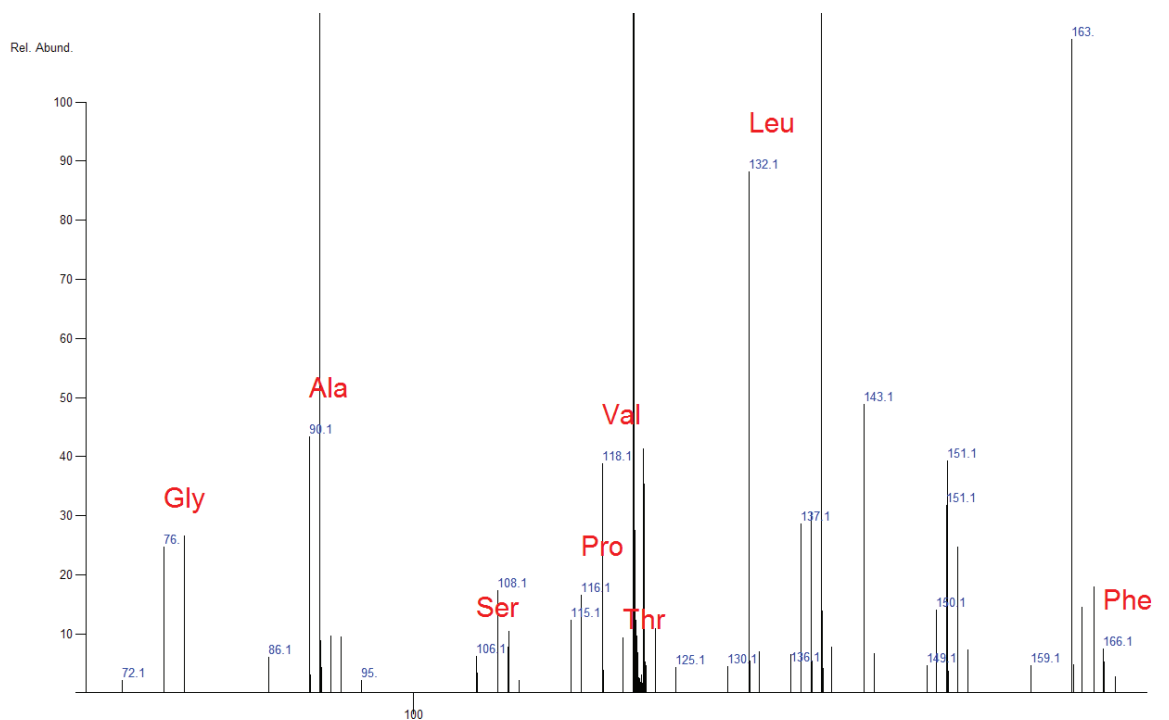


Figure 3. Amino acids A, F, G, I/L, S, P, T, and V detected with relative abundances between 0.5% and 18%

## Conclusion

DART can identify compounds in fingerprints, often making it possible to determine what substances a subject has been handling.





## Analysis of Biological Fluids

The AccuTOF-DART can detect a variety of substances in biological fluids such as urine, blood, and saliva with little or no sample preparation. These substances include drugs, amino acids, lipids, and metabolites.

Urine samples were analyzed by dipping a melting point tube in urine and placing the sample in front of the DART ion source. Figure 1 shows positive-ion DART mass spectra of a urine sample from a subject

taking ranitidine to reduce stomach acid production. The enlarged view in the inset shows the ranitidine metabolites desmethyl ranitidine and ranitidine N-oxide.

Figure 2 shows a negative-ion DART mass spectrum of urine from the same subject. Compounds detected that fall within 0.002 u within the theoretical masses for compounds in a target list include nucleotide bases, caffeine metabolites, uric acid and related compounds, and organic acids.

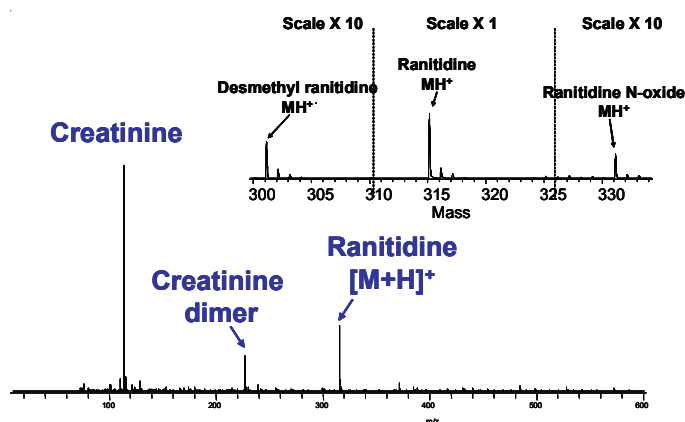


Figure 1. Ranitidine metabolites in human urine.

Name	Meas.	Calc.	Diff (u)	Rel. Abund.
GBL	85.0295	85.0290	0.0006	11.0317
Pyruvic_acid	87.0084	87.0082	0.0002	7.1700
Lactic_acid	89.0236	89.0239	-0.0002	8.3658
Cresol	107.0492	107.0497	-0.0004	0.9294
Creatinine	112.0513	112.0511	0.0002	81.6851
Purine	119.0354	119.0358	-0.0004	31.9510
Dihydro_methyluracil	127.0486	127.0508	-0.0021	23.3773
pGlu	128.0353	128.0348	0.0006	59.2337
Methylmaleic_acid	129.0212	129.0188	0.0024	37.1191
Me_succinate/diMe_malonate	131.0368	131.0358	0.0010	19.3593
Deoxyribose	133.0489	133.0501	-0.0012	28.3521
Hypoxanthine	135.0306	135.0307	-0.0001	100.0000
Methyl_hypoxanthine	149.0454	149.0463	-0.0009	37.5243
Hydroxymethyl_methyl_uracil	155.0453	155.0457	-0.0003	55.5832
Methylxanthine	165.0408	165.0412	-0.0004	32.4341
Hippuric_acid	178.0513	178.0504	0.0009	66.4487
Glucose	179.0552	179.0556	-0.0004	39.7499
Dimethylxanthine	179.0552	179.0569	-0.0017	39.7499
Dimethyluric_acid	195.0527	195.0518	0.0009	23.7577
AAMU (caffeine met.)	197.0667	197.0675	-0.0007	79.6617
Cinnamalidinemalonic_acid	217.0483	217.0501	-0.0017	60.5399
AFMU (caffeine met.)	225.0643	225.0624	0.0019	21.9092
Cytidine	242.0801	242.0777	0.0024	3.4545
Uridine	243.0641	243.0617	0.0024	21.1156
Phenylacetyl_glutamine	263.1033	263.1032	0.0001	48.9665
Ranitidine	313.1321	313.1334	-0.0013	8.7459
Ranitidine+Cl	349.1113	349.1101	0.0011	11.7296

Table I. Compounds identified by exact mass.

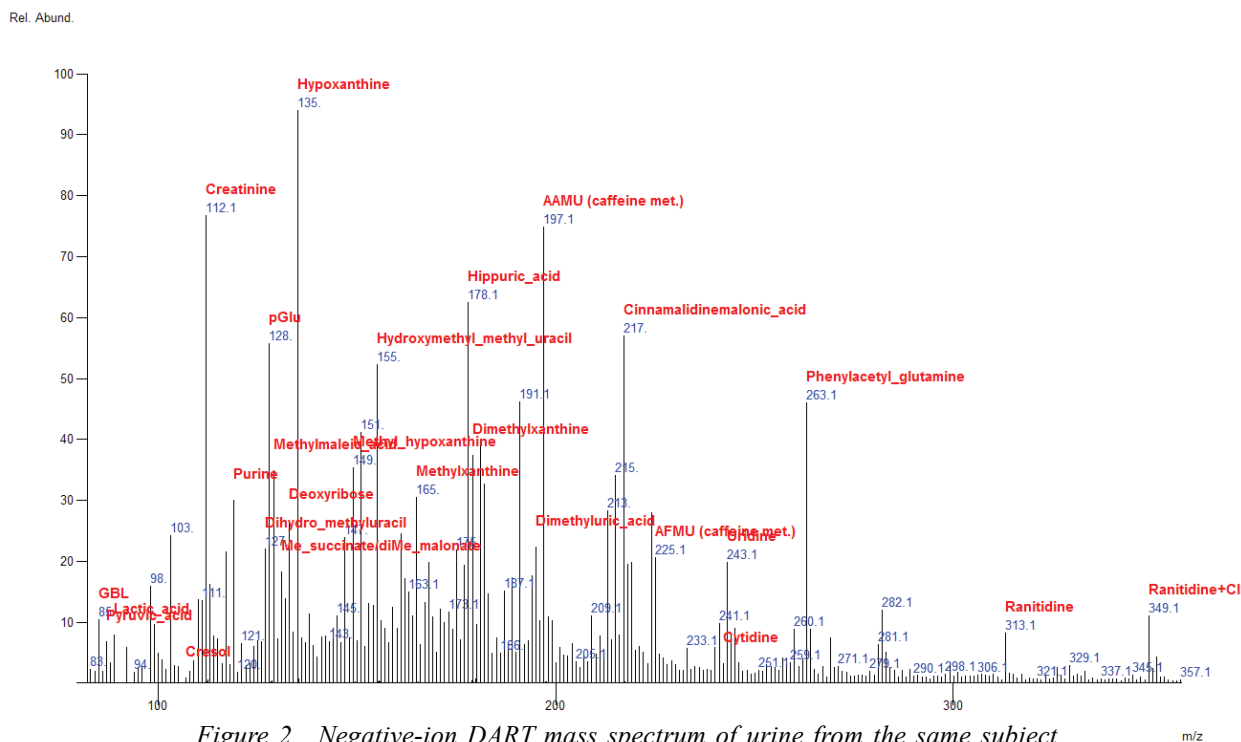


Figure 2. Negative-ion DART mass spectrum of urine from the same subject.



Quantitative analysis is possible. DART response is proportional to sample quantity. However, the absolute response is dependent on the position of the sample in the DART gas stream and on position of the sample relative to the mass spectrometer sampling orifice.

Addition of an internal standard can compensate for variations in ion abundance due to differences in placement of the sample tube in the DART ion source. Figure 3 shows the working curve obtained for urine samples that have been spiked with gamma hydroxy butyrate (GHB) at concentrations ranging from 0 ppm to 800 ppm. Samples were spiked with 50 ppm of a deuterated internal standard (d6-GHB). A melting point tube was dipped into the urine samples and then placed in front of the DART source. Results were obtained within seconds. Five replicates were measured for each concentration over a period of five days. Excellent linearity was observed.

Although some compounds can be detected in whole blood, whole blood is not well suited for analysis with no sample preparation. Minimal sample preparation can reveal compounds that are not readily detected in whole blood. Figure 4 shows amino acids detected in whole blood. Centrifuging the blood sample to remove blood cells makes it possible to detect triglycerides (Figure 5). The addition of acetonitrile to remove blood proteins makes it possible to detect other compounds, such as ranitidine (Figure 6).

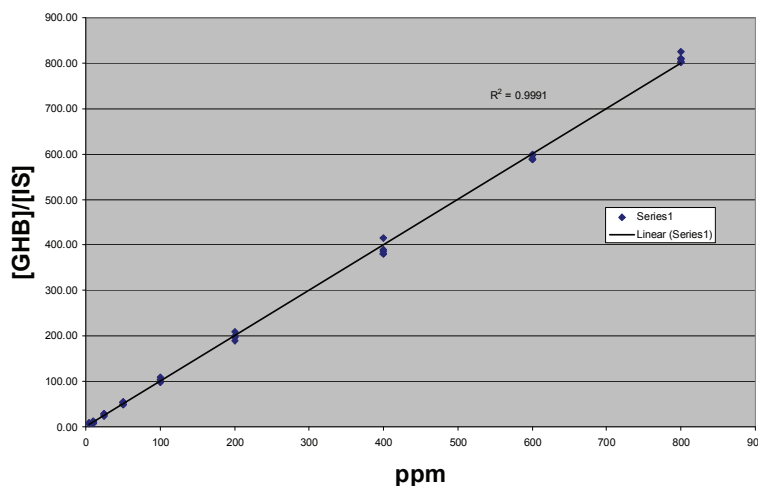


Figure 3. GHB in urine.

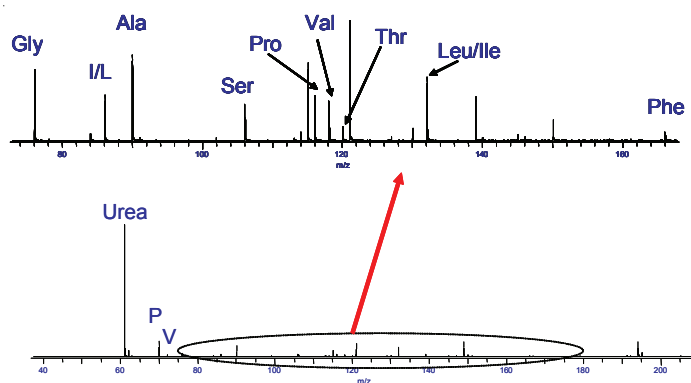


Figure 4. Amino acids in whole human blood.

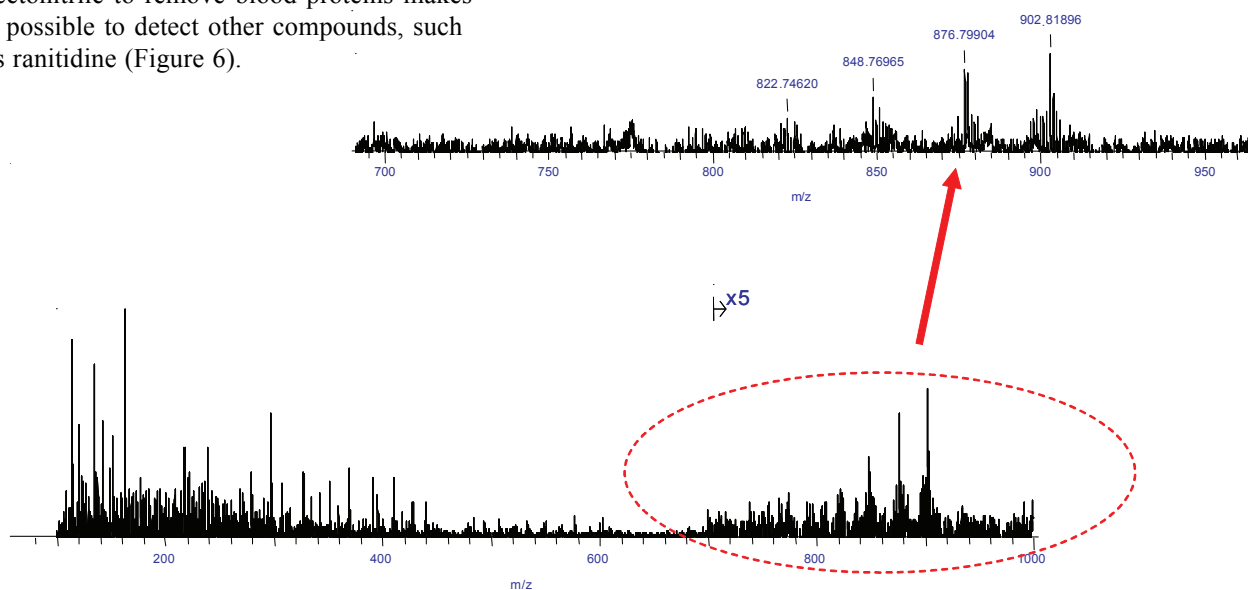


Figure 5. Triglycerides in human blood plasma.

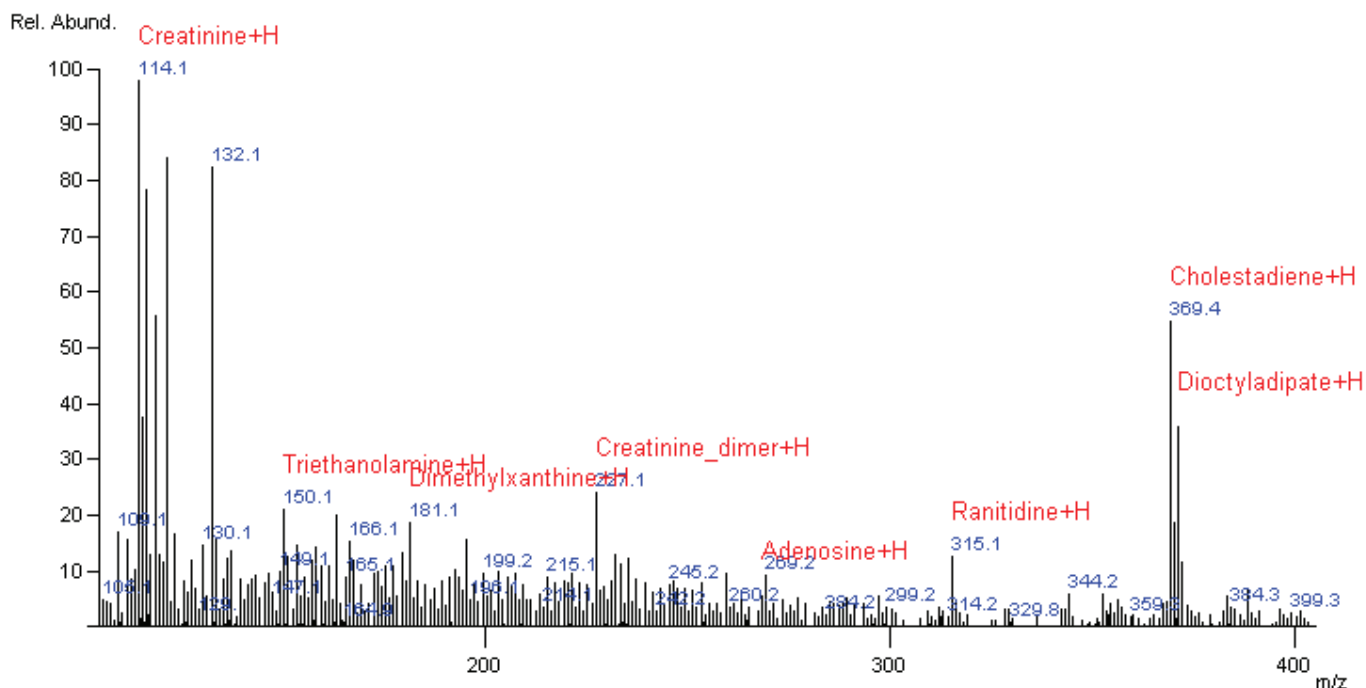


Figure 6. Compounds detected in human plasma after addition of acetonitrile. Amino acids A, P, V, L/I are detected, but not labeled in this figure. Note the presence of caffeine metabolites (dimethylxanthines). Triethanolamine is present in many consumer products and dioctyl adipate is a common plasticizer that may have been extracted from the plastic vial.

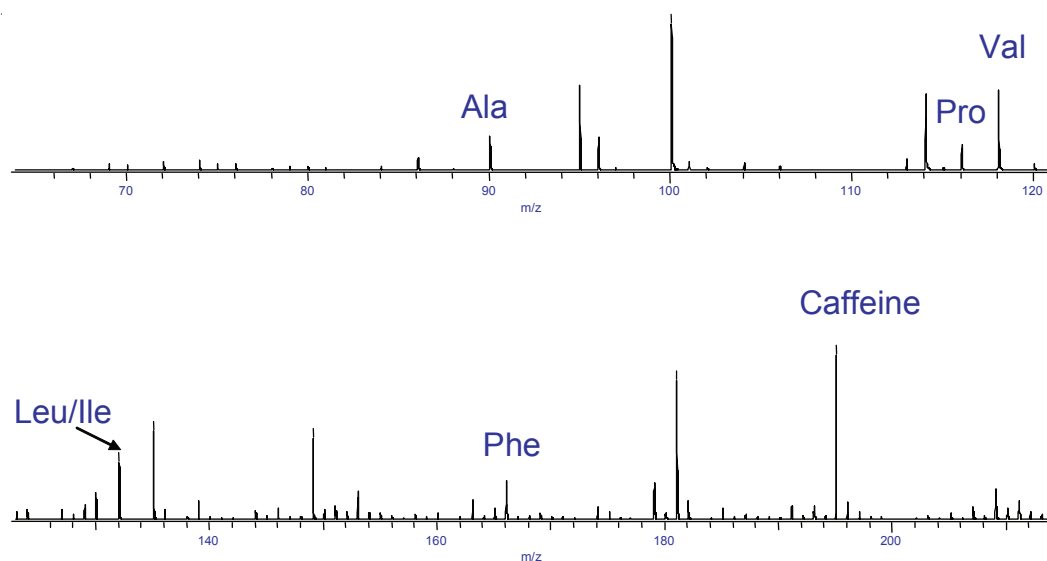


Figure 7. Amino acids and caffeine in saliva.

Analysis of other body fluids has been investigated briefly. Figure 7 shows the detection of amino acids and caffeine in a saliva sample from a coffee drinker.

Detection limits for many compounds with no sample preparation or preconcentration are in the high ppb to low ppm range.

### Conclusion

DART can be used to analyze biological fluids. Only a few drops of fluid are required for the analysis.



## End group structural analysis of polyphenylene sulfide by thermal desorption / pyrolysis DART-TOFMS

### Product used: Mass Spectrometers (MS)

Pyrolysis / gas chromatography / mass spectrometry (Py/GC/MS) and matrix-assisted laser desorption/ionization mass spectrometry (MALDI-MS) are powerful tools in polymer analysis. Py/GC/MS is a method in which a polymer sample is heated instantaneously and the volatile components generated by thermal decomposition are analyzed by GC-MS. Although it can be applied to polymers in various states and chemical information can be obtained, since the polymer is decomposed to the monomer level, average information of the sample can be obtained, but it is difficult to analyze the end group structure. MALDI can ionize polymers softly, and by selecting an appropriate matrix, it can ionize polymers with a molecular weight of several hundreds Da to several hundreds kDa. By combining with a high-resolution time-of-flight mass analyzer, if the sample has a molecular weight of up to about 10 kDa, a mixture of homopolymers with different end groups, a mixture of dissimilar polymers, or a copolymer can be mass-separated and the molecular weight distribution can be obtained. However, the elemental composition analysis of end groups by means of accurate mass is limited up to several kDa. While there are advantages and disadvantages in polymer analysis by Py/GC/MS and MALDI-MS, end group analysis of polymers by thermal desorption / pyrolysis (TDP) -DART-MS has been proposed [1]. This is a method of analyzing the volatile components generated when the polymer is gradually heated by a thermal desorption / pyrolysis device by using DART-MS. By gradual heating, unlike Py/GC/MS, moderately fragmented oligomer components can be analyzed by DART-MS. Some of the oligomer components generated include the end group structure by single cleavage of the main chain, which helps to analyze the structure of the polymer. Here, an analysis example of polyphenylene sulfide (PPS) using TDP-DART-MS is reported [2]. PPS is an engineering plastic with excellent heat resistance and chemical resistance. It is important to analyze the structure of the end groups because the difference in the manufacturing method appears in the end groups. However, it was difficult to analyze the end groups of PPS because it is insoluble in general organic solvents.

### Experimental

The sample used was a research grade PPS (Scientific Polymer Products). The ionRocket was used as the thermal desorption / pyrolysis (TDP) device. The gas generated from the TDP device was analyzed by the AccuTOF™ LC-plus 4G equipped with a DART™ ion source. The PPS sample was placed as a solid in a copper sample pot for ionRocket. The temperature of the ionRocket was held at room temperature for one minute and then raised to 600 °C with the rate of 100 °C/min. The helium gas temperature of the DART™ ion source was set to 450 °C. The measured mass range was  $m/z$  250 to 1,500, and the measurement was performed in the positive ion mode. The msRepeatFinder was used for Kendrick Mass Defect (KMD) analysis.

### Results

Figure 1a shows the change in total ion current (TICC) with heating. Gas began to be generated by pyrolysis from around 200 °C, reached its maximum around 550 °C, and then the amount of gas dropped sharply afterwards. Figure 1b shows the averaged mass spectrum from 180 °C to 500 °C. In the mass spectrum was observed a group of peaks with an interval of 108u, which was estimated from the measured accurate masses to be  $C_6H_4S$ , the monomer unit of PPS.

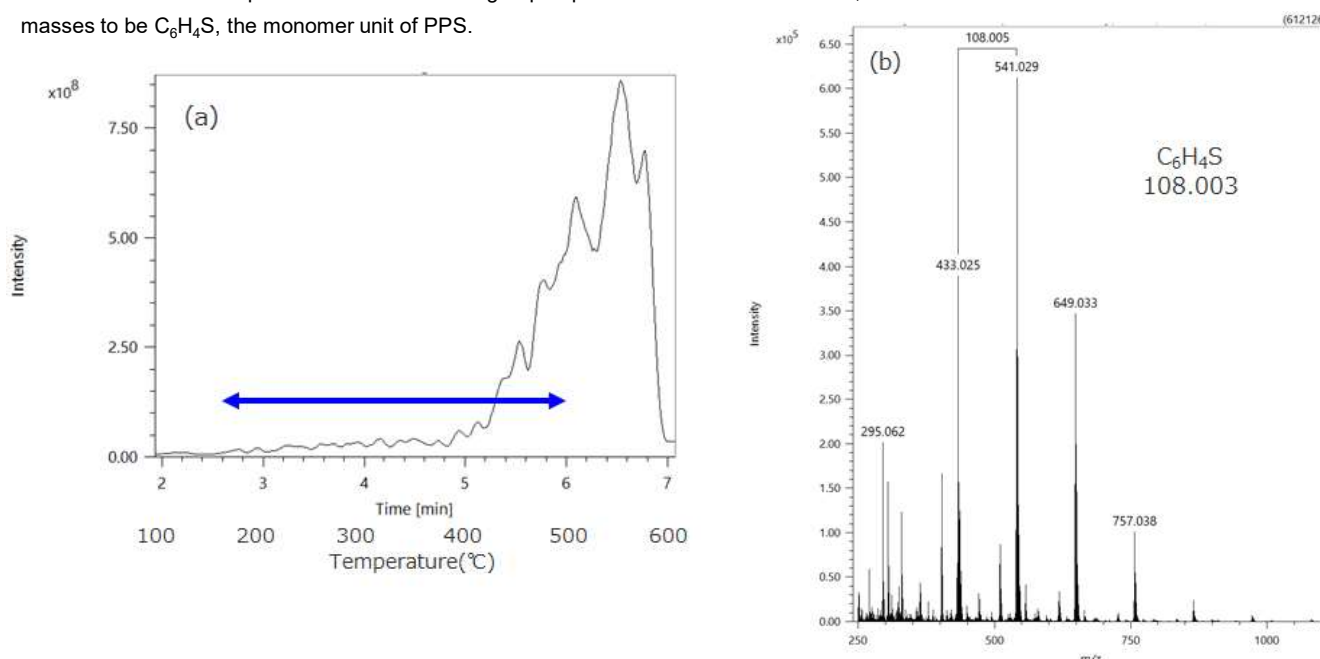


Figure 1. Evolution profiles of PPS in the TIC mode during the heating process(a) and mass spectra of heating temperature 180-500 °C (b).

Figure 2a is an expansion of the mass spectrum of Figure 1b into a KMD plot (base unit:  $C_6H_4S$ ). From the KMD plot, it was found that four main series were observed, and grouping was performed by msRepeatfinder. Structural elucidation was performed for each series from the measured accurate masses and isotope peak patterns. The results are shown in Figure 2b. The isotope patterns of series II and IV revealed that they contained one and two chlorines, respectively. The isotope pattern simulation and the enlarged view of the mass spectrum for  $n = 2$  in Series II were compared (Figure 2c). From the results of these end group analyzes, it can be inferred that this sample was synthesized by the Phillips method. Please refer to Reference [2] for the results of analysis of industrial PPS.

## Summary

As described above, the oligomers generated with a single cleavage of the polymer backbone by TDP device contain information on the end groups. By utilizing this, it is possible to obtain information on the structure of the end groups and the manufacturing method of the polymer.

## References

- [1] Sato Hiroaki, et al., BUNSEKI KAGAKU Vol. 69, No1•2, pp. 77-83 (2020)  
 [2] Sayaka Nakamura, et al. BUNSEKI KAGAKU Vol. 70, No1•2, pp. 45-51 (2021)

## Acknowledgement

This applications note was created with the cooperation of Dr. Hiroaki Sato, Dr. Shogo Yamane, and Dr. Sayaka Nakamura, Research Institute for Sustainable Chemistry, National Institute of Advanced Industrial Science and Technology. We would like to thank BioChromato Inc. for lending the ionRocket, a thermal desorption / pyrolysis device for DART, for experiments.

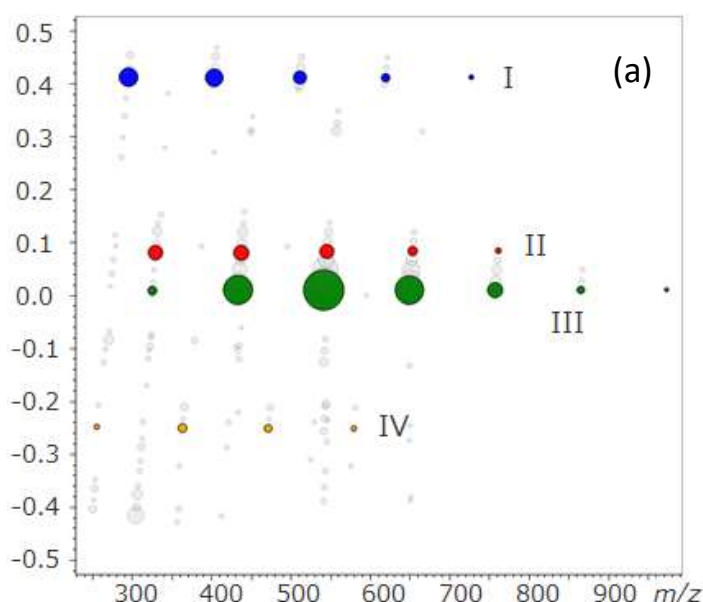
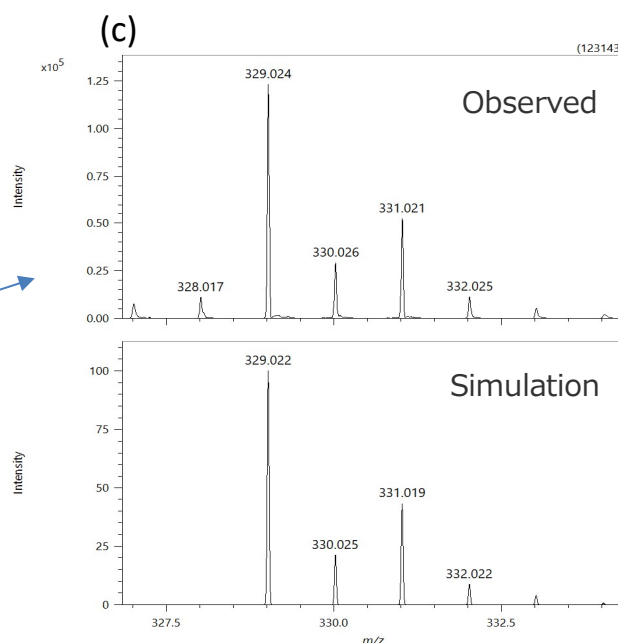


Figure 2 (a) KMD plots of Figure 1b(base unit  $C_6H_4S$ ).  
 (b)The estimated chemical structures of series I-IV found in KMD plot.

(c) Observed and simulated mass spectrum of  $[H(C_6H_4S)_2C_6H_4Cl + H]^+$  in series II.

(b)

Series	Estimated structures
I	$H-[C_6H_4-S]_n-C_6H_5$
II	$H-[C_6H_4-S]_n-C_6H_4Cl$
III	$[C_6H_4-S]_n$
IV	$Cl-C_6H_4-S-[C_6H_4-S]_n-C_6H_4Cl$



Copyright © 2022 JEOL Ltd.

Certain products in this brochure are controlled under the "Foreign Exchange and Foreign Trade Law" of Japan in compliance with international security export control. JEOL Ltd. must provide the Japanese Government with "End-user's Statement of Assurance" and "End-use Certificate" in order to obtain the export license needed for export from Japan. If the product to be exported is in this category, the end user will be asked to fill in these certificate forms.



## Analysis of polystyrene end group structure by thermal desorption/pyrolysis (TDP) DART-TOFMS

Product used : Mass Spectrometers (MS)

Pyrolysis-gas chromatography-mass spectrometry (Py-GC-MS) and matrix-assisted laser desorption/ionization mass spectrometry (MALDI-MS) are powerful tools in polymer analysis. Py-GC-MS is a method in which a polymer sample is instantaneously heated, and GC-MS analyzes the volatile components generated by thermal decomposition. Although it can be applied to polymers in various states and obtain chemical information, it is not easy to analyze the end group structure. Because the polymers decompose to the monomers and small oligomers, only average information about the sample can be obtained. MALDI-MS can ionize polymers softly, and by selecting an appropriate matrix, it can ionize polymers with a molecular weight of several 100 Da to several 100 kDa. Combining a high-resolution time-of-flight mass spectrometer, a mix of the same polymers with different end groups, a mix of polymers, or a copolymer can be mass-resolved. However, it can be obtained as long as its average molecular weight is up to 10 kDa. Furthermore, the elemental composition estimation of end groups using accurate mass is limited to several kDa.

While there are pros and cons to polymer analysis by Py-GC-MS and MALDI-MS, end group analysis of polymers by thermal desorption/pyrolysis (TDP) -DART-MS has been proposed [1]. This method generates volatile components by gradually heating a polymer sample with the thermal desorption/pyrolysis device and analyzing them with DART-MS. Unlike the rapid heating in Py-GC-MS, gradual heating generates larger oligomers, and DART-MS can detect them. Some of the generated oligomer components include end group structures, which can be a help in the structure analysis of polymers. In this report, we verify that the end group analysis of polystyrene by TDP-DART-MS examined in Reference [1] is possible by the TDP device ionRocket (BioChromato) and AccuTOF™ LC-plus 4G.

### Experimental

The samples used were standard polystyrenes for size exclusion chromatography (Tosoh Co.) with molecular weights of 5 kDa, 10 kDa, 100 kDa, and 400 kDa. The structures of PSs are shown in Figure 1. The ionRocket was used as the TDP device. The gas generated from the TDP device was measured by attaching a DART™ ion source to the AccuTOF™ LC-plus 4G. Polystyrene samples were prepared as 10 mg/mL tetrahydrofuran solutions, and 30 µL of a solution is deposited on a copper sample cup for ionRocket and dried. The temperature of the ionRocket was maintained at room temperature for one minute and then heated to 600 °C at 100°C/min. The helium gas temperature of the DART™ ion source was set to 450 °C. The measurement mass range was  $m/z$  250 to 1500, and the measurement was performed in the positive ion mode.

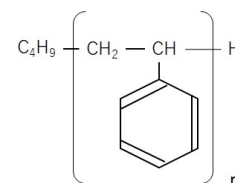


Figure 1 Chemical structure of polystyrene standards

### Results

Figure 2a shows the total ion current (TIC) with the temperature. Thermal desorption/pyrolysis products began to evolve around 200 °C, reached their maximum around 400 °C, and then dropped sharply. Figures 2(b) and (c) show mass spectra at 200-300 °C and 300-400 °C. The patterns of both spectra are significantly different. In Figure 2b, where the temperature is low, pyrolysis oligomers containing end groups are mainly observed, and in Figure 2c, where the temperature is high, pyrolysis oligomers generated from the inside of the backbone are mainly observed.

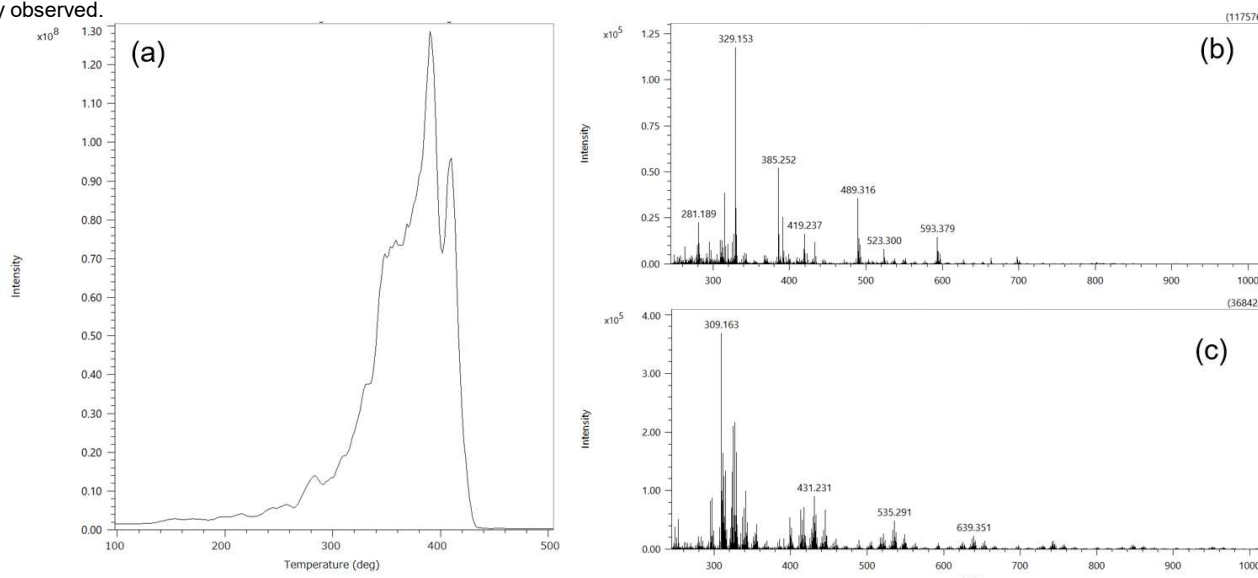


Figure 2. (a) Evolution profiles of polystyrene 5kDa in the TIC mode during the heating process. Mass spectra of heating temperature (b) 200-300 deg and (c) 300-400 deg.

Figure 3a is an enlargement of  $m/z$  475 to 715 of the mass spectrum of Figure 2b. Figure 3b also shows the KMD plot (base unit  $C_8H_8$ ). Two series of 104 u interval, which is the monomer mass of polystyrene, were observed. The structures estimated from the two series of observed accurate masses are shown in Figures 3c and d. In these two oligomer series, the polymer backbone was cleaved at one place during the pyrolysis process, and it is considered that the pyrolyzed incorporating oxygen were ionized as  $[M + H]^+$ . Since they are oligomers produced with single cleavage, they retain the end group structures. In this way, the composition of the end groups of the polymer can be considered by selecting and analyzing the mass spectrum of the pyrolyzed generated in the initial stage of gradual heating. In reference [1], series of oligomers produced by pyrolysis were observed as both  $[M + H]^+$  and  $[M + NH_4]^+$ , but here  $[M + H]^+$  was observed predominantly, and a simple mass spectrum was obtained. This is because the atmospheric pressure interface of the AccuTOF™ series has excellent vacuum pumping capacity and can be operated without using VAPUR interface, which assists the pumping of helium gas used for DART™ ion source. For the change of mass spectrum when VAPUR is attached, refer to the previous applications note MSTips No. 221 [2].

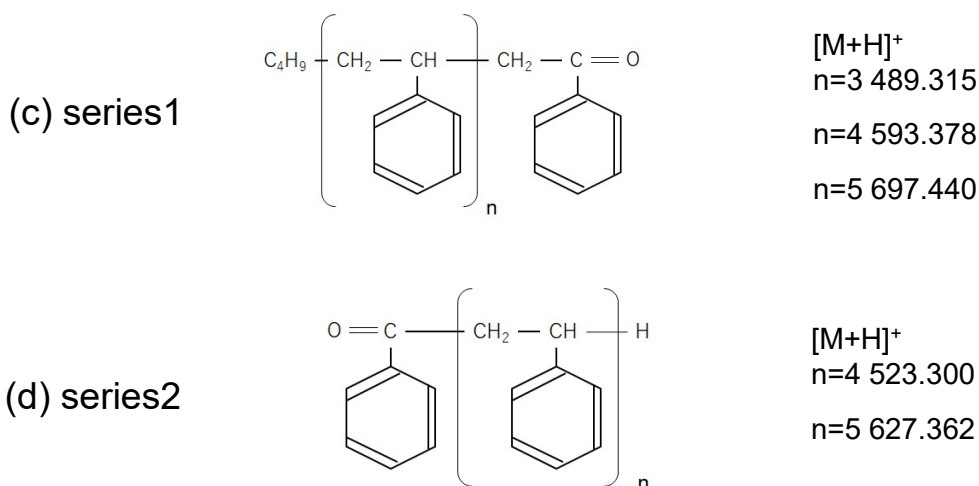
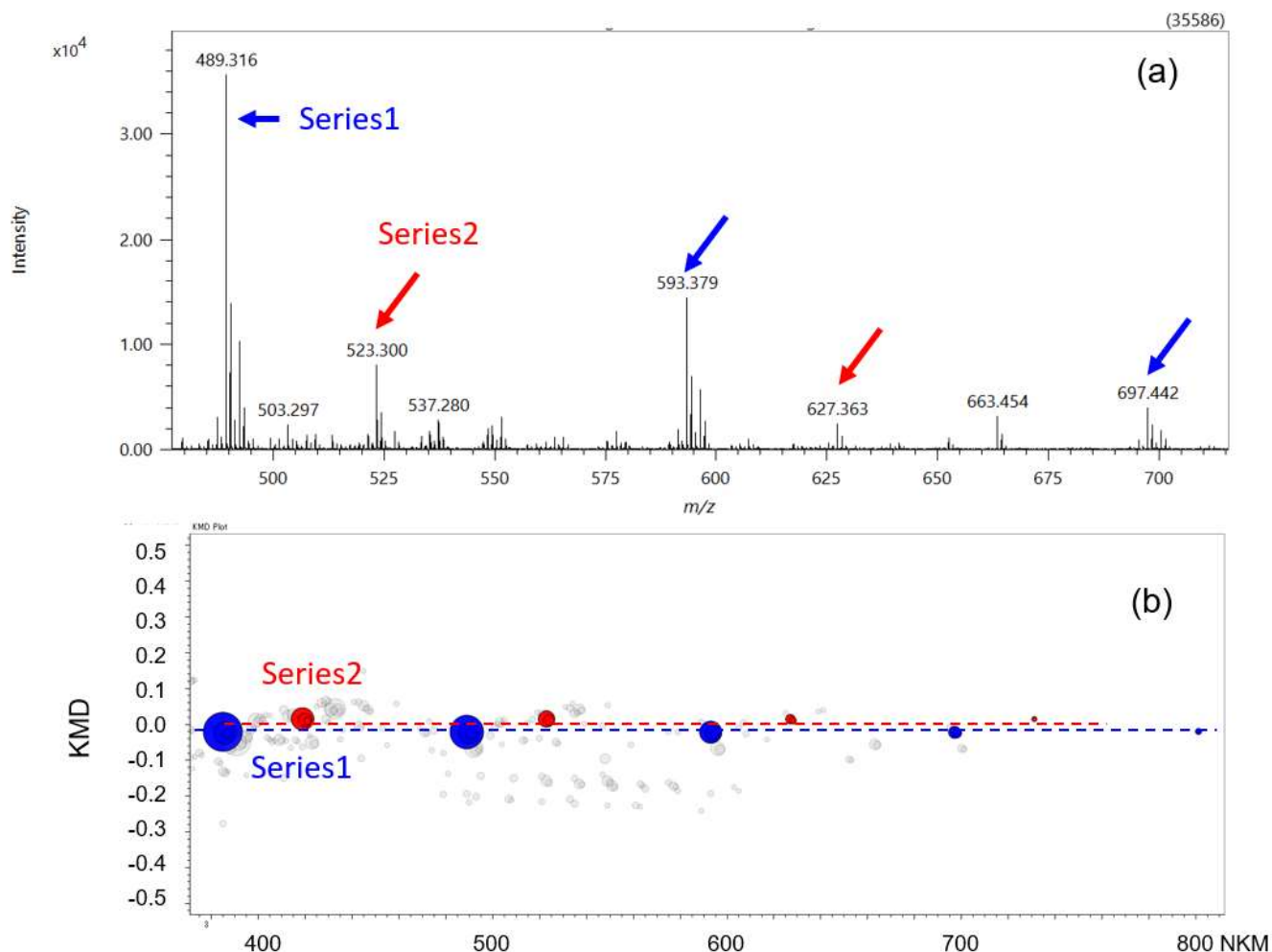


Figure 3 (a) Expanded mass spectrum of Figure 2b. (b) KMD plots of Figure 2b(base unit  $C_8H_8$ ). The estimated chemical structures and calculated masses of (c) series1 and (d) series 2.



Finally, we investigated changes in the relative ion intensity of pyrolysis oligomers (Series 1 on the previous page) containing end groups due to differences in the molecular weight of polystyrene samples. It can be seen that as the molecular weight increases, the relative intensity of pyrolysis oligomers containing end group information due to single-cleavage gradually decreases. Observing them for up to a molecular weight of about 100 kDa is possible, but it is challenging to observe them for above 400 kDa. With MALDI-TOFMS, the molecular weight distribution can be confirmed up to 100 kDa; however, it is difficult to obtain information on the end groups for high molecular weight samples[3]. It suggests that complementary information may be obtained by combining the MALDI-TOFMS and TDP-DART-MS.

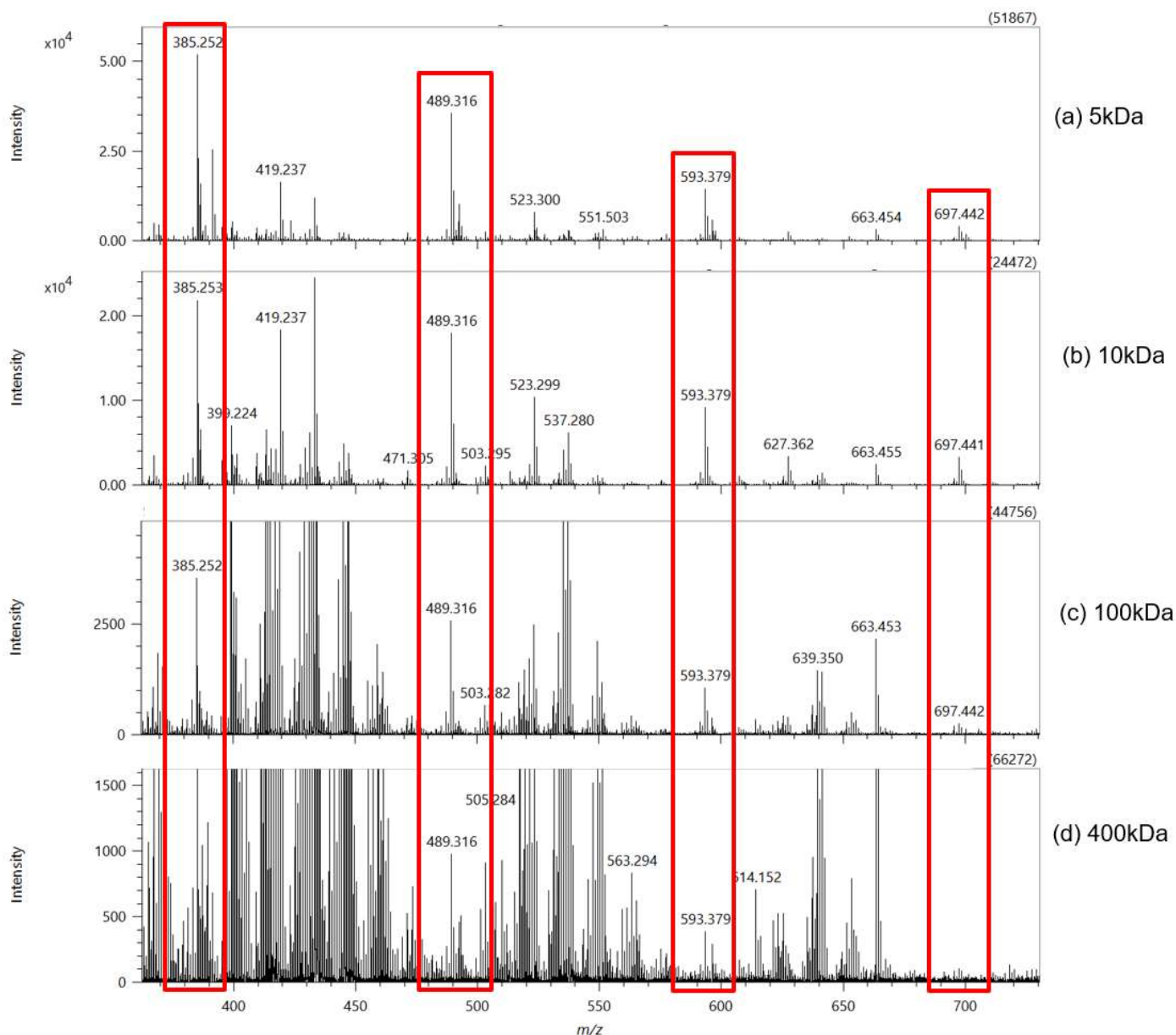


Figure 4 The mass spectra of polystyrene (a) 5kDa, (b) 10kDa, (c) 100kDa and (d) 400kDa using TDP-DART-MS.

## Summary

It was confirmed that information on the end groups can be obtained by detecting the oligomers produced by single-cleavage during gradual heating using TDP-DART-MS and estimating the elemental composition. It is expected that the structural analysis of polymers will be further advanced by using TDP-DART-MS in a complementary manner with the conventional Py-GC-MS and MALDI-MS.

## Acknowledgement

This document was created with the cooperation of Dr. Hiroaki Sato, Dr. Shogo Yamane, and Drs. Kiyoka Nakamura, Research Institute for Sustainable Chemistry, National Institute of Advanced Industrial Science and Technology.

We would like to thank BioChromato Inc. for lending the ionRocket thermal desorption / pyrolysis device for DART™ for the experiment.

## Reference

- 1) Hiroaki SATO, et al., BUNSEKI KAGAKU, Volume 69, Issue 1.2, p. 77-83 (2020)
- 2) "The AccuTOF™ Atmospheric Pressure Interface: an Ideal Configuration for DART™ and Ambient Ionization" in "AccuTOF™ LC series DART™ (Direct Analysis in Real Time) Applications Notebook"
- 3) MSTips No. 199 "Analysis of high molecular weight polystyrene standards by using JMS-S3000 "SpiralTOF™" with Linear TOF option."

Copyright © 2021 JEOL Ltd.

Certain products in this brochure are controlled under the "Foreign Exchange and Foreign Trade Law" of Japan in compliance with international security export control. JEOL Ltd. must provide the Japanese Government with "End-user's Statement of Assurance" and "End-use Certificate" in order to obtain the export license needed for export from Japan. If the product to be exported is in this category, the end user will be asked to fill in these certificate forms.





## Rapid Confirmation of Synthetic Compounds Using DART™ –Direct Mass Spectrometric Analysis from NMR Sample Tubes–

Product used : Mass Spectrometers (MS)

### Introduction

The DART™ (Direct Analysis in Real Time) ion source was conceived at JEOL USA, Inc. in 2003 as a pioneer of the “ambient ionization” that ionizes a sample under atmospheric pressure and performs direct mass spectrometric analysis. After various developments and improvements, it was launched in the market in 2005. Today, many applications using the DART™ ion source have been published, and the number of related papers exceeds 400.

Since the DART™ ion source enables analysis in an open air under atmospheric pressure, it can handle a wide range of samples such as solids, liquids, and gases. In addition, since the measurement is only to hold the sample over the gas flow expelled from the DART™ ion source, anyone can easily and quickly perform the measurement. Many applications have been published that utilize these characteristics of DART to quickly determine the elemental composition of organic compounds. This time, we report an application related to synthetic compound confirmation that combines nuclear magnetic resonance (NMR), which is indispensable for structural analysis of organic compounds, and mass spectrometry by DART.

### Results and discussion

Dulcine ( $C_9H_{12}N_2O_2$ ) was used as the sample, and DMSO and deuterated DMSO ( $DMSO-d_6$ ), which are often used in NMR, were used as the solvents. Samples were prepared at 20 mg / 0.6 mL for both DMSO solution and  $DMSO-d_6$  solution.

Fig. 1 shows the sampling method from the NMR sample tube. For sampling, an elongated glass rod was prepared and used. The measurement was carried out by immersing the tip of the glass rod in the sample solution in the NMR sample tube and holding it directly over the DART ion source. The measurement was completed in less than a minute.

Fig. 2 shows the DART mass spectrum of Dulcine in DMSO solution and  $DMSO-d_6$  solution. In DART, water molecules in the atmosphere are first ionized, and the sample molecules are ionized by the ion-molecule reaction between the water cluster ions and the sample molecules. Since hydrogen and deuterium contained in the solvent do not affect the ionization, protonated molecules ( $[M + H]^+$ ) are observed regardless of the composition of the solvent. As a result, the isotope peak pattern of the observed Dulcine protonated molecule agreed well with the theoretical isotope pattern. At the same time, an accurate mass analysis was carried out, and the elemental composition was confirmed with a good mass accuracy of 1.1 mDa or less. Since DART is not affected by deuterated solvents, it is possible to quickly and easily determine the molecular weight of the compound and elucidate the elemental composition of the molecular.



Fig.1 DART sampling

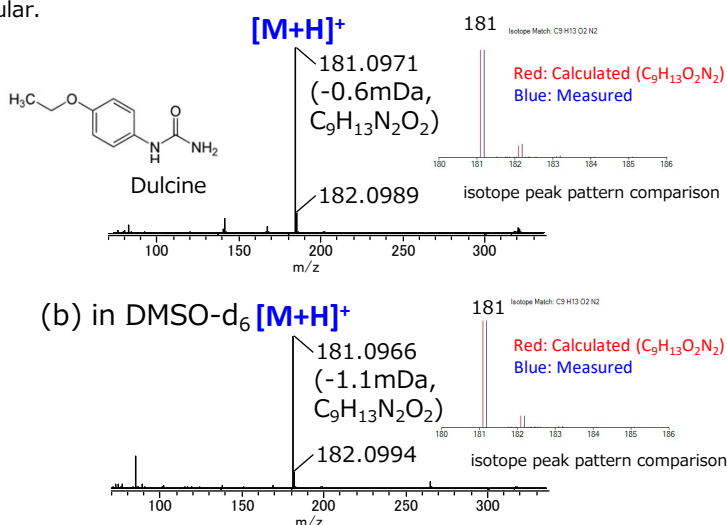
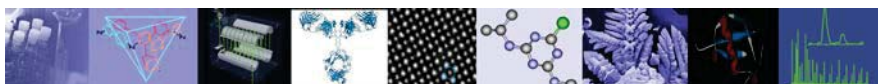


Fig.2 DART mass spectra of Dulcine  
(a) in DMSO, (b) in  $DMSO-d_6$

Copyright © 2021 JEOL Ltd.

Certain products in this brochure are controlled under the “Foreign Exchange and Foreign Trade Law” of Japan in compliance with international security export control. JEOL Ltd. must provide the Japanese Government with “End-user’s Statement of Assurance” and “End-use Certificate” in order to obtain the export license needed for export from Japan. If the product to be exported is in this category, the end user will be asked to fill in these certificate forms.





## Identification of Contamination on Welding Wires Using Cross-Platform Techniques in SEM and Mass Spec

### Introduction

A batch of contaminated welding wire received from a vendor by a customer was causing problems in a manufacturing process. Visual comparison of the clean and contaminated wire did not show any obvious differences, but the contamination was readily observed on backscatter electron images obtained with the JEOL IT300 scanning electron microscope (Figure 1).

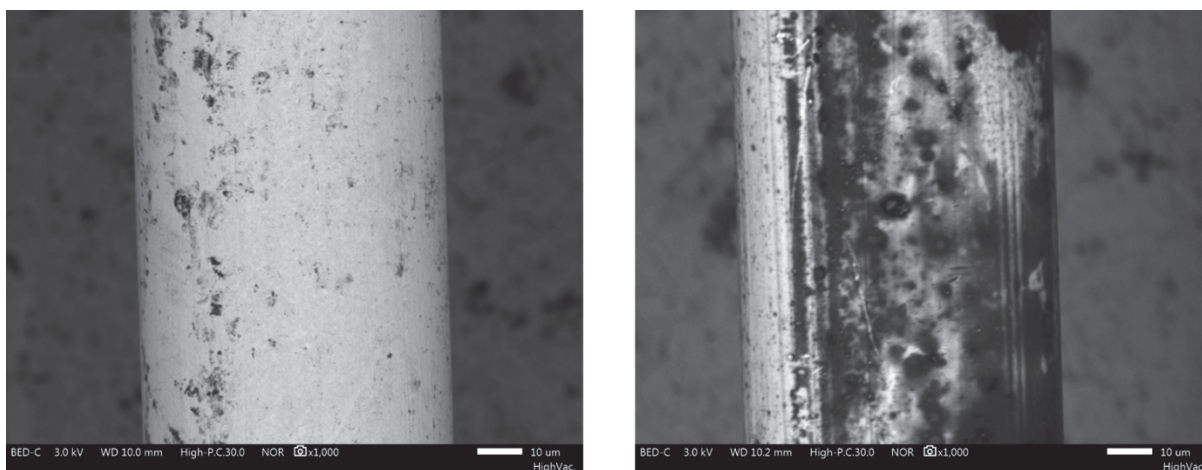


Figure 1. Backscatter electron images obtained at 3 kV of clean welding wire (left) and contaminated wire (right).

A JEOL *AccuTOF™-DART®* mass spectrometer equipped with a Biochromato *IonRocket™* thermal desorption and pyrolysis attachment were used to determine the chemical composition of the wire contamination. The *IonRocket* includes an oven and disposable sample holders that permit controlled heating of samples from ambient temperature up to 600°C. The resulting thermal desorption profiles facilitate the identification of volatile compounds and outgassing. At higher temperatures, pyrolysis products permit the identification of materials such as polymers.

### Experimental

Mass spectra were acquired in positive-ion mode with the DART ion source on the JEOL *AccuTOF-DART 4G* high-resolution time-of-flight mass spectrometer. Mass spectra were acquired with JEOL Mass Center software and data processing (mass calibration, spectral averaging, background subtraction, and mass chromatogram displays including 3D plots) was accomplished with TSS Unity software (Shrader Software Solutions, Detroit, MI). Mass spectral interpretation and compound identification were carried out with Mass Mountaineer software (mass-spec-software.com).

Scissors were used to cut small segments of wire (a few millimeters in length) that were placed onto the disposable copper sample stage for the *IonRocket*. Figure 2 shows the wire segments on the surface of the copper sample stage both before and after heating. The *IonRocket* oven was positioned directly under the DART ion source, and a glass tee was used to sample the gases desorbed from the sample into the DART helium gas stream. The *IonRocket* was programmed with a temperature ramp to heat the sample from ambient temperature to 600°C in 6 minutes.

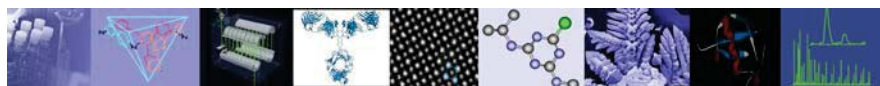


Figure 2. Segments of welding wire placed on the surface of the copper sample stages for the IonRocket. The left figure shows the wires placed on a fresh, clean sample stage, and the right side shows wire segments on the surface of a copper sample stage that was oxidized after heating to 600°C.

## Results

The 3D plots for clean and contaminated wires shown in Figure 3 provide an overview of the mass spectral analysis. The x-axis for each 3D plot indicates time and temperature. At a heating rate of 100°C min<sup>-1</sup>, 2 minutes is equivalent to 200°C, 4 minutes corresponds to 400°C, and 6 minutes corresponds to 600°C. The y-axis represents the mass-to-charge ratios ( $m/z$ ), and darker spots indicate higher relative abundance for the detected ions.

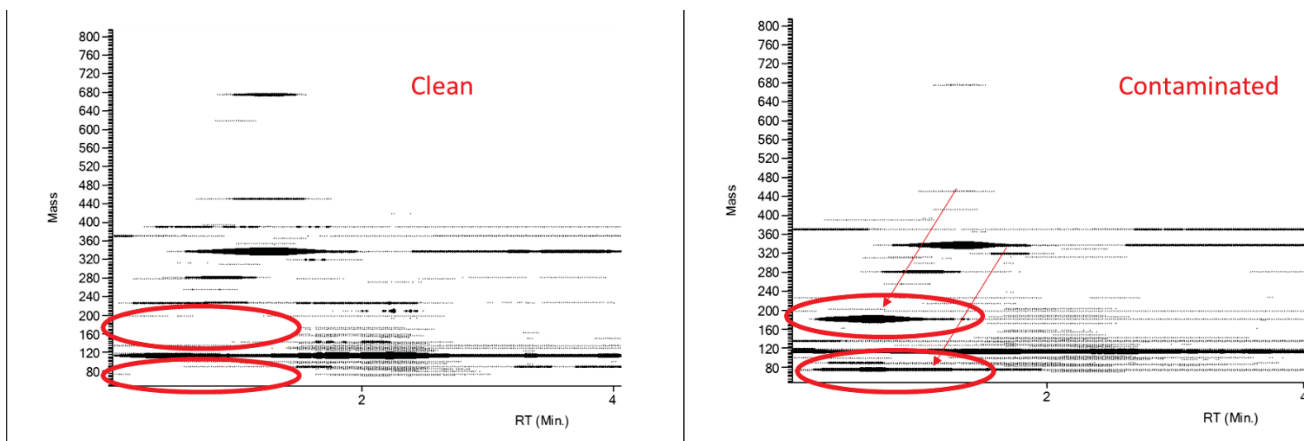


Figure 3. Comparison of the 3D plots for thermal desorption of clean (left) and contaminated (right) wires shows the presence of peaks at nominal  $m/z$  76 and  $m/z$  182 in the contaminated wires that are not present in the clean wires.

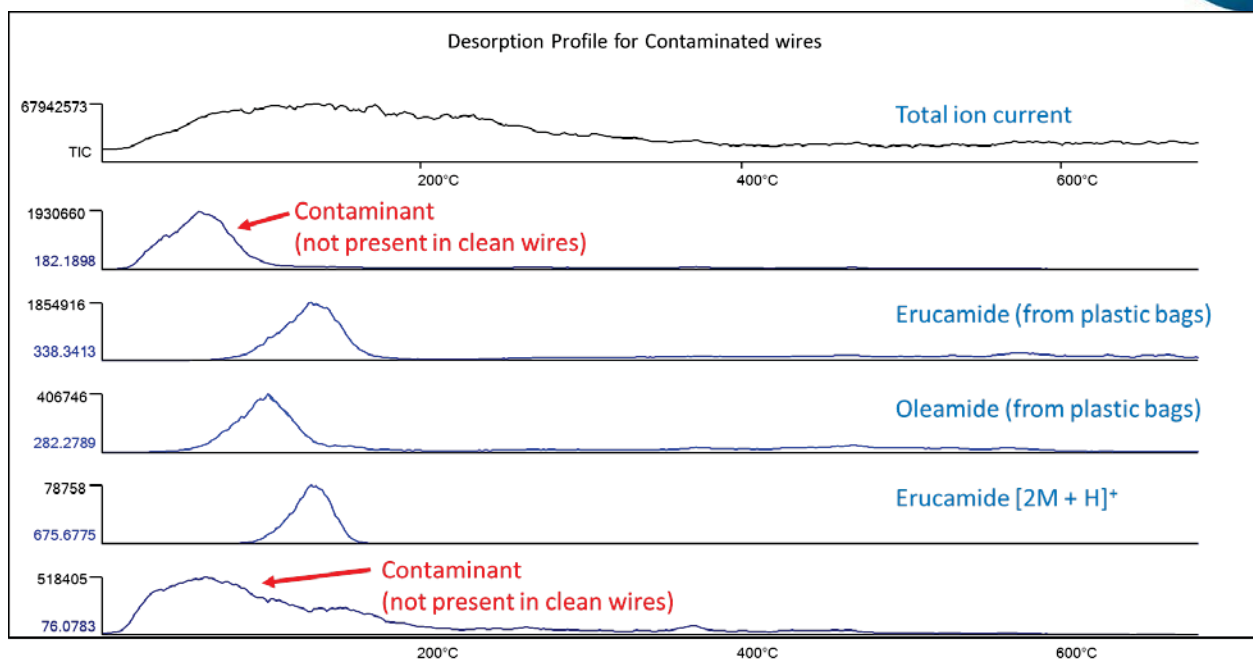
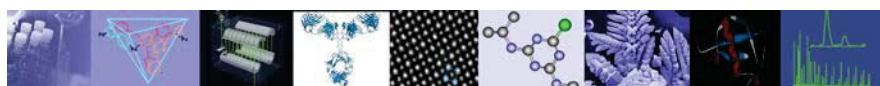


Figure 4. Thermal desorption profiles for selected components. Erucamide and oleamide are slip agents found on both clean and contaminated welding wires from the plastic bags used to ship the wires. The peaks at  $m/z$  76.0783 and  $m/z$  182.1898 were observed on the contaminated wires, but not on the clean wires.

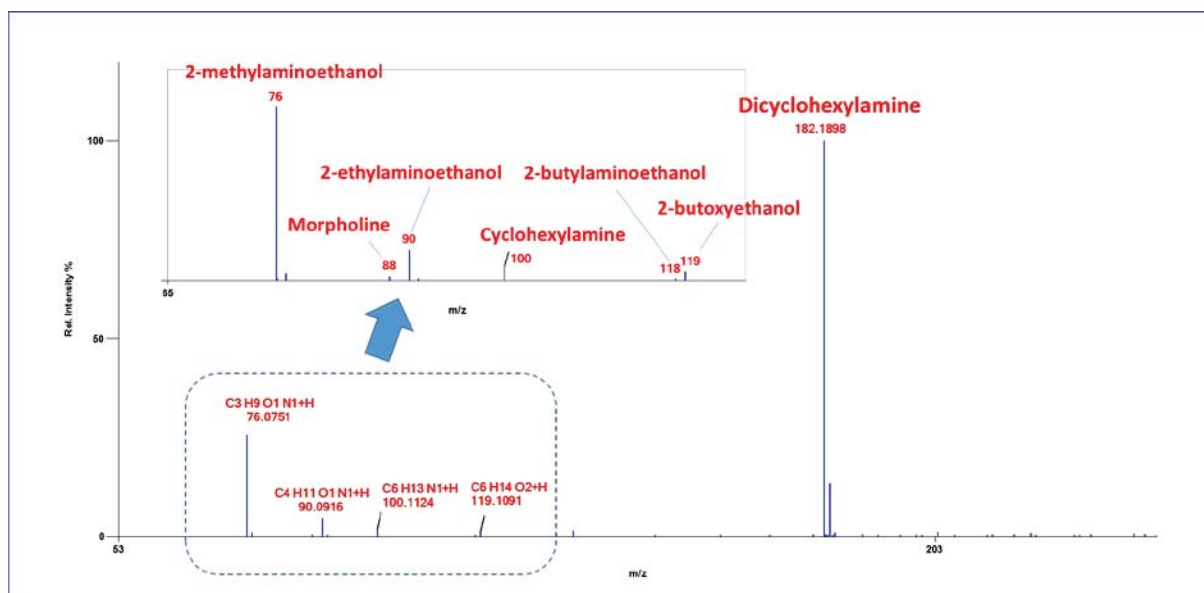
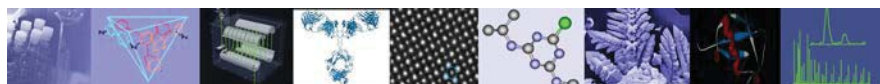


Figure 5. AccuTOF-DART mass spectrum of the contaminated wire at an IonRocket sample heater temperature of 65°C showing the presence of compounds used in metalworking fluids.





The temperature profiles for selected contaminants in the plastic bags containing the welding wires and the compounds found only on the contaminated wires are shown in Figure 4. Examination of the mass spectra at time 0.6 minutes shows that major peaks are present in the contaminated wire, but not in the clean wire, at  $m/z$  182.1898 and  $m/z$  76.0751. The mass spectrum in Figure 5 shows the peaks present in the contaminated wire that are not present in the clean wire. Exact mass measurements with isotope matching provide elemental compositions for each peak that are consistent with compounds used in metal working fluids. For example, the base peak at  $m/z$  182.1898 is identified as protonated  $C_{12}H_{23}N$  (dicyclohexylamine), the peak at  $m/z$  76.0751 is identified as protonated  $C_3H_9NO$  (2-methylaminoethanol) and other compounds are tentatively identified as protonated 2-ethylaminoethanol, 2-butylaminoethanol, morpholine, 2-butoxyethanol, and cyclohexylamine based on their elemental compositions.

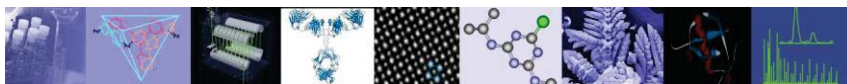
## Conclusion

The combination of SEM and Mass spectrometry, particularly *IonRocket* and *AccuTOF-DART*, permitted the identification of residual metalworking fluid on the contaminated samples, indicating that the wires were not adequately cleaned after fabrication.

While the contaminants could be detected with DART alone, the *IonRocket* facilitated handling for the small wire samples, permitted the analysis of multiple wire segments in a single measurement, and provided temperature-dependent desorption information about the contaminating compounds.

The Scanning Electron Microscope provides high magnification imaging of samples to identify quality control issues and reveal details that cannot be seen with the naked eye or optical microscope.

The *AccuTOF-DART* mass spectrometer with the *IonRocket* thermal desorption and pyrolysis accessory is a powerful tool for investigating problems related to materials and contamination.



## AccuTOF-DART analysis of motor oils

### Introduction

DART can characterize additives in lubricating oils directly without sample preparation. The additives generally produce a strong signal without interference from the base oil. However, complementary information about nonpolar components of the base oil can be obtained by  $O_2^{\bullet-}$  attachment chemical ionization, a simple analysis that can be easily and rapidly carried out with changing any hardware on the AccuTOF-DART mass spectrometer system.

### Experimental

All mass spectra were acquired with a JEOL AccuTOF-DART mass spectrometer equipped with a DART-SVP ion source.

Additives in motor oil were analyzed by dipping the sealed end of a melting point tube into each oil sample and suspending the tube in the DART gas stream. The DART was operated in positive-ion mode with helium DART gas and a gas heater temperature of 400°C. The mass spectrometer parameters were: RF ion guide voltage: 600V, ring lens = orifice 2 = 5V, orifice 1 = 20V.

The base oil was analyzed by diluting 10  $\mu$ L of oil into 300 10  $\mu$ L of hexane. The DART was operated as a source of  $O_2^{\bullet-}$  in negative-ion mode with helium gas. The AccuTOF mass spectrometer was operated in negative-ion mode with the RF ion guide set to 700V, ring lens = -3V, orifice 2 = -5V, and orifice 1 = -12V. Samples in hexane solution were rapidly aspirated from a narrow-diameter capillary (PCR pipette capillary) directly into orifice 1 (Figure 1). Rapid expansion of the solution into vacuum stabilized the weakly-bound oxygen adducts  $[M + O_2]^{\bullet-}$  for the nonpolar base oil components.

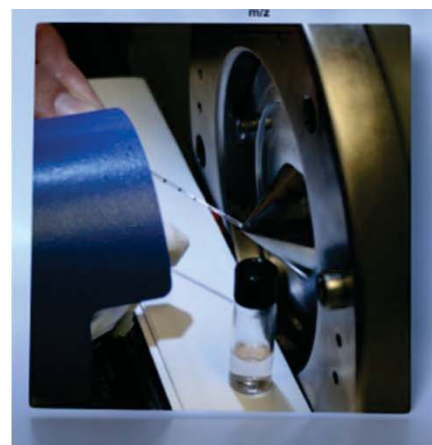
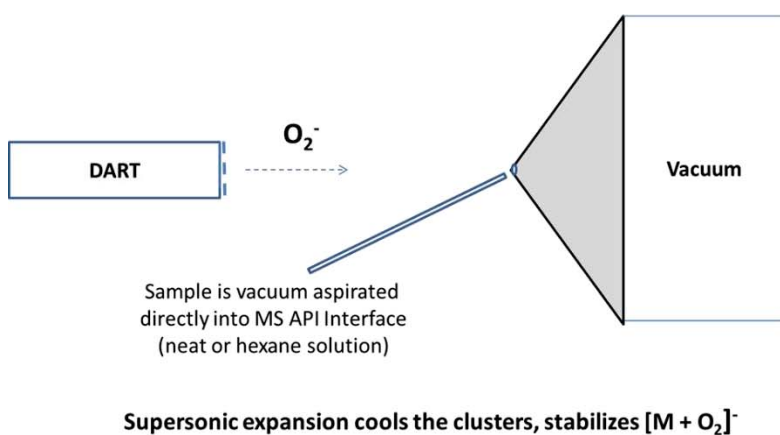
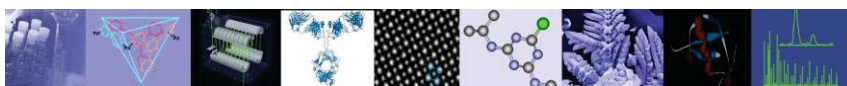


Figure 1. Schematic diagram and photograph of sample introduction for  $O_2^{\bullet-}$  attachment chemical ionization with the AccuTOF-DART.



## Complementary information about polar additives and nonpolar base oil components

Figure 2. shows the positive-ion DART mass spectrum (top) of a synthetic motor oil and the negative-ion  $O_2^{\bullet-}$  attachment chemical ionization mass spectrum (bottom) for the same oil sample. The positive-ion DART mass spectrum clearly shows the presence of polar dialkyldiphenylamine antioxidants and zinc dialkyldithiophosphate (ZDDP) anti-wear additives. The negative-ion  $O_2^{\bullet-}$  attachment mass spectrum shows the large alkanes  $C_nH_{2n+2}$  and an abundant alkylnaphthalene that comprise the base oil.

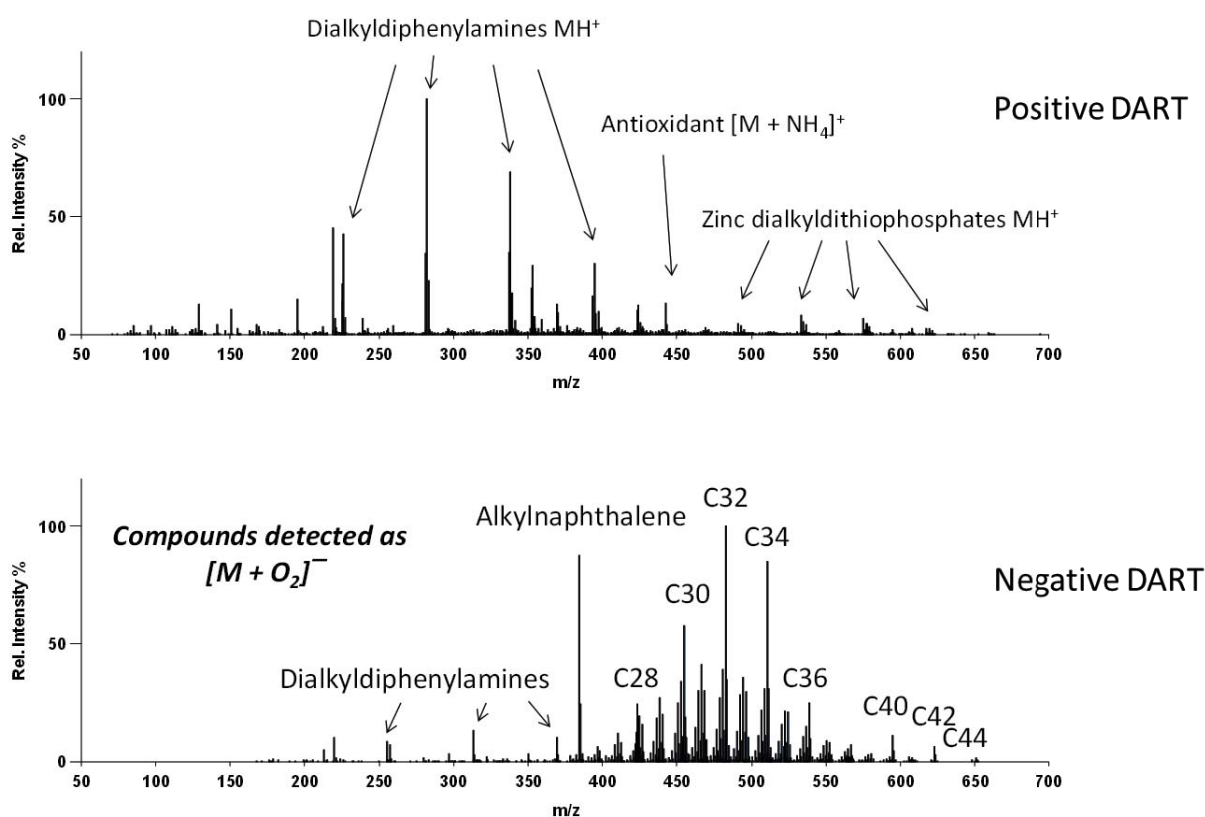
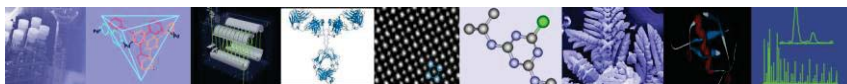


Figure 2. Positive-ion DART mass spectrum (top) showing the polar additives and negative-ion  $O_2^{\bullet-}$  attachment mass spectrum (bottom) showing the nonpolar base oil components of a synthetic motor oil.





### Comparison of the base oil composition of two different synthetic motor oils

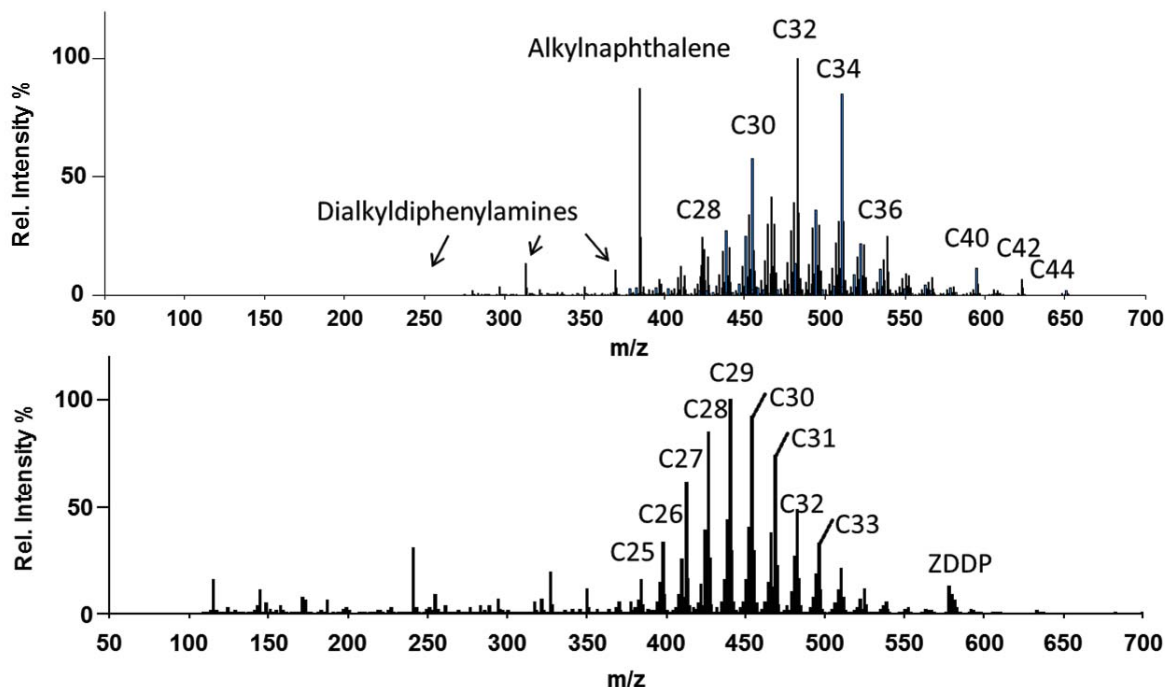
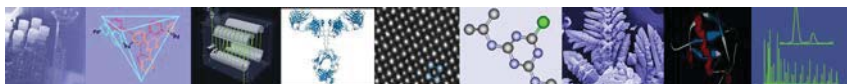


Figure 3.  $O_2^-$  attachment mass spectra showing differences in the base oil composition for two brands of synthetic motor oil.

### Conclusion

The AccuTOF-DART can be used to rapidly identify additives in motor oils and also to characterize the base oil composition. The AccuTOF-DART offers complementary ambient ionization techniques that can be easily carried out without requiring any hardware changes.





## Analysis of duct tapes by thermal desorption and pyrolysis mass spectrometry and X-ray-fluorescence spectroscopy

### Introduction

The identification of pressure-sensitive tapes such as duct tape and electrical tape is an important forensic application. Here we show the application of thermal desorption and pyrolysis combined with Direct Analysis in Real Time (DART) mass spectrometry to distinguish between manufacturers and brands of duct tapes. X-ray fluorescence (XRF) provides complementary information about the atomic composition of the different tapes.

### Experimental

#### Samples

Seven duct tape samples were analyzed by mass spectrometry and six by XRF: two Ace® Hardware tapes (one black and one gray), two 3M Scotch® duct tapes (one gray and one white), Rite-Aid® gray duct tape, Gorilla® black duct tape and Loctite Sumo black duct tape (not available when the other tapes were analyzed by XRF).

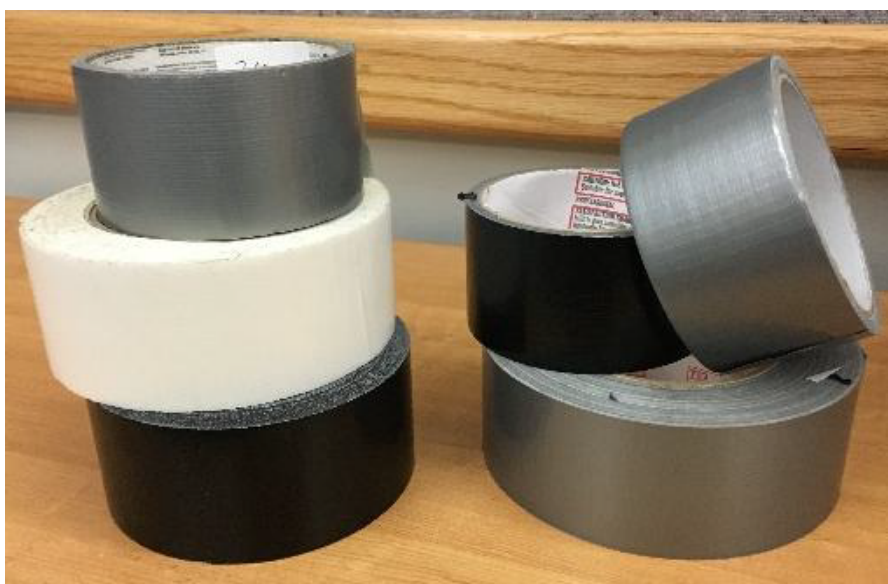
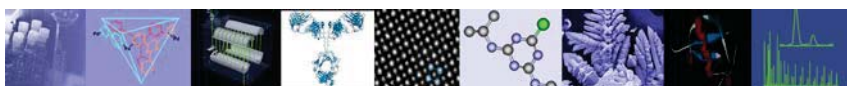


*Figure 1. Duct tapes analyzed in this study*



#### Thermal desorption/ pyrolysis DART mass spectrometry

Mass spectra were acquired by using a JEOL AccuTOF-DART® 4G mass spectrometer (Figure 2) equipped with a Biochromato, Inc. ionRocket thermal desorption and pyrolysis system (<http://biochromato.com/ionrocket/>).



Figure 2. The ionRocket thermal desorption/pyrolysis system mounted on the AccuTOF-DART 4G mass spectrometer

A small sample of each duct tape (roughly 1 mm in diameter) was placed into a disposable copper sample stage (or “pot”) for the *ionRocket* (Figure 3).



Figure 3. A copper pot used as a sample holder for the *ionRocket*

The copper sample stage was placed onto the *ionRocket* heater (Figure 4) and moved into position between the exit of the DART ion source and the sampling orifice of the AccuTOF-DART 4G mass spectrometer. A glass tee positioned above the sample (Figure 5) guides the thermal desorption and pyrolysis products into the DART gas stream.

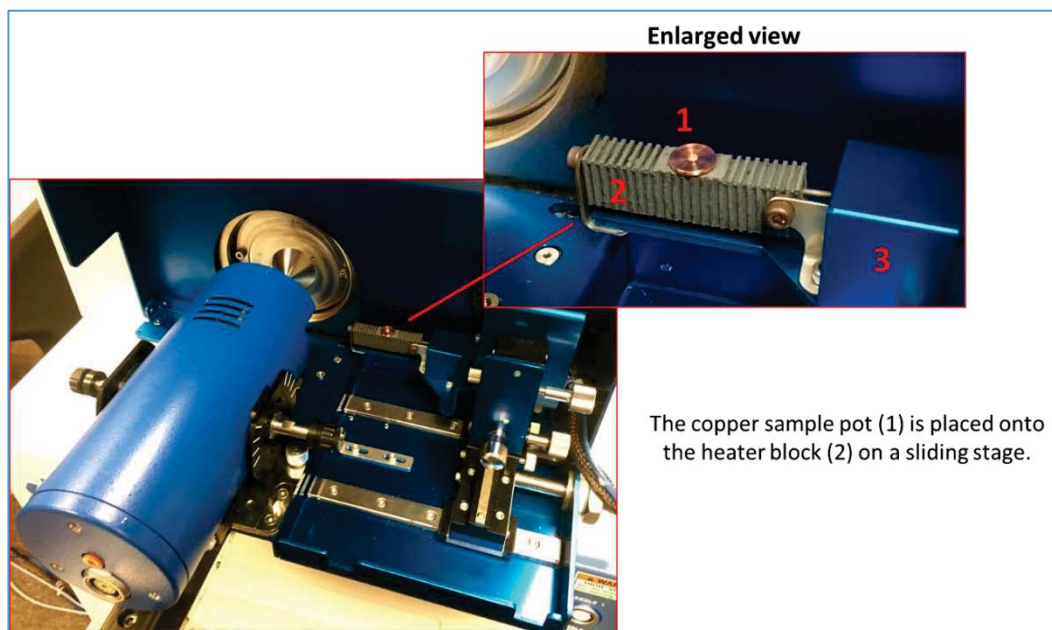
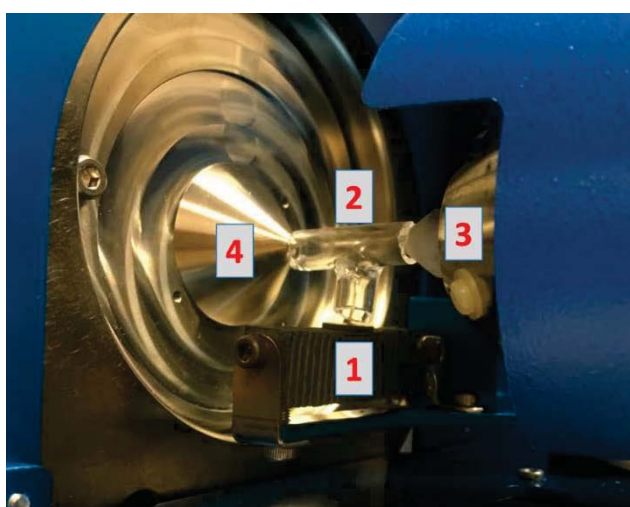


Figure 4. A sample mounted onto the ionRocket heater block.

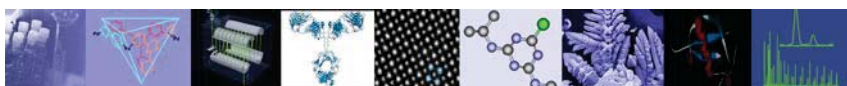


The sample pot and heater block (1) slide into position below a glass tee (2) mounted between the DART exit (3) and the mass spectrometer sampling orifice (4).

Figure 5. A sample mounted on the heater block, positioned below a glass tee.

The temperature ramp was programmed from ambient temperature to 600°C at a rate of 100°C min<sup>-1</sup>. Mass spectra were acquired at a resolving power of 10,000 in positive-ion mode at a spectral acquisition rate of 1 spectrum per second for the  $m/z$  range 50-1000.





### X-ray fluorescence (XRF)

A JEOL *Element Eye* (JSX-100S) benchtop x-ray fluorescence spectrometer (Figure 6) was used for all measurements using the *Quick and Easy Organic Analysis - Vacuum* solution. The vacuum condition was used to enhance sensitivity of light elements like silicon and aluminum. Measurement time was 60 seconds and a collimator setting of 9mm was set.



Figure 6. “Element Eye” benchtop x-ray fluorescence spectrometer

## Results

### Thermal desorption/DART/MS

Thermal desorption/DART mass spectra showed a clear and reproducible temperature dependence of polymer additives, natural rubber adhesive and pyrolysis products for each tape (Figure 7).

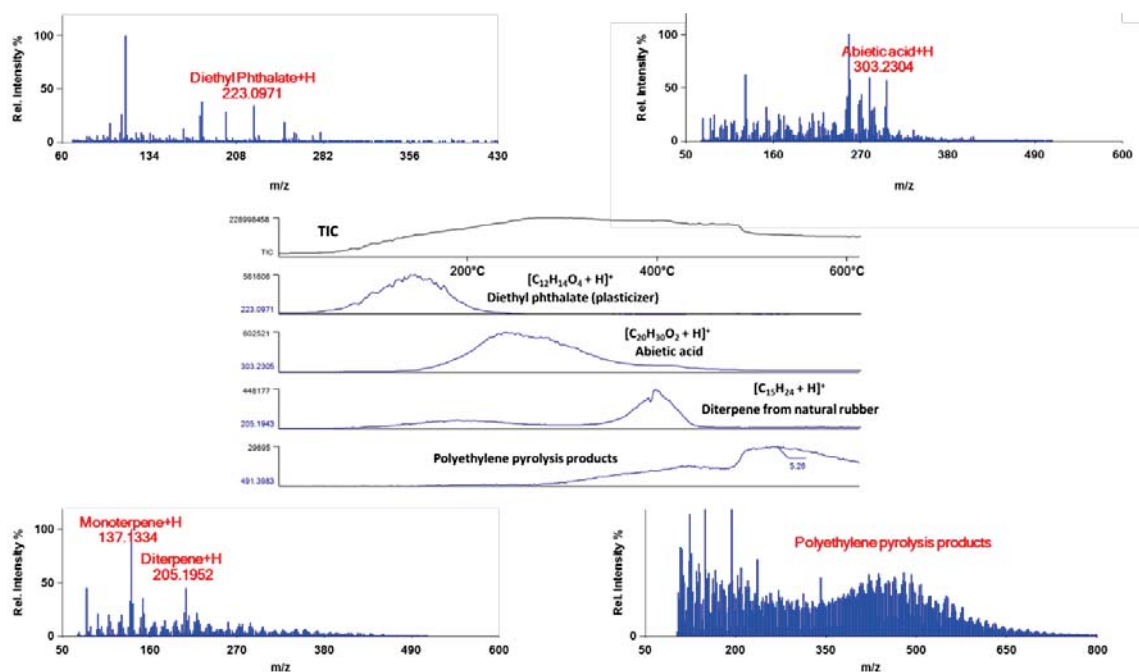


Figure 7. Temperature dependence and mass spectra for selected components



The thermal desorption profiles for certain components (for example abietic acid) differed reproducibly between samples (Figure 8).

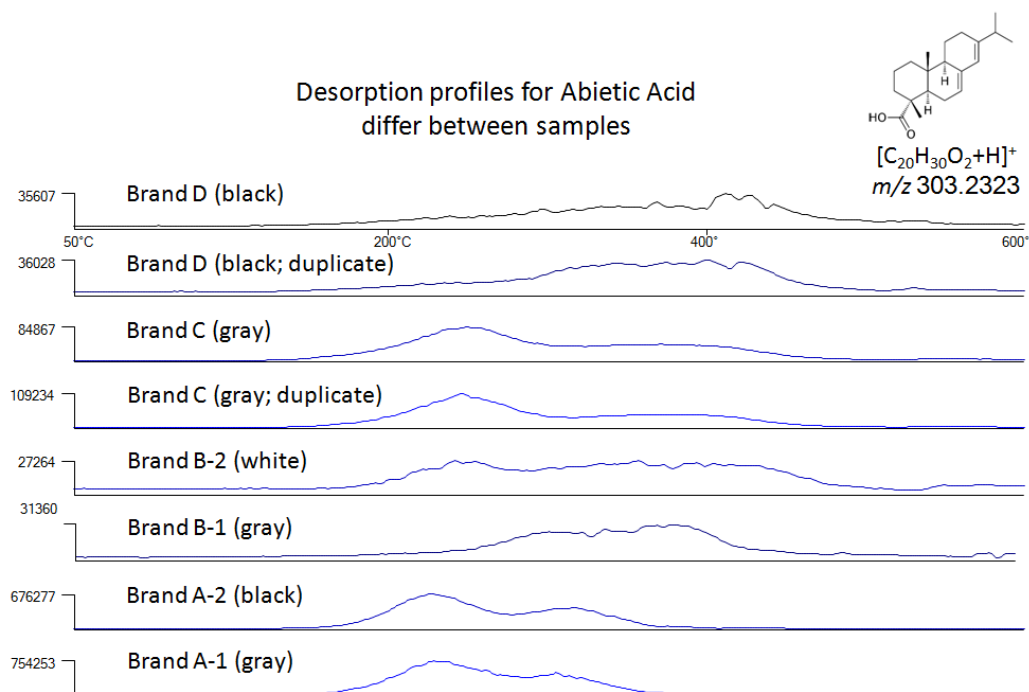
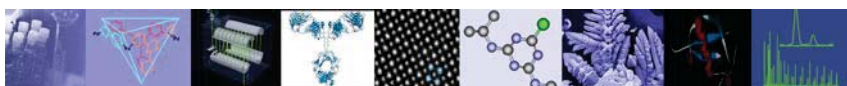


Figure 8. Thermal desorption profiles for abietic acid in different tapes.

The Brand A duct tapes (A-1 and A-2) showed nearly identical mass spectra and thermal desorption profiles, with one exception: a peak at  $m/z$  247.168 with the elemental composition  $[C_{16}H_{22}O_2 + H]^+$  was only present at significant levels in the gray tape, but not in the black tape.





Chemometric analysis of the thermal desorption mass spectra summed over the temperature range 144-166°C showed good separation between the different duct tapes. This temperature range was chosen because it highlighted differences between the additives in the different tapes without including excessive data from the natural rubber adhesive or pyrolysis products. The heat map (Figure 9) shows differences between the duct tapes. Kernel discriminant analysis (KDA, Figure 10) gave 100% accuracy for leave-one-out cross validation (LOOCV) using four principal components.

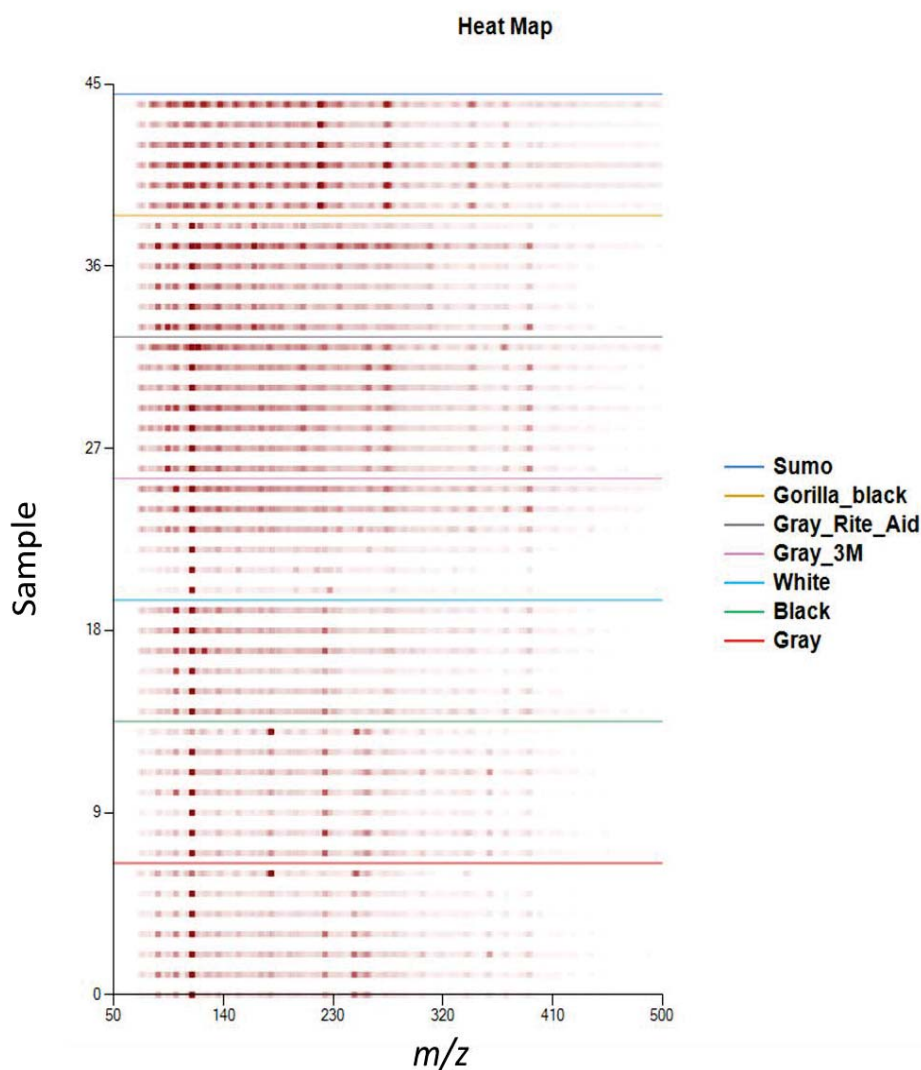


Figure 9. Heat map showing abundances for peaks in the mass spectra for each duct tape class.

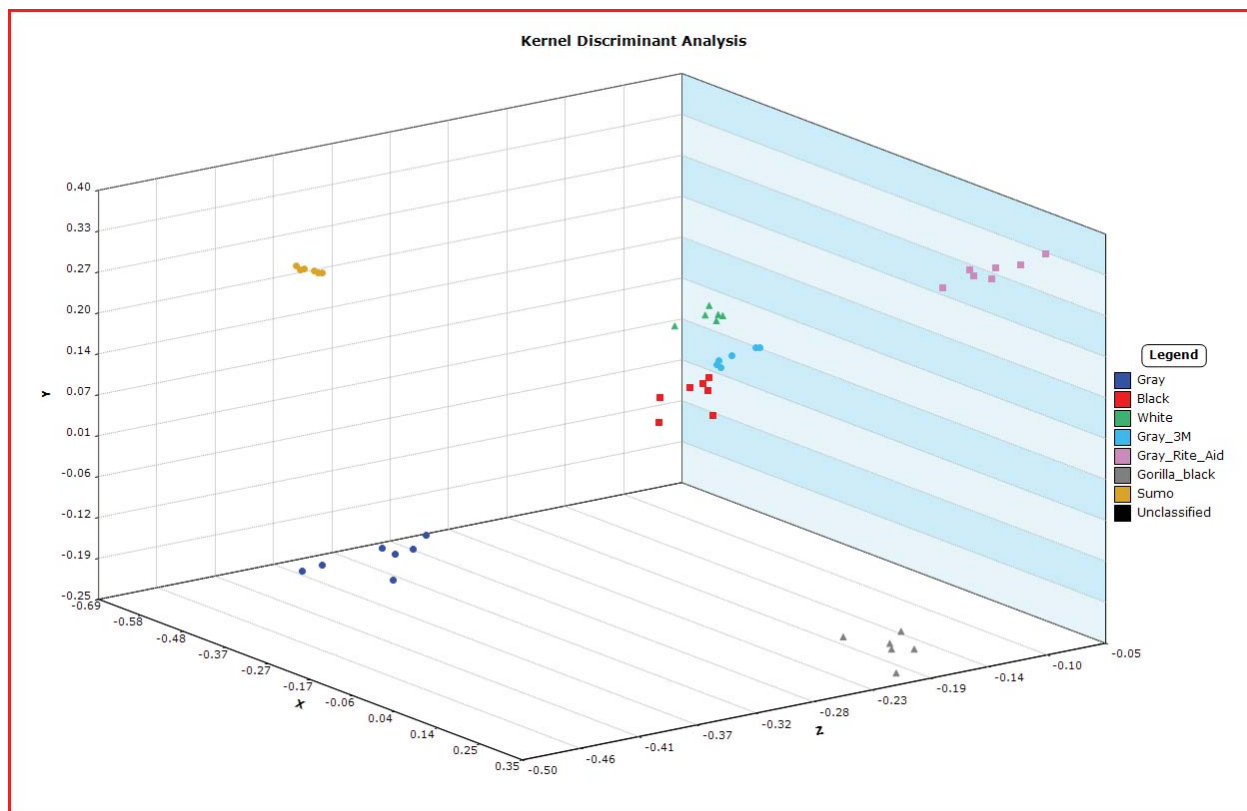
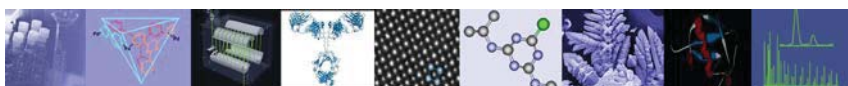
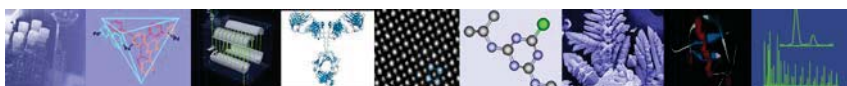


Figure 10. Kernel discriminant analysis of thermal desorption/pyrolysis DART mass spectra for seven duct tapes over the temperature range 144-166°C



## XRF

The XRF spectra showed differences in the atomic compositions for each tape. The gray tapes all contained significant amounts of aluminum, while the white tape showed abundant titanium (probably from  $\text{TiO}_2$  pigment). The black tape showed abundant Ti and also abundant Ca. A summary of the atomic compositions for each of six tapes is shown in Figure 11 along with images of the region analyzed.

	Weight %					
Element	A-1 (gray)	A-2 (black)	B-1 (gray)	B-2 (white)	C (gray)	D (black)
Al	0.50	0.06	0.50	0.08	0.92	0.02
Si	0.01	0.29	0.32	0.20	0.01	0.01
P		0.01	0.01	0.01		
S		0.02		0.00		0.05
Ca	1.67	3.47	6.63	6.46	0.71	8.21
Ti	0.26	0.51	0.25	2.32	0.59	0.08
Fe	0.01	0.02	0.02	0.02	0.00	0.02

Figure 11. Summary of XRF analysis of six duct tapes

## Conclusion

Mass spectra and thermal desorption profiles measured with the Biochromato *ionRocket* thermal desorption/pyrolysis system mounted on the JEOL *AccuTOF-DART* mass spectrometer showed clear and reproducible differences between the six different duct tapes. XRF data from the *Element Eye* showed distinct differences between each tape and provided information about the inorganic pigments used to color the tapes.

~ Application Note for DART ~

## Analysis of low polar compound by DART

~ analysis of organic electroluminescence materials ~

### Introduction

In MS Tips No. D031 we introduced the example of high polar compound analysis with DART. This application note introduces the example of the analysis of low polar compounds

For the mass spectrometric analysis of organic electroluminescence (EL) materials, which have been one of the typical luminescent materials in LC/MS (APCI, APPI), GC/MS (refer to MS Tips 78 and 87), MALDI-TOFMS, and TOFSIMS have been used.

This time, we have analyzed organic EL materials using DART as follows.

### Methods

The samples were adhered to the tip of a glass rod and presented directly to the DART™ ion source.

Sample	4,4'-Bis(carbozoi-9-yl)biphenyl (CBP) 4,4'-Bis(2,2-diphenyl-ethen-1-yl)biphenyl (DPVBi) (made by Luminescence Technology Corp., Taiwan)
Mass spectrometer	JMS-T100TD time-of-flight mass spectrometer
Ionization	DART (+)
Helium gas temperature	250 °C

### Results and discussion

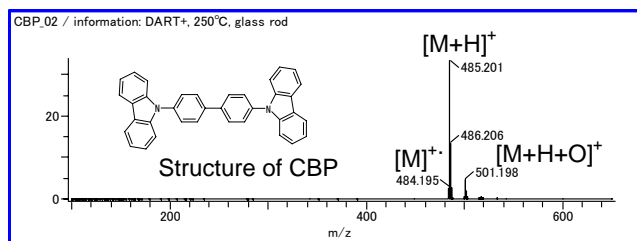


Fig. 1 DART(+) mass spectrum of CBP

Table 1 Estimated composition of CBP

Observed	Calculated	Error (10 <sup>-3</sup> u)	Estimated composition	Unsat.
485.20113	485.20177	-0.64	C <sub>36</sub> H <sub>25</sub> N <sub>2</sub>	25.5
501.19760	501.19669	0.92	C <sub>36</sub> H <sub>25</sub> N <sub>2</sub> O	25.5

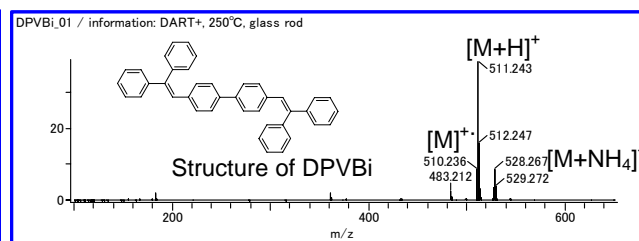


Fig. 2 DART(+) mass spectrum of DPVBi

Table 2 Estimated composition of DPVBi

Observed	Calculated	Error (10 <sup>-3</sup> u)	Estimated composition	Unsat.
511.24287	511.24258	0.29	C <sub>40</sub> H <sub>31</sub>	25.5
528.26722	528.26912	-1.90	C <sub>40</sub> H <sub>34</sub> N <sub>1</sub>	25.5

In both samples, [M+H]<sup>+</sup> was detected as base peak. In addition, [M+NH<sub>4</sub>]<sup>+</sup> and [M]<sup>+</sup> were also detected. With CBP, ion which can be deduced as [M+H+O]<sup>+</sup> from the accurate mass has also been detected. DART has been proven effective in the analysis of low polar compounds such as organic EL.

## ~ Application Note for DART ~

**Analysis of highly polar compound by DART**  
**~ analysis of ionic liquid ~****Introduction**

Direct analysis in real time (DART™) is applicable to a wide variety of samples; from low polar to highly polar compounds.

Ionic liquids have drawn much attention from various engineering fields, such as tribology, because of their unique properties of electrical conductivity, extremely low vapor pressure, low viscosity, low combustibility, etc. The sample was analyzed by dipping a glass rod to the sample and presented it directly to the DART™ ion source.

**Methods**

Sample	1-ethyl-3-methylimidazolium-bis(trifluoromethylsulfonyl)imide (EMI-TFSI)
Mass spectrometer	JMS-T100TD time-of-flight mass spectrometer
Ionization	DART (+), DART (-)
Helium gas temperature	200 °C

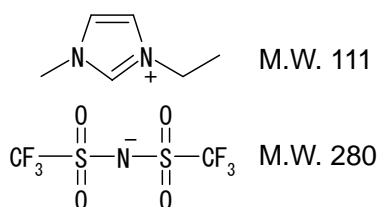
**Results and discussion**

Fig. 1 Structural formulae of EMI-TFSI

As shown in Fig. 2, base peaks were observed at  $m/z$  111 and  $m/z$  280 for DART(+) and DART(-) respectively. The elemental compositions of the cation and anion were confirmed by accurate mass measurements as shown in Table 1.

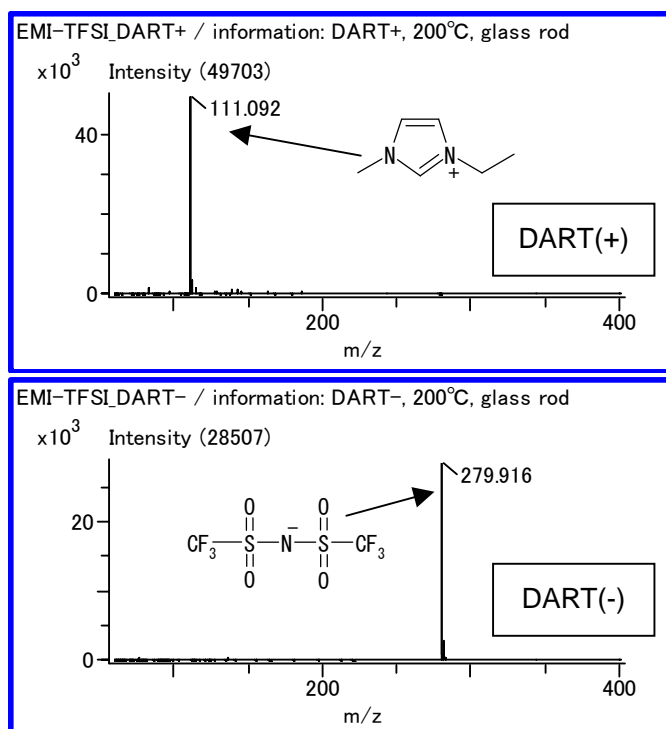


Fig. 2 DART mass spectra (top: DART(+)) bottom: DART(-)

	Measured	Theoretical	Error ( $10^{-3}$ u)	Elucidated formula	Unsaturation
Cation	111.09226	111.09222	0.04	$C_6H_{11}N_2$	2.5
Anaion	279.91569	279.91729	-1.60	$C_2F_6NO_4S_2$	2.5

## ~ Application Note for DART ~

**Analysis of Organic Contaminant on Metal Surface**

DART can ionize organic substance on solid surface in atmospheric pressure. By utilizing this feature, we analyzed organic contaminant adhered to a metal part (Fig. 1).

We wiped of the organic contamination on the metal surface by using ceramic fiber paper and analyzed it by holding up the ceramic fiber paper directly into the DART ion source. Peaks with 74 interval at  $m/z$  371,  $m/z$  445, and  $m/z$  519 are observed (Fig. 2; upper). The elemental compositions of these ions were deduced from their respective accurate masses (Table 1) and they were found to be poly(dimethylsiloxane) series.

One of the candidates for the contamination was silicone vacuum grease. The grease was analyzed separately by DART and the mass spectrum (Fig. 2; lower) was found to contain the same peaks. We concluded that the contamination was from the vacuum grease.



Fig. 1 Organic contamination on metal surface

**Conditions**

Ionization: DART (+)

Helium gas temperature: 250°C

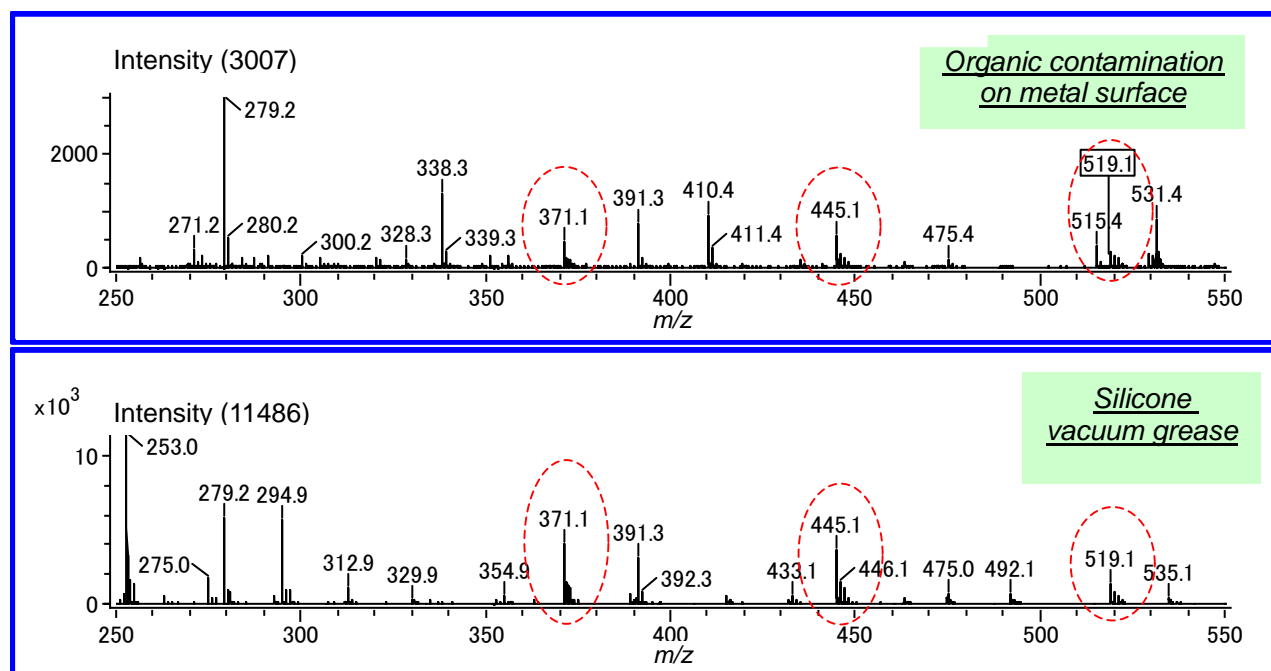


Fig. 2 DART (+) mass spectra

Upper: sample, lower: silicone vacuum grease

Table 1 Estimated elemental compositions of major ions from the sample

Observed $m/z$	Calculated $m/z$	Error (ppm)	Estimated composition	Unsaturation
371.10133	371.10178	-1.20	$12C_{10} 1H_{31} 16O_5 28Si_5$	0.5
445.12036	445.12057	-0.48	$12C_{12} 1H_{37} 16O_6 28Si_6$	0.5
519.13959	519.13936	0.44	$12C_{14} 1H_{43} 16O_7 28Si_7$	0.5

## Chemical Reaction Monitoring with the AccuTOF-DART™ Mass Spectrometer

### Introduction

DART provides a convenient means for monitoring the progress of chemical reactions. Reactants, intermediates, products and byproducts can be detected by simply dipping a glass rod into the reaction pot and then placing the rod in front of the DART ion source. The AccuTOF's ability to measure accurate masses and isotopic abundances makes it possible to confirm or identify the elemental compositions of peaks in the mass spectra. Here we show the use of AccuTOF-DART to monitor the acetylation of 1,5-hexanediol as a function of time.

### Experimental

600  $\mu$ l of 1,5-hexanediol (4.9 mmol) was mixed with 700  $\mu$ l (12.3 mmol) of glacial acetic acid and one drop of concentrated sulfuric acid in a loosely capped scintillation vial. The reaction was slowly warmed with a heat gun and a fume vent was positioned over the reaction vial and the DART source. Samples were taken periodically for analysis with the AccuTOF-DART by dipping a melting point tube into the reaction mixture and placing the tube in front of the DART ion source for a few seconds. The reaction progress was monitored by plotting the fractional

abundances of the protonated molecules ( $MH^+$ ) as measured for each component in the mass spectra.

### Results

Figure 1 shows the time dependence of the fractional abundances of unreacted 1,5-hexanediol ( $MH^+$  at  $m/z$  119.1072), the reaction intermediate 1,5-hexanediol monoacetate ( $MH^+$  at  $m/z$  161.1178) and the product 1,5-hexanediol diacetate ( $MH^+$  at  $m/z$  203.1283). At 20 minutes, roughly equal amounts of the intermediate monoacetate and the diacetate are present. At 90 minutes, the reaction was incomplete and unchanging because an insufficient excess of acetic acid was present. Adding another 100  $\mu$ l of acetic acid allowed the reaction to go to completion in 120 minutes.

### Conclusion

AccuTOF-DART provides a convenient and rapid means for monitoring the progress of chemical reactions. Reactants, intermediates, and products are readily detected.

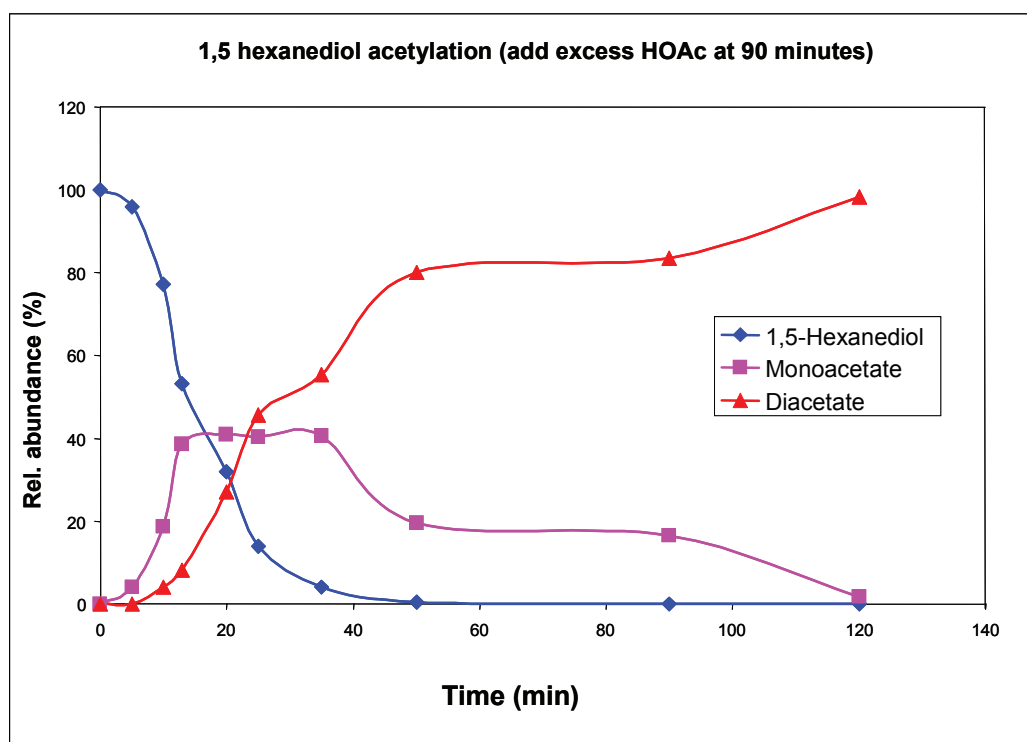


Figure 1. Synthesis of 1,5-hexanediol diacetate monitored by AccuTOF-DART.



## Direct Analysis of Organometallic Compounds

### Summary

Organometallic compounds play an important role in chemistry, as recently recognized by the awarding of the 2005 Nobel Prize in Chemistry to Chauvin, Schrock and Grubbs. Characterization of organometallic compounds by mass spectrometry can sometimes be complicated by problems with solubility and reactivity. Electron ionization can be used for some volatile organometallics. Fast atom bombardment (FAB) and electrospray ionization (ESI) are useful provided suitable solvents can be used. Field desorption (FD) is often effective, but FD emitters can be fragile and the analysis should be carried out by an experienced operator.

DART (Direct Analysis in Real Time) complements these methods and provides an alternative; it is fast and does not require solvents. The sampling area is purged

with an inert gas, reducing the likelihood of undesirable reactions. Further, AccuTOF-DART permits exact mass measurements without requiring the presence of a reference standard during the sample measurement. DART is extremely robust and does not require special operator training.

Mass spectra of several organometallic compounds were obtained by using DART. A few dry particles of each compound were placed in front of the DART source on a melting point tube and mass spectra were obtained within seconds. The best results were obtained by using small quantities of sample; very large quantities can result in ion-molecule reactions between sample ions and sample neutrals, resulting in isotopic patterns characterized by both  $M^+$  and  $[M+H]^+$ . All labeled assignments were confirmed by exact mass measurements and isotope pattern matching.

### Ferrocene: $Fe(C_5H_5)_2$

Ferrocene produces a molecular ion  $M^+$  for low sample quantities (micrograms or less). If a larger quantity is analyzed, ion-molecule reactions result in protonation of the molecule to produce  $[M+H]^+$ .

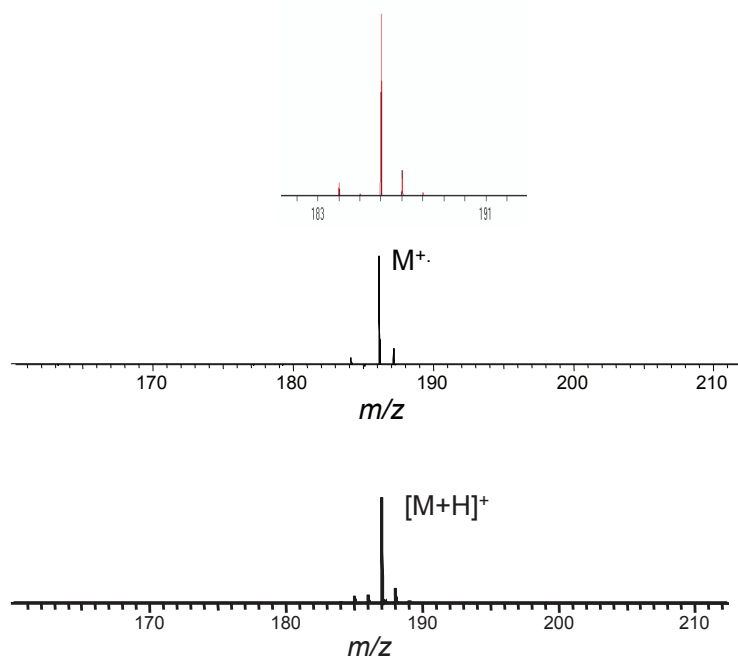


Figure 1. Top: Theoretical isotope pattern for  $Fe(C_5H_5)_2^+$ . Middle: Mass spectrum obtained by using a very small quantity of ferrocene. Bottom: Mass spectrum obtained by analyzing a large quantity of ferrocene on the melting point tube.

### Tungsten hexacarbonyl: $W(CO)_6$

Like ferrocene, tungsten hexacarbonyl produces mass spectra characterized by a molecular ion for low sample concentrations. A protonated molecule is observed if large sample quantities are presented to the DART source.

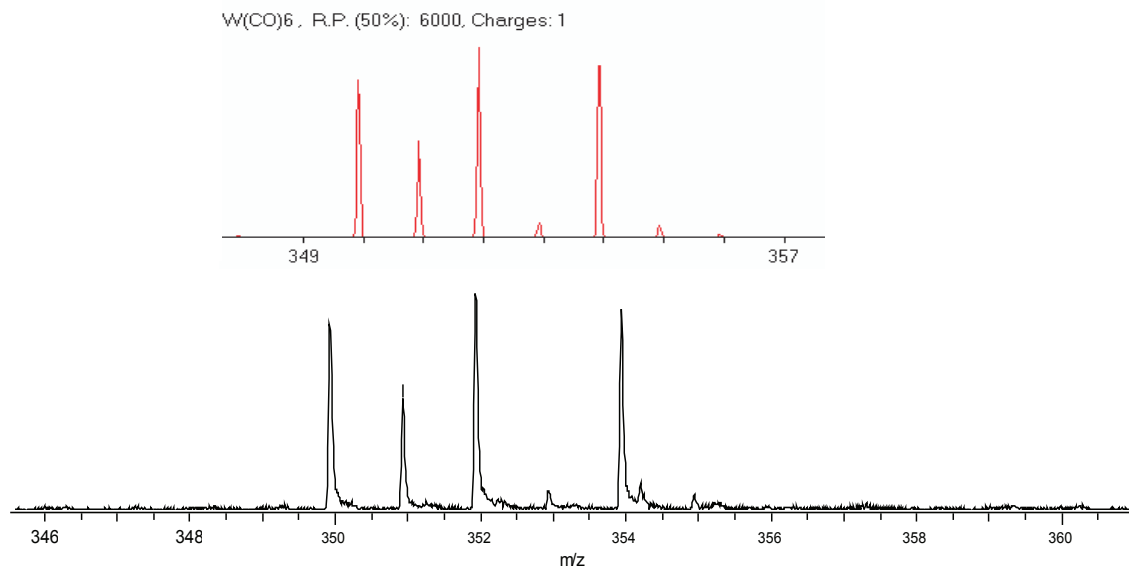


Figure 2. Top: theoretical isotope pattern for  $W(CO)_6^+$ . Bottom: measured mass spectrum for tungsten carbonyl.

### Acetylacetonato rhodium dicarbonyl: $C_5H_8O_2Rh(CO)_2$

This compound readily produces a molecular ion.

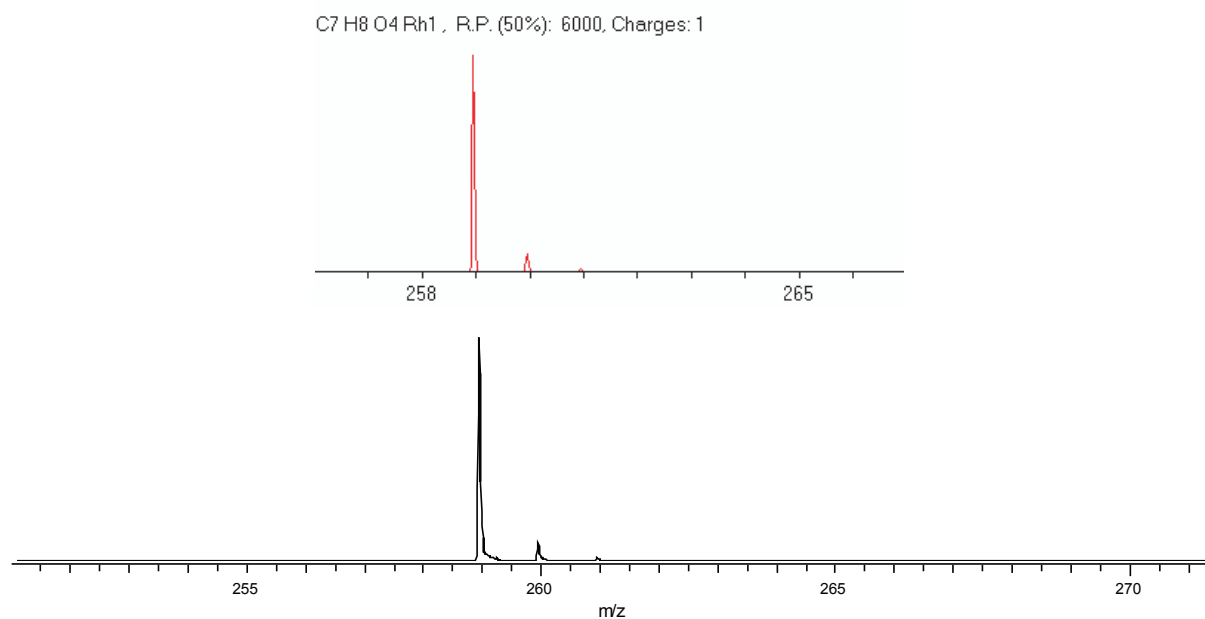


Figure 3. Top: theoretical isotope pattern for  $C_5H_8O_2Rh(CO)_2^+$ . Bottom: measured mass spectrum.

### (1,5-cyclooctadiene) platinum (II) chloride ( $C_8H_{12}PtCl_2$ )

This compound does not readily protonate. However, it produces an ammonium adduct if vapor from a dilute solution of ammonium hydroxide is present. Chloride loss and a related water adduct are also observed. A dimer  $((C_8H_{12}Pt)_2Cl_3)^+$  is also observed at higher mass (not shown).

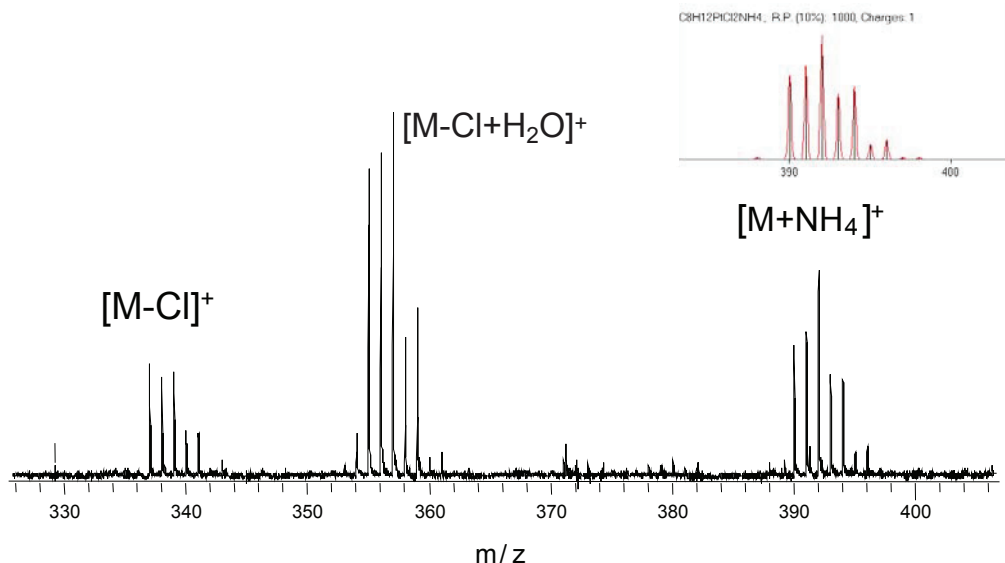


Figure 4. Top inset: theoretical isotope pattern for  $[C_8H_{12}PtCl_2+NH_4]^+$ . Bottom: measured mass spectrum.

### Bis(diphenylphosphoethane) platinum dichloride: $Pt(DPPE)Cl_2$

This compound behaves in a similar manner to (1,5-cyclooctadiene) platinum (II) chloride. An ammonium adduct can be observed, together with a chloride loss and a dimer  $[2M-Cl]^+$ .

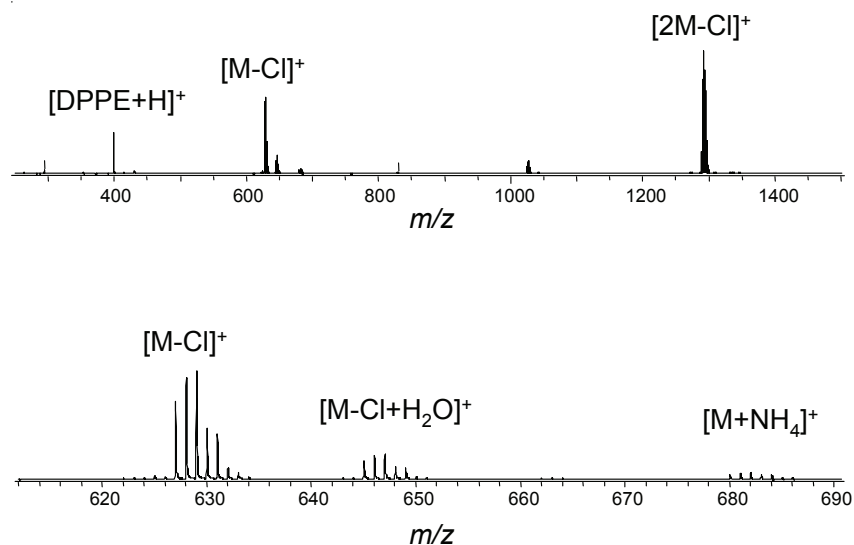


Figure 5. DART mass spectrum of  $Pt(DPPE)Cl_2$ . Top: mass spectrum for  $m/z$  350 to  $m/z$  1500. Bottom: enlarged view of region near  $[M-Cl]^+$ .

### Conclusion

AccuTOF-DART provides a convenient means for characterizing many organometallic compounds. No solvents are required and excellent agreement between theoretical and observed masses and isotopic abundances are obtained.



## Rapid Analysis of *p*-Phenylenediamine Antioxidants in Rubber

### Introduction

*p*-Phenylenediamine (PPD) and derivative compounds are commonly used as antioxidants and antiozonants in black rubber. These compounds can cause sensitization leading to contact dermatitis in susceptible individuals. Detection of additives in polymers such as rubber can be important for clinical, forensic, and manufacturing applications. Here we show that DART can be used to identify the presence of these compounds within seconds without requiring

any solvents or sample preparation.

### Experimental

Analysis was carried out by using the AccuTOF-DART. A piece of rubber from a mountain bike tire was placed in front of the DART ion source, which was operated with helium in positive-ion mode and a gas heater temperature of 250 degrees C. Signals appeared within seconds after placing the rubber in front of the DART source.

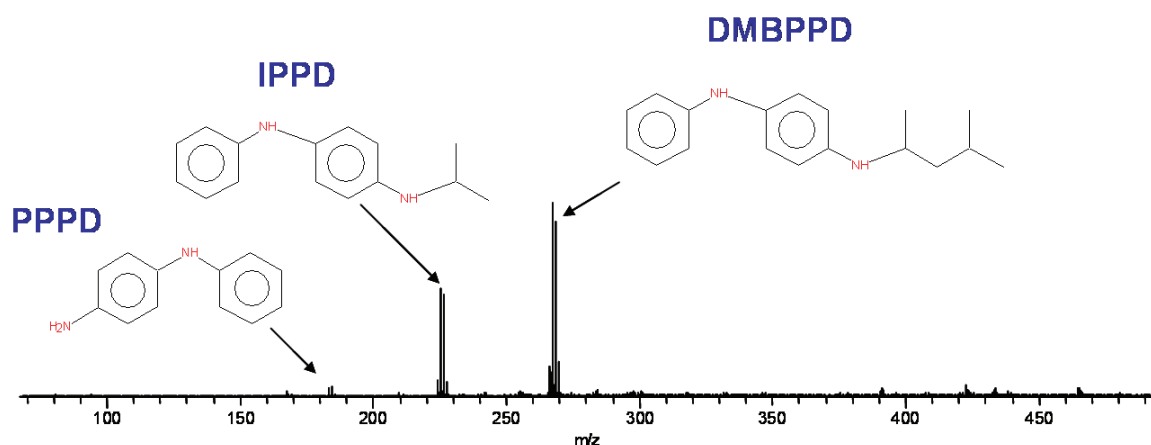


Figure 1. DART mass spectrum of a rubber particle from a mountain bike tire.

Meas. mass u	Abund. %	Diff. mmu	Unsat.	Compositions		
226.147202	0.00	0.20	8.0	C <sub>15</sub> H <sub>18</sub> N <sub>2</sub>	IPPD	M <sup>+</sup> .
227.154297	0.00	-0.53	7.5	C <sub>15</sub> H <sub>19</sub> N <sub>2</sub>	IPPD	[M+H] <sup>+</sup>
268.194214	0.00	0.27	8.0	C <sub>18</sub> H <sub>24</sub> N <sub>2</sub>	DMBPPD	M <sup>+</sup> .
269.201385	0.00	-0.40	7.5	C <sub>18</sub> H <sub>25</sub> N <sub>2</sub>	DMBPPD	[M+H] <sup>+</sup>

Table I.. Elemental compositions for *p*-phenylenediamine antiozonants in a rubber tire.

### Results

Exact mass measurements combined with accurate isotopic abundances provided elemental compositions (Table I) that were searched against the NIST mass spectral database. Three antiozonant compounds were recognized from their exact mass measurements

(see Table 1): N-Phenyl-*p*-phenylenediamine (PPD), N-Isopropyl-N'-phenyl-*p*-phenylenediamine (IPPD), and N-(1,3-Dimethyl butyl)-N'-phenyl-*p*-phenylene diamine (DMBPPD).



## Identification of Polymers

DART can be used to analyze polymers, cements, resins, and glues by increasing the gas temperature to 450-550° C to induce pyrolysis. This has been applied to a variety of polymers including Nylons, polypropylene and polyethylene, polyethylene terephthalate (PET), polyesters, poly(methyl methacrylate) (PMMA), polycarbonate, phenoxy resin, polystyrene, and cellulose. Examples are shown here for standard samples of Nylon, polystyrene, and cellulose.

The DART source was operated with helium in positive-ion mode. The gas heater was set to 475° C. Resins were cured in an oven for several hours before analysis; some resin samples had been cured for longer periods of time (months or years). Exact masses and accurate isotopic abundances were used to assign elemental compositions for peaks in the mass spectra. Nominal-mass spectra were exported into a library database in NIST format to facilitate identification of unknowns.

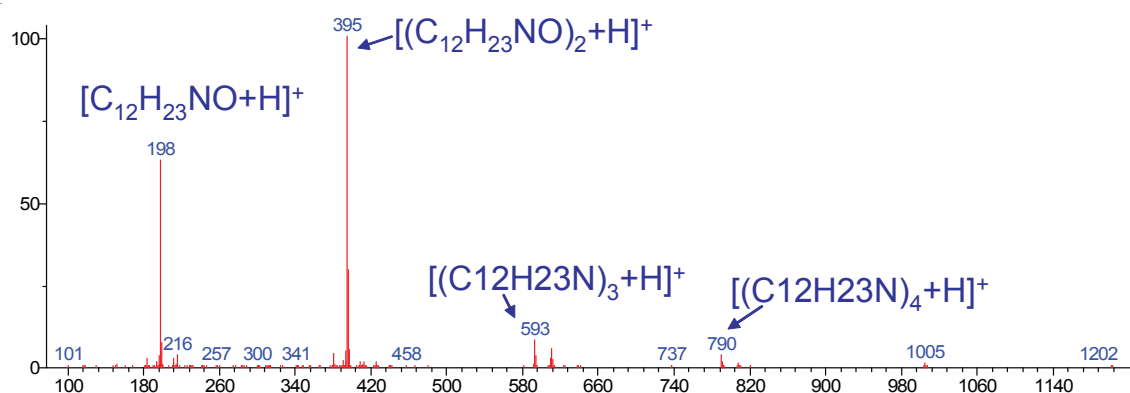


Figure 1. Nylon 12: Poly(lauryl lactam).

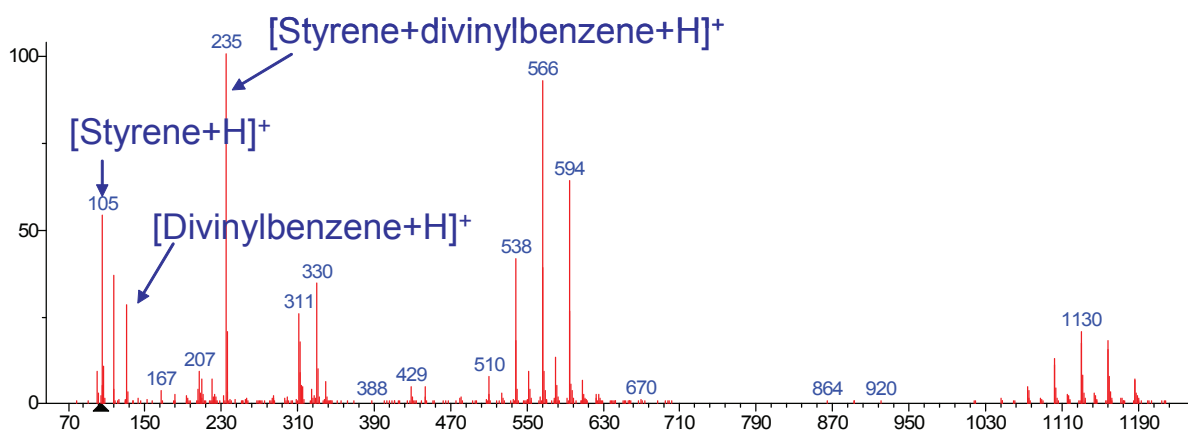


Figure 2. Polystyrene bead, average molecular weight ~ 240,000



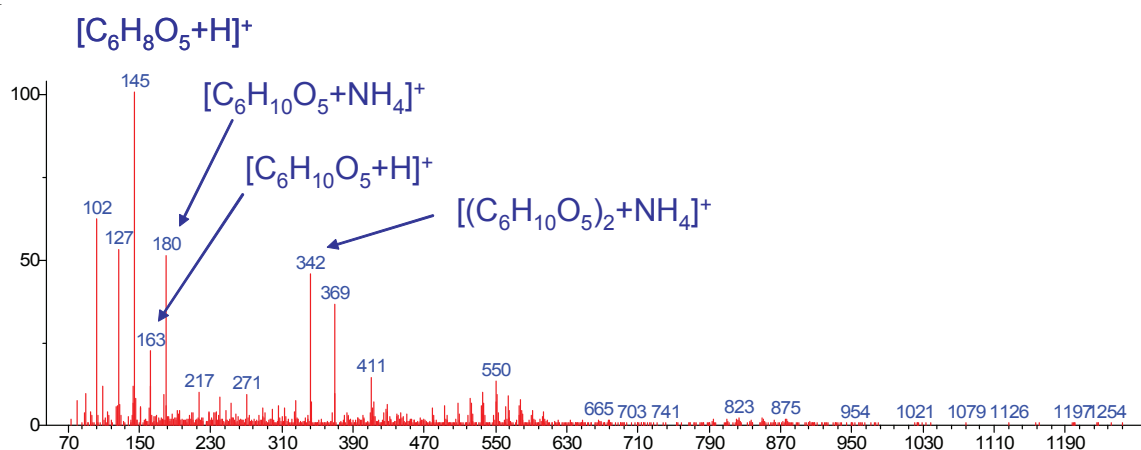


Figure 3. Cotton fibers showing peaks characteristic of cellulose  $(C_6H_{10}O_5)_n$ . Dilute ammonium hydroxide vapor enhanced  $[M+NH_4]^+$  formation.

It should be noted that mass spectra of commercial polymers may be dominated by plasticizers and other additives which can complicate the analysis. Nevertheless, it was possible to identify polyethylene in a milk bottle, poly(ethylene terephthalate) in a soda bottle, and polystyrene in a CD case and a mass spectrometer filament box.

### Conclusion

Polymers can be analyzed by DART. Fingerprint mass spectra are produced, and common formulation components can often be identified and confirmed by exact mass measurements.

## Rapid Analysis of Glues, Cements, and Resins

DART™ can be used to analyze polymers, cements, resins, and glues by increasing the gas temperature to 450-550° C to induce pyrolysis. This has been applied to a variety of glues and resins, including epoxies, polyimide resins, PVD cement, and cyanoacrylates. Examples are shown here for cured and uncured epoxy resin and cyanoacrylate glues.

The DART was operated with helium in positive-ion mode. The gas heater was set to 475° C. Resins were cured in an oven for several hours before analysis; some resin samples had been cured for longer periods of time (months or years). Exact masses and accurate isotopic abundances were used to assign elemental compositions for peaks in the mass spectra. Nominal-mass spectra were exported into a library database in NIST format to facilitate identification of unknowns.

The black component (Figure 1) of a common binary quick-curing epoxy is found to be bisphenol A diglycidyl ether

ether (DGEPA) and the white component (Figure 2) is the hardener DMP 30. The cured epoxy (Figure 3) shows some peaks common to both of these components, but new peaks are also observed from the polymerized resin.

Two different cyanoacrylate glues were examined. Both showed ethyl cyanoacrylate  $[M+H]^+$  ( $m/z$  126) and its fragments  $C_4H_2NO^+$  ( $m/z$  80) and  $C_4H_4NO_2^+$ . Product 1 also contained allyl methacrylate and a polymer component with ethylene oxide (EO) subunits. Product 2 contained the common plasticizers tributyl citrate and tributyl acetylacrylate.

### Conclusion

Glues, cements, and resins can be analyzed by DART. Fingerprint mass spectra are produced, and common formulation components can be identified and confirmed by exact mass measurements.

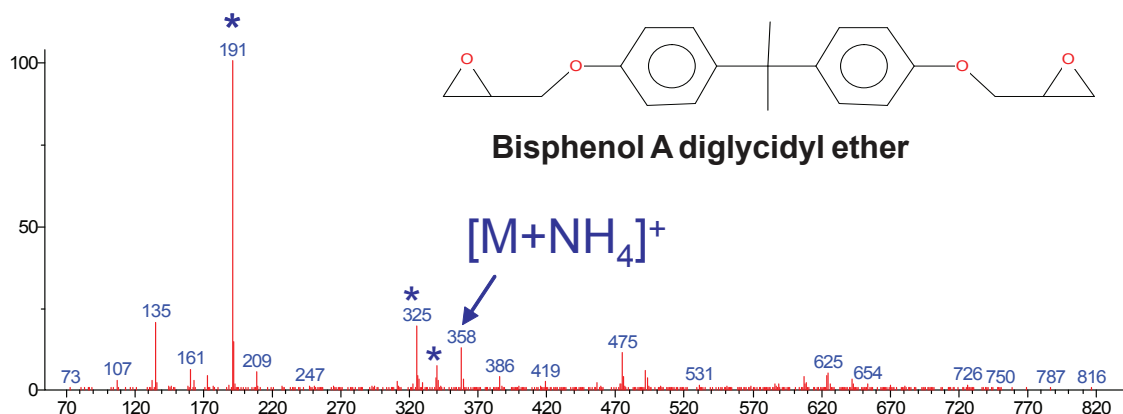


Figure 1. Uncured epoxy resin (black component)

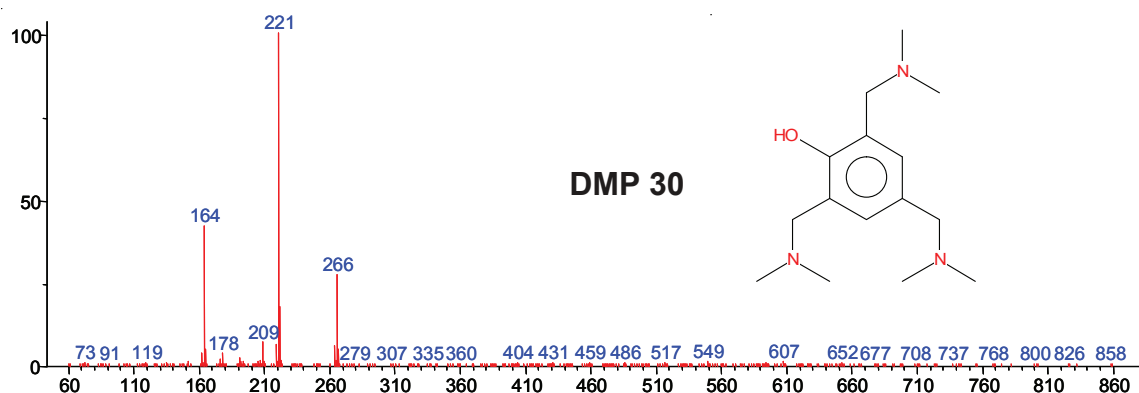


Figure 2. Uncured epoxy resin (white component)

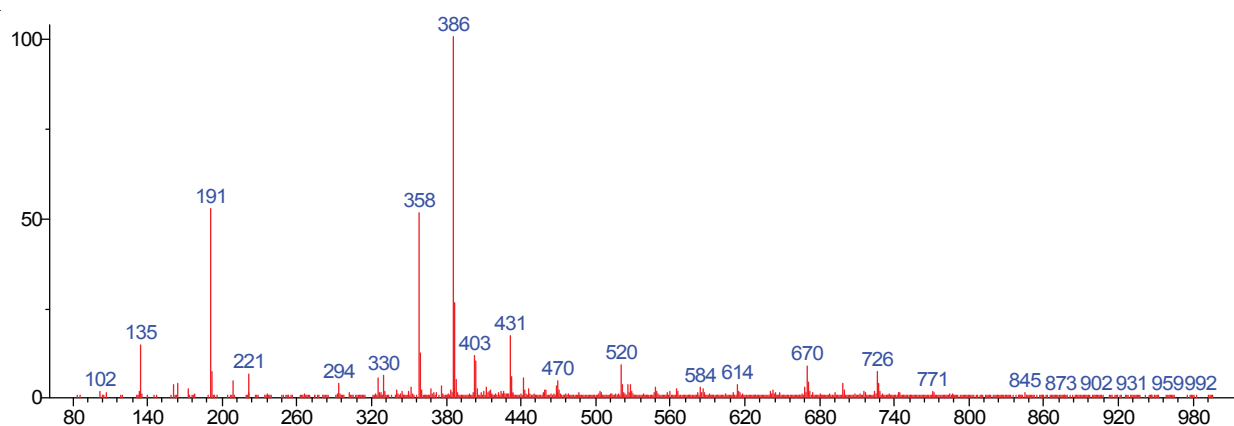


Figure 3. Cured epoxy resin on metal surface

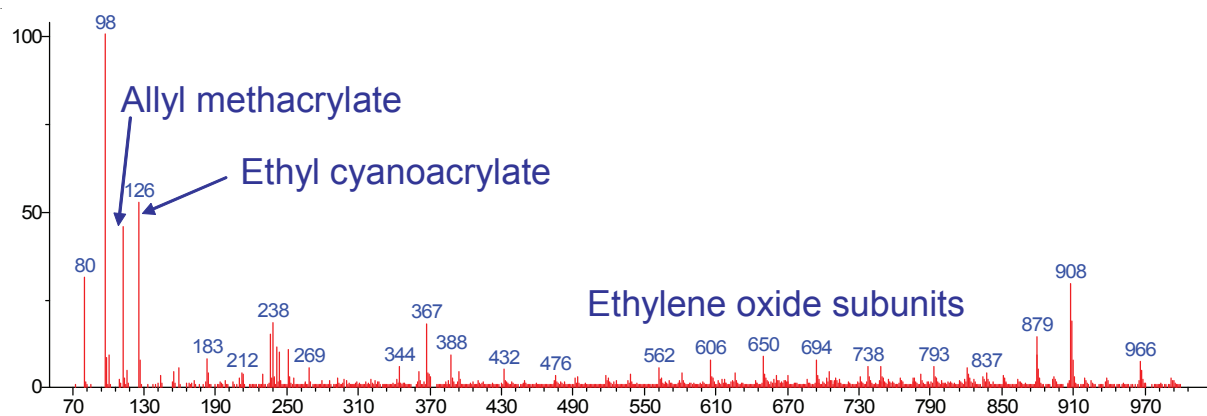


Figure 4. Cured cyanoacrylate glue product 1

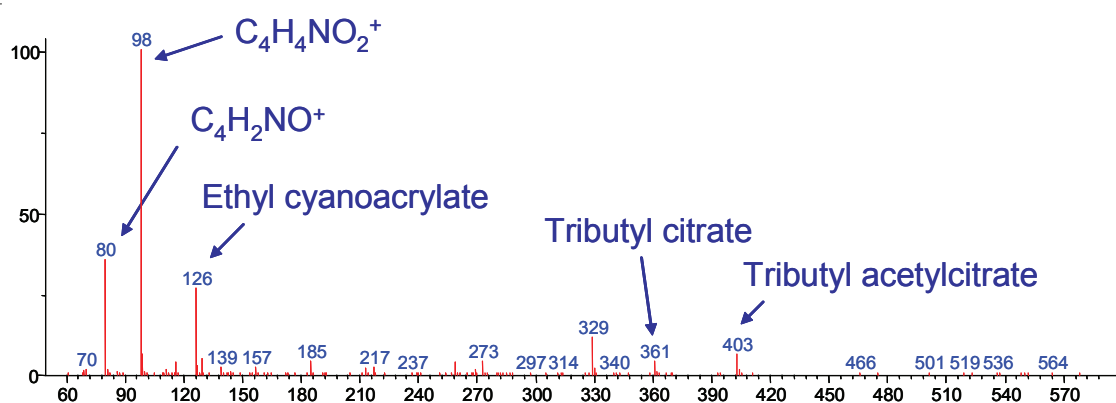


Figure 5. Cured cyanoacrylate glue product 2

## Direct Analysis of Adhesives

DART can be used with a heated gas stream to rapidly pyrolyze and identify low-volatility materials such as adhesives and resins, directly on surfaces. Although these materials are not pure compounds, a library of DART mass spectra can be created and searched to identify materials, and exact mass measurements coupled with accurate isotopic abundances can be used to identify unknown components. Examples are shown here for cured and uncured epoxies and acrylate adhesives on metal and glass.

All samples were analyzed by acquiring positive-ion mass spectra with the DART source operated with helium

and a gas heater setting of 450° C (helium temperature ~350° C). All mass spectra were measured over the  $m/z$  range 60-1000 at a resolving power of 6000. Following each analysis, a glass rod coated with PEG 600 was placed in front of the DART source to provide a calibration for exact mass measurements. A nominal-mass library of adhesive mass spectra was created by using the software link to the NIST version 2.0 mass spectra database search program. All figures shown here are copied from that library and only integer masses are shown although exact masses were recorded for all peaks.

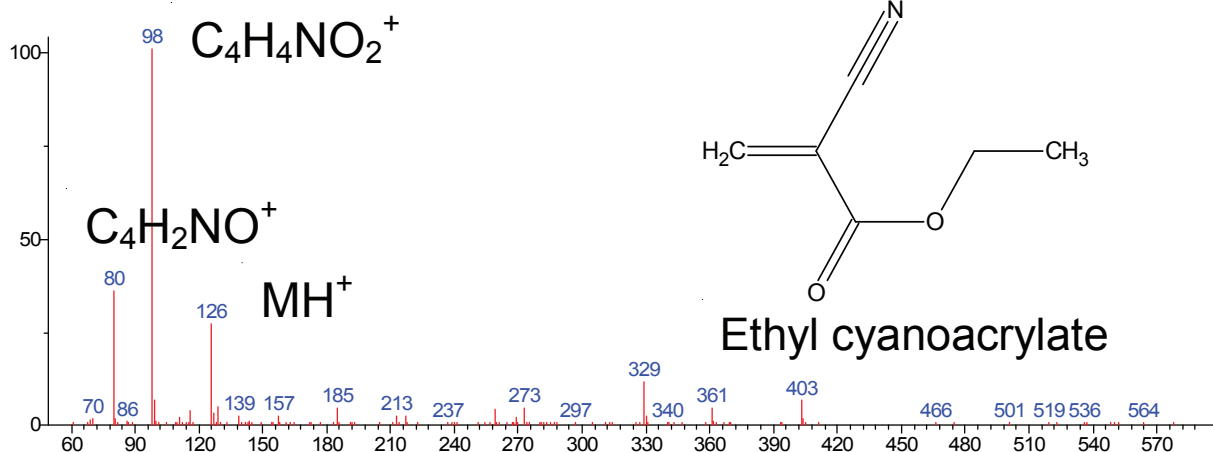


Figure 1. Cyanoacrylate adhesive on metal (Product 1)

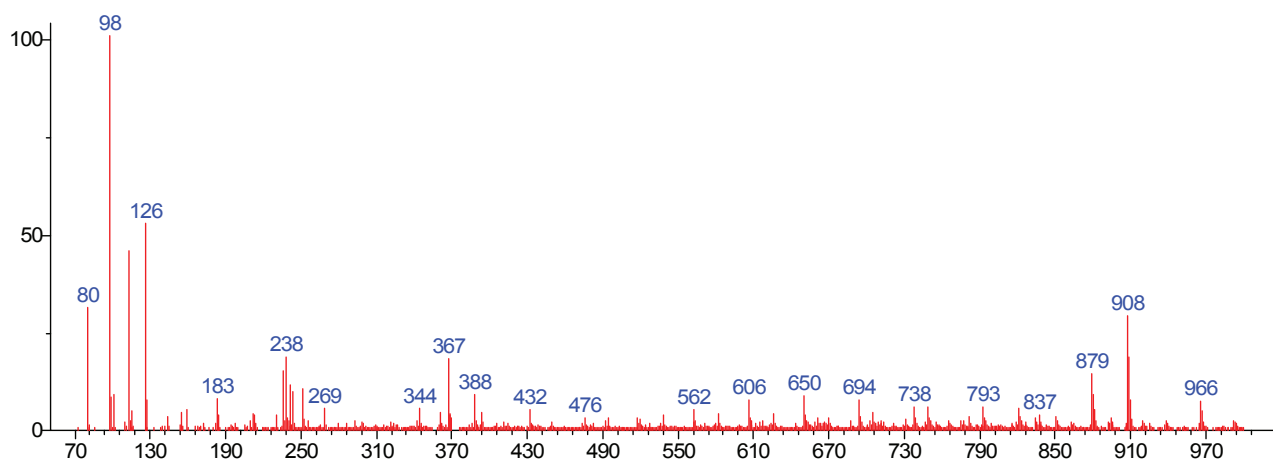


Figure 2. Cyanoacrylate adhesive on metal (Product 2)

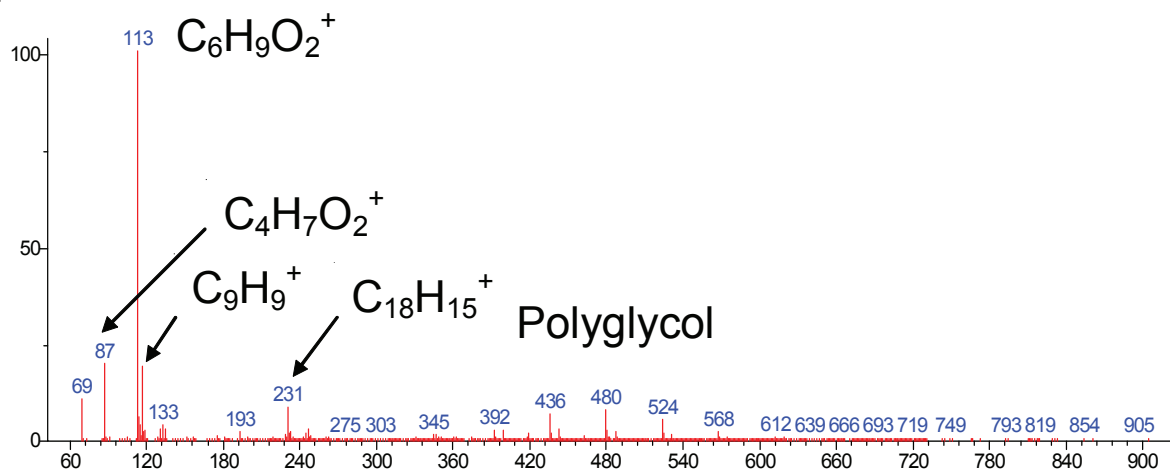


Figure 3. Methacrylate ester adhesive on glass (Product 3)

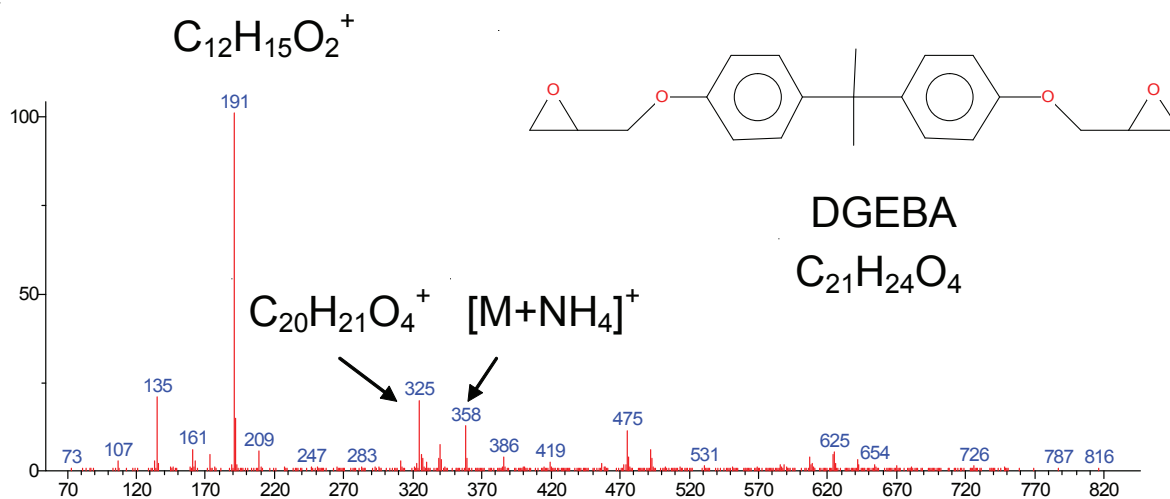


Figure 4. Epoxy resin (black component, uncured)

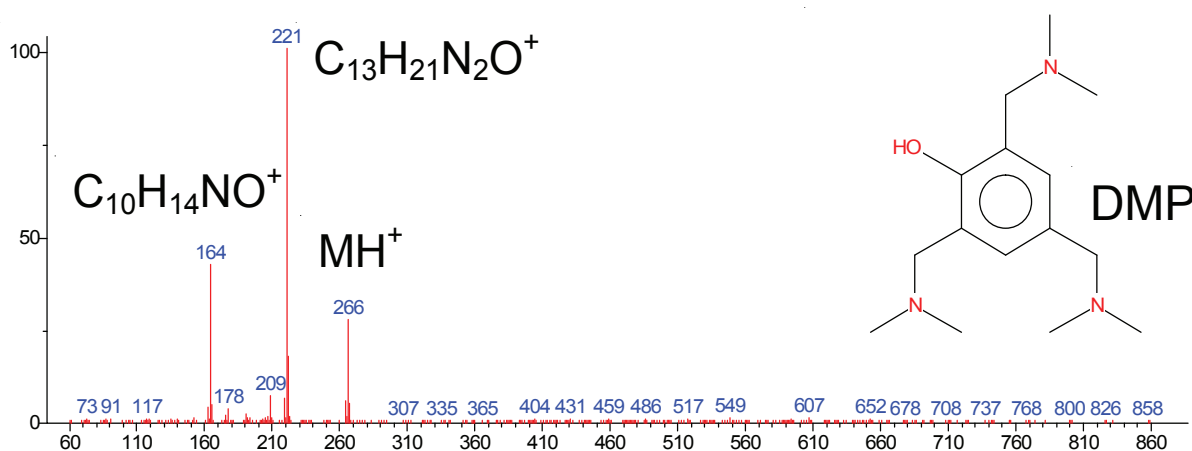


Figure 5. Epoxy hardener (white component)

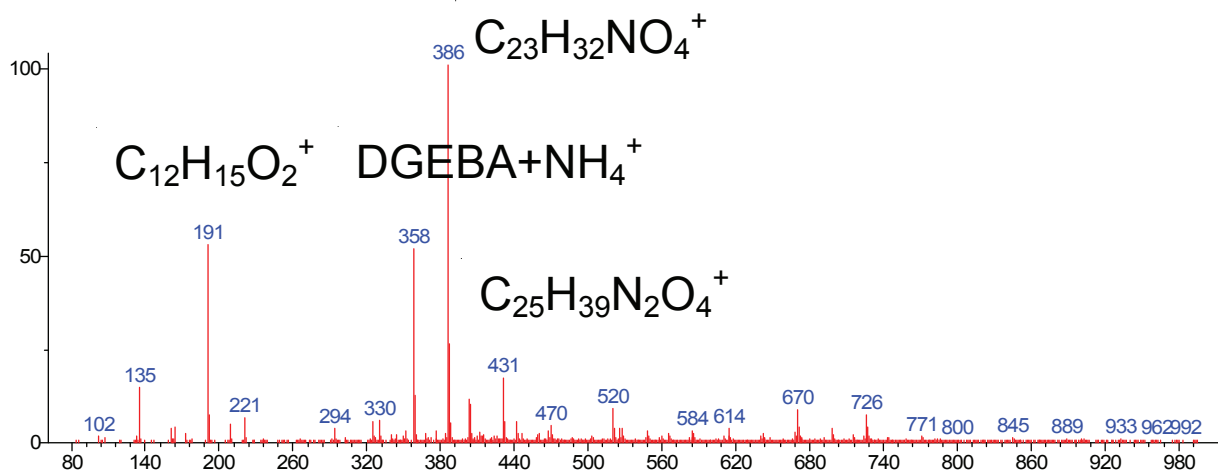


Figure 6. Cured epoxy

Both cyanoacrylate products show ethyl cyanoacrylate ( $m/z$  126.0555) and fragment ions  $C_4H_2NO^+$  ( $m/z$  80.0136) and  $C_4H_4NO_2^+$  ( $m/z$  98.0242). Product 2 shows an additional peak at measured  $m/z$  113.0602. This differs by only -0.05 u from the calculated  $m/z$  for  $C_6H_9O_2^+$ , tentatively assigned as  $[M+H]^+$  for allyl methacrylate. Product 2 also shows a series of high-mass peaks that differ by 44.0262, indicative of ethylene oxide based polymer subunits. A product described as a “methacrylate ester” (Figure 3) was dominated by the same  $C_6H_9O_2^+$  peak (assigned as allyl methacrylate), with methacrylic acid observed as  $C_4H_7O_2^+$  at  $m/z$  87.0447 (+0.1 mmu error).

Several binary epoxy formulations (separate resin and hardener) were examined. Figures 4 and 5 show the spectrum of two separate uncured components of a fast-curing epoxy and Figure 6 shows the cured epoxy.

The major compound in the uncured epoxy resin (black component) is identified by exact mass as the diglycidyl ether of bisphenol A or DGEBA. This has the composition  $C_{21}H_{24}O_4$  with  $[M+NH_4]^+$  observed at  $m/z$  358.2018. Fragments are seen at  $m/z$  191.1072

( $C_{12}H_{15}O_2^+$ ) and  $m/z$  325.143982 ( $C_{20}H_{21}O_4^+$ ). The major component in the hardener is identified as tris (2,4,6-dimethylaminomethyl) phenol (“DMP”), a widely used epoxy accelerator, with abundant fragments at nominal  $m/z$  164.1075 ( $C_{10}H_{14}NO^+$ ) and 221.165388 ( $C_{13}H_{21}N_2O^+$ ). Peaks corresponding to DGEBA and the accelerator are evident in the cured epoxy resin.

A variety of other glues, cements, and adhesives were examined. Each showed a characteristic pattern, permitting the identification of the material. Residual solvent, residual monomer, unreacted and partially reacted components were detected together with pyrolysis fragments.

## Conclusion

DART can be applied to the direct identification of adhesives and resins on surfaces. Exact mass measurements coupled with accurate isotopic abundances aid in the assignment of components in the adhesive formulations.





# SCIENTIFIC REPORTS



OPEN

## A High Throughput Ambient Mass Spectrometric Approach to Species Identification and Classification from Chemical Fingerprint Signatures

Received: 08 February 2015

Accepted: 29 May 2015

Published: 09 July 2015

Rabi A. Musah<sup>1</sup>, Edgard O. Espinoza<sup>2</sup>, Robert B. Cody<sup>3</sup>, Ashton D. Lesiak<sup>1</sup>, Earl D. Christensen<sup>4</sup>, Hannah E. Moore<sup>5</sup>, Simin Maleknia<sup>6</sup> & Falko P. Drijfhout<sup>5</sup>

A high throughput method for species identification and classification through chemometric processing of direct analysis in real time (DART) mass spectrometry-derived fingerprint signatures has been developed. The method entails introduction of samples to the open air space between the DART ion source and the mass spectrometer inlet, with the entire observed mass spectral fingerprint subjected to unsupervised hierarchical clustering processing. A range of both polar and non-polar chemotypes are instantaneously detected. The result is identification and species level classification based on the entire DART-MS spectrum. Here, we illustrate how the method can be used to: (1) distinguish between endangered woods regulated by the Convention for the International Trade of Endangered Flora and Fauna (CITES) treaty; (2) assess the origin and by extension the properties of biodiesel feedstocks; (3) determine insect species from analysis of puparial casings; (4) distinguish between psychoactive plants products; and (5) differentiate between *Eucalyptus* species. An advantage of the hierarchical clustering approach to processing of the DART-MS derived fingerprint is that it shows both similarities and differences between species based on their chemotypes. Furthermore, full knowledge of the identities of the constituents contained within the small molecule profile of analyzed samples is not required.

One of the manifestations of the genetic differences that distinguish one species from another is in the profile of constitutively present small molecules they contain, also known as the metabolome. Since the small-molecule profile of an organism ultimately reflects the genes that distinguish it, the information content of the metabolome might be just as well suited to genomic fingerprinting and assessment of genetic relatedness between species as the genomes themselves. There are several reasons why it would be useful to be able to accurately correlate the signature of small molecules observed within an organism to its overall systems biology. The observation of the composite of small-molecule biomarkers could provide a real-time view of gene expression activity, enable the monitoring of the status of cellular transcriptomes

<sup>1</sup>Department of Chemistry, University at Albany, State University of New York, 1400 Washington Avenue, Albany, NY 12222 USA. <sup>2</sup>U.S. National Fish and Wildlife Forensics Laboratory, 1490 East Main Street, Ashland, OR, 97520-1310, USA. <sup>3</sup>JEOL USA Inc., 11 Dearborn Road, Peabody, MA 01960 USA. <sup>4</sup>National Renewable Energy Laboratory, 15013 Denver West Parkway, MS-1634, Golden, CO 80401 USA. <sup>5</sup>Department of Chemical Ecology, School of Physical and Geographical Science, Keele University, Keele ST5 5BG, UK. <sup>6</sup>School of Biological, Earth and Environmental Sciences, University of New South Wales, Sydney, Australia. Correspondence and requests for materials should be addressed to R.A.M. (email: rmusah@albany.edu)

and proteomes, provide a means of assessing the evolutionary history of organisms, and provide an avenue for the rapid monitoring of the success of gene knockouts and knockdowns, among other uses. Although these applications can be accomplished by phylogenetic methods, the paucity of mapped and/or annotated genes for the vast majority of fauna and flora in existence makes this approach impossible for all but a select group of mostly model systems.

Convenient characterization of the defining features of an organism's real-time chemical portrait for the purpose of species classification has been hampered by several factors. These include: (1) the difficulty of acquiring a comprehensive small-molecule chemical map of an organism or its parts in real time; (2) the time-consuming nature of metabolome profiling by conventional methods; (3) the challenge of obtaining a faithful and consistent representation of defining chemical components or chemical component ratios that is divorced from biases or artifacts introduced by sample processing steps; and (4) distinguishing between chemicals that define a species and those that do not provide discriminatory information. However, the advent within the last decade of ambient ionization mass spectrometric methods that feature instantaneous real-time detection of fairly comprehensive small molecule profiles of matter in its native form, has the potential to revolutionize and simplify metabolome- and/or chemical fingerprint-based species characterization by circumventing to a large extent the aforementioned deficiencies of conventional methods. Additionally, the utilization of the comprehensive mass spectrometry-derived fingerprint, rather than a subset of small-molecule biomarkers, provides the opportunity to subject an entire dataset to multivariate statistical analysis to aid in species classification, as well as processing of the data through hierarchical clustering in order to assess genetic relatedness and distinguish between species.

Direct Analysis in Real Time (DART®)<sup>1</sup> is one of the most common of the new mass spectrometric "ambient ionization" sources<sup>2</sup> and was the first such source to be introduced as a commercial product. Following an early application note on the use of DART to analyze the flavor components and polyphenols in the leaves of two different basil cultivars<sup>3</sup>, there have been several reports on the application of DART to species biomarker identification. Fatty acid profiles measured by DART for different bacterial species have been shown to be distinct and reproducible<sup>4</sup>, volatiles release from Eucalypts of different species have been shown to be unique<sup>5,6</sup>, differentiation between red oak (*Quercus rubra*) and white oak (*Q. alba*)<sup>7</sup> by DART has been demonstrated, identification of printing and writing papers<sup>8</sup> based on chemical profile differences has been shown, and the identification of *Piper betel* cultivars<sup>9</sup>, ambiguous cubeb fruit<sup>10</sup> and varieties of the psychoactive plant *Mitragyna speciosa* ("Kratom")<sup>11</sup> have all been demonstrated utilizing ambient DART mass spectrometry. The U.S. Fish and Wildlife Services Forensic Laboratory has also used DART-MS to distinguish between species of *Dalbergia*<sup>12</sup> and agarwood<sup>12</sup>. Each of the aforementioned reports relied on visual examination of mass spectra or their corresponding heat maps for selection of *m/z* features that were then used in chemometric-based approaches including the unsupervised learning methods Principal Component Analysis (PCA) and Partial Least Squares Discriminant Analysis (PLS), and the supervised learning methods Linear Discriminant Analysis (LDA) and Kernel Discriminant Analysis (KDA), for distinguishing between species within a single genus. Successful application of these methods requires careful albeit *a priori* selection of the features (mass spectral peaks) that differentiate between species.

By combining mass spectrometric heat maps and chemometric protocols, we illustrate a high throughput method by which DART-MS-derived chemical signature profiles can be subjected to cluster analysis to not only distinguish between species, but provide information on genetic relations. An advantage of the hierarchical clustering approach to the processing of DART-derived fingerprint information is that it shows both similarities and differences between species based on their chemotypes as determined from DART-MS data. In contrast, previously described chemometric methods show only differences between classes, but do not indicate which classes have similar chemotypes. Furthermore, full knowledge of the identities of the constituents contained within the small molecule profile of the sample being analyzed is not required. The method is robust and rapid and the results are consistent. Here, we showcase several applications although these are by no means exhaustive and numerous other possibilities exist. In this work, we demonstrate how the method can be used to: (1) distinguish between endangered woods regulated by the Convention for the International Trade of Endangered Flora and Fauna (CITES) treaty; (2) assess the origin and by extension the properties of biodiesel feedstocks; (3) determine insect species from analysis of puparial casings; (4) identify psychoactive plant products; and (5) differentiate between Eucalyptus species.

## Results

**Detection of Illegally Traded Endangered Species in the Genus *Dalbergia*.** The convention for the international trade of endangered flora and fauna (CITES) which is enforced under the Endangered Species Act (ESA), bans the trade of tree species whose harvest has been deemed unsustainable. Visual inspection of harvested plant products in which leaves, flowers and other characteristic features have been retained can enable definitive identification of endangered species. However, since timber and sawn boards generally lack diagnostic morphological features, identification of wood products has historically relied on anatomical or chemical features associated with the hardwood. This process is laborious, time-consuming and can be prone to error.

The aforementioned challenge is further exacerbated not only by the plethora of colloquial terms used within the timber trade community for any one tree species, but also by the common use of a single name to refer to multiple species. For example, “*Dalbergia granadillo* Pittier” is a tree species of rosewood endemic to Mexico and northern Central America, whose common name is “granadillo”. However, this same name has been used to describe *Dalbergia retusa* (Leguminosae family), and several Fabaceae family trees including *Platymiscium yucatanum*, *Caesalpinia echinata*, and *C. platyloba*. Furthermore, *D. retusa* has a large number of synonyms including *Amerimnon lineatum*, *A. retusum*, *D. cuscatlantica*, *D. hypoleuca*, *D. lineata*, *D. pacifica*, *D. retusa* var. *hypoleuca*, and *D. retusa* var. *lineata*, with many xylarium collections still using historical nomenclature. The institution of correct *Dalbergia* classifications and nomenclature and the identification of illegally traded endangered *Dalbergia* species, has been stymied by the absence of a rapid and consistent mechanism by which to distinguish between species, and routinely detect those that are banned. In this work the chemical profile derived from a DART ion source coupled to a high-resolution time-of-flight (TOF) mass spectrometer was used to rapidly and consistently identify and distinguish between *Dalbergia* species.

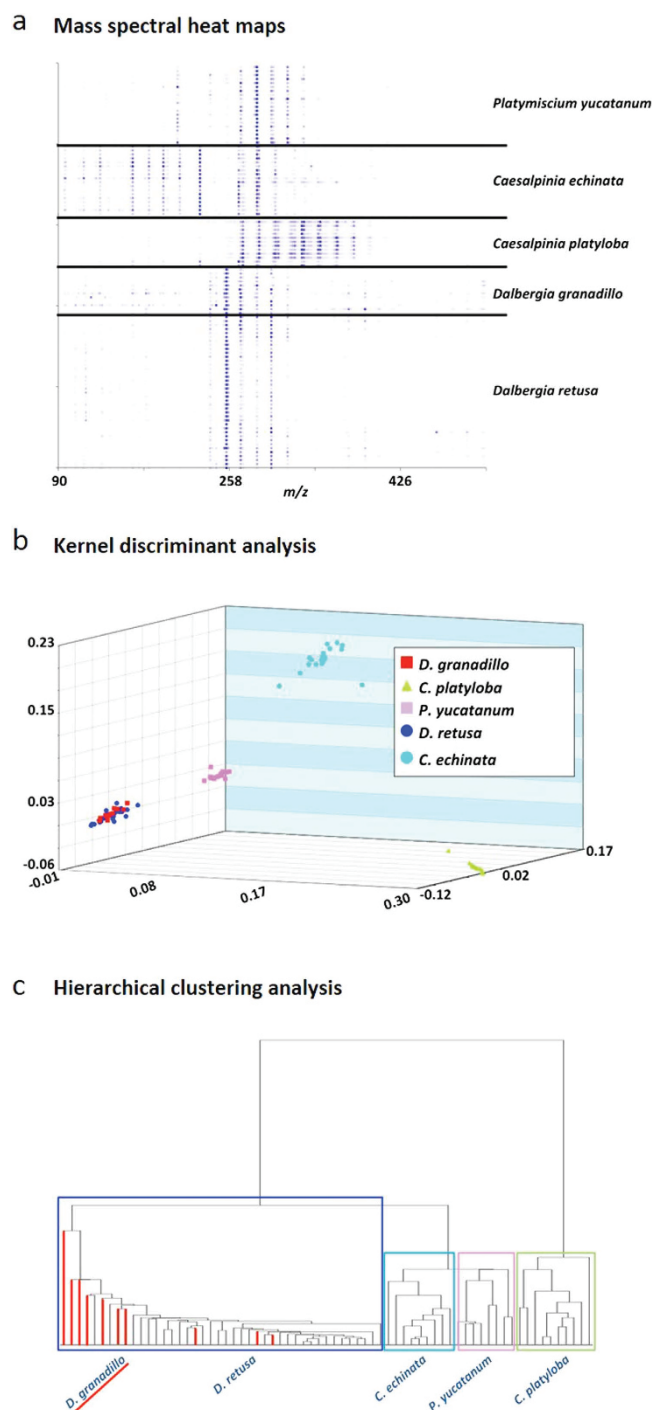
We proceeded on the premise that the rare *D. granadillo* was a synonymous species to other less cryptic taxa. Because the known curated xylarium reference samples of *D. granadillo* are extremely rare ( $n = 11$  worldwide), we decided to first compare the known xylarium-authenticated samples of *D. granadillo* hardwood by DART-TOF-MS to determine whether they exhibited similar chemical fingerprints. The results were then contrasted with the DART-TOF-MS spectra of five species of timber from a variety of sources that have been described by the common name of “granadillo” (i.e. *D. granadillo*, *D. retusa*, *P. yucatanum*, *C. echinata*, and *C. platyloba*—Supplementary Table 1). The mass spectra generated (Supplementary Figure 1) were rendered as heat maps using the Mass Mountaineer software suite. Supplementary Tables 2a–c show the corresponding measured  $m/z$  values and their abundances, and Fig. 1a illustrates the mass spectral heat maps. The results show that *D. retusa* and *D. granadillo* have similar compounds present in roughly the same relative amounts as indicated by the similar intensities of the indicated colors in the heat maps. The other three species show different and distinctive diagnostic ion patterns. The high-resolution masses of several of the molecules detected were consistent with those of compounds previously reported to be present in *Dalbergia*<sup>13,14</sup>.

Figure 1b is a graphical representation of the Kernel discriminant analysis (KDA) plot generated using 104 feature masses ranging from  $m/z$  107.037 –  $m/z$  527.155 from a training set of 102 spectra. The plot shows that *D. retusa* and *D. granadillo* form a single cluster that cannot be differentiated using KDA. The leave-one-out cross validation (LOOCV) for the KDA classification model analysis was fairly poor at 64.29%, reflecting the fact that these *Dalbergia* species could not be separated. The clustering of *D. retusa* and *D. granadillo* is supportive of our hypothesis that both represent one and the same species and therefore should be described by a single name. Indeed, when *D. retusa* and *D. granadillo* were joined into a single group under one name (*D. retusa*), the LOOCV of the KDA model rose to 98.98%. Thus, our observations support the premise that from the chemical profile of the heartwood, *D. granadillo* cannot be distinguished from *D. retusa* and that *D. granadillo* and *D. retusa* may be synonymous. Interestingly, we found that when the heat map data were imported into a third-party hierarchical clustering program such as Cluster 3.0, the resulting dendrogram classified the various *Dalbergia* samples according to species and illustrated their genetic relatedness. Cluster analysis was performed using uncentered correlation of 436 variables of the spectral data, and a typical result is shown in Fig. 1c. The leaves highlighted in red in Fig. 1c are *D. granadillo* specimens. The dendrogram shows that the *D. granadillo* clusters with the *D. retusa* samples, supporting the hypothesis that both represent the same species.

### Inferring the Phylogeny of Biodiesel Feedstocks From Fatty Acid Methyl Ester (FAME) Profiles.

Biodiesel is a renewable fuel derived from vegetable oils or animal fats by transesterification of triglycerides with an alcohol, generally methanol, in the presence of a catalyst<sup>15</sup>. The resulting mixture of fatty acid methyl esters (FAMEs) can be used to fuel diesel engines and is most often blended with petroleum diesel. The amount of biodiesel produced in the U.S. has increased significantly in recent years. In 2010 production was just over 300 million gallons, which increased to nearly 1 billion gallons in 2011. In 2013, production reached over 1.3 billion gallons<sup>16</sup>. Increased production and utilization of biodiesel has intensified interest in the properties of this fuel and how these properties impact engines and infrastructure. The feedstock from which biodiesel is derived determines many of the properties of the fuel. These properties are directly related to fatty acid makeup of different oil sources<sup>17</sup>. Desired properties such as cold weather operability and resistance to autoxidation are influenced by the acyl chain length and degree of unsaturation of the fatty acids in the feedstock<sup>18,19</sup>. If the feedstock used to manufacture a biodiesel is unknown to the user, the source may be determined from the FAME profile of the product if the unique fatty acid distribution of the source oil is known<sup>20</sup>. FAME profiling is commonly achieved with gas chromatography<sup>21</sup>. This analysis can be time consuming, particularly if a high degree of resolution is required to isolate FAMEs in more complex samples.

We determined that positive-ion DART can be used to rapidly determine the FAME profile of biodiesel, allowing for quick source and properties identification. The biodiesel samples utilized in this study included the most commonly used feedstocks in the United States<sup>22</sup>. Arugula (*Eruca sativa*), Brassica (*Brassica juncea*), Field Pennycress (*Thlaspi arvense*), Cress (*Lepidium sativum*), Camelina (*Camelina sativa*), Meadowfoam (*Limnanthes alba*), and Cuphea (*Cuphea lanceolata*) seed oils were provided by the



**Figure 1. DART-TOF mass spectral heat maps, kernel discriminant analysis (KDA) and hierarchical clustering analysis results derived from the DART-TOF mass spectra of *Dalbergia* wood species.** Panel **a**: DART-TOF mass spectra rendered as heat maps of the indicated species; Panel **b**: KDA based on 104 feature masses; 3 principal components accounted for 84.51 % of the variance. The LOOCV was 98.98%. Panel **c**: hierarchical clustering analysis dendrogram created from mass spectral heat map data, showing species classifications of the analyzed *Dalbergia* species woods. The leaves highlighted in red indicate *D. granadillo* specimens which cluster with *D. retusa*.

USDA National Center for Agricultural Utilization Research. The DART mass spectra (Supplementary Figure 2) obtained for hexane solutions of the aforementioned ten biodiesel feedstocks were dominated by both saturated and unsaturated FAMES ranging in size from 11–23 carbons (Supplementary Table 3). Hexane was used to dilute the samples because they proved to be too concentrated in their native form. The most abundant species in the majority of feedstocks (i.e. Brassica, Camelina, Canola, Cuphea,



Pennycress and Soy) were  $C_{19}$  FAMES (derived from  $C_{18}$  fatty acids). Nevertheless, the mass spectra were consistent for samples within the same species, but very clearly different between species (Supplementary Figure 2). Fifteen feature masses were used for principal component analysis (Fig. 2b). Species level clustering was observed in the covariance PCA plot with five principal components accounting for 92.6% of the variance and the LOOCV was 98.33%. Subjection of the corresponding mass spectral heat maps (Fig. 2a) to hierarchical clustering analysis showed that each species was clearly separated from the others (Fig. 2c). All members of Order *Brassicale* were clustered together with the exception of Canola, which is a cultivar that has been bred to have low erucic acid content. The remaining feedstocks (including the mixed biodiesel) belonging to different orders and/or families, comprised a separate cluster. Interestingly, Meadowfoam (order *Brassicale*, family *Limnathaceae*) was distinct from all of the other species. These observations illustrate that easily and rapidly acquired feedstock chemical profile information can be translated into dendrograms that clearly distinguish between genera to show their evolutionary relationships, and that the data can be generated in a high throughput fashion.

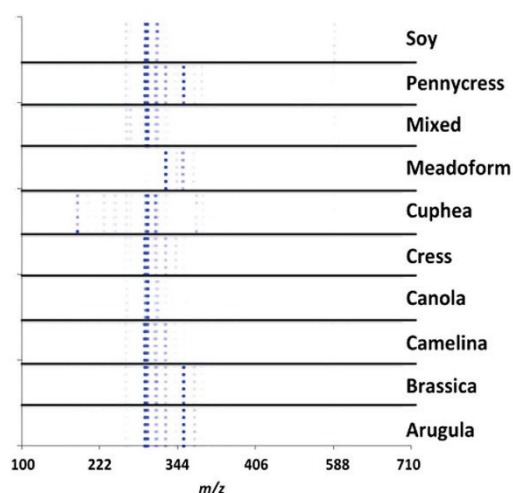
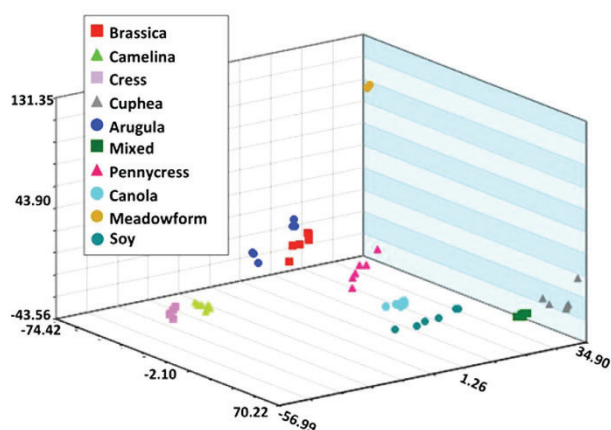
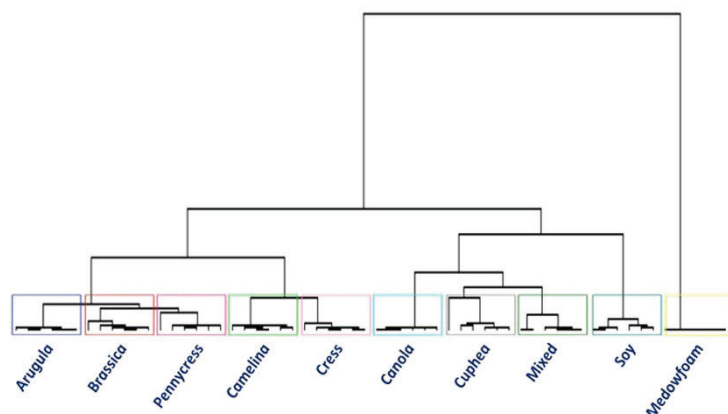
**Fly Species Identification from Insect Puparial Cases.** Blowflies (Diptera: Calliphoridae) are important to forensic entomology because they are often the first colonizers of decomposing remains and can offer significant diagnostic information towards calculating an accurate minimum post mortem interval ( $PMI_{min}$ ). Calliphoridae puparial cases are often the only persisting entomological evidence in criminal investigations involving highly decomposed remains<sup>23</sup>. These cases are the empty shells of the last layer of the larval stage (post feeding). Many studies have been published using larvae and pupal stages for PMI estimations<sup>24–28</sup>, but much less research has been published on puparial cases and currently, they are rarely used in criminal investigations due to the difficulty in identifying and ageing them. However, in the past decade, some studies have suggested that invaluable information can be extracted from puparial cases and hence, new methods to identify them are being developed<sup>23,29</sup>.

When an adult fly emerges from the case it does so from the mouth end, leaving the rest of the case intact. To correctly identify them, the same morphological features used for the pupae are examined (i.e. posterior spiracles, spines, and mouth piece if present). However, with empty cases, these morphological features have often been destroyed during emergence of the adult fly. It is well established that insect cuticular hydrocarbons have characteristic profiles for different species<sup>30–34</sup>. The same holds true for the hydrocarbon profiles of insect puparial cases<sup>35</sup>. Therefore, hydrocarbon analysis is advantageous because both young and aged cases retain definitive chemical information due to the stability of the constituent hydrocarbons despite weathering effects.

Positive-ion DART-MS was previously used to analyze the unsaturated cuticular hydrocarbons of awake behaving fruit flies (*Drosophila melanogaster*)<sup>36</sup>. However, this form of analysis does not give clear, unambiguous mass spectra for saturated alkanes. Recently, we reported that large polarizable alkanes, lipids and alcohols can be detected as  $O_2^-$  adducts ( $[M + O_2]^-$ ) by aspirating sample solutions directly into the mass spectrometer atmospheric pressure orifice in the presence of the  $O_2^-$  generated by the DART ion source<sup>37</sup>. We applied this technique to our analyses. The mass spectra typically observed are presented in Supplementary Figure 3 and the heat map renderings of these spectra are shown in Fig. 3a. The detected  $C_{27}$ – $C_{34}$  alkanes that were used as the basis for multivariate statistical analysis by supervised methods were easily observed as  $O_2^-$  adducts (see mass spectral peak assignments and molecule abundances in Supplementary Table 4). All species are distinctly separated within the PCA plot, demonstrating that their profiles have unique chemical differences (Supplementary Figure 3). However, there is less separation between *L. cuprina* and *L. sericata*. This is likely because they are from the same genus (*Lucilia*) and therefore their profiles share more similarities compared to the other species. It should be noted that this method does not distinguish between hydrocarbon isomers or provide any information about branching. Nevertheless, the results confirm that the hydrocarbon profiles measured by DART-MS clearly enable distinctions between species to be made.

A training set comprised of blowfly puparial case hexane extract mass spectra (i.e. *Chrysomya rufifacies*, *Lucilia sericata*, *L. cuprina*, and *Cochliomyia macellaria*) as well as spectra of puparial case extracts of the common house fly (*Musca domestica*) was created. Feature masses from these spectra were used for KDA, with the results featured in Fig. 3b. Excellent separation between the five different insect types was observed and LOOCV gave 100% correct identification for all samples. Five sets of puparial cases labeled “A” through “E” that were provided as blind samples were then analyzed. Samples A, B, C and D were correctly identified as *L. sericata*, *C. rufifacies*, *L. cuprina*, and *C. macellaria* respectively. Sample E gave a distinctly different profile. It was later revealed that it represented puparial cases for the common housefly, *Musca domestica*.

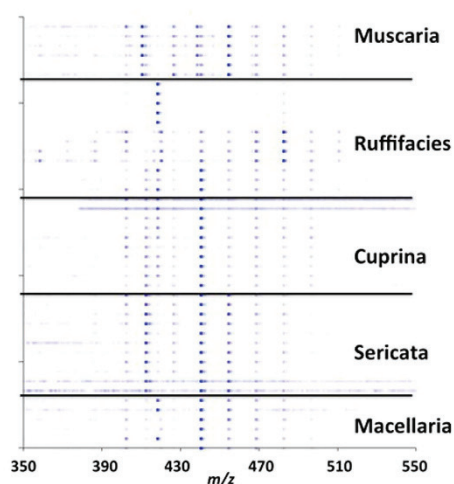
Although the mass spectral data for Sample B correctly clustered with that of *C. rufifacies*, it differed somewhat from the standard *C. rufifacies* samples measured one month earlier. This is illustrated in a comparison of the Sample B spectrum (Supplementary Figure 4) with that of the spectrum obtained for *C. rufifacies* (Supplementary Figure 3). The reason for this difference is not clear, but preliminary observations indicate that the alkane profiles for puparial cases of a given species may vary with age<sup>35</sup>. Although this difference is evident in the PCA plot (Fig. 3b), hierarchical clustering analysis of the mass spectral datasets that were rendered as heat maps showed the B samples and the *C. rufifacies* standards clustering together (Fig. 3c). The DART-MS derived small molecule fingerprint of a puparial case as a

**a Mass spectral heat maps****b Principal component analysis****c Hierarchical clustering analysis**

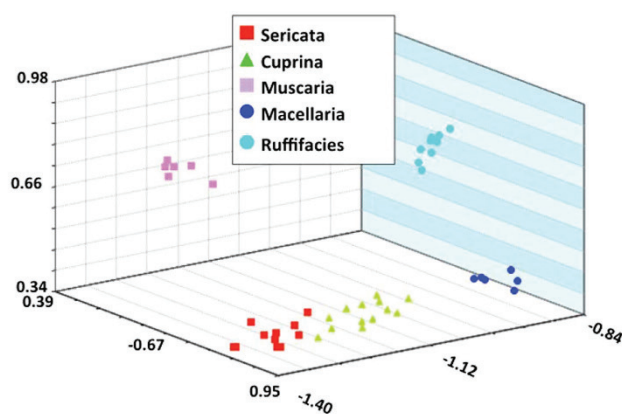
**Figure 2.** DART-TOF mass spectral heat maps, principal component analysis (PCA) and hierarchical clustering analysis results derived from the DART-TOF mass spectra of biodiesel feedstocks solubilized in hexane. Panel a: DART-TOF mass spectra rendered as heat maps of the indicated feedstocks; Panel b: PCA was based on sixteen feature masses; 3 principal components accounted for 73.4% of the variance and the LOOCV was 98.3%. Panel c: hierarchical clustering analysis dendrogram created from mass spectral heat map data, showing species-level classifications of the analyzed feedstocks.



**a** Mass spectral heat maps



**b** Kernel discriminant analysis



**c** Hierarchical clustering analysis

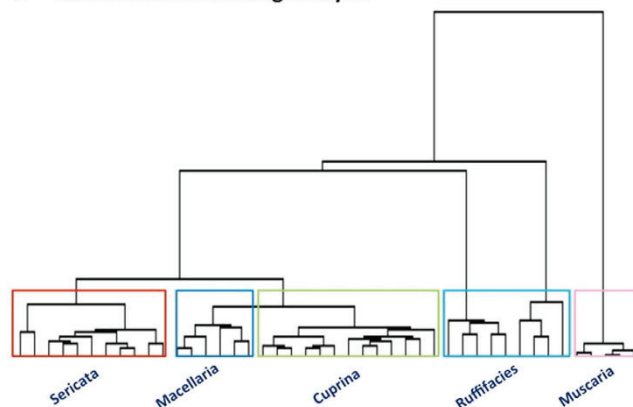


**Figure 3.** DART-TOF mass spectral heat maps, Kernel discriminant analysis (KDA) and hierarchical clustering analysis results derived from the DART-TOF mass spectra of hexane extracts of puparial cases of *C. ruffifacies*, *L. sericata*, *L. Cuprina*, and *C. macellaria* and *M. domestica*. Panel a: DART-TOF mass spectra rendered as heat maps; Panel b: Kernel discriminant analysis (KDA) was based on 10 feature values. Five principal components accounted for 96% of the variance. The LOOCV was 100%. Panel c: hierarchical clustering analysis dendrogram created from mass spectral heat map data, showing species classifications of the analyzed puparial cases.

function of its age is currently being investigated by the authors, as a correlation between the two could potentially serve as a tool in post mortem investigations.

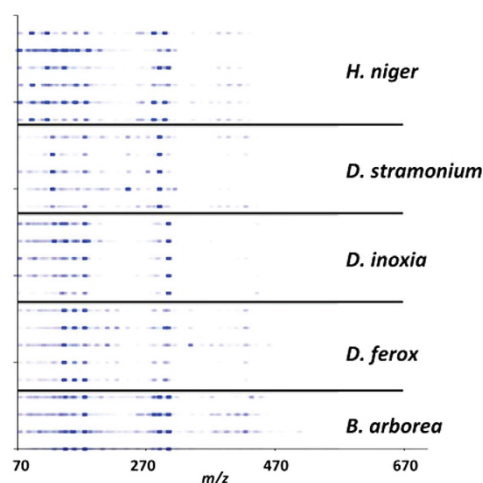
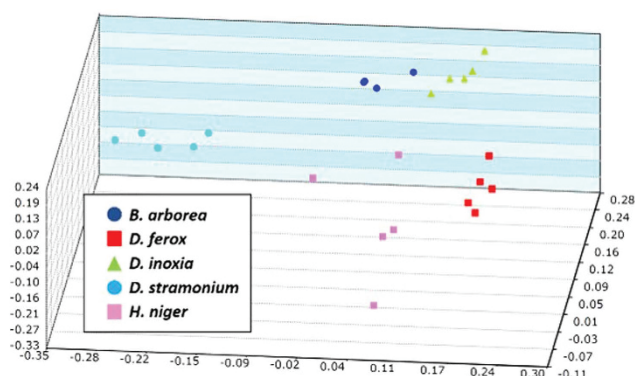
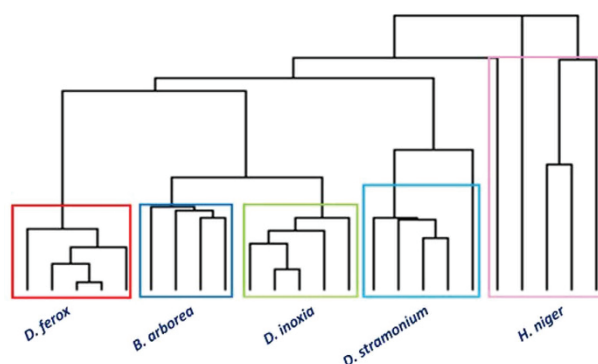
**Species Identification From Seeds of Plants Containing Belladonna Alkaloids.** The genus *Datura* contains multiple species of ornamental flowering plants of horticultural importance. They are a well-known source of belladonna alkaloids including scopolamine and atropine, whose hallucinogenic and narcotic properties have been exploited in traditional religious rituals, herbal and mainstream medicine, and more recently in recreational drug abuse using its seeds<sup>38</sup>. It is often difficult to distinguish *Datura* species due to similarities in the appearance of both their seeds and their aerial parts, and because their morphological features can vary depending on where the plants are grown<sup>39</sup>. *Datura* plants also often bear resemblance to those in the *Brugmansia* genus, and this has led to the misidentification of some genus *Brugmansia* plants as belonging to the *Datura* genus and vice versa, as well as misidentification of species within the *Datura* genus<sup>39</sup>. An additional challenge is that the morphological features that allow the plants to be distinguished, most notably the flowers and fruits, take months to years to appear, making species differentiation a long-term project. Furthermore, from a chemical profiling standpoint, the belladonna alkaloids found in *Datura* species also appear in *Brugmansia* and *Hyocyamus* species, making identification of plant material based on the presence of belladonna alkaloid biomarkers alone indeterminate. All of the aforementioned species are members of the large group of non-model plants that are poorly annotated and whose genomes have not been mapped, making phylogenetic species identification impossible. Here, direct analysis in real time-mass spectrometry (DART-MS) and hierarchical clustering analysis tools were applied to the seeds. The approach provided a rapid high throughput and viable method to test seeds directly for identification purposes, as well as for species differentiation and classification by cluster analysis.

Of the known *Datura* species, we used *D. ferox*, *D. stramonium* and *D. innoxia*, as these are commonly abused seeds. Since the belladonna alkaloids that serve as biomarkers for *Datura* species are also present in *Brugmansia* and *Hyocyamus* seeds, both were also analyzed to assess whether they could be distinguished as species unique from *Datura*. Figure 4a shows the mass spectral profiles of all five species, done in replicates of 3–5, rendered as heat maps. The corresponding raw mass spectra and the peak abundances are presented in Supplementary Figure 5 and Supplementary Tables 5a–5e respectively. The high resolution data revealed that several of the detected molecules had molecular formulas consistent with molecules that have been observed in *Datura* spp. such as tropine, scopoline, dihydroxytropine, hexose sugars, scopolamine, 3-tigloyloxy-6,7-dihydroxytropine, vanillin, linoleic acid and oleic acid (see Supplementary Tables 5b–5d)<sup>40–42</sup>. By visual inspection it was apparent that the mass spectra of each species were quite unique, even for the three *Datura* species. A total of 31 feature masses representing diagnostic peaks were used as a training set for the Kernel principal component analysis (KPCA). The results are shown in Fig. 4b. Each of the species was well clustered and could be distinguished from the others. Nevertheless, three principal components accounted for only 40% of the variance and increasing the number of principal components to 5 accounted for only 64% of the total variance. However, the LOOCV was 96%. The power of the chemical fingerprint signatures in permitting species differentiation and classification was demonstrated when the heat map data were imported into Cluster 3.0. Processing of the data in this manner furnished a dendrogram in which each of the seeds of the same species fell within clades that were representative of species classifications based on morphological feature differences, and were clearly distinct from one another (Fig. 4c).

**Species Differentiation of Eucalypts From Mass Spectrometry-derived Tissue-dependent Chemical Fingerprints.** The *Eucalyptus* genus covers a diverse range of flowing trees and shrubs with more than 700 species that are broadly distributed throughout the Americas, Australia, Africa, and Europe. They are commonly known as “gum trees” because of the distinct and pleasant volatile exudate that is produced in response to a tissue breach. Many species have attracted global attention as a source for fragrance oils, biofuels, a fast-growing wood source and other commercial applications<sup>43</sup>.

DART-MS profiling of eucalypt species was previously selected as a facile method to classify temperature-dependent emissions of volatile organic compounds (VOCs) for their atmospheric contributions in relation to changing climates and global warming, and to better estimate the range of biogenic pollutants released into the atmosphere during wildfires<sup>5,6</sup>. In that work, VOCs from stems and leaves of several eucalypts including *E. cinerea*, *E. citriodora*, *E. nicholii* and *E. sideroxylon* were identified. A wide range of compounds from simple organics (i.e. methanol and acetone) to a series of monoterpenes (i.e. pinene, camphene, cymene, eucalyptol) common to many plant species, as well as less abundant sesquiterpenes and flavonoids, were detected. This was achieved by stepwise adjustment of the DART helium gas temperature from 50 to 100 to 200 and to 300 °C, which enabled direct evaporation of compounds up to the onset of pyrolysis of plant fibres (i.e. cellulose and lignin). The identification of compounds was facilitated by correlating the observed high resolution accurate mass data to plant library compounds, and further matching their theoretical and experimental isotopic distributions.

In the current work the initial VOC temperature-dependent emission studies have been extended to chemometric-based processing of mass spectral data for species differentiation. DART-MS analyses of leaf samples at a fixed temperature of 300 °C for several eucalypts including *E. bridgesiana*, *E. cinerea*, *E.*

**a** Mass spectral heat maps**b** Kernel principal component analysis**c** Hierarchical clustering analysis

**Figure 4.** DART-TOF mass spectral heat maps, Kernel principal component analysis (KPCA) and hierarchical clustering analysis results derived from the DART-TOF mass spectra of *B. arborea*, *D. ferox*, *D. inoxia*, *D. stramonium* and *H. niger* seeds. Panel **a**: DART-TOF mass spectra of the five species rendered as heat maps; Panel **b**: Kernel principal component analysis (KPCA) based on 31 feature masses. Five principal components accounted for 64% of the variance. The LOOCV was 96%; Panel **c**: hierarchical clustering analysis dendrogram created from mass spectral heat map data, showing species classifications of the analyzed plant seeds.

*globulus*, *E. citriodora* and *E. polyanthemus* was conducted. The observed spectra, each of which represents the average of 5 individual spectra, are shown in Supplementary Figure 6, with the corresponding measured  $m/z$  and peak abundance values presented in Supplementary Tables 6a–6e. The heat map renderings of the spectra are shown in Fig. 5a. The results revealed the presence of a number of chemotypes common to all species including monoterpenes ( $m/z$  137,  $C_{10}H_{17}$ ) and various sesquiterpenes ( $m/z$  205,  $C_{15}H_{25}$ ). Several of the detected formulas are consistent with those of compounds isolated from the species (outlined in Supplementary Tables 6a–6e)<sup>44–46</sup>. Although all the species shared most of the dominant ions, they differed primarily in the relative abundance of detected compounds. A total of 15 feature masses representing  $m/z$  values varying from 155 to 509 were used for KDA. The resulting plot is shown in Fig. 5b. Three principal components accounted for 94% of the observed variance, and the LOOCV was 83%. When the mass spectral heat maps (Fig. 5a) were processed using Cluster 3.0, the resulting dendrogram (Fig. 5c) showed excellent species level discrimination, and none of the data were misclassified, thus demonstrating the robustness of the approach of using the entire mass spectral data set in providing the information needed for species-level distinctions to be made.

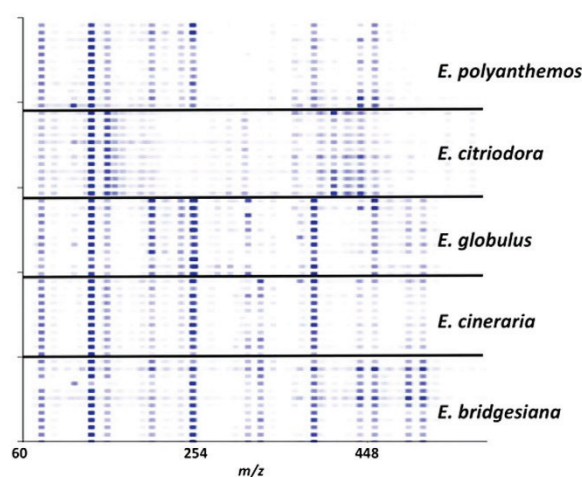
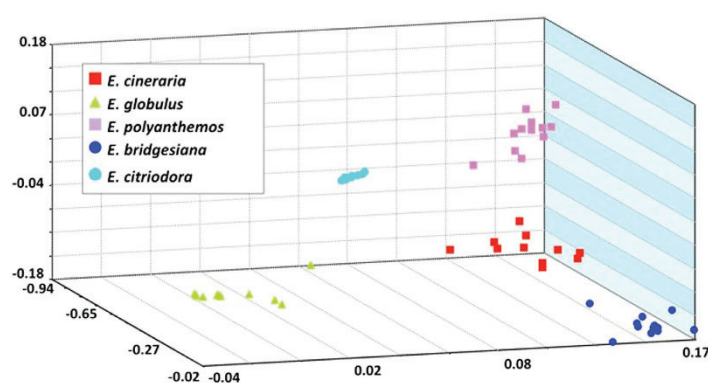
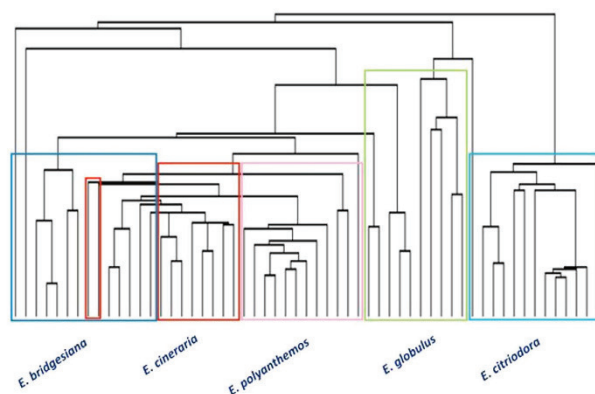
## Discussion

Statistical processing of the output of chemical analysis techniques for the purposes of typing and classification is not new. For example, hierarchical cluster analysis of Raman spectroscopic data has been used to classify tree pollens<sup>47</sup> and genus *Mentha* plants<sup>48</sup>. Multivariate statistical analysis has been applied to gas chromatographic results to classify the geographic origin of cocoa beans<sup>49</sup>, as well as <sup>1</sup>H NMR data for the analysis of wines<sup>50</sup>. Chemometric discrimination of coffee beans by area of origin has been demonstrated using Fourier transform infrared spectroscopy<sup>51</sup>.

The output of various mass spectrometric methods of small molecule profiling has also been similarly analyzed with varying results. Examples include multivariate statistical analysis of data generated using: (1) Curie Point pyrolysis mass spectrometry for classification of bacteria<sup>52</sup>; (2) paper spray mass spectrometry for determination of the geographic origin of coffee<sup>53</sup>; (3) HPLC-tandem MS of herbal medicines to determine country of origin<sup>54</sup>; (4) Ultraperformance liquid chromatography-time of flight mass spectrometry for classification of wheat lines<sup>55</sup>; (5) LC-MS/MS for the assessment of the utility of using bioactive components as the basis of distinguishing between herbal medicines<sup>56</sup>; (6) RPLC ESI-MS for standardization of *Ginkgo biloba* extracts<sup>57</sup>; (7) direct injection electrospray MS for classification of coffee trees<sup>58</sup>; (8) ion molecule reaction mass spectrometry for bacterial species differentiation<sup>59</sup>; (9) GC- and atmospheric pressure photoionization (APPI) MS for classification of natural resins<sup>60</sup>; (10) GC-GC TOF/MS for characterization and authentication of edible oils<sup>61</sup>, and (11) pyrolysis GC-MS profiling of eucalypt emissions in response to climate change and wildfires<sup>62</sup>, among other examples. The method described here differs from those outlined in the aforementioned studies in that in general, data acquisition is simpler, a broad range of compounds spanning the dielectric constant spectrum can be detected in a single experiment, and the entire information content of the observed DART-MS-derived chemical fingerprints is subjected to unsupervised hierarchical clustering (rather than using a subset of feature masses and/or chromatographic peaks).

Besides DART-MS, desorption electrospray ionization mass spectrometry (DESI-MS) is another ambient ionization mass spectrometry technique that exhibits advantages similar to those noted for DART-MS. However, relatively few studies featuring DESI-MS in metabolome profiling and/or chemical fingerprinting have appeared. Recently, Watrous *et al.*<sup>63</sup> demonstrated the use of “nanospray” DESI-MS for the *in vivo* metabolic profiling of bacterial colonies directly from a Petri dish. The report further illustrates the power of ambient ionization mass spectrometric methods to rapidly provide unprecedented glimpses of real-time changes in chemical fingerprint profiles in ways that are difficult and/or impossible to accomplish by more conventional methods.

In this report, we show that a variety of chemotypes from a diversity of samples can be readily detected under similar conditions. The high resolution *Dalbergia* species results have revealed the presence of several molecules with formulas consistent with those of compounds that have been identified in *Dalbergia* including neoflavonoid quinone derivatives such as the dalbergiones, various isoflavones, guainolide sesquiterpene lactones, auxins such as indole-3-acetic acid, pyrano- and furano-benzenes and diterpenes among many other polar and non-polar small molecules<sup>13,14</sup>. Both saturated and unsaturated biodiesel feedstock-derived FAMES of from 11 to 23 carbons were easily observed in positive ion mode. In analysis of the biofuels, we observed that the biodiesel was most conveniently analyzed by first diluting it with a non-polar solvent such as hexane, in order to make it less viscous. Alkanes and alkenes from 27–34 carbons long were observed as  $O_2^-$  adducts in hexane extracts of fly puparial cases, showing distinct variations in profile and abundance as a function of species. Our approach to the analysis of the puparial cases represents the first published application of the  $O_2^-$  attachment ionization technique to address an analytical problem. This novel method enabled us to easily detect large polarizable alkanes, lipids and alcohols as  $[M + O_2]^-$  adducts, by aspirating sample solutions directly into the mass spectrometer atmospheric pressure orifice in the presence of the  $O_2^-$  generated by the DART ion source<sup>37</sup>. The application of this technique necessitated the use of the solvent which, in this case, was hexane. Although these large non-volatile species could have been detected by GC-MS or field desorption, the former method is much slower than DART-MS analysis, while the latter requires introducing the sample into a vacuum on a fragile emitter. Neither approach is as convenient as the DART-MS analysis described

**a** Mass spectral heat maps**b** Kernel discriminant analysis**c** Hierarchical clustering analysis

**Figure 5.** DART-TOF mass spectral heat maps, Kernel discriminant analysis (KDA) and hierarchical clustering analysis results derived from the DART-TOF mass spectra of Eucalypt species leaves. Panel a: DART-TOF mass spectra of the five species rendered as heat maps; Panel b: KDA based on fifteen feature masses. Three principal components accounted for 93% of the variance. The LOOCV was 82.7%; Panel c: hierarchical clustering analysis dendrogram created from mass spectral heat map data, showing species-level classifications of the analyzed plant leaves.

here. In analysis of *Datura*, *Brugmansia* and *Hyocyamus* species plants, a range of compounds of varying polarities was observed, as illustrated in Tables 5a-e. Amines, sugars and fatty acids, among hundreds of



other compound types, were all detected in seconds in positive as well as negative ion modes. In the case of the Eucalypts, direct leaf analysis yielded spectra in which the presence of the odiferous mono- and sesquiterpenes for which this species is well known were all readily apparent.

It was the consistent and reproducible comprehensiveness of the rapidly acquired small molecule fingerprint in each of the biological samples surveyed in this work that was exploited to conduct successful species classification using multivariate statistical analysis tools. Using supervised methods such as PCA, KDA and KPCA, we determined that a small number of principal components could be used to account for ~40% - 90% of the observed variance, with LOOCVs from 80 - 100% probability depending on the sample analyzed. Hierarchical cluster analysis was applied to the entire mass spectral data set in each case as an unbiased approach to assess the extent to which the DART-MS-derived chemical fingerprint could enable species classification. The resulting dendrograms showed that in all cases, striking species level separations were accomplished, demonstrating that genomic distinctions between even closely related species manifest themselves in small molecule profile differences. A number of previous reports have demonstrated that hierarchical clustering of the type used here can be exploited for classification purposes. However, in the majority of these cases, distinguishing biomarkers or specific spectral features, rather than the entire small molecule fingerprint, were used. A recurring observation in these studies was the appearance of misclassifications, a not too unexpected consequence of the fact that (a) the selected principal components accounted for less than 100% of the variance; and (b) the information content of the chemical data that was used as the input for multivariate statistical analysis processing was not comprehensive, in that it was acquired using extracts, or the analysis was performed by a method in which certain molecules were preferentially detected over others. For the samples used in this work, no misclassifications were observed when the entire mass spectral dataset was used. This suggests that small molecule fingerprint-based classifications that can reflect genome differences are best acquired using the full fingerprint, rather than a subset of salient features. Of note is the fact that this method does not require that the identities of the fingerprint components be known. Nevertheless, the knowledge of the molecular weights and formulas of distinguishing molecules provides important information that can be used to eventually determine compound identity.

In summary, we have devised a rapid high throughput method for species identification and classification based on chemometric analysis of comprehensive DART-TOF-MS derived chemical signatures. The method entails introduction of the sample to the open air space between the DART ion source and the mass spectrometer inlet, followed by chemometric processing using the entire mass spectral dataset. A range of both polar and non-polar chemotypes are instantaneously detected, and matter in various forms (i.e. solid, liquid or gaseous) is easily analyzed with no need to change the method of sample introduction. The comprehensive small molecule signatures obtained serve as the input for unsupervised hierarchical cluster processing software, a number of open source versions of which are freely and readily available. The result of this processing tool is identification and species level classification based on the entire DART-derived chemical fingerprint. This methodology circumvents some of the pitfalls of the data selection bias that can accompany the use of supervised methods of statistical analysis on the one hand, and the deficiencies introduced by other instrument/chemical methods (such as extraction) on the other. Furthermore, it is significantly faster than conventional methods and can yield results from start to finish (including statistical analysis), in less than 3 min per sample. Given that the type of genome classification results consistently observed here are most often acquired using gene sequence information, and the time and resources required to generate it, the method outlined here provides a significant advancement in the determination of species level classifications. It supplies further evidence that inherent in the metabolome is the information content required to determine species level distinctions. In this work, we show the application of this methodology for rapid species-level identification of: endangered woods; biofuel feedstocks; insect puparial cases; plants; and tree species. These applications fall within the fields of forensic science, agronomy, agriculture, natural products chemistry, plant biochemistry and fuel chemistry among others, and it is anticipated that it could easily be used to further discoveries in a myriad of other areas.

## Methods

**Instrumentation.** An *AccuTOF* (JEOL Ltd., Akishima Japan) time-of-flight mass spectrometer equipped with a Direct Analysis in Real Time (DART) ion source (Ionsense LLC, Saugus, MA) was used for all measurements. Mass spectra were stored by the JEOL *Mass Center* data acquisition software at a rate of 1 per second for the  $m/z$  range 60 to 1000. The mass spectrometer resolving power was 6000 (FWHM) for protonated reserpine at  $m/z$  609.2812. The atmospheric pressure interface (API) conditions for positive-ion measurements were: orifice 1 = 20 V, ring lens = orifice 2 = 5 V. The RF ion guide voltage ("Peaks Voltage") was set to 600 V to permit analysis of ions greater than approximately  $m/z$  60. For all analyses except those of the seeds and Eucalyptus leaves, a sample of poly(propylene glycol) with average molecular weight of 600, also referred to as "polyethylene glycol" (PEG 600), was measured in each data file as a reference standard for mass calibration. For the remaining samples, Jeffamine M600 (Huntsman, The Woodlands, TX) was used as the calibrant. Unless otherwise stated, the DART was operated with helium and a gas heater setting of 350 °C. Sample extracts were analyzed by exposing the closed end of a Corning Pyrex melting point capillary tube (Capitol Scientific, Austin TX USA) that had been dipped into the extract, to the open air space between the ion source and the mass spectrometer inlet.

**Mass spectral data processing.** Data processing operations, including mass calibration, centroiding, spectral averaging and background subtraction were carried out with *TSSPro3* software (Shrader Software Solutions). *Mass Mountaineer* software (RBC Software, Portsmouth, NH) was used for classification chemometrics including heat maps, principal component analysis (PCA) and linear and kernel discriminant analysis (LDA and KDA respectively). Heat maps exported from *Mass Mountaineer* were imported into *Cluster 3.0* and *Java Treeview* (Stanford University) for hierarchical clustering analysis.

**Sample preparation and sample analysis.** *Dalbergia* species. Because of the common practice of using a single name to refer to multiple species within the *Dalbergia* genus, and the fact that many of the samples we analyzed are rare and illegal to trade, we conducted our analyses on samples from xylarium collections whose species identities had been verified. We then compared these to samples from commercial sources. Wood samples of known identity were sourced from the USDA Forest Product Laboratory (FPL), the USDA Animal and Plant Health Inspection Service (APHIS), the Oregon State University Xylarium (OSU), La Xiloteca del Instituto de Biología, UNAM, Mexico City, México (XIB), Eisenbrand Inc. Exotic Hardwoods, Torrance, CA, USA (EIEH), Cook Woods, Klamath Falls, OR, USA (CW), Carlton McLendon Inc., Atlanta, GA (CMI), PFC Shanty Navarro Hurtado, the Brazilian Federal Police (SNH), and the Botany collection at the University of South Carolina (USC). Furthermore, samples from multiple countries (Mexico, Guatemala, Nicaragua, Panama, Costa Rica and Brazil) were analyzed. The number of replicates that could be analyzed depended upon and was limited by species availability. The comprehensive list appears in Supplementary Table 1. Briefly, 11 *D. granadillo*, 34 *D. retusa*, 22 *P. yucatanum*, 21 *C. echinata* and 12 *C. playloba* species were analyzed. For sampling, wood slivers were shaved from the heartwood of the reference specimens and placed directly in the DART helium gas stream for six seconds each. A mass calibration standard of polyethylene glycol 600 (Ultra, Kingstown RI) was run between every 5<sup>th</sup> sample. For each species, sampling was conducted in replicates of 8–9.

**Biofuel feedstocks.** Soy-derived, canola-derived, and mixed feedstock biodiesels were obtained from Minnesota Soybean Processors (Brewster MN, USA), Archer Daniels Midland (Decatur IL, USA), and Future Fuel (Batesville, AR, USA), respectively. Non-commercial biodiesel samples were supplied by the United States Department of Agriculture, National Center for Agricultural Utilization Research, Agricultural Research Service (Peoria IL, USA). Hexane used to dilute samples for analysis was purchased from VWR (Denver CO, USA) and used as received. Biodiesel samples were measured by dipping the closed end of a melting point capillary tube into hexane solutions of each feedstock (30  $\mu$ L of feedstock dissolved in 100  $\mu$ L of hexane), and suspending the tube between the mass spectrometer inlet and the ion source. Solutions were sampled by DART-TOF-MS as described above in replicates of 5 for each feedstock.

**Pupal cases.** Pupal cases were provided by Dr. Jeffery Tomberlin (Texas A&M University, College Station TX USA) and Dr. Eric Benbow (Michigan State University, USA). Individual insect cases were deposited into vials containing 300  $\mu$ L of hexane (Thermo Fisher Scientific, Waltham MA USA) and allowed to stand for 5 min before DART sampling of the extract using the sealed end of a melting point capillary. The DART exit grid potential was set to +250 V. For every species, 5 cases were sampled in replicates of 5 each.

***Datura*, *Brugmansia* and *Hyocyamus* species differentiation.** *B. arborea* and *D. ferox* seeds were purchased from Georgia Vines (Claxton GA, USA). *H. niger*, *D. stramonium*, and *D. innoxia* seeds were purchased from Horizon Herbs (Williams OR, USA). Individual seeds were sampled by DART-TOF-MS using a vacuum tweezer apparatus to suspend the seeds between the ion source and the mass spectrometer inlet. For analysis, seeds were cut in half and one open half of the seed was oriented so that it faced the DART ion source. For each species, mass spectra were measured in replicates of 5.

***Eucalypt* analysis.** The species of *Eucalyptus* analyzed were *Eucalyptus polyanthemus* (10 plants with 5 replicates from each plant), *E. bridgesiana* apple (2 plants with 25 replicates from each), *E. globulus* (10 plants with 5 replicates each), *E. citriodora* (10 plants with 5 replicates each), and *E. cineraria* (4 plants with 17 replicates each). All plants except *E. bridgesiana* were purchased from Companion Plants Inc. (Athens, OH, USA). *E. bridgesiana* was purchased from Faddegon's Nursery (Latham, NY, USA). Plant leaves were sampled by removal of 6 mm diameter circular segments from the leaves of live soil bound plants with a paper hole punch and suspending the leaf sample in the open air space between the ion source and the mass spectrometer inlet.

**Multivariate statistical analysis.** Mass-calibrated and centroided mass spectra were exported from the data processing software (*TSSPro3*, Shrader Software Solutions, Detroit, MI) as text files for entry into the elemental composition and classification software (*Mass Mountaineer*, RBC Software, Portsmouth, NH, available from mass-spec-software.com). Principal components were calculated by using the correlation matrix. Abundances used for classification were selected from each mass spectrum for the indicated number of peaks having  $m/z$  values within 0.005–0.15 u of the target  $m/z$  value. Heat maps were rendered



as text files for import into Cluster 3.0 for single linkage hierarchical cluster analysis (Michiel de Hoon, University of Tokyo, adapted from the Cluster Program written by Michael Eisen, Stanford University, available at <http://bonsai.hgc.jp/~mdehoon/software/cluster/software.htm>). Dendrograms were observed using Java Treeview (written by Alok Saldanha, available at <http://jtreeview.sourceforge.net/>).

## References

- Cody, R. B., Laramée, J. A. & Durst, H. D. Versatile new ion source for the analysis of materials in open air under ambient conditions. *Anal. Chem.* **77**, 2297–2302 (2005).
- Domin, M. A., Cody, R. B. & Fernandez, F. M. *Ambient Ionization Mass Spectrometry*. (Royal Society of Chemistry, 2014).
- JEOL USA Inc. Flavones and Flavor Components in Two Basil Leaf Chemotypes. *Flavones and Flavor Components in Two Basil Leaf Chemotypes* (2006). Available at: <<http://www.jeolusa.com/DesktopModules/Bring2mind/DMX/Download.aspx?EntryId=42&PortalId=2&DownloadMethod=attachment>>. (Accessed: 25th March 2015).
- Pierce, C. Y. *et al.* Ambient generation of fatty acid methyl ester ions from bacterial whole cells by direct analysis in real time (DART) mass spectrometry. *Chem. Commun.*, 807–809 (2007).
- Maleknia, S. D. *et al.* Temperature-dependent release of volatile organic compounds of eucalypts by direct analysis in real time (DART) mass spectrometry. *Rapid Commun. Mass Spectrom.* **23**, 2241–2246 (2009).
- Maleknia, S. D., Bell, T. L. & Adam, M. A. Eucalypt smoke and wildfires: Temperature dependent emissions of biogenic volatile organic compounds. *Int. J. Mass Spectrom.* **279**, 126–133 (2009).
- Cody, R. B., Dane, A. J., Dawson-Andoh, B., Adedipe, E. O. & Nkansah, K. Rapid classification of white oak (*Quercus alba*) and northern red oak (*Quercus rubra*) by using pyrolysis direct analysis in real time (DART) and time-of-flight mass spectrometry. *J. Anal. Appl. Pyrol.* **95**, 134–137 (2012).
- Adams, J. Analysis of printing and writing papers by using direct analysis in real time mass spectrometry. *Int. J. Mass Spectrom.* **301**, 109–126 (2011).
- Bajpai, V., Sharma, D., Kumar, B. & Madhusudanan, K. P. Profiling of *Piper betle* Linn. cultivars by direct analysis in real time mass spectrometric technique. *Biomed. Chromatogr.* **24**, 1283–1286, doi: 10.1002/bmc.1437 (2010).
- Kim, H. J., Baek, W. S. & Jang, Y. P. Identification of ambiguous cubeb fruit by DART-MS-based fingerprinting combined with principal component analysis. *Food Chem.* **129**, 1305–1310 (2011).
- Lesiak, A. D., Cody, R. B., Dane, A. J. & Musah, R. A. Rapid detection by direct analysis in real time-mass spectrometry (DART-MS) of psychoactive plant drugs of abuse: The case of *Mitragyna speciosa* aka “Kratom”. *Forensic Sci. Int.* **242**, 210–218, doi: <http://dx.doi.org/10.1016/j.forsciint.2014.07.005> (2014).
- Lancaster, C. & Espinoza, E. Analysis of select *Dalbergia* and trade timber using direct analysis in real time and time-of-flight mass spectrometry for CITES enforcement. *Rapid Commun. Mass Spectrom.* **26**, 1147–1156, doi: 10.1002/rcm.6215 (2012).
- National Institute of Science and Technology. *KNAPSAck Family Databases* (2008). Available at: [http://kanaya.naist.jp/knapsack\\_jsp/result.jsp?sname=all&word=Dalbergia](http://kanaya.naist.jp/knapsack_jsp/result.jsp?sname=all&word=Dalbergia) (Accessed 25th March 2015).
- Afendi, F. M. *et al.* *KNAPSAck Family Databases: Integrated Metabolite–Plant Species Databases for Multifaceted Plant Research*. *Plant Cell Phys* **53**, e1, doi: 10.1093/pcp/pcr165 (2012).
- Gerpen, J. V. Biodiesel processing and production. *Fuel Process. Technol.* **86**, 1097–1107, doi: <http://dx.doi.org/10.1016/j.fuproc.2004.11.005> (2005).
- U.S. Energy Information Administration, *Monthly Energy Review* (2015). Available at: <http://www.eia.gov/totalenergy/data/monthly/pdf/mer.pdf>. (Accessed 21st May 2015).
- Knothe, G., Van Gerpen, J. & Krahl, J. *The Biodiesel Handbook*. 2nd edn, (AOCS Press, 2010).
- Knothe, G. & Dunn, R. A comprehensive evaluation of the melting points of fatty acids and esters determined by differential scanning calorimetry. *J. Amer Oil Chem Soc* **86**, 843–856, doi: 10.1007/s11746-009-1423-2 (2009).
- Knothe, G. Structure indices in FA chemistry. How relevant is the iodine value? *J. Amer Oil Chem Soc* **79**, 847–854, doi: 10.1007/s11746-002-0569-4 (2002).
- Spencer, G. F., Herb, S. F. & Gormisky, P. J. Fatty acid composition as a basis for identification of commercial fats and oils. *J. Am. Chem. Soc.* **53**, 94–96, doi: 10.1007/bf02635956 (1976).
- Pauls, R. E. A review of chromatographic characterization techniques for biodiesel and biodiesel blends. *J. Chromatograph. Sci.* **49**, 384–396, doi: 10.1093/chromsci/49.5.384 (2011).
- Alleman, T. L., Fouts, L. & Chiupka, G. *Quality Parameters and Chemical Analysis for Biodiesel Produced in the United States in 2011*. *NREL/TP-5400-57662*. Available at: <http://www.nrel.gov/docs/fy13osti/57662.pdf> (Accessed: 25th March 2015).
- Zhu, G. H., Xu, X. H., Yu, X. J., Zhang, Y. & Wang, J. F. Puparial case hydrocarbons of *Chrysomya megacephala* as an indicator of the postmortem interval. *Forensic Sci. Int.* **169**, 1–5, doi: 10.1016/j.forsciint.2006.06.078.
- Ames, C., Turner, B. & Daniel, B. Estimating the post-mortem interval (I): The use of genetic markers to aid in identification of *Dipteran* species and subpopulations. *International Congress Series* **1288**, 795–797, doi: <http://dx.doi.org/10.1016/j.ics.2005.09.088> (2006).
- Adams, Z. J. O. & Hall, M. J. R. Methods used for the killing and preservation of blowfly larvae, and their effect on post-mortem larval length. *Forensic Sci. Int.* **138**, 50–61, doi: 10.1016/j.forsciint.2003.08.010.
- Donovan, S. E., Hall, M. J. R., Turner, B. D. & Moncrieff, C. B. Larval growth rates of the blowfly, *Calliphora vicina*, over a range of temperatures. *Med. Vet. Entomol.* **20**, 106–114, doi: 10.1111/j.1365-2915.2006.00600.x (2006).
- Greenberg, B. Flies as Forensic Indicators. *J. Med. Entomol.* **28**, 565–577 (1991).
- Wang, J., Li, Z., Chen, Y., Chen, Q. & Yin, X. The succession and development of insects on pig carcasses and their significances in estimating PMI in south China. *Forensic Sci. Int.* **179**, 11–18, doi: 10.1016/j.forsciint.2008.04.014.
- Ye, G., Li, K., Zhu, J., Zhu, G. & Hu, C. Cuticular hydrocarbon composition in pupal exuviae for taxonomic differentiation of six necrophagous flies. *J. Med. Entomol.* **44**, 450–456 (2007).
- Lavine, B. K. & Vora, M. N. Identification of Africanized honeybees. *J. Chromatograph. A* **1096**, 69–75, doi: <http://dx.doi.org/10.1016/j.chroma.2005.06.049> (2005).
- Page, M., Nelson, L., Blomquist, G. & Seybold, S. Cuticular hydrocarbons as chemotaxonomic characters of pine engraver beetles (*Ips* spp.) in the grandicollis subgeneric group. *J. Chem. Ecol.* **23**, 1053–1099, doi: 10.1023/B:JOEC.0000006388.92425.ec (1997).
- Drijfhout, F. P. in *Current Concepts in Forensic Entomology* (ed J. Amendt, Campobasso, C. P., Goff, M. L., Grassberger, M.) 179–204 (Springer, 2010).
- Brown, W. V., Rose, H. A., Lacey, M. J. & Wright, K. The cuticular hydrocarbons of the giant soil-burrowing cockroach *Macropanesthia rhinoceros* saussure (Blattodea: Blaberidae: Geoscapheinae): analysis with respect to age, sex and location. *Com. Biochem. Physiol. B, Biochem. Mol. Biol.* **127**, 261–277 (2000).
- Haverty, M., Collins, M., Nelson, L. & Thorne, B. Cuticular Hydrocarbons of Termites of the British Virgin Islands. *J. Chem. Ecol.* **23**, 927–964, doi: 10.1023/b:joec.0000006381.75185.86 (1997).

35. Moore, H. E. *Analysis of cuticular hydrocarbons in forensically important blowflies using mass spectrometry and its application in post mortem interval estimations* Ph.D. thesis, Keele University, (2013).
36. Yew, J. Y., Cody, R. B. & Kravitz, E. A. Cuticular hydrocarbon analysis of an awake behaving fly using direct analysis in real-time time-of-flight mass spectrometry. *Proc. Natl. Acad. Sci.* **105**, 7135–7140, doi: 10.1073/pnas.0802692105 (2008).
37. Cody, R. B. & Dane, A. J. Soft ionization of saturated hydrocarbons, alcohols and nonpolar compounds by negative-ion direct analysis in real-time mass spectrometry. *J. Am. Soc. Mass Spectrom.* **24**, 329–334, doi: 10.1007/s13361-012-0569-6 (2013).
38. Oerther, S., Behrman, A. D. & Ketcham, S. Herbal hallucinations: common abuse situations seen in the emergency department. *J. Emerg. Nurs.* **36**, 594–596, doi: 10.1016/j.jen.2010.07.018 (2010).
39. Preissel, U. & Preissel, H.-G. *Brugmansia and Datura: Angel's Trumpets and Thorn Apples*. (Firefly Books Ltd., 2002).
40. El Bazaoui, A., Bellimam, M. A. & Soulaymani, A. Nine new tropane alkaloids from *Datura stramonium* L. identified by GC/MS. *Fitoterapia* **82**, 193–197, doi: 10.1016/j.fitote.2010.09.010 (2011).
41. Schmelzer, G. H. Gurib-Fakim. "Datura" *Plant Resources of Tropical Africa-Medicinal Plants*. (Wageningen: PROTA Foundation, 2008).
42. Temerdashev, A. Z., Kolychev, I. A. & Kiseleva, N. V. Chromatographic determination of some tropane alkaloids in *Datura metel*. *J. Anal. Chem.* **67**, 960–966, doi: 10.1134/s1061934812120040 (2012).
43. Coppen, J. J. W. *Eucalyptus: the Genus Eucalyptus*. (Taylor and Francis, 2001).
44. Bignell, C. M., Dunlop, P. J. & Brophy, J. J. Volatile Leaf Oils of some South-western and Southern Australian Species of the Genus *Eucalyptus* (Series I). Part XV. Subgenus *Symphomyrtus*, Section *Bisectaria*, Series *Levispermae*. *Flavour Frag. J.* **12**, 185–193, doi: 10.1002/(sici)1099-1026(199705)12:3<185::aid-ff627>3.0.co;2-b (1997).
45. Bignell, C. M., Dunlop, P. J., Brophy, J. J. & Fookes, C. J. R. Volatile Leaf Oils of some South-western and Southern Australian Species of the Genus *Eucalyptus* (Series I). Part XIV. Subgenus *Monocalyptus*. *Flavour Frag. J.* **12**, 177–183, doi: 10.1002/(sici)1099-1026(199705)12:3<177::aid-ff626>3.0.co;2-9 (1997).
46. Siddiqui, B. S., Sultana, I. & Begum, S. Triterpenoidal constituents from *Eucalyptus camaldulensis* var. obtusa leaves. *Phytochemistry* **54**, 861–865, doi: http://dx.doi.org/10.1016/S0031-9422(00)00058-3 (2000).
47. Schulte, E., Lingott, J., Panne, U. & Kneipp, J. Chemical characterization and classification of pollen. *Anal. Chem.* **80**, 9551–9556, doi: 10.1021/ac801791a (2008).
48. Rösch, P., Kiefer, W. & Popp, J. Chemotaxonomy of mints of genus *Mentha* by applying Raman spectroscopy. *Biopolymers* **67**, 358–361, doi: 10.1002/bip.10099 (2002).
49. Hernandez, C. V. & Rutledge, D. N. Multivariate statistical analysis of gas chromatograms to differentiate cocoa masses by geographical origin and roasting conditions. *Analyst* **119**, 1171–1176, doi: 10.1039/an9941901171 (1994).
50. Godelmann, R. *et al.* Targeted and nontargeted wine analysis by <sup>1</sup>H NMR spectroscopy combined with multivariate statistical analysis. Differentiation of important parameters: grape variety, geographical origin, year of vintage. *J. Agric. Food Chem.* **61**, 5610–5619, doi: 10.1021/jf400800d (2013).
51. Wang, N., Fu, Y. & Lim, L.-T. Feasibility study on chemometric discrimination of roasted Arabica coffees by solvent extraction and Fourier transform infrared spectroscopy. *J. Agric. Food Chem.* **59**, 3220–3226, doi: 10.1021/jf104980d (2011).
52. Nilsson, T., Bassani, M. R., Larsen, T. O. & Montanarella, L. Classification of species in the genus *Penicillium* by Curie point pyrolysis/mass spectrometry followed by multivariate analysis and artificial neural networks. *J. Mass. Spectrom.* **31**, 1422–1428, doi: 10.1002/(sici)1096-9888(199612)31:12<1422::aid-jms442>3.0.co;2-5 (1996).
53. Garrett, R., Rezende, C. M. & Ifa, D. R. Coffee origin discrimination by paper spray mass spectrometry and direct coffee spray analysis. *Analyt. Method.* **5**, 5944–5948, doi: 10.1039/c3ay41247d (2013).
54. Hwang Eui, C. *et al.* Articles : HPLC-tandem mass spectrometric analysis of the marker compounds in *Forsythiae Fructus* and multivariate analysis. *Nat. Prod. Sci.* **17**, 147–159 (2011).
55. Matthews, S. B. *et al.* Metabolite profiling of a diverse collection of wheat lines using ultraperformance liquid chromatography coupled with time-of-flight mass spectrometry. *PLoS ONE* **7**, e44179, doi: 10.1371/journal.pone.0044179 (2012).
56. Wu, Y. *et al.* Comparative studies on *Ophiopogonis* and *Liriope*s based on the determination of 11 bioactive components using LC-MS/MS and hierarchical clustering analysis. *Food Res. Int.* **57**, 15–25, doi: http://dx.doi.org/10.1016/j.foodres.2014.01.004 (2014).
57. Medvedovici, A., Albu, F., Naşcu-Briciu, R. D. & Sârbu, C. Fuzzy clustering evaluation of the discrimination power of UV-Vis and (±) ESI-MS detection system in individual or coupled RPLC for characterization of *Ginkgo Biloba* standardized extracts. *Talanta* **119**, 524–532, doi: http://dx.doi.org/10.1016/j.talanta.2013.11.035 (2014).
58. Montero-Vargas, J. M. *et al.* Metabolic phenotyping for the classification of coffee trees and the exploration of selection markers. *Mol. Biosyst.* **9**, 693–699, doi: 10.1039/c3mb25509c (2013).
59. Dolch, M. E. *et al.* Volatile organic compound analysis by ion molecule reaction mass spectrometry for Gram-positive bacteria differentiation. *Eur. J. Clin. Microbiol. Infect. Dis.* **31**, 3007–3013, doi: 10.1007/s10096-012-1654-2 (2012).
60. Rhourri-Frih, B. *et al.* Classification of natural resins by liquid chromatography-mass spectrometry and gas chromatography-mass spectrometry using chemometric analysis. *J. Chromatograph. A* **1256**, 177–190, doi: http://dx.doi.org/10.1016/j.chroma.2012.07.050 (2012).
61. Xu, B., Zhang, L., Wang, H., Luo, D. & Li, P. Characterization and authentication of four important edible oils using free phytosterol profiles established by GC-GC-TOF/MS. *Anal. Method.* **6**, 6860–6870 (2014).
62. Maleknia, S. D. Environmental effects of wildfire emissions associated with changing climates. *AQCC J.* **48**, 33–36 (2014).
63. Watrous, J. *et al.* Metabolic Profiling Directly from the Petri Dish Using Nanospray Desorption Electrospray Ionization Imaging Mass Spectrometry. *Anal. Chem.* **85**, 10385–10391, doi: 10.1021/ac4023154 (2013).

## Acknowledgments

The support of the Research Foundation of SUNY, a grant from the U.S. National Science Foundation to RAM and RBC (grant #1310350), a fellowship from the Winston Churchill Memorial trust as well as financial support from Keele University for HM, and the support of the U.S. Department of Energy, Office of Vehicle Technologies under Contract DEAC36-99GO10337 with the National Renewable Energy Laboratory, are appreciated. The assistance of Justine Giffen with preparation of the Eucalypt samples and Dr. Bryan Moser of the USDA in supplying biodiesel samples is gratefully acknowledged. Thanks are also extended to Professors Jeffery Tomberlin and Eric Benbow who supplied the puparial cases. The findings and conclusions in this article are those of the authors and do not necessarily represent the views of the U. S. Fish and Wildlife Service.

### Author Contributions

Experiments were performed by R.A.M., E.O.E., R.B.C., A.D.L., E.C. and H.E.M. The manuscript was written by R.A.M., E.O.E. and R.B.C. E.C., H.E.M. and S.M. contributed to the writing of the manuscript. R.A.M., E.O.E., R.B.C., E.D.C., H.E.M. and F.P.D. conceived of various aspects of the research ideas described.

### Additional Information

**Supplementary information** accompanies this paper at <http://www.nature.com/srep>

**Competing financial interests:** The authors declare no competing financial interests.

**How to cite this article:** Musah, R. A. *et al.* A High Throughput Ambient Mass Spectrometric Approach to Species Identification and Classification from Chemical Fingerprint Signatures. *Sci. Rep.* **5**, 11520; doi: 10.1038/srep11520 (2015).



This work is licensed under a Creative Commons Attribution 4.0 International License. The images or other third party material in this article are included in the article's Creative Commons license, unless indicated otherwise in the credit line; if the material is not included under the Creative Commons license, users will need to obtain permission from the license holder to reproduce the material. To view a copy of this license, visit <http://creativecommons.org/licenses/by/4.0/>



Certain products in this brochure are controlled under the "Foreign Exchange and Foreign Trade Law" of Japan in compliance with international security export control. JEOL Ltd. must provide the Japanese Government with "End-user's Statement of Assurance" and "End-use Certificate" in order to obtain the export license needed for export from Japan. If the product to be exported is in this category, the end user will be asked to fill in these certificate forms.



JEOL Ltd.

3-1-2 Musashino Akishima Tokyo 196-8558 Japan Sales Division Tel. +81-3-6262-3560 Fax. +81-3-6262-3577  
www.jeol.com ISO 9001 • ISO 14001 Certified

• **AUSTRALIA & NEW ZEALAND** /JEOL (AUSTRALASIA) Pty.Ltd. Suite 1, L2 18 Aquatic Drive - Frenchs Forest NSW 2086 Australia • **BELGIUM** /JEOL (EUROPE) B.V. Planet II, Gebouw B Leuvensesteenweg 542, B-1930 Zaventem Belgium  
• **BRAZIL** /JEOL Brasil Instrumentos Cientificos Ltda. Av. Jabaquara, 2958 5º andar conjunto 52 - 04046-500 Sao Paulo, SP Brazil • **CANADA** /JEOL CANADA, INC. 3275 1ere Rue, Local #8 St-Hubert, QC J3Y-8Y6, Canada • **CHINA** /JEOL (BEIJING) CO., LTD. Zhongkeziyuan Building South Tower 2F, Zhongguancun Nansanjie Street No. 6, Haidian District, Beijing, P.R.China • **EGYPT** /JEOL SERVICE BUREAU 3rd Fl. Nile Center Bldg., Nawal Street, Dokki, (Cairo), Egypt • **FRANCE** /JEOL (EUROPE) SAS Espace Claude Monet, 1 Allée de Giverny 78290, Croissy-sur-Seine, France • **GERMANY** /JEOL (GERMANY) GmbH Gute Aenger 30 85356 Freising, Germany • **GREAT BRITAIN & IRELAND** /JEOL (U.K.) LTD. Silver Court, Watchmead, Welwyn Garden City, Hertfordshire AL7 1LT, U.K. • **INDIA** /JEOL INDIA PVT. LTD. Unit No.305, 3rd Floor, ABW Elegance Tower, Jasola District Centre, New Delhi 110 025, India /JEOL INDIA PVT. LTD. Hyderabad Office 422, Regus Solitaire Business centre, 1-10-39 to 44, level 4, Gumidelli Towers, Old Airport Road, Begumpet, Hyderabad - 500016, India • **ITALY** /JEOL (ITALIA) S.p.A. Palazzo Pacinotti - Milano 3 City, Via Ludovico il Moro, 6/A 20079 Basiglio(MI) Italy • **KOREA** /JEOL KOREA LTD. Dongwoo Bldg. 7F, 1443, Yangjae Daero, Gangdong-Gu, Seoul, 05355, Korea • **MALAYSIA** /JEOL (MALAYSIA) SDN.BHD. 508, Block A, Level 5, Kelana Business Center, 97, Jalan SS 7/2, Kelana Jaya, 47301 Petaling Jaya, Selangor, Malaysia • **MEXICO** /JEOL DE MEXICO S.A. DE C.V. Arkansas 11 Piso 2 Colonia Napoles Delegacion Benito Juarez, C.P. 03810 Mexico D.F., Mexico • **QATAR** /Mannai Trading Company W.L.L. ALI Emadi Complex, Salwa Road P.O.Box 76, Doha, Qatar • **RUSSIA** /JEOL (RUS) LLC Office 351, floor 3, 23, Novoslobodskaya St, Moscow 127055, Russia • **SCANDINAVIA** /SWEDEN JEOL (Nordic) AB Hammarbacken 6A, Box 716, 191 27 Sollentuna Sweden • **SINGAPORE** /JEOL ASIA PTE.LTD. 2 Corporation Road #01-12 Corporation Place Singapore 618494 • **TAIWAN** /JIE DONG CO., LTD. 7F, 112, Chung Hsiao East Road, Section 1, Taipei, Taiwan 10023 (R.O.C.) • **THE NETHERLANDS** /JEOL (EUROPE) B.V. Lireweg 4, NL-2153 PH Nieuw-Vennep, The Netherlands • **USA** /JEOL USA, INC. 11 Dearborn Road, Peabody, MA 01960, U.S.A.